Identification and Characterisation of Differentially Methylated Regions within the human Major Histocompatibility Complex

Eleni M. Tomazou

The Wellcome Trust Sanger Institute
University of Cambridge
Clare College

This dissertation is submitted for the degree of Doctor of Philosophy

Declaration

This thesis describes my work undertaken in the laboratory of Prof. Stephan Beck at the Wellcome Trust Sanger Institute while member of Clare College, University of Cambridge. It is submitted in fulfilment of the requirements for the degree of Doctor of Philosophy. The work described here has not been submitted for any degree, diploma, or any other qualification. This thesis does not exceed 300, single-sided pages of double spaced text, not including the bibliography and appendices.
This dissertation is the result of my own work and includes nothing that it is the outcome done in collaboration except as detailed in the text below.

Microarray data analysis was done with the help of Gregory Lefebvre (Wellcome Trust Sanger Institute).

Bioinformatics analysis for identification of genomic features of tDMRs was performed with the help of Stephan Rice (Wellcome Trust Sanger Institute).

MHC tile-path array was printed by the Wellcome Trust Sanger Institute Microarray facility.

Eleni M. Tomazou
Cambridge, 21 July 2008

Abstract

DNA methylation is one of several epigenetic marks capable of modulating genome function. Alterations to the temporal or spatial patterns of DNA methylation give rise to differentially methylated regions (DMRs). DMRs can arise during normal development and can be associated with specific tissues (tissue-specific DMRs, tDMRs) as well as during the development of aberrant phenotypes (phenotype specific DMRs, pDMRs) and in many cases can be implicated in the aetiology of complex diseases.

This dissertation describes an array-based assay for the unbiased identification and characterisation of DMRs (both tDMRs and pDMRs) within the human Major Histocompatibility Complex (MHC). The MHC, a 4Mb region on chromosome 6, is an ideal model system for studying DMRs as it is gene dense and associated with many complex diseases including immune-linked diseases as well as cancer.

I identified and characterised 55 MHC loci as tDMRs of which about 27% could be correlated with tissue specific gene expression. This implicates DNA methylation as an additional regulatory layer in the control of MHC loci. DNA methylation was also found to be associated with the regulation of genes involved in the MHC class I antigen processing and presentation pathway. Cell lines that displayed the MHC class I^- phenotype, which is a common disease phenotype, were tested for the presence of pDMRs. I identified two pDMRs that were correlated with the down-regulation of the *HLA-A*, *HLA-B*, *TAP1* and *PSMB8* genes and 14 pDMRs associated with *PSMB9* up-regulation. Three DMRs were identified within the TNF gene cluster which may contribute to the development of the MHC class I^- phenotype. Finally, two DMRs within the promoter regions of the *PSMB8* and *B2M* genes showed strong correlation with low expression levels. These findings are consistent with previous studies supporting the notion that transcriptional gene silencing promotes DNA hypermethylation or vice versa. The former implies that, in some cases, DNA hypermethylation may be the consequence rather than the cause of gene silencing.

The genomic features and functional aspects of some of the identified DMRs were tested and it was shown that DNA methylation inhibitors can restore parts of the MHC class I pathway that were silenced by hypermethylation.

The results presented in this thesis support the role of DNA methylation in phenotypic plasticity. They complement the extensive amount of genetic data available for the MHC and open the way for the development of integrated (epi)genetic approaches to complex phenotypes and common diseases.

Publications

Publication list arising from the work described in this thesis at the time of submission:

1. **Tomazou EM** and Powell GT. Look who's talking too: graduates developing skills through communication. ***Nat Rev Genet***. 2007 Sep;8(9):724-6

2. **Tomazou EM**, Rakyan VK, Lefebvre G, Andrews R, Ellis P, Jackson DK, Langford C, Francis MD, Bäckdahl L, Miretti M, Coggill P, Ottaviani D, Sheer D, Murrell A, Beck S. Generation of a genomic tiling array of the human Major Histocompatibility Complex (MHC) and its application for DNA methylation analysis. ***BMC Med Genomics***. 2008 May 30;1:19.

3. Down TA, Rakyan VK, Turner DJ, Flicek P, Li H, Thorne NP, Kulesha E, Gräf S, **Tomazou EM**, Bäckdahl L, Johnson N, Herberth M, Howe KL, Jackson DK, Miretti MM, Marioni JC, Birney E, Hubbard TJP, Durbin R, Tavare S, Beck S. A Bayesian de-convolution strategy for immunoprecipitation-based DNA methylation analysis. ***Nat Biotechnol***. 2008 Jul 8;26(7):779-785.

4. Rakyan, VK, Down TA, Thorne NP, Flicek P, Kulesha E, Gräf S, **Tomazou EM**, Bäckdahl L, Johnson N, Herberth M, Howe KL, Jackson DK, Miretti MM, Fiegler H, Marioni JC, Birney E, Hubbard TJP, Carter NP, Tavare S, Beck S. An integrated resource for genome-wide identification and analysis of human tissue-specific differentially methylated regions (tDMRs). ***Genome Res***. 2008 Jun 24 (online)

5. Ottaviani D, Lever E, Mitter R, Jones T, Forshew T, **Tomazou EM**, Beck S, Krawetz SA, Platts AE, Segarane B, Sheer D. Recruitment of Genome Anchors to the Nuclear Matrix: a Novel Mechanism for Regulating Expression of the Human MHC? ***Genome Res***. accepted

Acknowledgments

Stephan Beck, my supervisor. Thank you for your support, advice, for keeping up my enthusiasm, and for always remembering my birthday. I could not have asked for a better mentor.

Mike Stratton for his constructive comments, as a member of my thesis committee, and for his support during the last year. It has been really helpful. Thank you very much.

Vardhman Rakyan my lab-mate, bench-mate, office-mate and a good friend. Thank you for introducing me to MeDIP and bisulphite sequencing and for the interesting discussions. Keep in touch!

Marcos Miretti, my favourite post-doc. Thank you for being there when the others had to go…Hope we meet in America – North and/or South…

Adele Murrell, my second supervisor. It was a pleasure meeting you and working with you.

ex-Team-50 members: Roger Horton, Penny Coggill, Liselotte Backdahl and Jen Sambrook. Thank you for all the good times in the office and for all the chocolate we have shared. Good luck to all of you and hope we meet again.

The Cancer Genome Project team, and especially Andy Futreal and Mike Stratton; thank you for letting me use your space, equipment and money during the last year.

The people in the analysis office; although we have not interacted a lot it was a great pleasure to meet you all!

Gregory Lefebvre, my statistician. Thank you very much for analysing my data. It was nice working with you and good luck in Lausanne.

The Wellcome Trust Sanger Institute Microarray Facilities and especially Cordelia Langford, Rob Andrews and Peter Ellis; thanks for your support during the last three years.

The Wellcome Trust Sanger Institute PhD program: for the generous financial support and training. A special thank you to Christina Hedberg-Delouka and Alex Bateman for always being helpful.

Antigone and Samrah, my ‘Cambridge family’. Thank you for proof-reading my thesis and for all the great times at the “spitaki” residence. I will miss you…

Lampros and Loukia, my lovely parents; thank you for letting me go… I miss you too…

Table of contents

List of figures

List of Tables

Abbreviations

5-aza-CR	5-Azacytidine
5-aza-CdR	5-Aza-2'-deoxycytidine
5m-CpG	methylated CpG at 5-carbon position of cytosine
aCGH	array comparative genomic hybridization
ASM	allele specific DNA methylation
bp	base pair
BAC	bacterial artificial chromosome
B2M	β2-microglobulin
BSA	bovine serum albumin
°C	degrees Celcius
CANX	calnexin
CALR	calreticulin
CGI	CpG island
ChIP	chromatin immunoprecipitation
CNV	Copy Number Variation
CpG	cytidine-guanosine dinucleotide
CIITA	MHC class II transactivator
Cy3	Cyanine 3-dCTP
Cy5	Cyanine 5-dCTP
DMR (tDMR, pDMR)	Differentially Methylated Region (tissue-specific-, phenotype-specific)
DMSO	dimethyl sulphoxide
DNMT	DNA methyltransferase
dNTP	2'-deoxyribonucleoside 5'-triphophate
ds	double stranded
EBV	Epstein-Barr Virus
ECR	Evolutionary Conserved Region
EDTA	ethylenediamine tetra-acetic acid
ER	Endoplasmatic Reticulum

FBS	Foetal Bovine Serum
GA	Genetic Analyser
HCMV	human cytomegalovirus
HERV	human endogenous retrovirus
HEP	Human Epigenome Project
HLA	human leukocyte antigen
HSP	heat shock protein
ICF	immunodeficiency syndrome
IFN	interferon
kb	kilobase pairs
LB	Luria-Bertani broth
LD	linkage disequilibrium
LINE	long interspersed nuclear element
LITAF	lipopolysaccharide-induced TNF-α factor
LM-PCR	Ligation Mediated PCR
LPS	lipopolysaccharide
LRES	long range epigenetic silencing
LTR	long terminal repeat
MeDIP	Methylated DNA Immunoprecipitation
MBD	methyl binding domain
μg	microgram
MHC	Major Histocompatibility Complex
min	minute
ml	millilitre
μl	microlitre
μM	micromolar
mM	millimolar
mm	millimetre
NAHR	non-allelic homologous recombination
NRM	nurim
MVP	Methylation Variable Position
NCBI	National Centre for Biotechnology Information
ncRNA	non-coding RNA
ng	nanogram

PAC	P1 artificial chromosome
PBS	phosphate buffer saline
PCR	Polymerase Chain Reaction
RFX	regulatory factor X
rpm	revolutions per minute
RRBS	Reduced Representation Bisulphite Sequencing
RT-PCR	Real Time PCR
SAM	S-adenosyl-methionine
SDS	sodium dodecyl sulphate
sec	second
SNP	Single Nucleotide Polymorphism
ss	single stranded
SSC	saline sodium citrate
TNF	Tumour Necrosis Factor
TSS	Transcription Start Site
Tris	tris(hydroxymethyl)aminomethane
U	unit
UCSC	University of California Santa Cruz
UTR	untranslated region
WTCCC	Wellcome Trust Case Control Consortium
WGA	whole genome association

Chapter 1

General Introduction

1.1 Introduction

One of the major challenges in genetics today is to understand the causes of complex diseases. Complex diseases refer to disorders that do not follow Mendel's laws of inheritance (Mendel, 1950; Wang et al., 2005). Such diseases are considered to derive from multiple heritable and environmental factors. Cancer, schizophrenia, diabetes, lupus and cardiovascular diseases are a few representative examples. Identifying the basis of complex diseases will be of great medical relevance (Kiberstis, 2002; Kiberstis, 2002; L, 2002; Lander and Schork, 1994).

In recent years, a lot of attention has been given to the genetic components of such diseases. Large, collaborative studies have been focused on the identification of single nucleotide polymorphisms (SNPs) (The International HapMap Project, 2003; WTCCC, 2007) and copy number variation (CNVs) (Beckmann et al., 2007; Redon et al., 2006) that could be associated with human diseases and eventually lead to new therapies. However, to date only a few genetic variants have a significant and replicated association to complex diseases indicating that other factors in addition to genetic variation may contribute to complex phenotypes.

Recent advances in high-throughput epigenomics (mapping of genome-wide epigenetic modifications) (Bernstein et al., 2007), have led to the concept of epigenetic variation which is now also considered to play an important role in the development of complex diseases (Hatchwell and Greally, 2007; van Vliet et al., 2007). A number of studies, including this thesis aim to elucidate the role of epigenetics in the context of such phenotypes.

I used the major histocompatibility complex (MHC) region (Horton et al., 2004), a 4Mb region on human chromosome 6, as a model system to elucidate the role of DNA methylation (the best-studied epigenetic mark to date) in the regulation of MHC loci. The MHC has been chosen because it is associated with susceptibility to more complex

diseases than any other region within the human genome (Lechler, 2000). Unravelling the epigenetic code of the MHC will give further insights into the impact of epigenetics in complex phenotypes.

1.2. The Major Histocompatibility Complex - MHC

The major histocompatibility complex (MHC) is a 4Mb region on the short arm of human chromosome 6 (6p21.3) (Horton et al., 2004). It is one of the most gene-dense and highly polymorphic regions of the human genome and it is associated with many complex diseases including infectious, autoimmune and inflammatory diseases as well as cancer, and it is important in transplant medicine.

The classical MHC is divided into three classes: Class I, Class II and Class III. Figure 1.1 shows the gene map of the MHC region indicating the order of the three classes (I, III, II) and their relative sizes as well as the genes encoded within each class. The concept of the extended MHC (xMHC) (although not discussed any further within this thesis) was recently established based on the finding that linkage disequilibrium (LD) and MHC-related genes exist outside the boundaries of the classical 4Mb MHC region (Horton et al., 2004).

1.2.1 MHC encoded genes

The gene map of the MHC region was completed and reviewed recently (Horton et al., 2004). The classical MHC comprises 224 gene loci, of which more than 57% are thought to be expressed. At least 10% of the MHC genes have functions related to the immune system. The MHC is divided into three regions in the following order: telomere – class I, class III, class II - centromere (figure 1.1):

i. MHC class I region

This region has a size of about 2Mb and contains the three main MHC class I genes, *HLA-A*, *HLA-B* and *HLA-C*, which are highly polymorphic and members of the immunoglobin superfamily (Lawlor et al., 1990). They present intracellular antigen peptides to the T-cell receptors of cytotoxic T-cells. Antigens, in order to be presented to the cell surface, go through a pathway called the antigen presenting pathway (Hewitt, 2003). These genes are expressed by most somatic tissues at varying levels. The MHC class I region also harbours the non-classical class I genes, *HLA-E*, *-F* and *–G*, which are less polymorphic and display a more restricted tissue expression compared to the classical genes (Geraghty, 1993). *HLA-G* is the only class I gene expressed in foetal trophoblast cells and may play a role in the maternal tolerance of the foetus (Loke and King, 1991; Parham, 1996). The MHC class I like genes *MICA* and *MICB* (Stephens, 2001) and a plethora of pseudogenes (Geraghty, 1993; Le Bouteiller, 1994) are also encoded within this region.

ii. MHC class II region

The class II region, 880 kb in size, contains one gene every 40kb on average. This class, similar to class I, encodes members of the immunoglobin superfamily *HLA-DP*, *-DQ*, *–DR* and pseudogenes (the classical MHC class II genes) (Andersson et al., 1987). However, these genes are expressed as heterodimers only on specialised antigen-presenting cells such as macrophages, B cells and some T cells. The former engulf and internalise exogenous antigens which are then presented to helper T cells by class II members of the immunoglobin superfamily. The non-classical class II genes, *HLA-DM* and *–DO*, are not expressed on the cell surface, but form heterotetrameric complexes involved in peptide exchange and loading onto classical class II molecules (Alfonso and Karlsson, 2000).

The class II region also encodes *PSMB8*, *PSMB9*, *TAP1*, *TAP2* and *TAPBP*. The products of these genes are involved in the MHC class I antigen processing and presentation machinery (Androlewicz, 1999; Lehner and Trowsdale, 1998; van Endert, 1999).

iii. MHC class III region

This is a very gene dense region of about 100 kb and contains at least 70 genes with diverse functions (Aguado, 1996). Examples of class III genes are *C2* and *C4* which are members of the complement system. *C2* and *C4* gene products mediate phagocytosis and lysis of bacterially infected cells leading to inflammatory response. Members of the tumour necrosis family, *TNF-*α, *LTA* and *LTB*, which are cytokines that control inflammation, are also encoded within this region (Gruss and Dower, 1995). Three heat shock proteins (HSP) are also encoded in the class III region. They are involved in stress-induced signalling of immune responses mediating the elimination of damaged, infected or malignant cells (Gleimer and Parham, 2003)

1.2.2 MHC Polymorphism

HLA class I and class II genes are highly polymorphic (Robinson et al., 2003) and *HLA-B* has been reported to be the most polymorphic gene in the human genome (Mungall et al., 2003). The extensive polymorphism of the MHC loci is believed to enhance immune defence by broadening the array of antigenic peptides available for T-cell recognition. MHC encoded molecules govern immune responses by presenting antigen peptides to T-cells (figure 5.2). Genetic polymorphism within the MHC region also facilitates variable susceptibility to MHC-linked diseases as well as to pathogens (Goulder and Watkins, 2008). Single nucleotide polymorphisms are the most common type of variation within the MHC. Recently, four-independent re-sequencing projects have significantly expanded our knowledge of variation within the MHC (Horton et al., 2008; Raymond et

al., 2005; Shiina et al., 2006; Smith et al., 2006). However, polymorphism is not restricted to genetic variation (SNPs). Structural copy number variation (CNVs) (Redon et al., 2006) also exist within the MHC (Stewart et al., 2004). More specifically, two hyper-variable regions have been reported to have CNVs: (i). the RCCX region (within the MHC class III region) which contains duplications of *C4, TNXA, CYP21A1P* and *STK19P* pseudogenes (Chung et al., 2002; Yang et al., 1999), and (ii). the *DRB* locus (within the MHC class II region) between *HLA-DRB1* and *HLA-DRB9* which shows haplotype-specific rearrangements (Marsh, 2000) .

In addition, polymorphism resulting from the presence or absence of retroviral sequences (LINEs, Alu, HERV, LTR, MER and SVA) (Stewart et al., 2004) has been observed. The retroviral insertions are often located either in the *HLA-DR* region or near the MHC class I genes, possibly promoting molecular evolution. Recently a HERV-derived gene, *HCP5*, has been implicated in HIV-1-host interaction (Fellay et al., 2007).

1.2.3 MHC-linked diseases

The MHC is associated with many diseases including most if not all autoimmune diseases (Lechler, 2000). A representative list of MHC-linked diseases is given in table 1.1. In most of the cases listed, the disease causing mutation/variation is not yet known. Disease-causing and disease-associated genes are indicated in table 1.1.

The involvement of the MHC in many complex diseases was confirmed further by whole genome association (WGA) studies (WTCCC, 2007). A recent study has shown that MHC-class I mediated events, mainly involving a *HLA-B* locus, contribute to the aetiology of type I diabetes, which is an autoimmune disease (Nejentsev et al., 2007), whereas the role of three other polymorphic MHC loci (*HLA-B, HLA-C* and *ZNRD1*) were reported to influence the host response to HIV-1 (Fellay et al., 2007). The latter supports the role of the MHC in conferring resistance to infectious diseases.

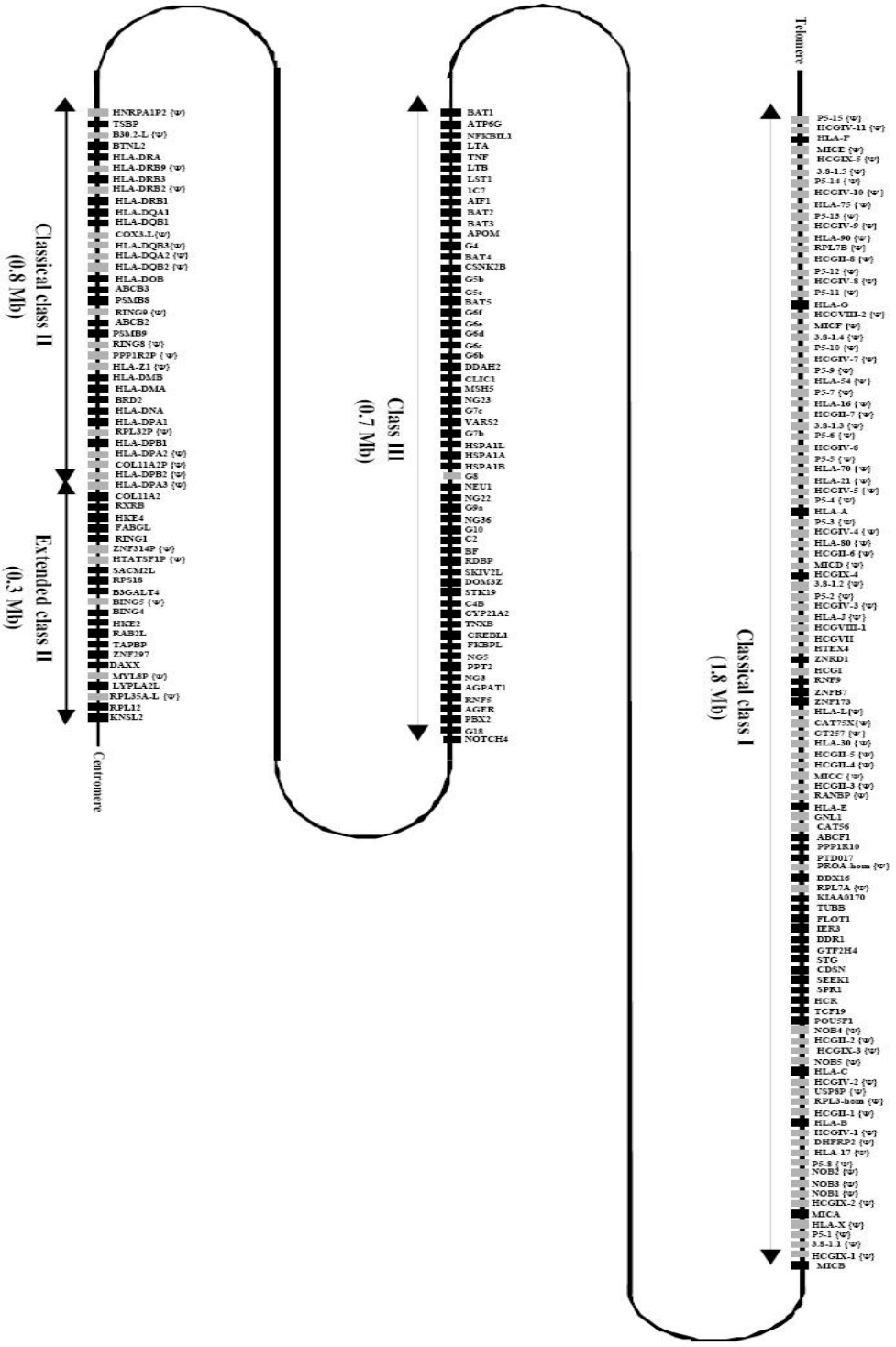

Figure 1.1. **Gene map of the human MHC**. Genes are displayed in order from telomere to centromere but are not drawn to scale. Solid black boxes indicate the loci that have been

investigated by the HEP (see below). {Ψ} indicates the presence of a pseudogene. Figure was taken from Novik et al. (Novik et al., 2002).

1.2.3.1 Future challenges in studying MHC-linked diseases

The MHC provides a prototype for the study of complex diseases. Although past studies have generated extensive data for the genetics of the MHC resulting in important contributions to medicine (de Bakker et al., 2006; Rioux and Abbas, 2005; Vyse and Todd, 1996), further studies are necessary to improve our understanding of the causes of MHC-linked diseases. As summarised in figure 1.2, complex MHC-linked diseases, like autoimmune diseases, are the result of complex interactions between genetic, epigenetic and environmental factors. Epigenetic factors include DNA methylation, histone modifications and non-coding RNAs (see below).

Elucidating the epigenetic code of the MHC can be expected to be highly beneficial to biomedical research.

1.2.4 MHC and Epigenetics – What is known so far

Emerging evidence suggests that epigenetic events are associated with the regulation of MHC gene expression. This is based on the below findings:

i. The MHC class II transactivator (CIITA) and the regulatory factor X (RFX) proteins serve as focal points for recruiting histone modifying enzymes to MHC class II promoters, whereby CIITA itself is regulated by DNA methylation, histone modifications and ncRNAs (Wright and Ting, 2006; Zika and Ting, 2005).

ii. Treatment of melanoma and esophageal cell lines with the DNA methylation inhibitor 5-aza-2'-deoxycytidine (see below) led to restoration of MHC class I expression (which is suppressed in these cell lines), implicating DNA

methylation in the expression of MHC class I genes (Maio et al., 2003; Nie et al., 2001; Serrano et al., 2001)

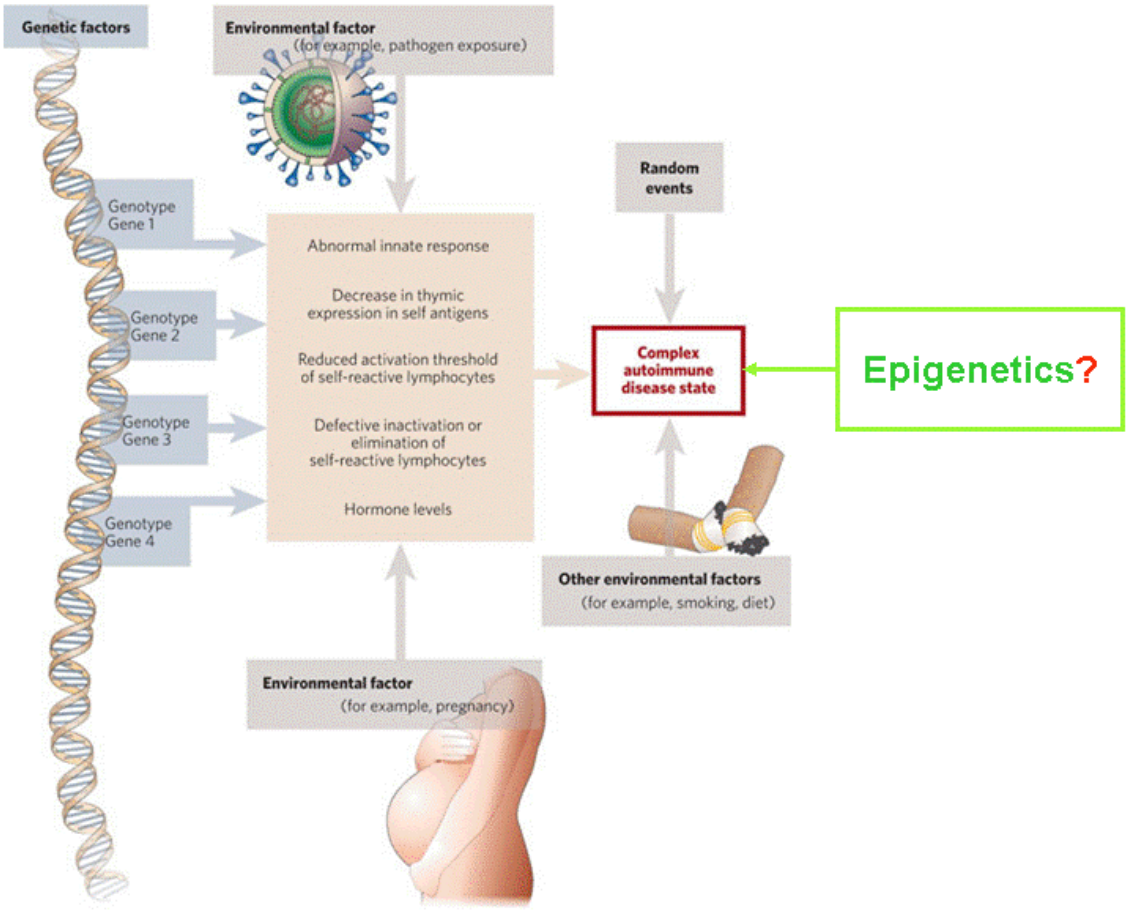

Figure 1.2. **Autoimmune diseases caused by complex traits.** In complex traits, the clinically recognised disease state results from interactions between multiple genotypes and the environment. Recently the role of epigenetics in such complex diseases has been implicated. The question mark next to 'epigenetics' reflects that the contribution of epigenetics is still not well understood. A lot of current studies aim to elucidate the impact of genetics, epigenetics and environmental factors in susceptibility, disease progression and clinical management. Figure was taken (with some modifications) from Rioux and Abbas (Rioux and Abbas, 2005).

MHC class I region	
HLA-G	Associated with *Pemphigus vulgaris* in Jewish patients
HLA-A	Associated with autoimmune diseases; for example, birdshot chorioretinopathy
HLA-E	Associated with type 1 *Diabetes mellitus*; also influences age of onset of disease
MDC1	Associated with inadequate DNA damage responses owing to MDC1-deficiency
CDSN	Causes hypotrichosis simplex of the scalp
PSORS1C1	Associated with psoriasis
PSORS1C2	Associated with psoriasis
C6orf18	Associated with psoriasis
HLA-C	Associated with autoimmune diseases; for example, psoriasis
HLA-B	Associated with autoimmune diseases; for example, ankylosing spondylitis or Behcet disease
MICA	Associated with autoimmune diseases; for example, rheumatoid arthritis and coeliac disease
MICB	Associated with coeliac disease
MHC class III region	
NFKBIL1	Associated with rheumatoid arthritis
LTA	Associated with myocardial infarction
TNF	Associated with septic shock, cerebral malaria
LTB	Associated with infective/inflammatory diseases
NCR3	Associated with impairment of NK cell function in HIV-1 infected patients
BAT2	Associated with influence on age at onset of type 1 *Diabetes mellitus*
NEU1	Causes type I and II sialidosis
C2	Causes C2 deficiency
C4B	Causes C4 deficiency
C4A	Causes C4 deficiency
CYP21A2	Causes several disorders owing to 21-hydroxylase deficiency
TNXB	Causes Ehlers–Danlos syndrome (hypermobility type) owing to tenascin X deficiency
AGER	Associated with amplification of inflammatory responses in rheumatoid arthritis
MHC class II region	
HLA-DR loci	Associated with autoimmune diseases; for example, rheumatoid arthritis, type 1 and type 2 *Diabetes mellitus*
HLA-DQ loci	Associated with autoimmune diseases; for example, narcolepsy
TAP2	Causes bare lymphocyte syndrome type I owing to TAP2-deficiency; associated with various diseases; for example, rheumatoid arthritis
TAP1	Causes bare lymphocyte syndrome type I owing to TAP1-deficiency; associated with various diseases; for example, vitiligo in Caucasian patients that are young in age at onset
BRD2	Associated with juvenile myoclonic epilepsy
HLA-DP loci	Associated with autoimmune diseases; for example, chronic beryllium disease

Table 1.1. **Genes in the MHC in which variation has a relationship to disease.** Table was taken from Horton et al. (Horton et al., 2004)

iii. The HEP study has shown that at least 10% of the MHC loci analysed show tissue-specific methylation patterns, implicating DNA methylation in tissue-specific expression of MHC genes (Rakyan et al., 2004).

iv. A non-coding RNA (microRNA), encoded by human cytomegalovirus (HCMV) during infection, might regulate the expression of a 'stressed-induced' MHC gene (*MICB*) (Stern-Ginossar et al., 2007).

v. It should be noted that extensive the genetic polymorphism within the MHC makes the latter an ideal region for studying interaction between the genome and the epigenome and the formation of hepitypes (see section 1.3.7.1). It can be postulated that SNPs that result to gain or loss of one or more critical CpG sites may affect the overall methylation profile of a locus. Alternatively, non-CpG SNPs located within an epigenetically sensitive regulatory element may also influence the epigenetic make-up of a region.

Based on the above observations I reasoned that epigenetics may be important in the regulation of genes encoded within in the MHC, and hence be associated with MHC-linked phenotypes.

In the following sections I introduce the concept of epigenetics, refer in detail to DNA methylation and epigenetic variation in the form of differentially methylated regions (DMRs), and discuss how DMRs can be linked to complex phenotypes. The rationale of my study, which aimed to identify DMRs within the MHC, is given in the last section of this chapter.

1.3 Epigenetics

1.3.1 Definition

The term epigenetics was first introduced by Conrad Waddington in 1942 (Waddington, 1942). It was used to describe the interactions of genes with their environment “to bring a phenotype into being”. Today epigenetics refers to mitotically and, in some cases, meiotically heritable states of gene expression that are not due to changes in the DNA sequence (Allis et al., 2007). The Greek prefix ‘epi-‘ implies features that are “in addition” to genetics, and this is reflected in the current definition.

1.3.2 Epigenetic Modifications in Mammalian Genomes

Epigenetic modifications are stable modifications of the DNA or chromatin that do not alter the primary nucleotide sequence. They can alter the functions of associated genes by modulating DNA accessibility, protein recruitment and chromatin structure (figure 1.3a).

Histones are the major protein component of chromatin. The core histones, including H2A, H2B, H3 and H4, make up the nucleosome and are subjected to post-translational modifications at specific positions within the amino-terminus of their tails. These modifications include for instance acetylation, methylation, phosphorylation and ubiquitination (figure 1.3b) and they are correlated with chromatin accessibility and transcriptional activity or repression (Berger, 2007; Kouzarides, 2007).

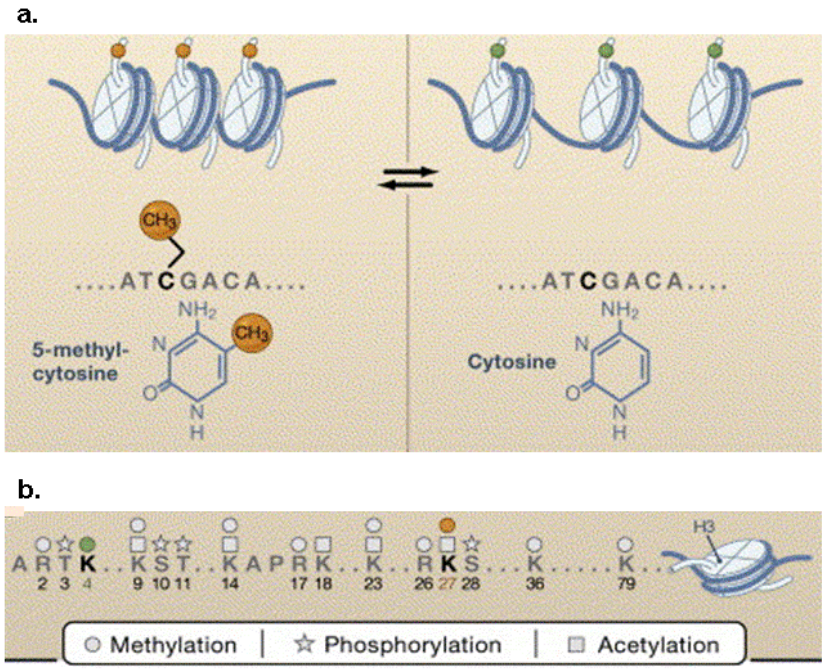

Figure 1.3. **DNA methylation and histone modifications**. Cytosine methylation is the only known covalent modification of DNA in mammals. In contrast, histones are subject to different combinations of modifications, including acetylation, methylation, phosphorylation and ubiquitination. Part a. illustrates the structure and effects of cytosine methylation (repressive/orange, activating/green). Part b. illustrates the diversity of histone H3 modifications. Figure was taken from Bernstein el al., (Bernstein et al., 2007).

DNA methylation is a covalent modification of the 5-carbon position of cytosine. The reaction involves the addition of a methyl group (figure 1.3a) and it is catalysed by DNA methyltransferases (DNMTs) with S-adenosyl-methionine (SAM) as the methyl donor (figure 1.4). In mammals this occurs predominantly in the context of cytidine-guanosine (CpG) dinucleotides (Bird, 2002) but non-CpG methylation has also been reported in certain cell types, and is common in plants (Finnegan and Kovac, 2000; Grandjean et al., 2007; Ramsahoye et al., 2000).

Recently, non-coding RNAs (ncRNAs) have been recognised as an additional component associated with epigenetic modulation and have been reported to be

involved in X-chromosome inactivation, chromatin structure, DNA imprinting and DNA demethylation (Costa, 2005).

DNA methylation is the epigenetic mark studied in this thesis and is discussed in more detail in the following sections.

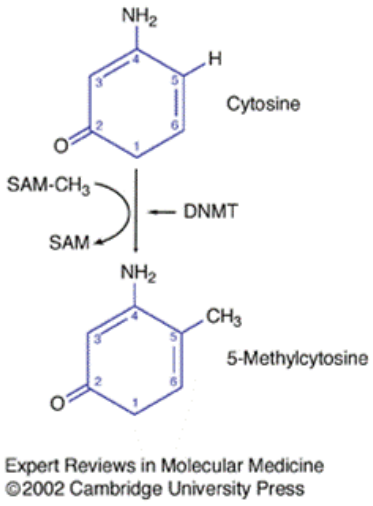

Figure 1.4. **Mechanism of DNA methylation.** 5-Methylcytosine is produced by the action of the DNA methyltransferases (DNMT 1, 3a or 3b), which catalyse the transfer of a methyl group (CH_3) from *S*-adenosylmethionine (SAM) to the 5-carbon position of cytosine.

1.3.3 DNA methylation in mammals

DNA methylation is the most stable epigenetic modification known to date. Cytosine methylation patterns are propagated through cell division and this involves the action of specific DNA methyltransferases (DNMT1) (Bird, 2002; Goll and Bestor, 2005). Methylation patterns are established during early mammalian development starting with the paternal genome undergoing active demethylation shortly after protamine-histone exchange in the male pro-nucleus. The maternal genome also undergoes demethylation probably through a passive DNA replication mechanism (Reik et al., 2001; Santos et al., 2002). Genome-wide methylation levels increase rapidly in the blastocyst by the action of the *de novo* DNA methyltransferases DNMT3A and DNMT3B (Bestor, 2000) which

ultimately lead in the formation of methylation patterns found in adult somatic cells. These physiological patterns of cytosine methylation can be disrupted to cause disease, the best-studied example being cancer, in which abnormal methylation is common and implicated in pathologic events such as silencing of tumour-suppressor genes (Robertson, 2005). In addition to DNMT1, DNMT3A and DNMT3B a fourth DNA methyltransferase, DNMT2, is known to date. DNMT2 has low methyltransferase activity *in vitro* and its absence has no discernable effect on DNA methylation levels (Bestor, 2000).

In mammalian somatic cells, DNA methylation occurs at the 5-carbon position of cytosine at CpG dinucleotide (5m-CpG) sites (figures 1.3a and 1.4). About 70% of CpGs are methylated (hypermethylated), amounting to about 1% of total DNA bases in the human genome (Ehrlich et al., 1982). In normal somatic cells, 5m-CpG sites predominantly occur in repetitive DNA elements, satellite DNAs, non-repetitive intergenic DNA and exons. Regions with high G+C and CpG content, termed CpG islands (Cross and Bird, 1995; Klose and Bird, 2006), have been considered to be mostly unmethylated. CpG islands cover about 0.7% of the human genome and contain 7% of the CpG sites. The unmethylated status of CpG islands, at least in the germ line, protects them from CpG depletion caused by spontaneous deamination of methylated cytosines. The mismatch repair system can accurately recognize and correct the deamination product of cytosine bases (uracil), but not the deamination product of methyl-cytosine (thymine). About 60% of human gene promoters are associated with CpG islands whereas there are about 8,500 autosomal non-promoter CpG islands within the human genome (Hubbard et al., 2007).

Recent studies indicate that a subset of promoter CpG islands are subjected to *de novo* methylation during normal development and tumourigenesis (Meissner et al., 2008), and this has been reported to be associated with repression of CpG island-promoters

(Eckhardt et al., 2006; Estecio et al., 2007; Jones and Baylin, 2002; Khulan et al., 2006; Rakyan, 2008; Weber et al., 2007). Concerning non-promoter CpG islands only 27% were found to be unmethylated compared to 67% of promoter CpG islands that are constitutively unmethylated (Rakyan et al., 2008). Correlation with expression data suggested that approximately half of the currently annotated non-promoter CpG islands are likely to have similar functions as promoter CpG islands (see below).

1.3.4 Function of DNA methylation

In mammals, DNA methylation plays a vital role in a diverse range of cellular functions, including tissue-specific gene expression, imprinting, X-chromosome inactivation, cell differentiation and the regulation of chromatin structure (Bird, 2002). It is also associated with many diseases including cancer and ageing (Robertson, 2005).

Mechanistically, a methylated cytosine (frequently referred as the fifth base) can be recognised by a number of regulatory proteins and alter the transcriptional potential of genomic regions. DNA methylation has been mainly implicated with transcriptional repression especially when it occurs within promoter regions or in close proximity to the transcription start sites (TSS) of genes (Bird, 2002). However, recent evidence suggest that it also facilitates transcription when it occurs downstream of promoter regions within gene bodies. Recent studies have shown a positive correlation between gene-body DNA methylation and gene expression (Eckhardt et al., 2006; Rakyan, 2008; Rakyan et al., 2004). This is consistent with data generated for the X-chromosome where hypomethylation at gene promoters and hypermethylation of gene bodies was associated with active transcription (Hellman and Chess, 2007). DNA methylation is also involved in the global maintenance of the genome, protection against mobile elements and inhibition of cryptic transcription. These will be discussed below.

i. *DNA methylation and gene expression silencing*

There are two basic models that underpin the relationship between DNA methylation of promoter regions and gene silencing (figure 1.5):

1. Direct model – DNA methylation represses transcription by directly blocking the recruitment of transcriptional activators to the cognate DNA sequence (Watt and Molloy, 1988).

2. Indirect model – additional factors, like the methyl binding domain (MBD) containing proteins, including MeCP2, MBD1 and MBD2, that bind to methylated DNA are required for the recruitment of transcription repression complexes (figure 1.5) (Ballestar et al., 2003; Ballestar and Wolffe, 2001).

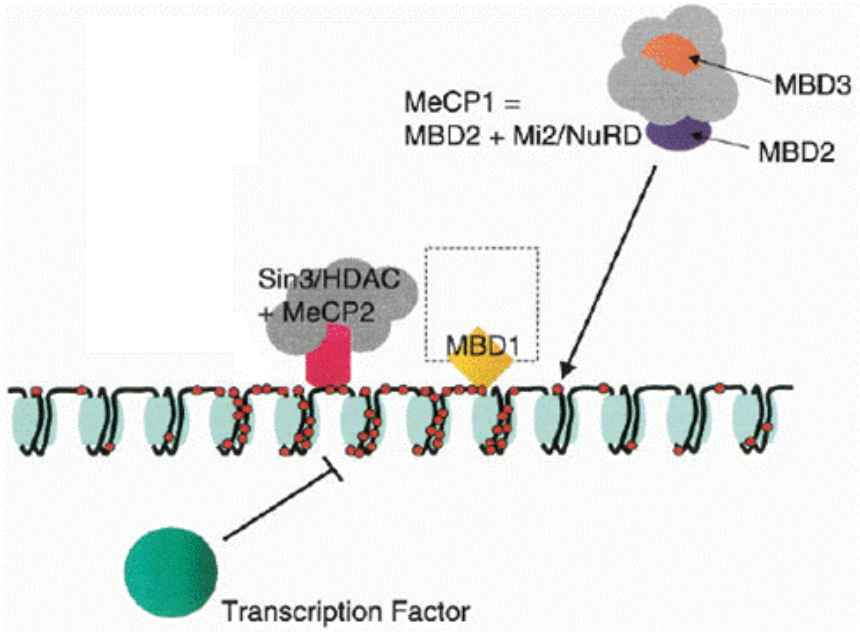

Figure 1.5. **Transcriptional repression by DNA methylation.** A stretch of nucleosomal DNA is shown with all CpGs methylated (red circles). Below the diagram is a transcription factor that is unable to bind its recognition site when it is methylated. The top of the diagram illustrates protein complexes that can be attracted by methylation, including the methyl-CpG binding protein MeCP2 (plus the Sin3A histone deacetylase complex), the MeCP1 complex comprising MBD2 plus the NuRD corepressor complex, and the uncharacterized MBD1 complex. MeCP2 and MBD1 are chromosome bound proteins, whereas MeCP1 may be less tightly bound (reviewed in (Bird, 2002). Figure was taken from Bird (Bird, 2002).

It is also worthy of mention that there are several lines of evidence supporting the notion that DNA methylation does not mediate silencing of active promoters but rather affects

genes with low transcriptional activity, suggesting that DNA methylation is a secondary event during the gene silencing process (Bird, 2002; Clark and Melki, 2002; Stirzaker et al., 2004; Turker, 2002). Examples of *de novo* methylation by DNMTs following gene inactivation include methylation of genes that are already silenced during X-inactivation, and hypermethylation of *GSTP1* CpG island promoter which is initiated by a combination of gene silencing and spreading of DNA methylation. This is consistent with a recent study looking for changes in methylation patterns upon differentiation proposing a "Use it or Lose it" model. According to this model, genes with low levels of transcriptional activity in a given cell type are likely to be locked in this state by DNA methylation (Meissner et al., 2008). This can be the result of changes in the balance of chromatin modifying enzymes (e.g. decreased H3K4 de-methylase activity) due to transcriptional silencing. It has been shown that DNA methylation is in inverse correlation with methylation of H3K4 (Meissner et al., 2008).

ii. *Inhibition of cryptic transcription initiation*

DNA methylation within coding regions has been confirmed by many recent studies (Eckhardt et al., 2006; Meissner et al., 2008; Rakyan et al., 2008; Rakyan et al., 2004; Weber et al., 2007). One potential role for intragenic methylation could be inhibition of cryptic transcription initiation outside gene promoters (Zilberman et al., 2007). It is possible that the transcription machinery itself disrupts chromatin structure and exposes cryptic initiation sites to be methylated (Carrozza et al., 2005).

iii. *Protection against mobile elements*

In mammalian genomes, most repetitive DNA sequences are found to be methylated (Rollins et al., 2006). Work in Dnmt1$^{-/-}$ mice supports the notion that methylation leads to silencing of repeats (Walsh et al., 1998), and hence to immobilization of mobile elements which is important to insure genomic integrity.

iv. Maintenance of genome stability

Several lines of evidence indicate that global hypomethylation can lead to increased genomic instability in mammalian cells. In human cell lines, deletion of DNMTs induces chromosomal abnormalities (Chen et al., 2007) and partial loss of DNMT3b is linked to the immunodeficiency (ICF) syndrome, which is characterised by chromosomal rearrangements in centromeric regions (Xu et al., 1999). Global hypomethylation in the gene bodies and repetitive elements is a well known characteristic of human cancer cells. This phenomenon has been linked to increased chromosomal instability and tumour progression (Eden et al., 2003), and it was also shown to precede copy number changes in gastrointestinal cancer (Suzuki et al., 2006).

1.3.5 DNA methylation inhibition assay

The correlation between loss and gain of DNA methylation, and activation and repression of transcription of the associated genes can be verified by the use of DNA methyltransferase inhibitors. One class of methylation inhibitors are nucleoside analogues which have a modified cytosine ring attached to either a ribose or deoxyribose moiety (Jones and Taylor, 1980) (figure 1.6a). These analogues can be metabolised into nucleotides, and hence incorporated into DNA and/or RNA (Li et al., 1970). Treatment of cultured cells with such analogues can lead to loss of DNMT activity, as the latter becomes irreversibly bound to the analogues, resulting in passive loss of DNA methylation (figure 1.6b). Two cytosine analogues, 5-Azacytidine (5-Aza-CR) and 5-Aza-2'-deoxycytidine (5-Aza-CdR) are commonly used in cell culture DNA methylation studies and they have been widely studied for cancer treatment (Christman, 2002; Yoo and Jones, 2006). Both 5-Aza-CR and 5-Aza-CdR were recently approved by the U.S. Food and Drug Administrator (FDA) (with the clinical names Vidaza and Decitabine respectively) for treatment of myelodysplastic syndrome, a preleukemic disease (Gal-Yam et al., 2008; Kaminskas et al., 2005; Kantarjian et al., 2007).

Cells cultured in the presence of 5-Aza-CdR incorporate it into DNA during DNA replication which leads into the formation of stable covalent complexes between the DNA molecule and DNMTs (Santi et al., 1983). The modification at the C5 position prevents the release of the enzyme (figure 1.6.c). This prevents further methylation of the genome and results to progeny cells with reduced DNA methylation.

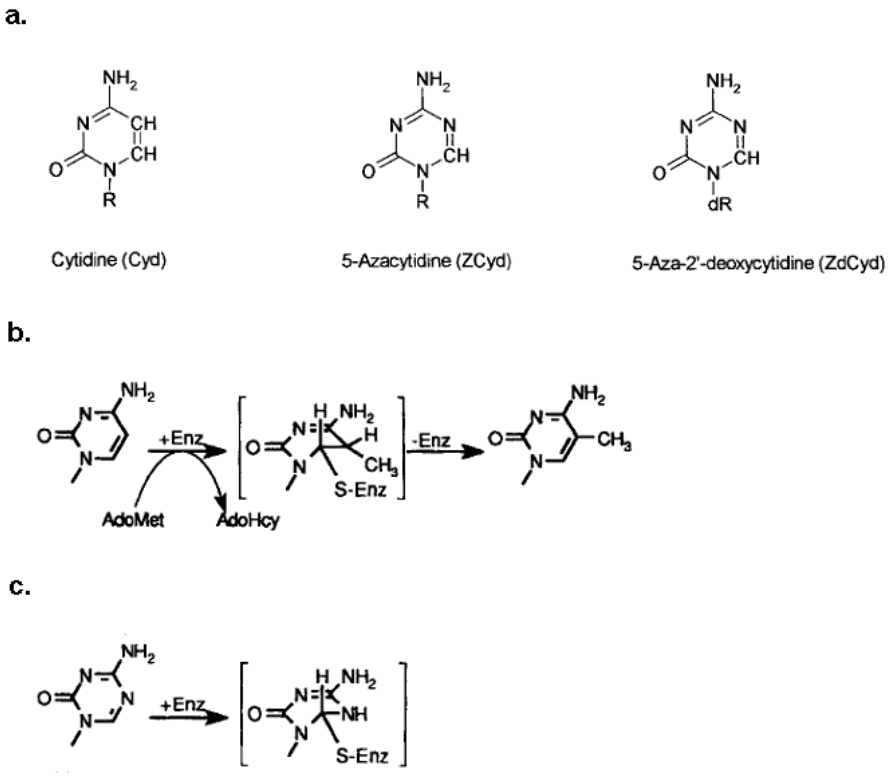

Figure 1.6. **DNA methylation inhibitors.** Cytidine analogues have a modified cytosine ring, preventing methylation. Part a. Structure of cytidine and its 5-aza analogues. R=ribose, dR=deoxyribose. Part b. Methylation of cytidine at the 5-carbon position. Part c. DNMTs bind irreversibly to cytidine analogues and block DNA methylation. Figure was taken from Christman (Christman, 2002).

1.3.6 Methodologies for detection of DNA methylation

Many methods of DNA methylation analysis have been developed over the years. DNA methylation detection approaches are based on one of three techniques: bisulphite conversion, digestion with methylation-sensitive restriction enzymes and affinity purification (reviewed in (Beck and Rakyan, 2008; Weber and Schubeler, 2007;

Zilberman and Henikoff, 2007). Bisulphite sequencing and the immunoprecipitation approach for capturing methylated DNA are introduced below and used extensively for the work described within this thesis.

1.3.6.1 Bisulphite Sequencing

The gold standard approach for methylation analysis is 'bisulphite sequencing'. Bisulphite sequencing involves treating DNA with sodium bisulphite to convert unmethylated cytosines to uracils (figure 1.7). Converted DNA is subjected to PCR amplification using primer sets corresponding to the regions of interest. Primers are specific for converted DNA and do not contain CpG sites. The last step involves conventional DNA sequencing; unmethylated cytosines will be read as thymine, while methylated cytosines will be read as cytosine (Frommer et al., 1992) (figure 1.7).

Typically in tissue samples, because they contain a mixture of different cells, methylation levels for a specific CpG site appear to be heterogeneous. Hence, it is necessary to quantify the proportion of methylated CpG sites under investigation after bisulphite sequencing. An algorithm called ESME was developed as part of the Human Epigenome Project (HEP) (see below) and was applied to estimate methylation levels from signal ratios of the corresponding sequence traces (Lewin et al., 2004). It has been demonstrated that this method can detect differences in methlyation rates of 20% highly accurately.

Recently bisulphite conversion has been adapted for large scale DNA methylation analysis. Meissner and colleagues have developed a bisulphite conversion-based method called reduced representation bisulphite sequencing (RRBS) (Meissner et al., 2005) which was successfully combined with next generation sequencing technology (Meissner et al., 2008). In a similar manner bisulphite converted DNA was subjected to deep sequencing using an Illumina Genetic Analyser (GA) for the analysis of the *A.*

thaliana methylome (methylC-seq) (Lister et al., 2008). Bisulphite conversion has also been combined with microarray platforms for large-scale methylation analysis (Adorjan et al., 2002; Gitan et al., 2002; Reinders et al., 2008).

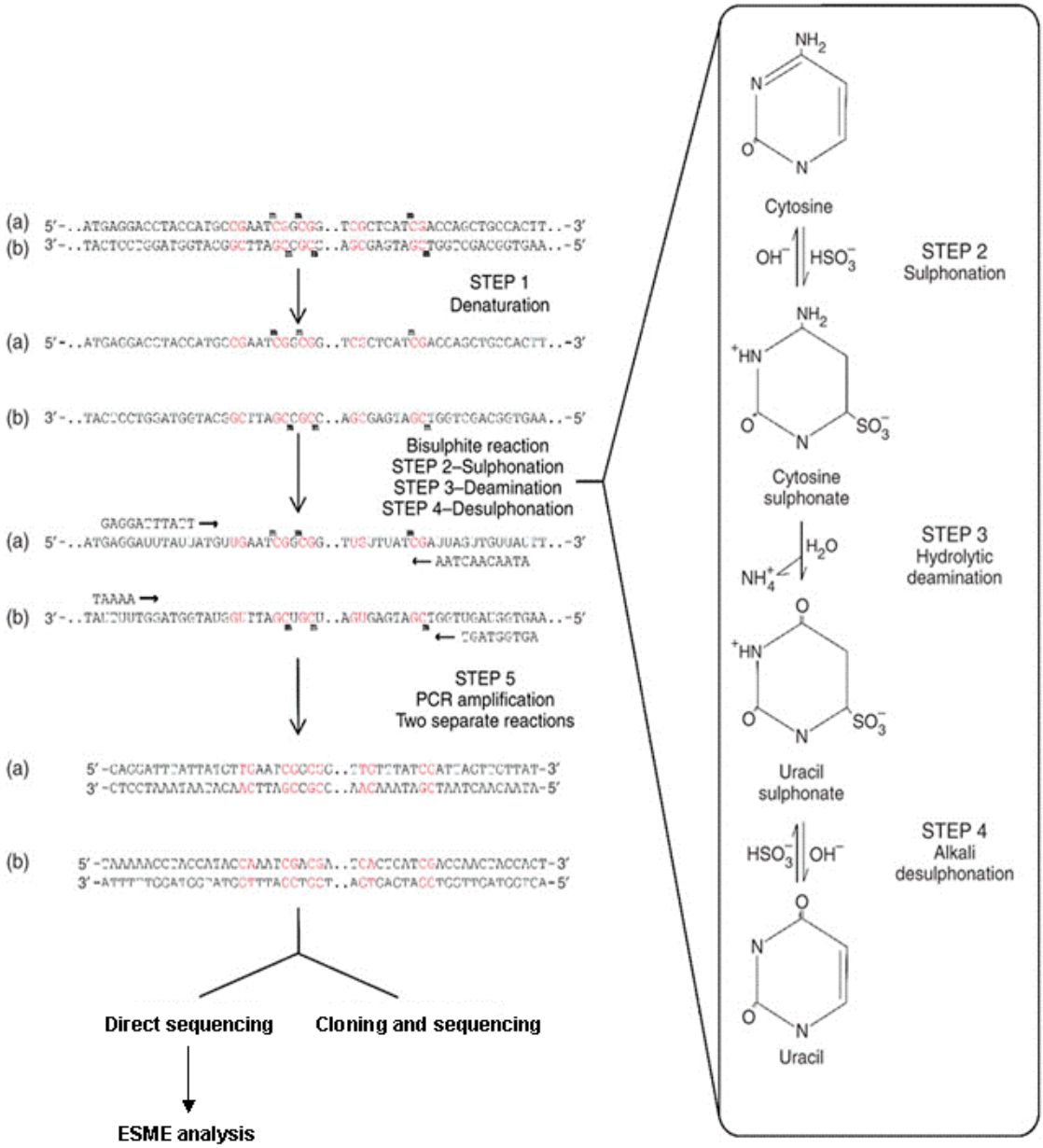

Figure 1.7. **Bisulphite conversion**. An example DNA sequence, 5' to 3' orientation, with the complementary plus (a) and minus (b) DNA strands is shown. The CpG sites are colored red and methylation of a CpG site is indicated by ^{m}CpG. After denaturation, the DNA is single stranded and each strand, a and b, can be amplified independently with strand-specific bisulphite-specific primers to determine

the methylation state of each strand. Example strand-specific and bisulphite-specific PCR primers are indicated above and below the DNA strands (in reality, primers are longer). In the forward primers, the cytosine bases are replaced by thymine bases and, in the reverse primers, the guanines (complementary base to cytosine) are replaced by adenine residues. Detailed design parameters of the bisulphite-specific PCR primers are given in section 2.2.3.1. After PCR amplification, methylation of the CpG sties in the target sequence can be determined by either direct PCR sequencing of the product or cloning and sequencing. Figure was taken (with some modifications) from Clark et al. (Clark et al., 2006).

1.3.6.2 Methylated DNA Immunoprecipitaton – MeDIP

Methylated DNA Immunoprecipitation (MeDIP) has been developed recently (Keshet et al., 2006; Weber et al., 2005) and since then has been used extensively especially for large-scale methylation studies (see below). In the MeDIP assay, a monoclonal antibody against methylated cytosines is used to enrich methylated DNA fragments. In brief, genomic DNA is fragmented to an average size between 300 and 600 bp and denatured to generate single-stranded DNA fragments. Methylated single-stranded DNA fragments are immunoprecipitated after incubation with an antibody that has affinity for the methyl group of methylated cytosines (figure 1.8).

The immunoprecipitated DNA can be used for the analysis of the methylation status of a particular genomic region by employing specific primers. However, the importance of this technique is underlined by the fact that MeDIP can be easily adapted for large-scale or even genome-wide methylation analysis studies (figure 1.8). MeDIP has already been combined with microarray technologies to generate methylation profiles in cancer and normal tissue samples (Illingworth et al., 2008; Keshet et al., 2006; Mohn et al., 2008; Rakyan et al., 2008; Weber et al., 2005; Weber et al., 2007; Zhang et al., 2008; Zhang et al., 2006; Zilberman et al., 2007). Recently MeDIP was combined with next-generation sequencing technology leading to the first mammalian methylome (Down et al., 2008). Human sperm DNA was used for this purpose. Such advances in methylation profiling are promising great potential for future studies of DNA methylation in humans.

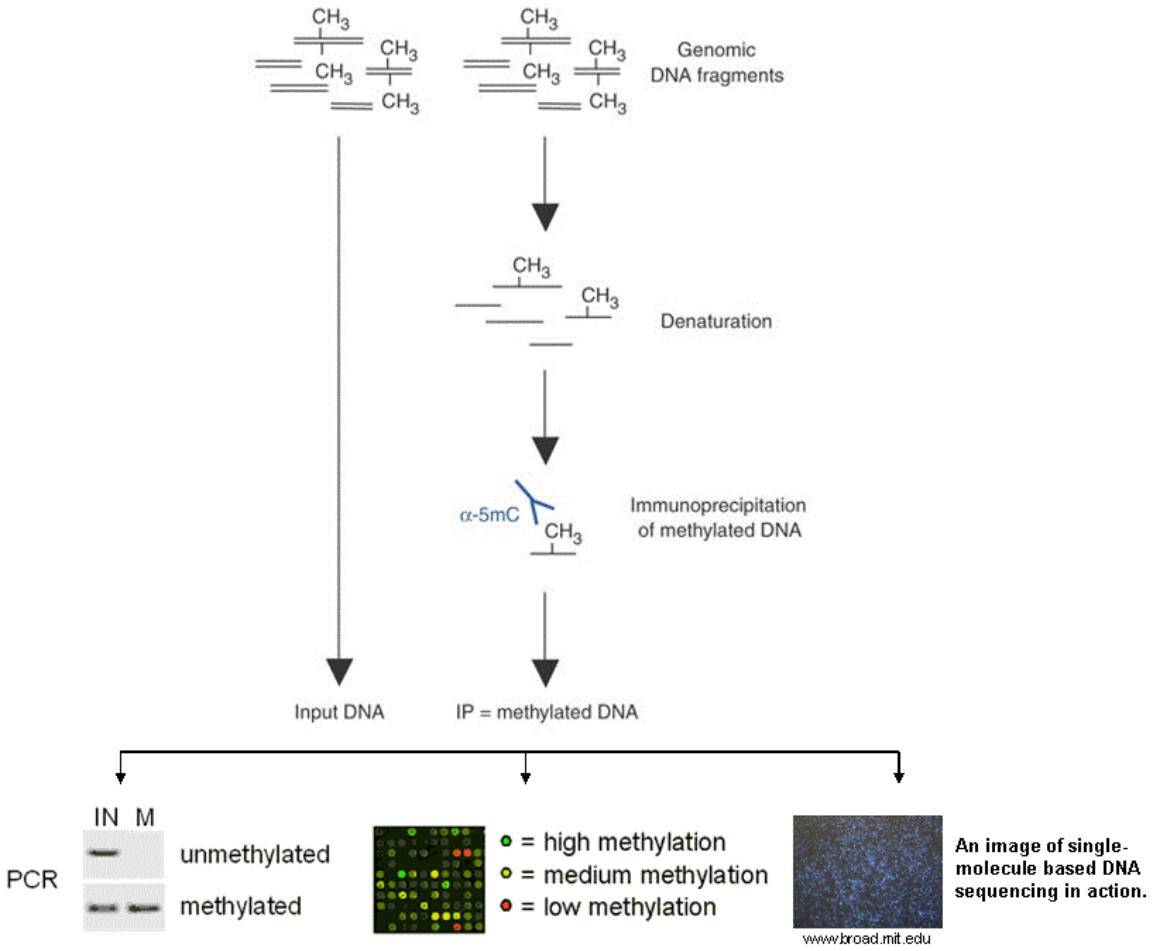

Figure 1.8. **Methylated DNA immunoprecipitation (MeDIP).** Denatured genomic DNA of desired fragment length (generated by restriction or sonication) is incubated with an antibody directed against 5-methyl-cytosine (a-5mC), and methylated DNA is isolated by immunoprecipitation. Enrichment of target sequences in the methylated fraction can be quantified by standard DNA detection methods such as PCR, by comparing input (IN) to MeDIP (M) DNA, microarrays (MeDIP-chip) or by next generation sequencing technology (MeDIP-seq). Figure was adapted from Weber et al (Weber et al., 2005).

1.3.7 Epigenetic variation in humans

The diversity of human phenotypes is the result of genetic and epigenetic variation and the interaction of these two biological variables with the environment (Hoffmann and Willi, 2008; Jaenisch and Bird, 2003). Although a number of studies have focused on studying genetic variation (Beckmann et al., 2007), the scale and significance of epigenetic variation has only begun to be elucidated (Rakyan and Beck, 2006).

The need to consider epigenetic alongside genetic variation in the context of complex diseases, has been highlighted by: (i). the finding of disease discordance in monozygotic twin studies (especially those living in the same environment) and (ii). the confirmation that epigenetic factors play a decisive role in the aetiology of many of human diseases (Robertson, 2005). To this effect the first systematic effort for cataloguing epigenetic variation was launched in 1999 (Beck et al., 1999). The resulting Human Epigenome Project (HEP) aimed to identify methylation variable positions (MVPs), which are akin to SNPs, promising to advance the understanding and diagnosis of human diseases. Following HEP, recent advances in epigenome mapping (Beck and Rakyan, 2008; Mendenhall and Bernstein, 2008) were beneficial in conducting large-scale comprehensive epigenetic studies looking for epigenetic variation. These studies are expected to have a high impact on our understanding, diagnosis and treatment of complex diseases in the next few years.

1.3.7.1 Differentially Methylated Regions - DMRs

The most frequent and stable form of epigenetic variation is differential DNA methylation. Alterations to the temporal or spatial patterns of DNA methylation which are indicative of local changes in genome functionality can lead to the formation of differentially methylated regions (DMRs). DMRs can vary in size from a few to hundreds or thousands of base pairs and, based on context, can be associated with: (i). specific tissues or cell types (tissue specific DMRs – tDMRs) and (ii). specific phenotypes or disease conditions (phenotype specific DMRs – pDMRs).

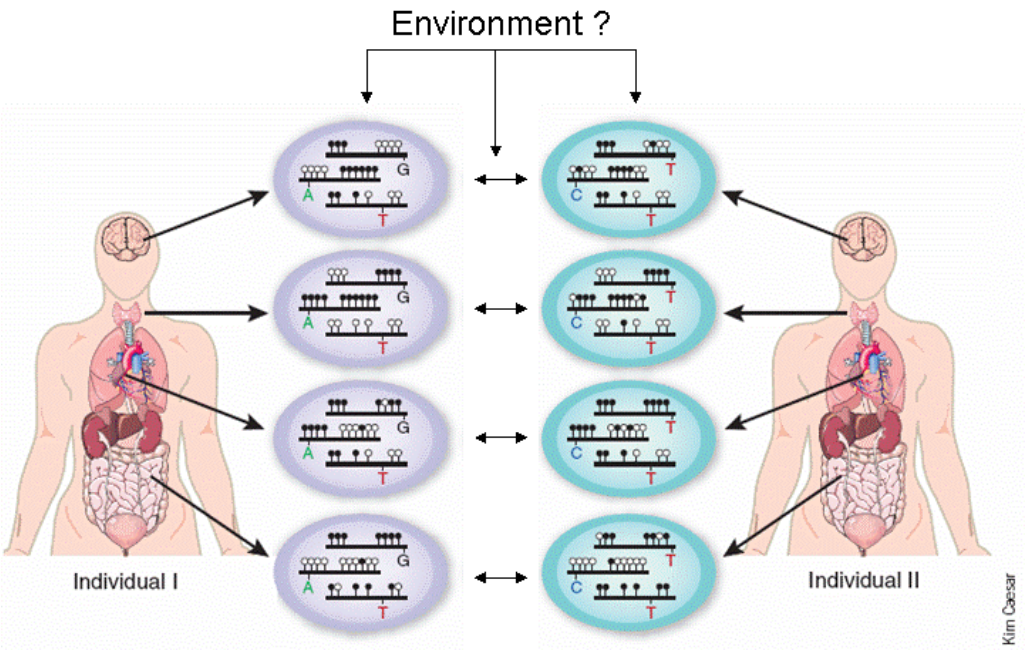

Figure 1.9. **DNA methylation heterogeneity among individuals and cell types**. Cell type–specific and tissue-specific DNA methylation are illustrated by organ-to-organ variations in the clusters of methylated CpGs within the same individual. Despite overall consistency in tissue-specific DNA methylation patterns, variations in these patterns exist among different individuals. Methylated CpGs are indicated by a filled circle and unmethylated CpGs by an open circle. SNPs are indicated by the corresponding base. The potential role of the environment in heterogeneous methylation patterns is also indicated. Figure was adapted from Brena et al. (Brena et al., 2006).

i. Tissue specific DMRs - tDMRs

tDMRs refer to methlyation differences between different cell types with otherwise identical genetic material (figure 1.9). Several large scale DNA methylation studies have started to catalogue such tissue-specific methylation differences (tDMRs) (Eckhardt et al., 2006; Illingworth et al., 2008; Rakyan et al., 2008; Rakyan et al., 2004; Shiota, 2004; Weber et al., 2007). Identification of tDMRs at a genome-wide scale will eventually lead to a better understanding of the role of DNA methylation in setting up and maintaining tissue-specific expression patterns. Comparison of tDMRs within gene loci and gene expression profiles suggested that tDMRs are involved in regulating tissue-specific gene expression. Interestingly, the majority of tDMRs were not within the 5'UTRs of genes but

rather in exons and introns of functionally diverse genes whereas a significant proportion of them found to overlap with evolutionary conserved, non-protein coding regions (ECRs). The latter supports the notion that tDMRs may have a functional role beyond the mere control of transcription via promoter methylation.

One interesting question arising from the existence of tDMRs is the mechanism by which they occur. Large-scale analysis using pluripotent cells suggest that they may arise at early stages of development processes. Comprehensive DNA methylation studies using ES and lineage committed cells (Bibikova et al., 2006; Farthing et al., 2008; Meissner et al., 2008; Mohn et al., 2008) will give insights into whether epigenetic marks in early development have a primary role in determining tissue-specific expression patterns and hence tissue-specific identities.

ii*. Phenotype specific DMRs – pDMRs*

pDMRs reflect epigenetic variation within cell types from the same origin between different individuals (figure 1.9). Based on the source of this variability inter-individual DMRs can be divided into two classes:

1. DMRs that are driven by genetic variation. Variation in DNA methylation levels can be affected by genetic variation directly by the introduction or removal of CpG sites, or indirectly by the introduction of sequences (e.g. repeat elements or transposons) (Lippman et al., 2004) that affect methylation in *cis*. It has been shown that in Beckwith-Wiedeman syndrome (BWS) patients, specific haplotypes within the IGF2 locus have been associated with loss of methylation (Murrell et al., 2004), supporting the notion that the genotype can act synergistically with the epigenotype. This led to the introduction of the term ‘hepitype’ which combines the contribution of a haplotype and an epitype to a given phenotype (Murrell et al., 2005). This concept was further supported by a recent study reporting allele-specific DNA methylation (ASM) at 16 SNP-tagged loci distributed across various chromosomes (Kerkel et al., 2008). The authors of this paper introduced

the term ‘epihaplotype’, which is akin to ‘hepitype’ (Murrell et al., 2005), to describe sequence-depended DNA methylation patterns. These findings can be useful for fine mapping and interpretation of non-coding RNAs and for their association with complex diseases.

2. DMRs that are generated by stochastic events independently of genetic variation. Such DMRs can arise due to errors during DNA replication. Stochastic events that lead to variation in DNA methylation patterns can occur in cell culture condition (*in vitro*) or *in vivo* during ageing. This is supported by a recent study reporting epigenetic differences between aging monozygotic twins (Fraga et al., 2005). However, as this study did not examine the same individuals serially over time, it is not clear if the methylation differences observed occurred over time or were present historically. A subsequent study found no age-related variation in DNA methylation, but again this study did not track the same individuals over time.(Eckhardt et al., 2006). Such DMRs can lead, in many cases, to cancer development (the single leading risk factor for cancer is age) and they may explain the adult onset of a number of complex, non-malignant diseases (Feinberg, 2004; Feinberg, 2008).

These stochastic events can be influenced by the environment. It has been reported that decreased grooming and nursing by rat mothers reduced DNA methylation at a glucocorticoid receptor gene promoter in the hippocampus of the offspring, resulting in increased stress response in later life (Weaver et al., 2004). This example demonstrates how environmental stimuli during childhood could affect phenotypic outcomes in later life through the epigenome. This might have great relevance to phenotypic differences observed between monozygotic twins growing up in different environments.

1.3.7.2 DMR identification goes global in the human genome

The first large scale study for DMR identification was launched in 1999 by Stephan Beck and colleagues (Beck et al., 1999). The Human Epigenome Project (HEP) aimed to generate methylation data for selected regions of the human genome in both normal and disease tissues by bisulphite sequencing (see above) using locus specific PCR primers. HEP has generated DNA methylation profiles for three human chromosomes (6, 20 and 22) in 12 different tissues revealing novel insights in tissue specificity of DNA methylation patterns (Eckhardt et al., 2006; Rakyan et al., 2004).

Since then, and as DMRs and epigenetic variability in general have been recognised as an important factor in determining genome functionality, other large-scale efforts have emerged aiming for systematic mapping of the human epigenome. Both bisulphite sequencing and MeDIP-technology (see above) have been adapted to be used with microarray and next-generation sequencing platforms. Application of MeDIP together with illumina GA platform led to the first human methylome (Down et al., 2008). Figure 1.10 summarises major landmarks form the launch of the HEP (1999) to the first human methylome (2008).

It is now clear that global DNA methylation profiling has come of age. Continuous efforts in comprehensive cataloguing of DMRs in multiple tissues and cell types as well as during differentiation and phenotype development will provide a broad basis for future studies aiming to understand how the (epi)genome functions in health and disease.

.

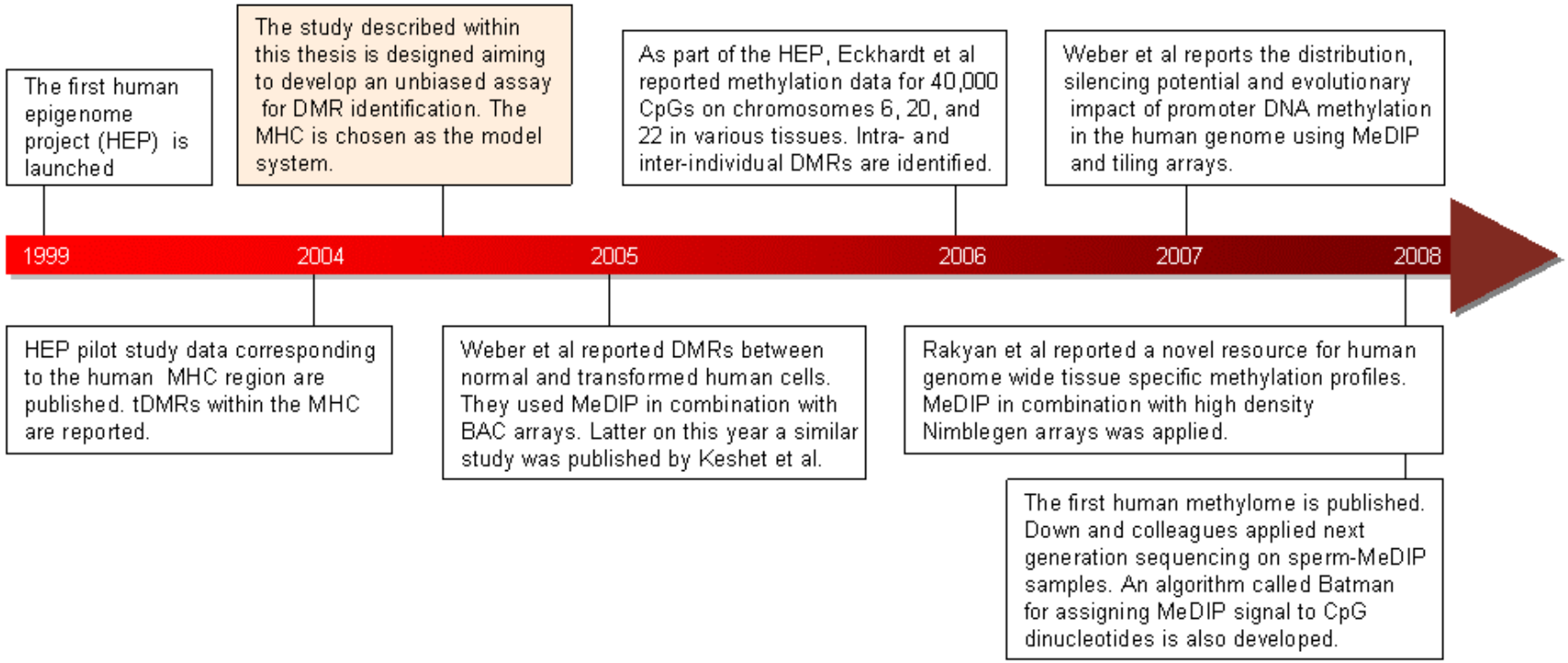

Figure 1.10. **Selected landmarks in large-scale DNA methylation studies and DMR identification in the human genome.**

1.4 Rationale of my thesis

The aim of this project was to identify and characterise differentially methylated regions (DMRs) that can contribute to phenotypic plasticity. This study was designed in April 2005. At that time the HEP pilot study had been published, reporting the existence of DMRs within the MHC region and Weber and colleagues had at this time developed MeDIP. MeDIP was used in combination with BAC arrays (100 kb resolution) for methylation profiling and, more specifically, for the identification of DMRs between normal and cancer samples (figure 1.10) (Weber et al., 2005).

In this context, I chose to use the MHC as a model system and develop a higher resolution array-based assay for the unbiased identification of DMRs. The assay involved MeDIP in combination with an MHC tiling array covering the whole MHC at 2kb resolution (chapter 3). This assay was used to perform two screens: (1). tDMR screen, looking for DMRs associated with specific tissues (chapter 4) aiming to give insights in the role of DNA methylation in tissue specific gene expression, and (2). pDMR screen, looking for DMRs associated with a particular phenotype (chapter 5) and aiming to elucidate the role of epigenetic variation in complex diseases. The phenotype I tested is the MHC class I down-regulation (MHC class I^- phenotype).

Both screens were successful, verifying further the implication of DMRs, and of epigenetic variation, in the regulation of MHC loci and hence in MHC-linked phenotypic plasticity.

In addition, I performed DNA methylation and gene expression analysis of genes that may be implicated in the MHC class I^- phenotype and are encoded outside the MHC region (chapter 6). The findings of this analysis verify further the complexity of MHC-linked phenotypes.

Finally I discuss and summarise my findings (chapter 7) and discuss future directions for studies to elucidate complex diseases associated with the MHC region.

In summary the work described within this thesis supports the notion that epigenetic variation plays a decisive role in the development of normal and aberrant phenotypes and hence it should necessarily be considered, together with genetic variation, as an important factor when studying complex diseases.

Chapter 2

Materials & Methods

2.1 Materials

2.1.1 Reagents (listed in alphabetical order)

Antibodies

5-methylcytidine, purified (Eurogentec)

Chemicals

All chemicals used for this thesis were purchased from Sigma.

Enzymes

AmpliTaq Gold Polymerase (Applied Biosystems)

EcoRI (New England Biolabs)

Proteinase K (Roche)

Ribonuclease A (Sigma)

T4 DNA ligase (New England Biolabs)

T4 DNA polymerase (New England Biolabs)

Fluorophores

Cyanine 3-dCTP (Perkin Elmer)

Cyanine 5-dCTP (Perkin Elmer)

Primer Pairs

All primers were purchased from Sigma. List and sequences of primer pairs are provided in Appendix table 2.1. The table section numbers are referenced in the relevant sections of this thesis.

Other Reagents

Big Dye (Applied Biosystems)

dNTP set - 100mM each (GE Healthcare)

Dynalbeads M-280 Sheep-anti mouse IgG (DynalBiotech)

Human Cot1 DNA (Invitrogen)

Human Genomic DNA (Roche)

SYBR Green MasterMix Plus (Eurogentec)

Yeast tRNA (Invitrogen)

2.1.2 Commercial kits

BD Advantage–GC Genomic PCR BD (Biosciences)

DNeasy Tissue Kit (QIAGEN)

Expand Kit (Roche Diagnostics)

EZ-meth Kit (Genetix)

PCR purification Kit (QIAGEN)

RNeasy Mini Kit (QIAGEN)

TOPO TA cloning kit (Invitrogen)

Transcriptor First Strand cDNA synthesis Kit (Roche)

Zymo DNA clean up concentrator-5 (Genetix)

2.1.3 Solutions & Buffers (listed in alphabetical order)

Note: HPLC water was used to prepare solutions & buffers

10mM dNTP	10mM each dNTP (dCTP, dATP, dGTP, dTTP)
(mix for PCR)	
10 x dNTP	0.5mM dCTP
(mix for DNA labelling)	2mM each of dGTP, dTTP and dATP
2 x IP buffer	20mM sodium phosphate (pH 7.0)
	280mM NaCl
	0.1% Triton X-100
EcoRI buffer	New England Biolabs
GTE buffer	20% Glucose
	1M Tris-HCl, pH 8.0

	0.1M EDTA
Hybridization buffer	2 x SSC
	50% deionised formamide
	10 mM Tris-Cl (pH 7.4)
	5% dextran sulphate
	0.1% Tween-20
Proteinase K buffer	10mM Tris-Cl (pH 7.8)
	5mM EDTA
	0.5% SDS
Wash solution 1	2 x SSC
	0.03% SDS
Wash solution 2	0.2 x SSC
Wash solution 3	1 x PBS
	0.05% Tween 20 (Sigma)
Precipitation Mix	100ml 96% ethanol
	200μl 3M sodium acetate
	400μl 0.1mM EDTA

Sequencing Reaction Buffer (x4)

0.32M Tris Base pH 9.0

0.006M $MgCl_2$

9.9% Tetramethylene Sulfone (Sigma)

0.18% Tween-20 (Sigma)

5.9% glycerol

1.0% formamide

1x Restriction Enzyme Buffer 2 New England Biolabs

50 mM NaCl

10 mM Tris-HCl

10 mM $MgCl_2$

1 mM Dithiothreitol

pH 7.9 at 25°C

25mM $MgCl_2$ Applied Biosystems

10 x PCR Gold buffer Applied Biosystems

100 x BSA New England Biolabs

Phosphate Buffer Saline (PBS) pH 7.4

137mM NaCl

2.7mM KCl

10mM Na_2HPO_4

2mM KH_2PO_4

10 x Tris-borate EDTA electrophoresis buffer (TBE) pH 8.3

0.9M Tris-borate

20mM EDTA

10 x TE (Tris-EDTA) buffer pH: 8.0

100mM Tris-Cl

10mM EDTA

LB medium

10 mg/ml Bacto-tryptone

5 mg/ml yeast extract

10 mg/ml NaCl

pH 7.4

LB plates LB medium

15 g/l agar

75 μg/ml Ampicillin

2.1.4 DNA used for tDMR screen – chapter 4

Human DNA samples from healthy individuals were obtained from AMS Biotechnology (Oxon, UK), Analytical Biological Services (Wilmington DE, USA) and from the MHC Haplotype Project (Turner et al., 2008). Samples included DNA extracted from two tissues (liver and placenta) and two cell types ($CD8^+$ lymphocytes and sperm). Additional information on those samples is summarized in Table 2.1.

Donor Information						
Index	**Tissue**	**Replicate**	**Age (yrs)**	**Sex**	**Ethnicity**	**Supplier**
1	Liver	1	37	M	Caucasian	ABS, Wilmington, DE, USA
2	Liver	2	29	M	Caucasian	BCI, Haywatd, CA, USA
3	Placenta	1	29 (mother)	F	Caucasian	ABS, Wilmington, DE, USA
4	Placenta	2	31 (mother)	F	Caucasian	ABS, Wilmington, DE, USA
5	Sperm	1	20-49	M	Caucasian	MHC Haplotype Project (Turner et al., 2008)
6	Sperm	2	20-49	M	Caucasian	MHC Haplotype Project (Turner et al., 2008)
7	T-cells $CD8^+$	1	41	M	Caucasian	ABS, Wilmington, DE, USA
8	T-cells $CD8^+$	2	27	F	African American	ABS, Wilmington, DE, USA

Table 2.1. **Tissues and cell types used in this study.**
ABS: Analytical Biological Services
BCI: BioChain Institute

2.1.5 Cell Lines used for pDMR screen – chapter 5

Cancer cell lines K562, MCF7, 578T, H69, CCRF-CEM, Colo-205, MDA-MB-231, MDA-MB-361 and T47D were provided by the Cancer Genome Project (Wellcome Trust Sanger Institute). The EBV-transformed B-lymphoblastoid cell lines GM10851 and GM15510 were provided by Nigel Carter (The Wellcome Trust Sanger Institute).

2.1.6 Cell Culture Media and Reagents

Cell Culture Media

All media listed in table 2.2 apart from Iscoves Modified DM were purchased from Invitrogen. Iscoves Modified DM was purchased from LGC Promochem.

Cell Culture Reagents

Insulin solution from bovine pancreas (Sigma-Aldrich)

5-aza-2'-deoxycytidine (Sigma-Aldrich)

Foetal Bovine Serum - FBS (Invitrogen)

Penicillin/Streptomycin (Invitrogen)

Dimethyl Sulphoxide - DMSO (Sigma-Aldrich)

Non-essential amino acids (Invitrogen)

D-(+)-Glucose Solution (Sigma-Aldrich)

Sodium biocarbonate (Sigma-Aldrich)

Trypsin/EDTA solution (Invitrogen)

2.1.7 Bacterial Clones

Recombinant pUC plasmid clones were used for the construction of the MHC array (section 2.2.7). These clones were generated at the Wellcome Trust Sanger Institute as part of the HapMap project (The International HapMap Project, 2003). In total 1662 clones were selected. These clones cover the entire MHC (approximately 4Mb). Clones corresponding to gaps and controls were generated as described in section 2.2.7.2. Clone names and genome coordinates of their respective inserts can be found in appendix table 2.2.

2.1.8 Key World Wide Web addresses

Website	Address
Ensembl	http://www.ensembl.org/index.html
GNF - Atlas of Gene Expression	http://expression.gnf.org/cgi-bin/index.cgi
HUGO gene nomencalture	http://www.genenames.org/index.html
Primer3	http://frodo.wi.mit.edu/cgi-bin/primer3/primer3_www.cgi
Reverse Complement	http://www.bioinformatics.org/sms/rev_comp.html
The Wellcome Trust Sanger Institute	http://www.sanger.ac.uk
UCSC genome browser	http://genome.ucsc.edu/
Vega	http://vega.sanger.ac.uk/index.html
zPicture	http://zpicture.dcode.org/

2.2 Methods

2.2.1 Tissue Culture

2.2.1.1 Culturing of Cell Lines

All cell lines were cultured in media with 10% foetal bovine serum and 1% penicillin-streptomycin solution. Table 2.2 provides the information about the media and supplements used for each cell line. All cell lines had the media changed every two days.

Cell Lines	Media	Supplements	Growth Properties
K562	Iscove's Modified DM		suspension
MCF7	Eagle's MEM	0.01mg/ml bovine insulin 0.1 x non essential amino acids	adherent
T47D	RPMI-1640	0.01mg/ml bovine insulin 2mM L-glutamine 1.5 g/L sodium bicarbonate 4.5 g/L glucose 10 mM HEPES 1.0 mM sodium puruvate	adherent
578T	DMEM	0.01mg/ml bovine insulin	adherent
Colo 205	RPMI-1640		mixed
CCRF-CEM	RPMI-1640	2mM L-glutamine 1.5 g/L sodium bicarbonate 4.5 g/L glucose 10 mM HEPES 1.0 mM sodium puruvate	suspension
MDA-MB-231	Leibovitz's L-15		adherent
MDA-MB-361	Leibovitz's L-15		loosely adherent
H69	RPMI-1640	2mM L-glutamine	suspension
GM10851	RPMI-1640	10 mM HEPES	suspension
GM15510	RPMI-1640	10 mM HEPES	suspension

Table 2.2 **List of all cell lines used.** Note: All cell lines were grown under 5% CO_2 at 37°C in flasks with vented caps (Corning). Only exceptions were MDA-MB-231 and MDA-MB-361 which were cultured in 100% air and in flasks with plug seal caps (Corning).

Once cell growth was confluent, the following steps were taken:

Adherent Cell Lines

1. Culture medium was removed using sterile 2ml aspirating pipette attached to vacuum trap.

2. Monolayer of cells was washed with PBS

3. Cells were trypsinised using trypsin/EDTA solution. Flask was placed in 37°C incubator for 5 min. Equal volume of 10% FBS medium was added to inactivate trypsin.

4. Cells were transferred into 50 ml Falcon tubes and harvested at 1700 rpm for 5 min.

5. Cell pellet was washed once with PBS.

6. Cells were counted with a haemocytometer with a 0.1 mm sample depth under a light microscope (Olympus).

7. Cell pellet was suspended in medium and moved to a bigger flask, split into more flasks, cryo-preserved or used for DNA/RNA extractions as described later in this chapter.

Suspension Cell Lines

A similar procedure, as for adherent cell lines, was followed but excluding steps 2 and 3.

2.2.1.2 Cell cryo-preservation

Cell pellet was resuspended to 10^6 – 10^7 cells/ml in 10% (v/v) DMSO in 10% FCS culture medium, and transferred into polypropylene cryo-tubes. Cryo-tubes were placed in a freezing vessel primed with 250 ml Isopropanol and stored at -70°C overnight. Finally cryo-tubes were transferred to the gas phase of a liquid nitrogen vessel (-180°C) for permanent storage.

2.2.1.3 5-Aza-2'-Deoxycytidine Treatment

Cell lines MCF7 and 578T were treated with 5-aza-2'-deoxycytidine as described below. 5-aza-2'-deoxycytidine was always added fresh to the media.

MCF7 cells

1 x 10^5 MCF7 cells were plated into a 100mm dish (Corning) and, 24h later (day 1), they were treated with 0, 0.8, 2.4, 4.8 and 9.6 μM 5-aza-2'-deoxycytidine (Sigma-Aldrich). The culture was then replenished with fresh drug-containing medium every 48h. DNA and RNA were isolated from the drug treated culture on day 6 as described in sections 2.2.1.4 and 2.2.1.5

578T cells

4 x 10^5 MCF7 cells were plated into a 100mm dish (Corning) and, 24h later (day 1), they were treated with 0, 4 and 8 μM 5-aza-2'-deoxycytidine (Sigma-Aldrich). The culture was then replenished with fresh drug-containing medium every 48h. DNA and RNA were isolated from the drug treated culture on day 6 as described in sections 2.2.1.4 and 2.2.1.5

2.2.1.4 DNA extraction and manipulation

Total genomic DNA was extracted from all cell lines listed in table 2.2. DNA extraction was performed using the DNeasy Tissue Kit in accordance with the manufacturer's protocol. Approximately 5x10^6 cells were used for each DNA extraction. The concentration of the DNA was determined using a Nanodrop (using 1 OD_{260}=50μg ds DNA).

The integrity of DNA was confirmed by visualization on 1.5% agarose gels using ethidium bromide staining.

2.2.1.5 RNA manipulation

All reagents for RNA work were prepared with Diethylene Pyrocarbonate (DEPC) treated water. Bench surfaces and lab ware were cleaned before use with RNAseZap (Ambion).

2.2.1.5.1 RNA extraction

Total RNA was prepared from all cell lines listed in table 2.2 using the RNeasy Mini kit in accordance with the manufacturer's protocol. RNA was eluted with 35 μl of DECP-treated water.

The integrity of the RNA was confirmed by visualization on 1.5% agarose gels using ethidium bromide staining. The concentration of RNA was determined by using a Nanodrop (using 1 OD_{260}= 40μg RNA). A_{260}/A_{280} ratios were also calculated for each sample. Samples with ratios smaller than 1.7 or greater than 2.1 were discarded.

2.2.1.5.2 cDNA synthesis

cDNA was synthesised from total RNA (1μg) using Transcriptor First Strand cDNA synthesis Kit. Anchored-oligo$(dT)_{18}$ primers were used to prime the cDNA synthesis. The synthesis was completed in accordance with the manufacturer's instructions. The resulting cDNA was diluted to 10ng/μl and was stored at -20°C.

2.2.2 Methylated DNA Immunoprecipitation (MeDIP)

MeDIP was done essentially as described before (Keshet et al., 2006; Weber et al., 2005) with some modifications as described below.

2.2.2.1 Sonication of genomic DNA

10μg of genomic DNA resuspended in 100μl of water, was randomly sheared to fragments of 300 to 1000 bp using a Virtis sonicator on full power. DNA was sonicated twice for 75 sec with 1 min incubation on ice in between.

The size of fragments was confirmed by visualization on 1.5% agarose gels stained with ethidium bromide (section 3.3.1).

2.2.2.2 Immunoprecipitation - pDMR screen (chapter 5).

1. 4 µg of sheared genomic DNA resuspended in 240 µl of water were denatured for 10 min at 95-100°C and then placed on ice for 5 min.

2. 250 µl of 2 X IP buffer and 10 µl of 5MeC-mAb (10µg) were added to the DNA sample and incubated at 4ºC with slow rotation for 2 hours.

3. 30 µl of Dynabeads were washed twice with 700 µl of 1 X IP buffer.

4. Dynabeads were magnetically captured using a magnetic rack.

5. DNA-5MeC-Ab sample was added to the pre-washed beads and incubated at 4°C with slow rotation for two hours.

6. Dynabeads were magnetically captured and washed three times with 700µl of 1 x IP buffer.

7. Dynabeads were resuspended in 200 µl of Proteinase K buffer and 2 µl of proteinase K was added to the solution.

8. Solution was incubated at 50°C for 2 hours with rotation in a hybridization oven.

9. Dynabeads were magnetically captured and sample was removed using a P200 gilson pipette.

10. 700 µl of binding buffer (Zymo kit) was added to the sample.

11. Sample was applied to a filter column (Zymo kit) and centrifuged for 10 sec at maximum speed.

12. Filter columns were washed twice with wash buffer (Zymo kit)

13. Immunoprecipitated DNA was eluted twice with 15 µl water (1 min incubation at room temperature prior to centrifugation).

14. The DNA concentration was determined with a NanoDrop (using 1 OD_{260} = 33µg ssDNA)

2.2.2.3 Immunoprecipitation - tDMR screen (chapter 4).

For this screen (due to restricted DNA availability) MeDIP and input DNA was amplified by ligation-mediated PCR (LM-PCR) (Oberley et al., 2004) following the procedure below:

1. 2.5 μg sheared DNA was incubated with 1 X buffer 2, 10 X BSA, 1.2μl dNTP mix (10mM each), 3 Units of T4 DNA polymerase and distilled water to a final volume of 120μl for 20 minutes at 12°C.

2. The reaction was cleaned up using a Zymo-5 kit according to the manufacturer's instructions but the final elution was done in 30μl of TE buffer pH 8.5.

3. The adaptors JW102 (5'-gcggtgacccgggagatctgaattc–3') and JW103 (5'-gaattcagatc-3') were ligated to the cleaned-up DNA by incubation overnight at 16ºC in a reaction containing 40 μl adaptor mix (50μM each), 6 μl T4 DNA ligase 10 X buffer, 5 μl T4 DNA ligase (400U/μl) and distilled water to a final volume of 100μl.

4. DNA was cleaned up as described above.

5. To fill in the overhangs, the sample DNA was incubated at 72ºC for 10 min with 1μl dNTP mix (10mM each), 5μl 10 X AmpliTaq Gold PCR buffer, 3μl $MgCl_2$ (25mM), 5U AmpliTaq Polymerase and distilled water to a final volume of 50μl.

6. DNA was cleaned up as described above.

7. 50 ng of the ligated DNA sample was set aside as the input fraction.

8. 1.2 μg of the ligated DNA sample was denatured for 10 min at 100°C and then placed on ice for 5 min.

9. Immunoprecipitation was performed in 1 X IP buffer and 3 μl of 5-MeC-mAb with incubation at 4ºC with slow rotation for 2 hours.

10. 10 μl Dynabeads (6.7 x 10^8 beads/ml) were washed in 1 X IP buffer according to the manufacturer's instructions and, added to the DNA-antibody mixture and then incubated at 4ºC with slow rotation for 2 hours.

11. The Dynabead-Ab-DNA mixture was washed three times with 500 µl IP buffer and finally resuspended in 100 µl of Proteinase K buffer.

12. 1µl of proteinase K (50 U/ml) was added and incubated at 50ºC for 2 hours with rotation.

13. The sample was cleaned up using a Zymo kit-5 (using 700 µl binding buffer).

14. The DNA concentration was determined with a NanoDrop (using 1 OD_{260} = 33µg ssDNA) and diluted to 1 ng/µl.

15. Two separate LM-PCRs were performed for IP and input fraction respectively. LM-PCR was performed in a final volume of 50µl containing 10 µl distilled water, 10 µl Advantage-GC buffer, 10 µl GC- melt, 3.1 µl 25 mM $Mg(OAc)_2$, 5 µl JW-102 primer (10 µM), 1.4 µl dNTPs, 1 µl Advantage-GC polymerase and 10 µl DNA (1ng/µl). Reaction conditions were as follows: 1 cycle at 95ºC for 2 min for initial denaturation, 20 cycles at 94ºC for 30 sec, 68ºC for 3 min and 1 cycle at 68ºC for 10 min.

16. After LM-PCR, the reactions were cleaned up using a QIAquick PCR Purification kit and eluted with 50µl of water (pre-heated to 50ºC).

2.2.3 Bisulphite Sequencing

2.2.3.1 Primer Design

1. Primers were designed to complement bisulphite treated DNA

2. Primers were designed using primer 3 (Rozen and Skaletsky, 2000)

3. Primers were designed to be 22 bp long (where possible), to have about 30-40% GC content and a melting temperature around 58°C. All primers were designed to contain at least two C to U transitions as a marker of successful bisulphite treatment and to exclude CpG sites, where methylation can vary. Primer sets were further designed to yield amplicons of 300 to 400 bp in size.

The complete list of all primer pair sequences is provided in appendix table 2.1.

2.2.3.2 Bisulphite treatment

Genomic DNA (500 ng) was subjected to sodium bisulphite conversion using the EZ DNA methylation Kit according to the manufacturer's instructions. Elution step was performed with 20 μl elution buffer. The basis of bisulphite treatment is described in chapter 1 (section 1.3.6.1).

2.2.3.3 PCR amplification of bisulphite treated DNA

20 ng of bisulphite converted DNA was used for each PCR. Reactions (25 μl) were set up in 96-well plates (Applied Biosystems) and contained 17.5 μl water, 1 x AmpliTaq Gold buffer, 2 μl primer mix (10 mM each), 2mM $MgCl_2$, 0.5 μl dNTP mix (10 mM each) and 1U of AmpliTaq Gold. The thermal cycling conditions were as follows:

i. 95°C for 5 min

ii. 94°C for 30 sec

iii. 57°C for 1 min

iv. 72°C for 1 min

v. steps ii to iv were repeated 40 times

vi. 72°C for 5 min

PCR products were confirmed by visualization on 1.5% agarose gels using ethidium bromide staining. PCR products were cleaned up using Millipore PCR filter plates as follows. After adding 40 μl of water to the PCR reactions, they were loaded into the filter plate. Plate was placed on a vacuum manifold (10 mmHg for 12 min). Subsequently, 25 μl of water were loaded on the filter plate. After vortexing the plate for 10 min, purified PCR products were retrieved by aspiration.

2.2.3.4 Sequencing

Cleaned PCR fragments were sequenced from both ends using the dideoxy chain terminator method (Sanger et al., 1977), with V3.1 Bigdye terminator chemistry. Sequencing reactions (10 μl) were set up in 96 well plates and contained 0.5 μl Big Dye, 2 μl sequencing reaction buffer, 3 μl primer (3μM), 4μl of cleaned PCR product (section 2.2.3.3) and 2.5 μl water. Thermal cycling conditions were as follows: 1min at 96°C and 45 cycles at 96°C for 10 sec; 50°C for 10 sec; 60°C for 2 min.

Sequencing clean up was performed as follows:

1. 10μl water was added to the samples (total 20 μl).
2. 50 μl of precipitation mix was added, plate was sealed and agitated briefly
3. Plate was centrifuged at 4000 rpm for 20 min at 4°C.
4. Supernatant was tipped off and plate was drained by placing it upside down on tissue paper.
5. 100 μl of chilled 70% ethanol was added to each well.
6. Plate was centrifuged at 4000 rpm for 3 min at 4°C.
7. Steps 4-6 were repeated.
8. Plate was centrifuged upside down on a tissue at 250 rpm for 1 min.
9. Plate was left unsealed in the dark for an hour to evaporate any residual ethanol.
10. Plate was given to the Wellcome Trust Sanger Institute sequencing facilities. Sequencing reactions were analyzed on 3730 ABI sequencing machines (Applied Biosystems, USA).

2.2.3.5 ESME analysis

Quantitative methylation rates were estimated from bisulphite sequence traces using the ESME software (Lewin et al., 2004). ESME estimates, at any given CpG site, the average methylation level from all the copies of DNA amplicons generated during PCR and is therefore, compared to sub-cloning, a more accurate representation of

methylation levels. ESME calculates quantitative methylation values from signal proportions represented by different dyes in four-dye sequence trace files after correcting for imbalanced and over-scaled signals, incomplete bisulphite conversion, quality problems and base-call artefacts. ESME is useful for estimating methylation levels in samples with heterogeneous methylation levels (e.g. human tissues) and it has been used extensively by the HEP (see also section 1.3.6.1) (Eckhardt et al., 2006; Rakyan et al., 2004).

2.2.4 Quantitative real-time PCR

2.2.4.1 Primer Design

Primer pairs for all qRT-PCR assays were designed with Primer 3. The amplicons generated by these primers were 100 to 200 bp long. Primer pairs used for expression studies were designed for regions across intron-exon boundaries to avoid false positives arising from amplification of contaminating genomic DNA. The complete list of primer sequences is provided in appendix table 2.1.

2.2.4.2 qRT-PCR amplification

qRT-PCR was performed using an ABI Prism 7300 Sequence Detection System, using Optical MicroAmp 96-well plates and optical adhesive covers (Applied Biosystems). For each qRT-PCR reaction (total volume of 13.5 μl), 6.5 μl SYBR Green PCR master mix and 2.5 μl primer mix (1.5 μM each.) were used. 15 ng of cDNA and 30 ng of DNA were used for expression and MeDIP validation assays respectively.

Reaction conditions were as follows: 1 cycle at 50°C for 2 minutes, 1 cycle at 95°C for 10 minutes, 40 cycles at 95°C for 15 sec and at 60°C for 1 minute. Reactions were done in triplicates.

2.2.4.3 qRT-PCR assay data analysis

The efficiency, reproducibility and dynamic range of the assay was determined by constructing a standard curve using serial dilutions of a known template every time a new primer pair was used. Primer pairs were used only if efficiency of the assay was 90 to 100%, the slope of the curve around 3.0 and the Ct values for all technical replicates were similar. The presence of non-specific products was identified by constructing melting curves for each primer pair at 0.1°C intervals between 60°C and 95°C.

MeDIP validation assay

To evaluate the relative enrichment of target sequences after MeDIP, the C_t of the MeDIP fraction was normalized (for each sequence tested) to the C_t of the input (ΔC_t). Subsequently I normalised the ΔC_t of each target sequence to the ΔC_t of an unmethylated control sequence ($\Delta\Delta C_t$). Finally I calculated the enrichment as follows:

$$E = 2^{-\Delta\Delta Ct}$$

Expression assay

Gene expression in the cancer cell lines used in this study was determined in relation to a reference gene. As reference, the *ubiquitin C* gene (*UBC*) was used. (Vandesompele et al., 2002). Additional housekeeping genes (*RPL13A* and *GAPDH1*) were also tested and based on validation experiments UBC was assessed to be an adequate representative (figure 2.1). The EBV-transformed cell lines GM10851 and GM15510 were used as controls for normal *UBC* expression.

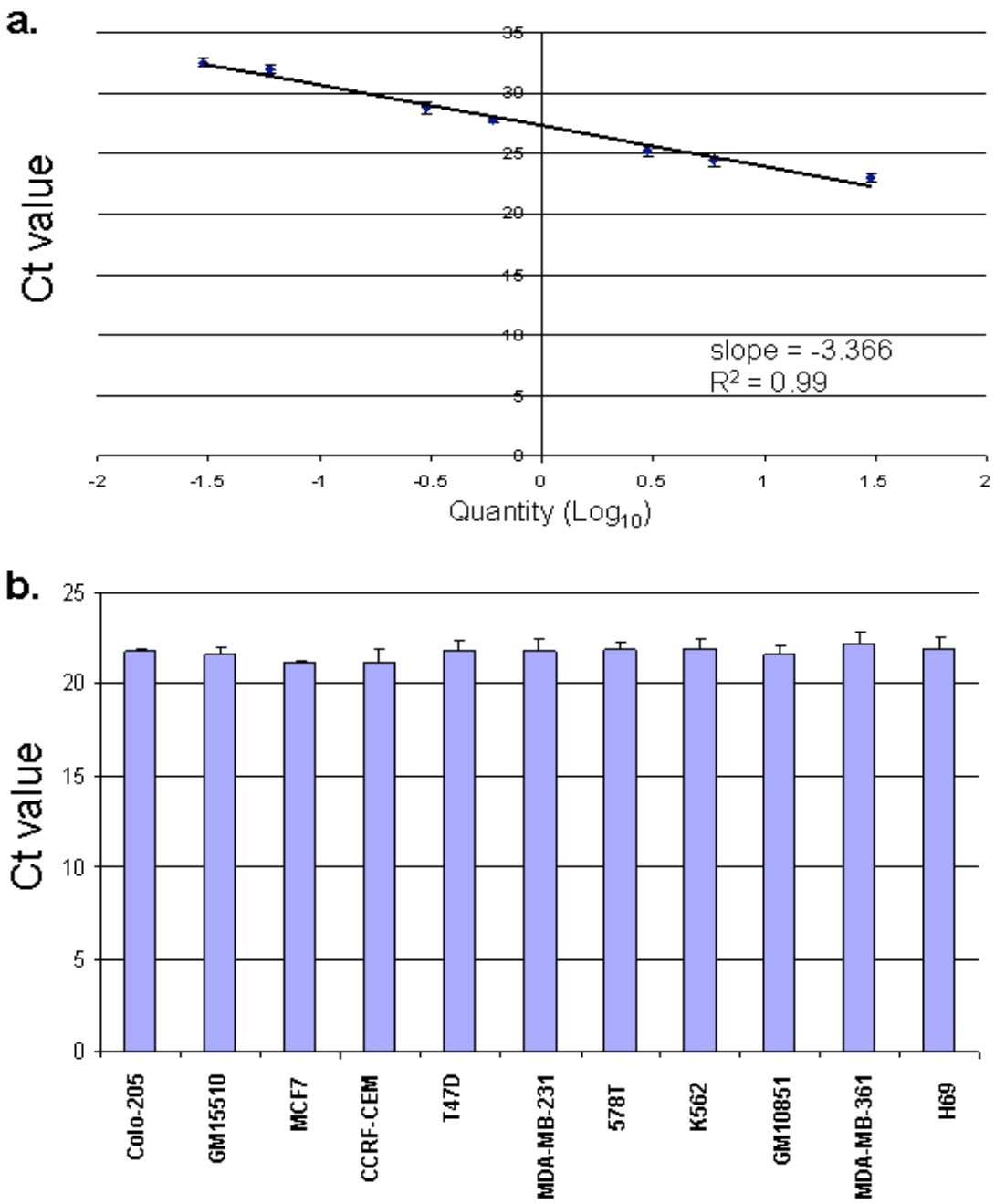

Figure 2.1 **Validation of UBC primers**. a). UBC detection by RT-PCR. UBC was detected by serial dilutions of human genomic DNA. The figure shows a standard curve generated from the real time amplification plot. Figure shows the average of three independent experiments. The efficiency of the reaction was 99% (R^2 =0.99) b). UBC detection in various cell lines. UBC detection by RT-PCR was performed on 15ng cDNA originated by the 11 cell lines tested for the pDMR screen (chapter 5). In all cases UBC detected within the same range of PCR cycles (Ct value close to 22 in all cases). Figure shows the average of three independent experiments for each cell line.

The relative difference in expression level of a target gene in cancer cell lines (test sample) compared to the EBV-transformed cell lines (controls) was determined as follows:

First the C_T of the target gene was normalized to the C_T of the reference gene for both test sample and control sample as follows:

$$\Delta C_{T(test)} = C_{T(target, test)} - C_{T(ref, test)}$$

$$\Delta C_{T(control)} = C_{T(target, control)} - C_{T(ref, control)}$$

Second, the ΔC_T of the test sample was normalised to the ΔC_T of the control as follows:

$$\Delta\Delta C_T = \Delta C_{T(test)} - \Delta C_{T(control)}$$

Finally the expression ratio was calculated as follws:

$$2^{-\Delta\Delta C_T} = \text{Normalised expression ratio}$$

2.2.5 Bacterial Cloning

Cloning of PCR fragments was performed using the TOPO TA Cloning Kit following the manufacture's protocol. Briefly, 1μl of PCR product was added to a mixture containing 4μl water, 1μl salt solution (1.2 M NaCl, 0.06 M $MgCl_2$) and 0.083μl TOPO vector. After 30 min incubation at room temperature 25μl of TOPO chemically competent cells were added to the mixture. Cells were heat-shocked for 45 sec at 42°C and 150μl of SOC medium was added immediately to the cells. Cells were grown for 1h (37°C, 200 rpm) before plating onto LB-amp plates.

2.2.6 Mini-preps of plasmid DNA

A single colony was inoculated into 1ml of LB broth containing ampicillin and grown overnight at 37°C at 320 rpm. For this purpose sterile 96 deep well blocks (2ml capacity) were used. On the following day the cells were pelleted for 2 min at 4000 rpm and resuspended in 120μl GTE buffer on ice. After ensuring complete resuspension of the pellet 120μl NaOH/SDS and 120μl KoAc were added to the cells.

140μl of the cell lysates were removed from the bottom of each deep well and dispensed into a Costar filter plate, which was placed on top of a Costar 3365 storage plate containing 140μl of 100% isopropanol, per well. Plates were centrifuged for 15 min at 400rpm and 4°C. Filter plate was discarded and isopropanol tipped-off. After addition of 100μl of 70% ethanol to the wells and 5 min centrifugation (4000rpm, 4°C) the plate was dried. Finally plasmids were dissolved by adding 60μl of water in each well.

2.2.7 Restriction Digests

Restriction digests of plasmid DNA (up to 10μg) were carried out using 1 x EcoRI buffer and 20 units of EcoRI enzyme. Samples (20μl reaction) were incubated at 37°C for 2 hours, and the resulting digest was confirmed by agorose gel electrophoresis.

2.2.8 Colony PCR

Following bacterial transformation (section 2.2.5) individual colonies were picked using sterile toothpicks and resuspended in 25μl PCR reaction buffer. For this purpose 96 well plates kept on ice were used. M13 forward and reverse primers were used for colony PCR. PCR conditions were as follows:

i. 95°C for 8 min
ii. 94°C for 30 sec
iii. 55°C for 30 sec
iv. 72°C for 1 min
v. Steps ii to iv repeated 30 times
vi. 72°C for 10 min

PCR products were confirmed by agarose gel electrophoresis and staining with ethidium bromide.

2.2.9 MHC tile path array

2.2.9.1 Generation of amino-linked probes

A total of 1747 overlapping plasmid clones were used to generate the array. Of those, 1662 clones (average insert size 2 kb) were picked from the HapMap chromosome 6 library (The International HapMap Project, 2003) and 85 clones were generated by cloning gap-spanning PCR amplicons (average insert size 332 bp). In addition, I generated and included 43 PCR-derived clones as controls. Generation of gap and control clones is described in the following section (2.2.9.2).

Double-stranded amino-linked amplicons were generated from each clone using vector-specific PCR in 50 mM KCl, 5 mM Tris pH 8.5 and 2.5 mM $MgCl_2$ (10 min at 95°C; followed by 35 cycles of 95°C for 1 min, 60°C for 1.5 min, 72°C for 7 min; and a final extension of 72˚C for 10 min - Forward primer 5'-CCCAGTCACGACGTTGTAAAACG-3'; Reverse primer 5'-AGCGGATAACAATTTCACACAGG-3'). In order to generate strand-specific array probes, two separate PCR reactions were performed for each clone, in one case using a 5'-aminolinked primer for the forward strand, and in the other case, for the reverse strand. After quality assessment of the products by gel electrophoresis, spotting buffer was added directly to a final concentration of 250 mM sodium phosphate pH 8.5, 0.00025% w/v sarkosyl, 0.1% sodium azide, and the products were filtered (Multiscreen-GV filter plates, Millipore).

2.2.9.2 Gap closure and control clones

As mentioned in the previous section (2.2.9.1) 85 gap and 45 control clones were generated. Using the appropriate primer pair (appendix table 2.1.1.1), amplicons corresponding to gap regions and control regions were generated by PCR. For this purpose commercially available human genomic DNA was used. Generation of clones for the gaps and controls was performed as described in section 2.2.5 and

2.2.6. Successful cloning amplicons confirmed by restriction digestions (2.2.7) and colony PCR (2.2.8)

2.2.9.3 Array printing and processing

Array printing and processing were performed at the Wellcome Trust Sanger Institute Microarray Facility as follows:

1. Array probes were printed onto amino binding slides (Motorola) at 20-25ºC, 40-50% relative humidity using a MicroGrid II arrayer (Biorobotics/Apogent Discoveries).

2. The array probes were printed in a 24 block format with spots in duplicates.

3. The slides were transferred into a microscope slide rack and placed in a humid chamber (NaCl saturated with water in an air-tight container) and incubated for 24-72 hours at room temperature.

4. The slides were removed from the humidity chamber and immersed in a 1% (w/v) solution of ammonium hydroxide and incubated for 5 minutes with gentle shaking.

5. The slides were then transferred to a solution of 0.1% (w/v) sodium dodecyl sulphate and incubated for 5 min with gentle shaking.

6. The slides were briefly rinsed in Milli-Q ddH2O (Miili-Q plus 185 purification system) at room temperature and then placed in 95ºC Milli-Q ddH2O for 2 minutes to completely denature the bound DNA elements resulting to single-stranded strand-specific array probes.

7. The slides were transferred to ice-cold Milli-Q ddH2O and then briefly rinsed two times in Milli-Q ddH2O at room temperature.

8. The slides were dried by spinning at 180 g for 5 min.

9. The slides were stored in a slide box and kept at room temperature in a cool dry place until used.

10. The final slide consists of 24 blocks (19 x 20) and a total of 7832 probes.

2.2.10 Microarray hybridization

Fluorescent labelling was performed using a modified Bioprime labelling kit in a 130.5 μl reaction (topped up with distilled water) containing 100 ng DNA, 15 μl dNTP mix (2 mM dATP, 2 mM dTTP, 2 mM dGTP, and 0.5 mM dCTP), and 1.5 μl Cy5/Cy3 dCTP (1mM). The reactions were purified using Micro-spin G50 columns (Pharmacia-Amersham) in accordance with the manufacturer's instructions. Reference and test samples were combined and precipitated with 55 μl of 3 M sodium acetate (pH 5.2) in 2.5 volumes of ethanol with 90 μg human C_ot1 DNA. The DNA pellet was resuspended in hybridization buffer (see Materials) containing 300 μg yeast tRNA. Hybridization was performed for 24 hours at 37°C on a MAUI hybridization platform. Finally, the arrays were washed serially in wash solution 1 for 5 min at room temperature, in wash solution 1 for 5 min at 60°C, four times in wash solution 2 for 20 min at room temperature, in wash solution 3 for 10 min at room temperature and finally in HPLC water for 10 min at room temperature. Subsequently the arrays were dried (by centrifugation – 3 min at 800 rpm) and stored in the dark.

2.2.11 Microarray Scanning

Microarrays were scanned using a ScanArray Express HT scanner (PerkinElmer) as follows:

1. Cy3 and Cy5 images at 5 μm resolution were acquired using the ScanArray 4000 confocal laser-based scanner (Perkin-Elmer) at laser power of 100% and a photo multiplier tube (PMT) value of 75% and 70% respectively. All arrays were scanned using the same parameters to avoid introducing another variable as part of the scanning process.

2. The software ScanArray Express (Perkin Elmer) was used to quantify the fluorescent intensities of the spots using the fixed circle quantisation and the TOTAL normalization method. This software can automatically locate the spot position on the

scanned image of the array to obtain the signal intensity values. Mean intensity ratios (intensity-background) were reported for each spot representing an array element.

2.2.12 Microarray Data Analysis

For each sample we analysed two biological replicates. All hybridizations were performed with fluorochrome-reversed pairs of two-colour labelled probes (two dye swaps as technical replicates). For the purpose of this analysis I treated the forward and reverse probes as replicates. Hence, for each sample tested, I obtained 16 measurements derived from quadruplicate spots on 4 array hybridizations (two biological replicates plus dye swaps). Fluorescence intensities were determined using the ScanArray Express software (PerkinElmer). Fusion of dye-swap and biological replicate results and subsequent analyses were performed using R packages from Bioconductor (Gentleman et al., 2004). For each probe, log-ratios were normalised within arrays using a Local Linear Regression (loess) which is efficient in removing dye effects (Smyth and Speed, 2003) and average intensities were normalised between arrays (Yang, 2003) leaving previously normalised ratios unchanged. Dye-swapped samples and biological replicates were defined in a design matrix where rows represent samples (observations) and columns represent effects of interests (parameters). Subsequent analyses were performed according to the design matrix by fitting a gene-wise generalised linear model to log-ratios with the generalised least squares method. This analysis takes advantage of the correlation structure arising from the four duplicated spots (Smyth, 2005) which is expected to be constant. Finally, ranking of the features according to their evidence of discrepancy between effects as defined in the design matrix, was performed by using empirical Bayes methods (Smyth, 2004) where moderated t-statistics test each individual effect equal to zero. Estimated p-values were subjected to multiple testing by using the False Discovery Rate (FDR) method (Benjamini, 1995). A threshold of p-value < 0.001 was used.

This analysis was performed by Dr. Gregory Lebfevre at the Wellcome Trust Sanger Institute.

2.2.13 Identification of genomic features of DMRs

I used the Application Programme Interface (API) to extract the features that are in the Ensembl functional genomics dataset. The whole chromosome 6 was scanned using a 2 kb sliding window in 1 kb steps. For each window, I counted the number of each type of feature within the bounds of the window. This way, a discrete probability distribution was generated, which, for a randomly selected window, determines how likely is to observe a certain number of features.

Windows that overlap an assembly gap were ignored, as this would bias the results.

For each DMR and for feature type, I used the feature count and the probability distribution to calculate:

1. The probability that a random window of that size would have exactly that number of features.

2. The probability that a random window of that size would have more or the same number of features (the right-hand tail of the distribution: if this value is small, it would suggest that the feature is enriched); 95% confidence interval was used.

3. The probability that a random window of that size would have less or the same number of the feature (the left-hand tail of the distribution: if this value is small, it would suggest that the feature is depleted); 95% confidence interval was used.

It should be noted that the probability distribution was generated for a 2 kb window, but DMRs were not exactly 2 kb, so some scaling was done to allow for this difference, i.e. if a DMR was 4 kb and had 6 features, then for a 2 kb window it would be scaled to 3 features.

This analysis was performed by Dr. Stephen Rice at the Wellcome Trust Sanger Institute.

Chapter 3

Development and validation of an array-based assay for the identification of DMRs

3.1 Introduction

The availability of genomic sequences of various organisms, including human, has provided an important resource in the effort of understanding biological functions. This resource has been exploited extensively by micro-array technology, including the development of DNA tiling arrays (Bertone et al., 2005; Hoheisel, 2006; Mockler et al., 2005; Yazaki et al., 2007). DNA tiling arrays represent a complete tile path of non-repetitive DNA over a locus, complex, chromosome or entire genome at various sequence resolutions. The exclusion of repetitive elements and other non-unique sequences from tiling array designs aims to reduce non-specific background signals that mask the signal resulting from specific probe hybridization. Probes used for the construction of such arrays can be partially overlapping, tiled end to end or may be spaced at regular intervals. DNA tiling arrays have enabled the discovery of novel transcribed sequences and transcription factor binding sites and, during the past few years, they have led the way for DNA methylation profiling.

DNA methylation analysis techniques, including bisulphite conversion, methylation sensitive restriction and immunoprecipitation (reviewed in (Beck and Rakyan, 2008; Weber and Schubeler, 2007; Zilberman and Henikoff, 2007) have been adapted successfully to be used in combination with DNA tilling arrays (Illingworth et al., 2008; Keshet et al., 2006; Mohn et al., 2008; Rakyan et al., 2008; Rakyan, 2008; Weber et al., 2005; Weber et al., 2007; Zhang et al., 2008; Zhang et al., 2006; Zilberman et al., 2007). The first array-based methylome has already been reported for *Arabidopsis thaliana* (Zhang et al., 2008; Zhang et al., 2006), and recently, by using Nimblegen array platforms, comprehensive genome-wide DNA methylation data have been generated for several human tissues (Rakyan et al., 2008).

My objective was to develop an unbiased tiling array-based assay for the identification of differentially methylated regions (DMRs) within the MHC region. DMRs refer to temporal or spatial patterns of DNA methylation and can be indicative of local changes in genome functionality (see section 1.3.7). To this end:

(i). I constructed and validated a tiling path micro-array covering the MHC region on chromosome 6.

(ii). I optimised and validated a protocol for the immunoprecipitation of methylated DNA fractions (MeDIP).

(iii). I tested the application of the MHC tiling array for DMR identification in combination with MeDIP.

3.2 MHC tiling array

3.2.1 Chemistry of the MHC tiling array.

The construction of the MHC tiling array was based on the 5'amino-link array surface chemistry developed at the Wellcome Trust Sanger Institute (Dhami et al., 2005) which allows single strands of DNA derived from double stranded PCR products to be retained on the surface of the micro-array slide. This is accomplished by the incorporation of a 5'-amino-linked modification at the end of one strand of a double stranded PCR product using modified primers (either forward or reverse). The 5'-amino-linked modification facilitates a covalent bond between the modified strand and the surface of the slide. Upon slide processing, the strand attached to the slide is retained, whereas the unmodified strand is removed. The single stranded DNA molecules attached at one end of the surface of the slide provide an ideal substrate for hybridization with labelled DNA samples (figure 3.1).

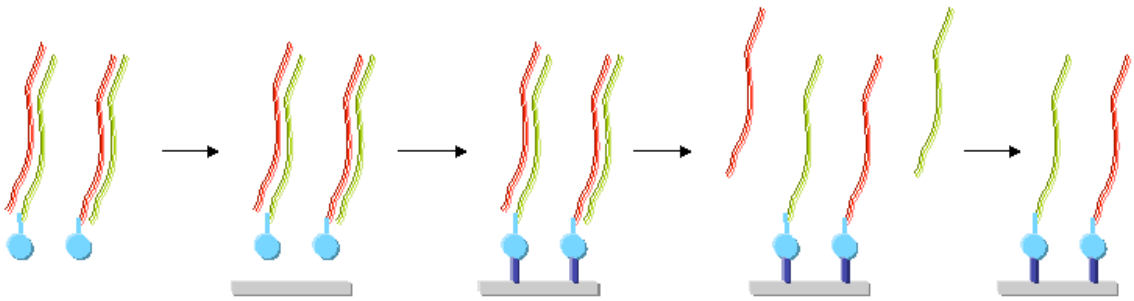

Figure 3.1. **Diagrammatic representation of processing of single-stranded array probes.** Double-stranded PCR products (red/green denote forward and reverse strands respectively) containing a 5'-amino-linked modification on one strand (blue sphere) are arrayed onto the surface of the slide (grey bar). Covalent attachment occurs via the 5'

amino-link (dark blue line) and the slide surface. Denaturation of the PCR product renders them single-stranded and suitable as hybridization substrates.

3.2.2 Generation and quality control of MHC array probes

The probes were designed to cover the entire MHC region as a minimally overlapping tile path, with appropriate controls. For this purpose I used the freely available clones from the HapMap project (The International HapMap Project, 2003). A total of 1747 overlapping plasmid clones were used to generate the array. Of those, 1662 clones (average insert size 2 kb) were picked from the HapMap chromosome 6 library and 85 clones were generated by cloning gap-spanning PCR amplicons (average insert size 332 bp). Some repeat-rich regions (about 12 kb in total) proved to be refractory to PCR amplification, and are thus missing from the array. Therefore, the total coverage represents 99.67% of the MHC region. It should be noted that at the time of the array design, the average probe size (2kb) was adequate as a comparable resolution was also used (e.g. the ENCODE project; The ENCODE project 2004). The main advantage of using the clones from the HapMap project was that all probes could be generated with the same primer set (section 2.2.9), making the process of array construction reproducible and economical.

In addition, I generated and included 43 PCR-derived clones as controls, covering: i) CpG islands of *BRCA1, GSTP1, RARB2* and *MLH1* genes as controls for studying methyl-binding domain (MBD) proteins (Ballestar et al., 2003), ii) imprinted regions (*H19, IGF2, KvDMR1, HSIGF2G, IGF2RDMR2* and *DMR0*) (Lewis and Murrell, 2004), as controls for studying imprinted regions (work in progress by Adele Murrell) iii) gene poor regions of chromosome 6; iv) matrix attachment regions of the *β-globin* gene cluster (Ottaviani et al., 2008); v) loop-associated DNA of the *PRM2* gene; vi) promoter regions of the *GAPDH* and *IRF1* genes; vii) replication origin of the *LB2* gene; vii) replication origin-lacking region of the *β-globin* locus; and viii) DNAase I-hypersensitivity sites of the *β-globin* locus control region. Controls iii to viii were used

to study higher-order structure such as matrix attachment regions (MARs) within the MHC (Ottaviani D., et al., 2008) Ten genes from the *Arabidopsis thaliana* genome (spotted in replicates, distributed across the array) that can be used to assign DNA barcodes as internal controls were also included. In addition, 192 Cy3 spots were printed on each array that can be used for calibration and orientation. MHC probe coordinates and primer sets used for the generation of gap-spanning and control clones are provided in appendix tables 2.1 and 2.2. Except for the Cy3 spots, none of the other controls were used for the analysis described in this thesis, but may be useful for other types of analyses.

In order to generate strand-specific array probes, two separate PCR reactions were performed for each clone using universal M13 primers: one reaction using a 5'-amino-linked primer for the forward strand, and one using a 5'-amino-linked primer for the reverse strand.

The array probes were assessed visually by agarose gel electrophoresis (figure 3.2).

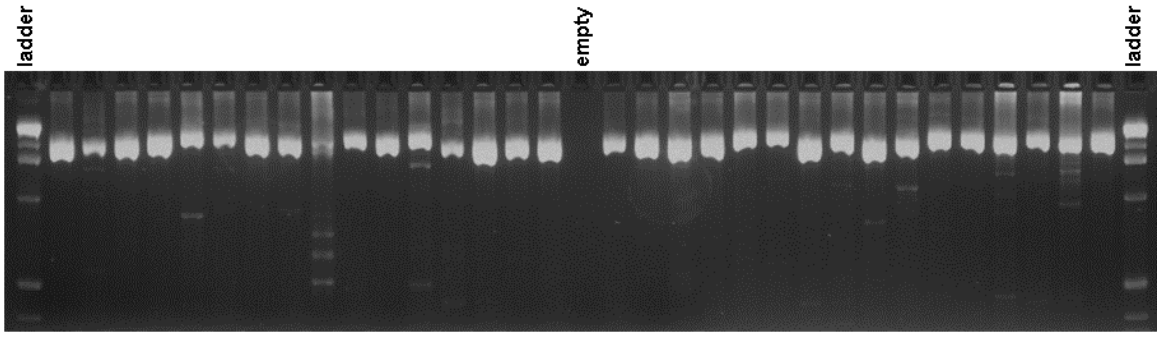

Figure 3.2. **Quality control of PCR-amplified probes.** All probes were electrophoresed on agarose gels and their bands were scored visually. Probes were electrophoresed on 2.5% agarose 1xTBE gels and visualized with ethidium bromide (a representative gel is shown).

Finally, the identity of randomly selected 240 clones (15 % of total) was confirmed by re-sequencing. Of the clones tested 7 failed to match to the expected reference sequences. From this partial analysis, I extrapolate that about 97% of the probes are correct and should be informative. Table 3.1 summarizes the characteristics of the array probes.

		No. of probes spotted on the array		
	No. of MHCclones	forward	reverse	**total**
No of MHC probes	1747	3494	3494	6988
No. of control probes	43	86	86	172
Cy3 spots				192
Arabidopsis regions				480
Total No. of array probes				**7832**

Table 3.1. **Summary of MHC tiling array probes**. The table lists the total number of probes used for the array construction. Probes were validated visually by agarose gel electrophoresis and by re-sequencing. In total 7832 probes were spotted on the array.

3.2.3 Validation of the MHC tiling array

In total 7832 probes were spotted to produce the 2kb MHC tile path array (table 3.1). Initial validation of the array was performed directly after spotting. The quality of array spots was tested using Cy3 dye and only those arrays that had less than 2% of the total spots not fluorescing or merged were used further.

The quality of array probes was further validated by performing input to input hybridization. Fragmented genomic DNA (average size 300 – 1000 bp) was labeled with Cy3 and Cy5 dyes and hybridized on the MHC tiling array. Calculation of $\log_2$ ratios (Cy3/Cy5) showed values very close to zero (figure 3.3a) indicating absence of hybridization variation within the array probes. On the other hand, when MeDIP to input hybridization was performed (see below) the range of $\log_2$ ratio was between 2 and -2 (figure 3.3b), as expected.

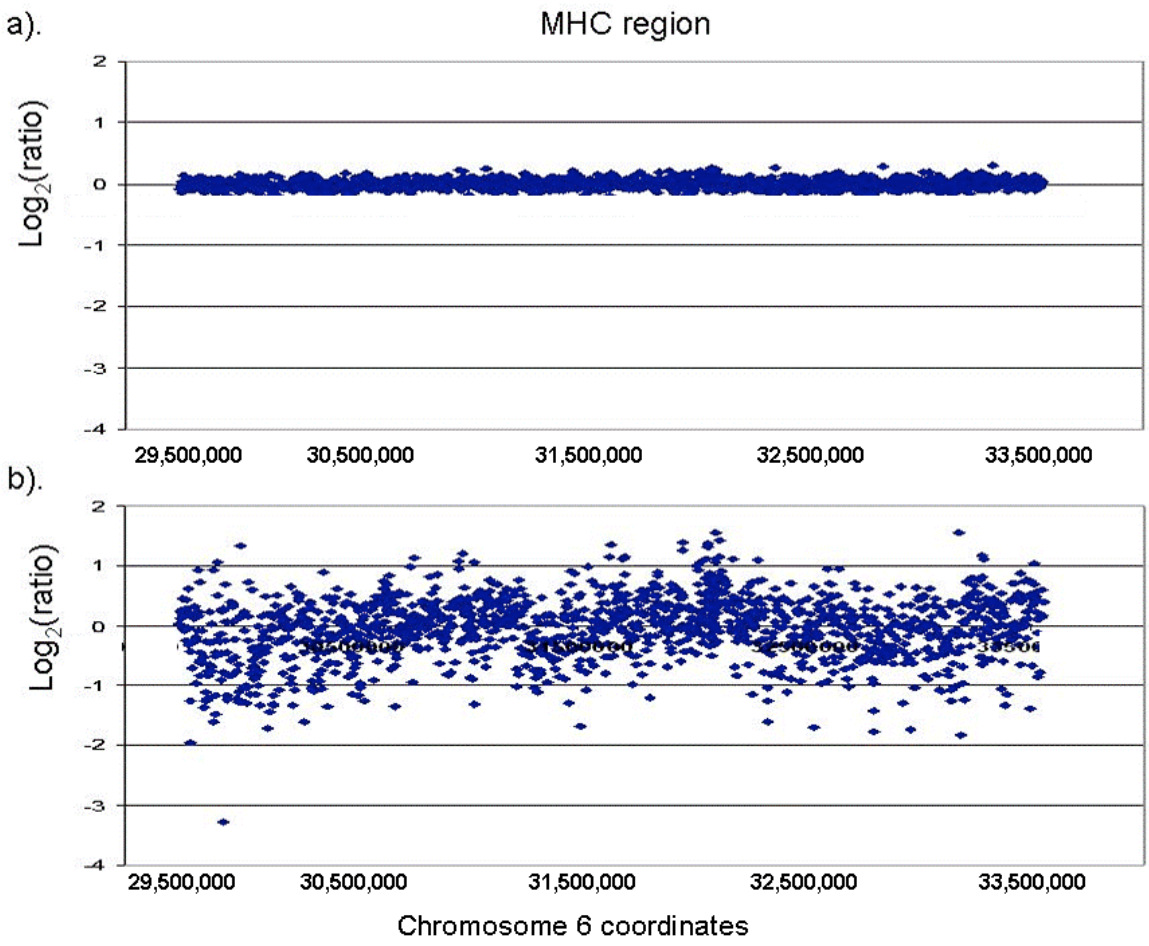

Figure 3.3. **Hybridization variation.** a) Input versus input hybridization of sperm DNA. b). MeDIP versus input hybridization on sperm DNA. Plotted are log_2-transformed hybridization ratios against the linear map position of the MHC probes. Log_2 ratios of input to input hybridization are close to zero whereas ratios corresponding to MeDIP to input hybridization range from 2 to -2.

3.2.4 Repetitive elements

Compared to most commercial and custom tiling arrays, the MHC tiling array also contains repeat elements, allowing such sequences to be analysed as well if desired. Figure 3.4a shows the distribution and frequency of repeat sequences within the probes on the array. About 9% of the probes have low (0-5%) repeat content and around 11% have high (95-100%) repeat content. The majority (80%) of probes have a random repeat content ranging from 6-94%. For studies that are not designed to interrogate repeat sequences (as in the study presented here) I show that repeat sequences can be efficiently blocked by the addition of human Cot-1 DNA during

hybridization (Figure 3.4b). Human Cot-1 DNA is commonly used to block non-specific hybridization in microarray screening. It is derived from placental DNA, about 50 to 300 bp in size and is enriched for repetitive DNA sequences such as the *Alu* and *Kpn* family members (Marx et al., 1976). I compared the probe intensities of the Cy5 channel for two hybridizations, one with and the other without Cot-1 DNA. In the presence of Cot-1 DNA, the intensities of repeat-containing probes are clearly reduced to the same level detected for repeat-free probes, indicating that undesired repeat signals can be blocked and that the unique parts of repeat-containing probes remain to be informative and can be kept for further analysis.

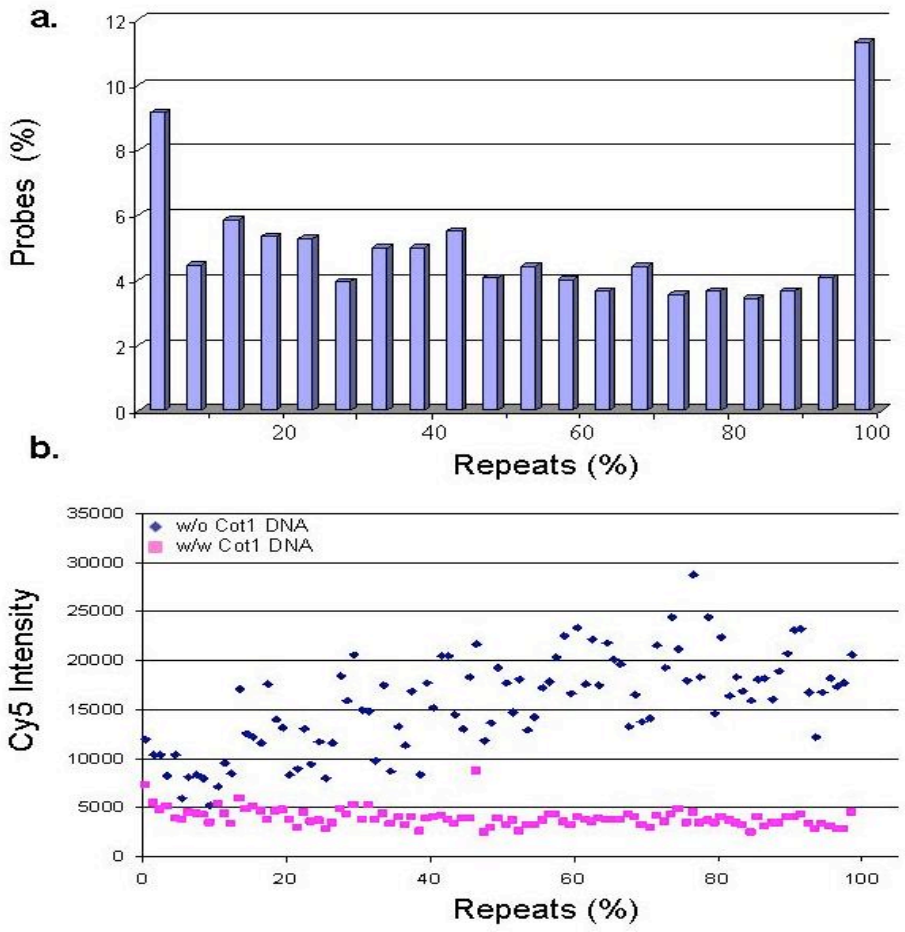

Figure 3.4. **Distribution and suppression of repeat sequences.** (a) Distribution and frequency of repeat sequences within probes on the array. (b). Suppression of repeat-specific signal using Cot1 DNA. Two independent hybridizations were carried out using genomic DNA extracted from $CD8^+$ lymphocytes. In both experiments total DNA was labelled with Cy5 dye.

Only in one of these was unlabelled Cot1 DNA added. In the hybridization without Cot1 DNA, Cy5 intensity increases almost linearly with repeat density until it reaches a plateau (around 25,000 Cy5 intensity). In the presence of Cot1 DNA, Cy5 intensity of highly repetitive probes is comparable to those of repeat-free probes.

3.3 MeDIP optimization and validation

Immunoprecipitation-based protocols for methylation analysis, methylated DNA immunoprecipitation (MeDIP) and methyl-cytosine immunoprecipitation (mCIP), were developed independently by two groups (Keshet et al., 2006; Weber et al., 2005). Both protocols are very similar and both were used as a point of reference while optimising the immunoprecipitation protocol for this study. In order to avoid confusion I refer to this technique as MeDIP in this thesis. MeDIP was first described in August 2005 and since then it has been used to generate comprehensive methylation profiles in mammals and plants as well as for DMR detection in cancer cells (Keshet et al., 2006; Rakyan, 2008; Weber et al., 2005; Zhang et al., 2006; Zilberman et al., 2007). In brief the MeDIP assay involves immunoprecipitation of methylated DNA fragments using an antibody that binds specifically to methylated cytosines. MeDIP was described in detail in section 1.3.6.2. In the below section I refer to the critical genomic DNA fragmentation step (3.3.1) and validation of MeDIP by quantitative real time qPCR (3.3.2).

3.3.1 Genomic DNA fragmentation

The first step of the MeDIP assay is genomic DNA fragmentation. Fragmentation of genomic DNA was performed by sonication. Sonication gives random, overlapping target fragments and clear interpretation of data (figure 3.5).

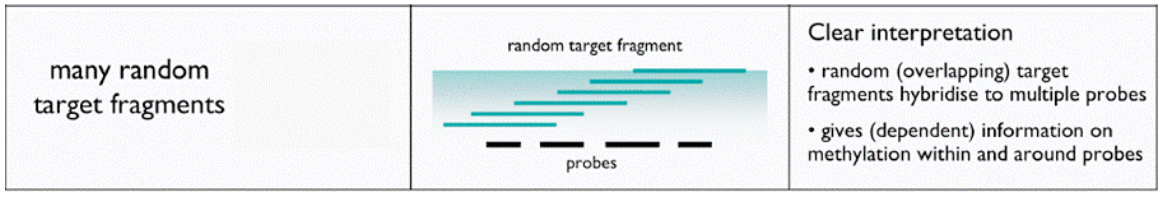

Figure 3.5. **Relationship between target fragments and array probes in methylation analysis.** Figure was adopted from Thorne (Thorne NP, 2006).

After sonication the size of the fragmented DNA ranges from 300 to 1000 bp (figure 3.6). It was important to keep the size range constant for all MeDIP experiments performed for this study.

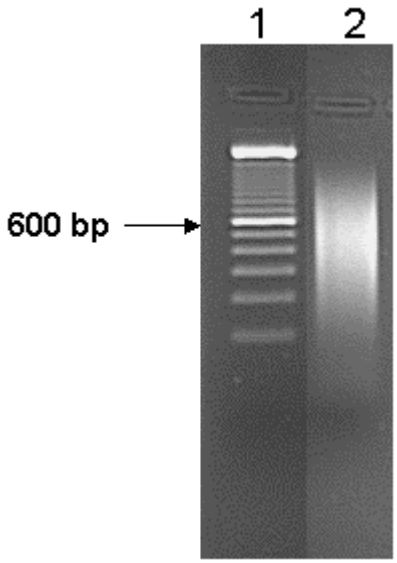

Figure 3.6. **Fragmentation of genomic DNA.** Genomic DNA was fragmented by sonication using a Virtis sonicator to generate fragments of a size range from 300 to 100bp. 500 ng of sonicated DNA was loaded onto a 2% agarose gel (lane 2). Size of fragmented DNA was estimated using 100bp ladder as a size marker (lane 1). Average size of DNA fragments is about 600bp, as indicated.

3.3.2 Validation of MeDIP

Enrichment of methylated DNA in the MeDIP fraction can be measured by qRT-PCR. I validated MeDIP by performing qRT-PCR to test the enrichment of regions with varying CpG densities for which the methylation status was known from the Human Epigenome Project (Eckhardt et al., 2006; Rakyan et al., 2004). It should be noted that CpG sites are unequally distributed within mammalian genomes and that the number of CpGs within a target region as well as their methylation status can influence target sequence enrichment in the MeDIP fraction. I showed that following

MeDIP methylated regions are enriched approximately proportionally to their CpG densities, and no significant enrichment irrespective of CpG density was observed for unmethylated regions (figure 3.7a).

Using a threshold of ≥5-fold enrichment, the MeDIP assay is therefore sensitive for regions of ≥1% CpG density. Using this threshold (actual enrichment range was 5-80 fold), I generated DNA methylation profiles of the entire MHC as described below.

In some cases (tDMRs screen, chapter 4) I had to introduce an amplification step while performing MeDIP assay due to limited starting DNA material. A ligation mediated PCR (LM-PCR) step was introduced as described previously (Oberley et al., 2004). In brief, the LM-PCR technique involves blunt ending of the fragmented DNA, ligation of a uni-directional double stranded oligo-nucleotide linker, and finally PCR amplification of the resultant DNA population after MeDIP. qRT-PCR analysis on MeDIP-LM-PCR DNA (post_LM-PCR) revealed similar enrichment for both methylated and unmethylated fractions as for non-amplified MeDIP fractions (pre_LM-PCR) (figure 3.7a,b), indicating that LM-PCR does not introduce an amplification bias. This was further supported by comparison of pre- and post-LM-PCR MeDIP-array analysis on the MHC-tile path array (see below).

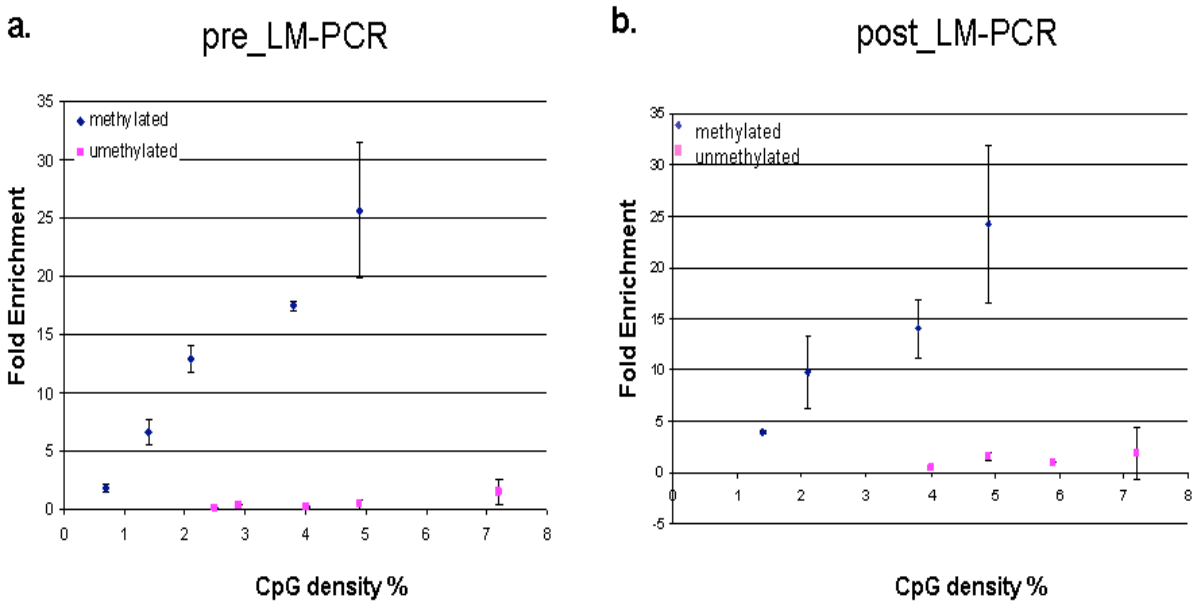

Figure 3.7. **Correlation between enrichment after MeDIP and CpG density**. Control sequences that are methylated, unmethylated or lack CpG sites were selected from HEP. MeDIP was done using liver genomic DNA. The relative enrichment of the MeDIP versus input fractions was calculated based on qRT-PCR data. Graph a. validation of MeDIP without amplification step. Graph b. Validation of MeDIP after amplification by LM-PCR. In both cases a specific and efficient enrichment of methylated over unmethylated fractions was shown. Enrichment of methylated and unmethylated fractions lies between the same range for both pre- and post-LM-PCR samples. The error bars indicate the variance of two independent measurements. Methylated amplicons display an approximately linear dependency on CpG density.

3.4 Application of the MHC tiling array for methylation analysis.

The MHC tiling array has been designed to be compatible with chromatin immunoprecipitation (ChIP), methylated DNA immunoprecipitation (MeDIP), array comparative genomic hybridization (aCGH) and expression profiling, inclusive of non-coding RNAs. In this section I demonstrate the utility of the MHC tiling path array for methylation analysis and DMR identification.

I used the array in conjunction with MeDIP. After performing MeDIP, MeDIP-enriched fractions and input fractions were differentially labelled with Cy3 and Cy5 and hybridized on the MHC tiling array. Following completion of appropriate quality control experiments DMRs were identified and validated.

In the next sections I describe how normalization of the array data was performed, how the quality of array hybridizations was tested and finally how I identified and validated DMRs.

3.4.1 Normalization of MHC tiling array data

Microarray screening can be affected by multiple sources of variation including array construction process, preparation of samples, hybridization process and the quantification of spot intensities (Repsilber and Ziegler, 2005). Normalization of array data attempts to remove such variation which might affect the outcome of the subsequent analysis.

Normalization usually applies to the $\log_2$ ratio of Cy3 and Cy5 intensities (corrected for the background) which will be: $M=\log_2 Cy3 - \log_2 Cy5$. The log-intensity of each spot is: $A = (\log_2 Cy3+\log_2 Cy5)/2$, a measure of the overall brightness of a spot. For the normalization of the MeDIP-MHC array data I applied local linear regression (loess) (Smyth and Speed, 2003) which fits a robust local regression to the relation between M and A. The normalized M values is the original one minus the loess fitted one, and thus should correct for spatial effects and for effects related to intensity. Figure 3.8 shows how data differ before and after normalization (MA plots).

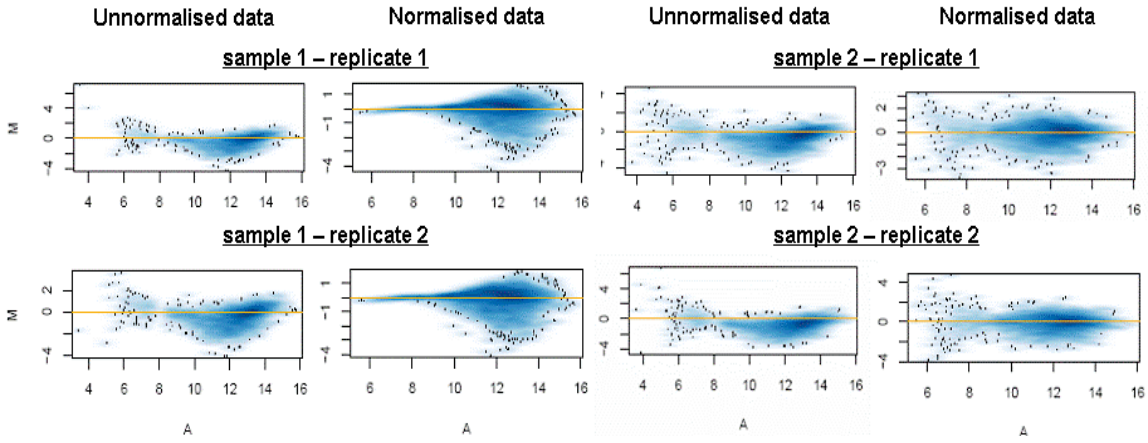

Figure 3.8. **Normalization within arrays.** Figure illustrates MA plots generated for four hybridization experiments. MeDIP-enriched and input fractions from a single sample were co-hybridized to each array. MA plots for two different samples and two biological replicates of each sample are shown. M represents the $\log_2$ ratio of the Cy3 and Cy5 intensities and A represents the $\log_2$ geometric mean of the Cy3 and Cy5 channel intensities.

3.4.2 MeDIP-MHC tiling array hybridization quality control

Methylation analysis across the MHC was performed by using the MHC tiling array in combination with MeDIP. I tested the reproducibility of this approach. I used DNA extracted from sperm (two biological replicates) and I performed MeDIP and the MHC array hybridization for each of the DNA samples before and after LM-PCR (see above). In both cases the correlation coefficient between biological replicates was high (R^2 >0.82) (figure 3.9a and b). In addition, I tested if LM-PCR introduces a bias in the methylation analysis. I compared hybridizations of pre– and post-LM-PCR

samples (sperm DNA) and showed that LM-PCR does not have a major effect on the analysis (R^2 = 0.88) (figure 3.9c). Finally fluorochrome-reversed pairs of 2-colour labelled probes (dye swaps) were performed for LM-PCR samples. It has been shown that using standard direct labelling techniques introduce a bias to incorporation of the dye during the labelling reaction. In order to test for this I compared dye-swap hybridizations (figure 3.9d) and I found that the correlation coefficient was at least 0.72 (R^2 = 0.72).

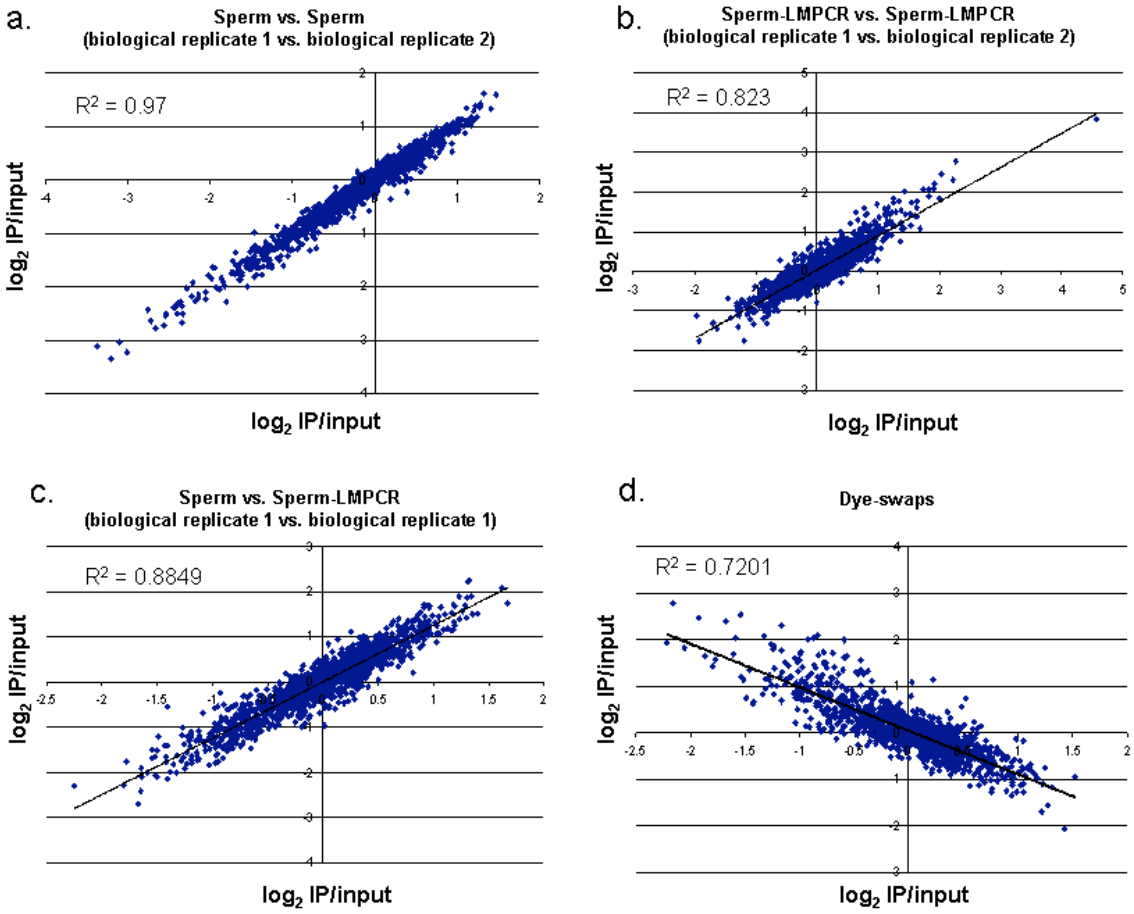

Figure 3.9. **Comparisons of MHC tiling array hybridizations.** Scatter-plots show: a). Comparison of biological replicates; b). Comparison of biological replicates after LM-PCR; c). Comparison of profiles pre- and post-LMPCR; d). Comparison of Dye swaps after LM-PCR. In all comparisons sperm DNA was used. Correlation coefficients are given for each comparison.

3.4.3 DMR identification and validation

The efficiency of immunoprecipitation in MeDIP depends on the density of methylated CpG sites, which vary greatly within any given mammalian genome, making it difficult to distinguish variations in enrichment from confounding CpG density effects (Weber et al., 2005; Weber et al., 2007). Hence, until recently, it has not been possible to estimate absolute methylation levels from MeDIP-array experiments. The on-going development of a novel algorithm employing a Bayesian de-convolution strategy to normalize MeDIP array data for CpG density is likely to overcome this current limitation in the near future (Down et al., 2008).

Determining absolute methylation values along the MHC region was beyond the scope of this study. I aimed to identify DMRs between samples. To this end I followed an experimental design as shown in figure 3.10. DMRs were identified by performing direct pair-wise comparisons and by applying t-test statistics. A threshold of p-value < 0.001 was employed.

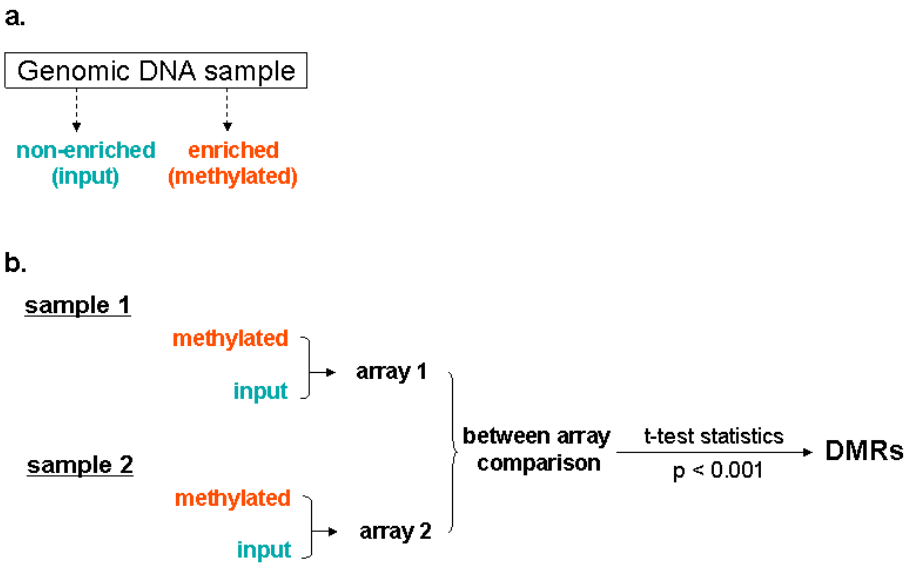

Figure 3.10. **Design of approach for calling DMRs.** (a). Target fractions after MeDIP experiment. (b). Calling of DMRs. For DMR identification, comparisons between arrays were performed. Significance of methylation differences between samples was calculated by t-test statistics. A threshold of p-value < 0.001 was used.

This approach was applied successfully for the identification of tDMRs and pDMRs (chapters 4 and 5). The approach was validated further by correlating the tDMRs identified by this study with tDMRs identified by an additional independent study, the Human Epigenome Project (HEP) (Eckhardt et al., 2006; Rakyan et al., 2004). DMRs were also validated by bisulphite sequencing. In all cases, DMR status could be confirmed, indicating that the array is suitable for DMR identification (chapter 4 and 5).

3.5 Discussion

The array reported in this chapter is the first genomic tiling array (2kb resolution) of the entire MHC. Commercially available tiling arrays usually exclude repeat sequences and therefore cover only about 50% of the genomic sequence. At the time of array design, whole-genome tiling arrays that included the MHC were constructed from P1 artificial chromosomes (PACs) and bacterial artificial chromosomes (BACs), resulting in a resolution of approximately 100 Kb. By utilizing a public clone resource, the MHC array was generated at a fraction of the costs associated with commercial arrays, albeit at lower resolution than is now achievable with these platforms. The array is compatible with standard array processing and scanning platforms and contains 7832 features. Of these 6988 correspond to the MHC region on chromosome 6. According to quality control experiments I performed, 97% of the probes can be informative for analysis of the MHC region. Upon request, the MHC array is freely available from the Microarray Facility at the Wellcome Trust Sanger Institute.

The array has been designed to be compatible with chromatin immunoprecipitation (ChIP), methylated DNA immunoprecipitation (MeDIP), array comparative genomic hybridization (aCGH) and expression profiling, inclusive of non-coding RNAs.

In this chapter I described how the array can be used for methylation analysis. To this end, MeDIP was optimised and validated showing its efficiency for

immunoprecipitation of methylated genomic fragments (300-1000bp) with at least 1% CpGs.

The utility of the MHC array in conjunction with MeDIP for DMR identification was tested and validated. This approach allows DMR identification at 2kb resolution and used for the identification of tissue and phenotype specific DMRs as described in chapters 4 and 5 respectively.

3.6 Conclusion

I have generated and validated a genomic tiling array and I have demonstrated its utility for DNA methylation profiling and the identification of DMRs when combined with MeDIP. Chapters 4 and 5 describe the application of this approach for tDMR and pDMR identification respectively.

Chapter 4

Tissue-specific DMR (tDMR) screen

4.1 Introduction

Tissue specific gene expression in higher eukaryotes involves the activation or silencing of transcription at the appropriate time, and at the right genomic location during cell differentiation. Gene expression is controlled by promoter sequences located immediately upstream of the transcription start site (TSS) of a gene, and by additional regulatory elements located close to the gene that they control, or at a certain distance, or even on a different chromosome (figure 4.1) (Maston et al., 2006).

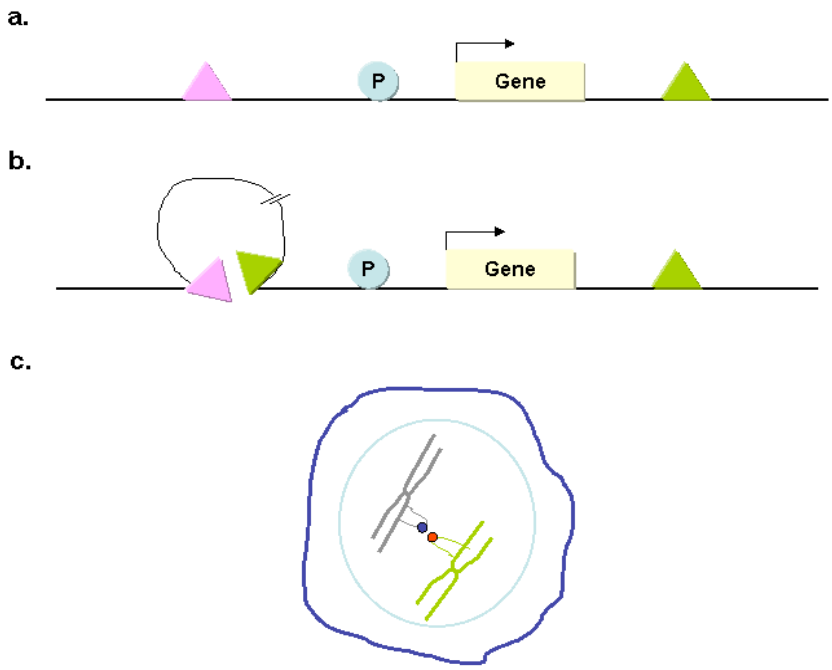

Figure 4.1 **Regulation of gene expression.** a. Linear view of gene regulation. The promoter (P) near the start of a gene provides the minimal information needed for gene expression. The function of the promoter is supplemented by enhancers or silencers farther away (triangles), where regulatory proteins bind to activate or repress transcription of the gene (arrow). b. The looping model of gene regulation. Proteins binding to control regions (triangles) scan through large portions of DNA, looping the intervening region out, until they find the relevant gene. c. Genes from different chromosomes might come into contact when the chromatin containing them loops out from their chromosome 'territory'. Figure was adapted (with some modifications) from Kioussis D., 2005 (Kioussis, 2005).

What determines the gene expression pattern that uniquely defines different tissues with otherwise identical genetic material remains a fundamental biological question.

Landmark publications in the mid-1970s speculated on the role of differential methylation of CpG sites in tissue specific gene expression (Holliday and Pugh, 1975; Riggs, 1975). However this idea remained controversial as a number of studies failed to correlate promoter methylation with expression of known tissue specific genes (Walsh and Bestor, 1999; Warnecke and Clark, 1999). It was almost 20 years later when a study by Futscher BW., et al (Futscher et al., 2002) showed that promoter methylation of the MASPIN gene controls its cell type specific expression.

It is of note that all studies referenced above looked only at the methylation patterns of the promoters of genes with known tissue specific gene expression. However, it should be kept in mind that expression is not controlled solely by promoter regions (figure 4.1). Hence, a different way to investigate if there is a contribution of DNA methylation in tissue specific gene expression is to first identify regions with tissue specific methylation patterns (tDMRs), and subsequently try to correlate them with tissue-specific gene expression.

Advances in methylation analysis technology (section 1.3.6) have eased the way for tDMR identification. Large-scale studies were reported during the past few years that aimed to identify tissue-specific methylation patterns (Eckhardt et al., 2006; Illingworth et al., 2008; Rakyan et al., 2004). One such study, the Human Epigenome Project (HEP), was launched in 1999 and aimed to systematically analyse DNA methylation in the regulatory regions of all known genes in most major tissues and cell types using bisulphite sequencing (Beck et al., 1999). About 25% of the amplicons investigated by the HEP were tDMRs. Interestingly, tDMRs present within CpG islands (CGIs) were located several kilobases away from the nearest annotated genes (Eckhardt et al., 2006). This possibly explains why previous studies reported few tissue specific methylation patterns.

However, when my study was designed (April 2005), only data from the pilot HEP study were available (figure 1.10) (Rakyan et al., 2004). The latter has generated DNA methylation data for about 2.5% of the human MHC region. A significant

proportion (10%) of the MHC loci analysed showed tissue-specific DNA methylation patterns.

In this chapter I will describe a more comprehensive study looking for tDMRs within the entire MHC region. This was part of an effort to identify epigenetic control elements that may be involved in the regulation of MHC genes. For this purpose I generated a MHC tiling array, which I used in combination with MeDIP to enable me to generate methylation data for about 97% of the MHC region (chapter 3). Four samples, also tested as part of the HEP study, were used. In the following sections I present the tDMRs I identified and their characteristics, including correlation with tissue-specific gene expression.

4.2 Samples used for the tDMR screen.

For the tDMR screen, DNA extracted from two tissues (liver and placenta), $CD8^+$ T lymphocyte cells and sperm was used. Two biological replicates of each sample were tested (table 2.1)

These samples were chosen because they have been used previously for methylation analysis across the MHC as part of the HEP study (Eckhardt et al., 2006; Rakyan et al., 2004). Based on HEP, MHC associated tDMRs are present within these tissues. Based on previous studies failing to identify significant sex-specific DNA methylation differences on autosomes (excluding imprinted regions) and the MHC (Rakyan et al., 2004, Weber et al., 2005, Eckhardt et al., 2006), the samples studied here were not controlled for sex.

Tissue-specific DNA methylation profiles of the MHC

Comprehensive methylation profiles of the MHC region were generated using the MHC tiling array in conjunction with Methylated DNA Immunoprecipitation (MeDIP). For this purpose, DNA extracted from 2 tissues (liver and placenta), $CD8^+$ T lymphocytes and sperm was used (section 4.2). I co-hybridised each immunoprecipitated sample with its corresponding untreated sheared control DNA on

the MHC array and analysed the data as described in chapters 2 and 3. Methylation profiles along the MHC region in the four samples tested are shown in figure 4.2.

At this (megabase) resolution, three main observations can be made: (i) The overall profiles correlate significantly ($0.83 < R^2 < 0.93$), suggesting few or no large-scale (>100 Kb) differences in DNA methylation, except perhaps in liver, where some regions appear to be lower in methylation than in other tissues. (ii) As expected from the MeDIP validation qRT-PCR data (figure 3.7) (although CpG density was analysed here), the profiles correlate very well with C+G content, clearly demarcating the boundaries of the MHC class I, II, III and extended class II regions. (iii) The profiles further show the vast improvement in coverage compared to the 253 amplicons, analysed as part of the Human Epigenome Project (Rakyan et al., 2004).

These profiles were used for the identification of tDMRs within these four samples as described in the following section (section 4.4).

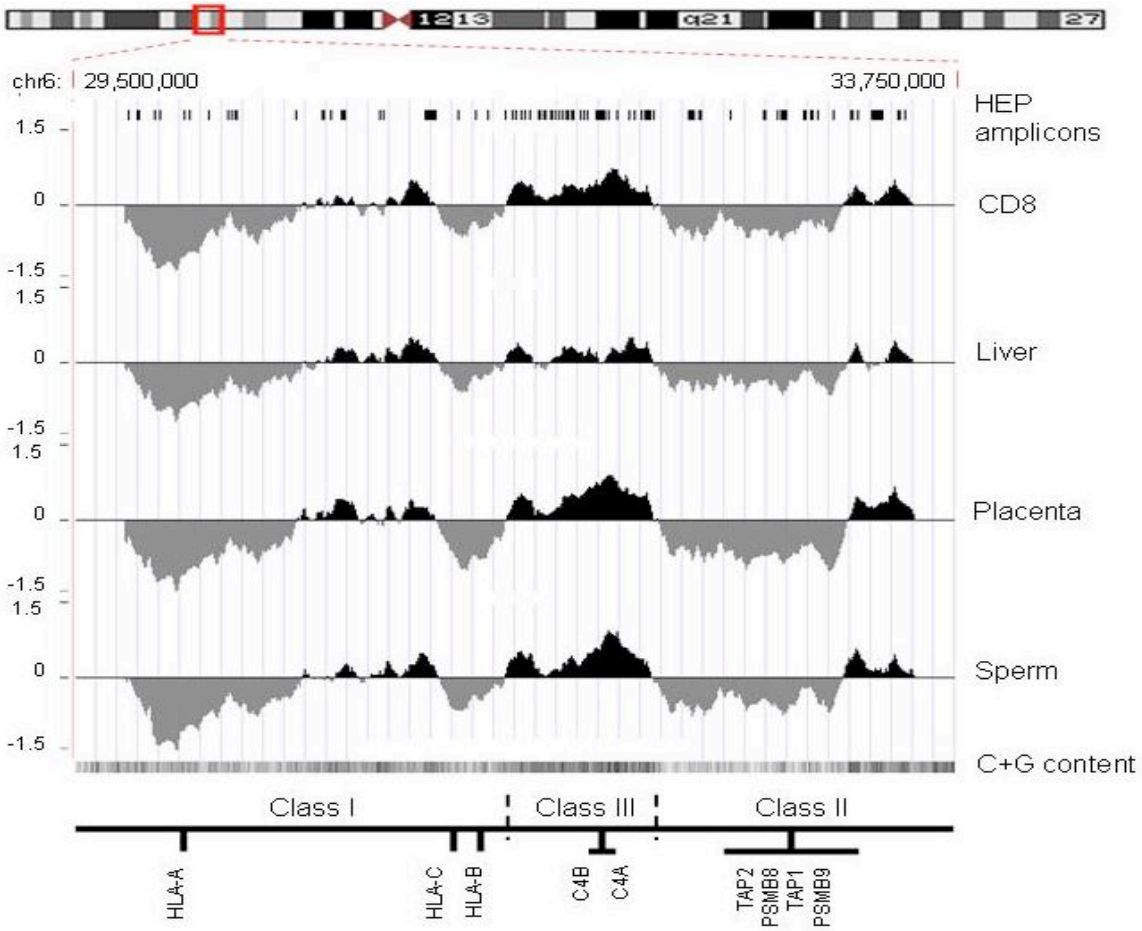

Figure 4.2 **DNA methylation profiles of the MHC.** For each of the four samples tested ($CD8^+$ lymphocytes, liver, placenta, sperm), the log_2 signal ratios (MeDIP/input) were uploaded as individual tracks to the UCSC genome browser using the 'smooth' function. Regions enriched or depleted in DNA methylation are shaded in black and grey, respectively. Also shown are the locations of HEP amplicons and a track of the C+G content (the darker the shading, the higher the C+G content). For orientation, the approximate positions of the MHC class I, II and II subregions and some landmark genes are indicated.

4.4 tDMR identification

For the identification of tDMRs, I performed pair-wise comparisons (six in total – $CD8^+$ T lymphocytes versus placenta, liver versus placenta, placenta versus sperm, $CD8^+$ T lymphocytes versus sperm, liver versus sperm, and liver versus $CD8^+$ T lymphocytes) of the array-derived DNA methylation profiles (section 4.3). At 2 kb, the probe resolution was not high enough to determine if more than one tDMR was contained within a probe or if positive, adjoining probes were part of the same tDMR. Therefore, each differentially methylated probe was considered to be a separate tDMR. According to this definition, I identified a total of 90 putative tDMRs of which 35 were present in more than one comparison (Figure 4.3; Appendix table 4.1).

According to the pair-wise analyses, sperm is most frequently differentially methylated which agrees with the findings of the Human Epigenome Project. The majority of tDMRs identified in sperm are hypomethylated compared to the other samples (65% of tDMRs in placenta-sperm comparison; 93% of tDMRs in CD8-sperm comparison; 32% of tDMRs in liver-sperm comparison). It is known that DNA extracted from sperm is hypomethylated compared to somatic cell DNA (Farthing et al., 2008; Reik, 2007; Schaefer et al., 2007). Notable exceptions are the tDMRs identified in the complement region which seem to be less methylated in liver than any of the other samples. DMRs within this region are discussed further in section 4.6.

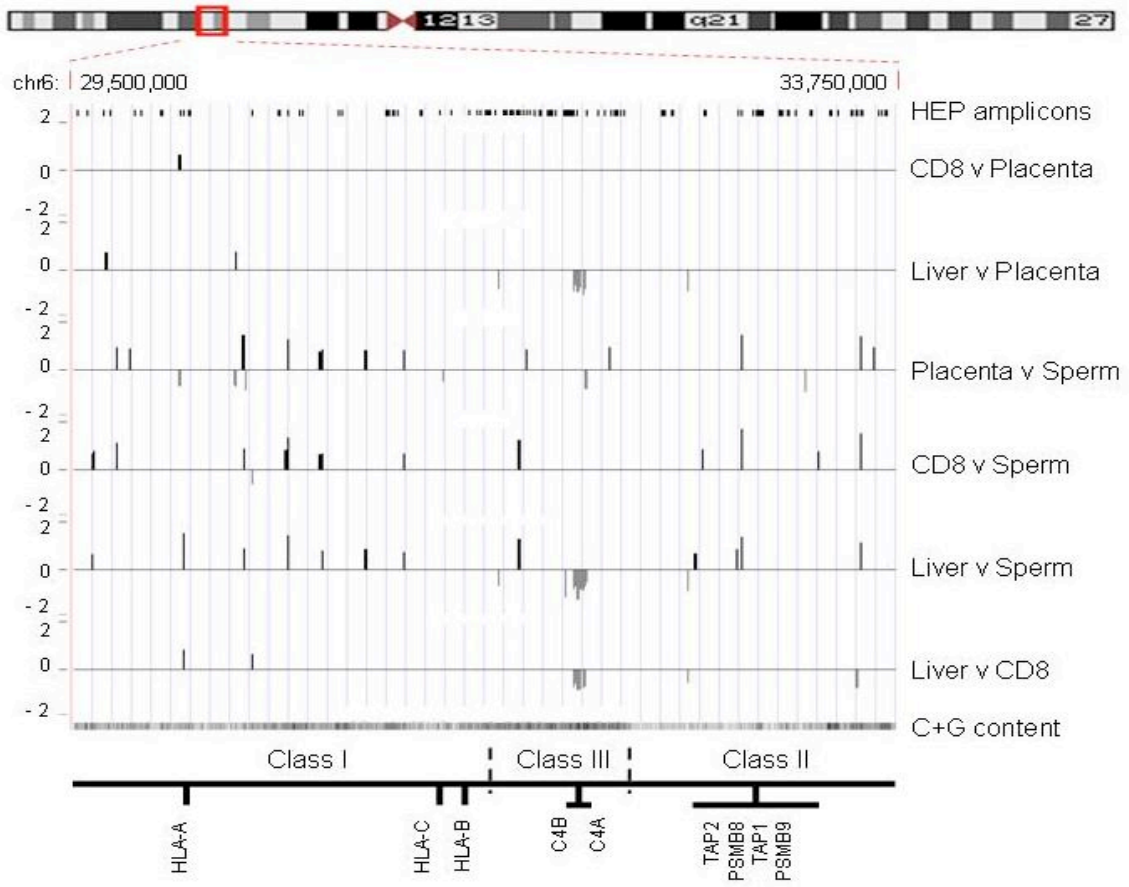

Figure 4.3 **tDMRs within the MHC region.** Pair-wise comparisons (six in total) of the MHC array-derived DNA methylation profiles were performed using t-statistics. A threshold of p-value < 0.001 was used. In total 90 putative tDMRs were identified. Vertical axis shows the $\log_2$ ratio of the two corresponding methylation profiles. Each line represents a tDMR (average size 2kb). Black lines represent tDMRs more methylated in one sample compared to the other (the identities of the pair-wise comparisons are given on the right) whereas grey lines represent less methylation. The majority of tDMRs are present in comparisons with sperm. The locations of HEP amplicons, a track of the C+G content and the approximate positions of the MHC class I, II and II subregions and some landmark genes are also indicated. The Class III region encoding for C4 genes seems to be less methylated in liver.

4.5 Validation of tDMRs

In this section I describe the validation of the tDMRs reported in the previous section (section 4.4). This was done in two steps:

4.5.1. I randomly selected six tDMRs and subjected them to independent methylation analysis using bisulphite DNA sequencing.

4.5.2. I correlated the tDMRs identified by my analysis with the corresponding HEP data (Eckhardt et al., 2006; Rakyan et al., 2004).

4.5.1 Validation of tDMRs by bisulphite sequencing.

I randomly selected six tDMRs, irrespective of their functional relevance, and I subjected them to bisulphite sequencing analysis. The latter is an independent method for methylation analysis (section 1.3.6.1). While with the MeDIP-MHC tiling approach I could only identify methylation differences between two samples (DMRs) (chapter 3), bisulphite sequencing analysis assigns absolute methylation values for each CpG site within a region of about 300- 400 bp. Hence, it is not appropriate to directly compare data generated by the two approaches. However, it is possible to compare relative methylation differences between two samples based on data generated independently by the two methods.

Figure 4.4 shows the genomic locations of the six tDMRs (a), their methylation status based on comparison of their respective MeDIP array profiles (b) and their absolute methylation values based on bisulphite sequencing (c). In all six cases, the bisulphite sequencing results were consistent with the array data, indicating that that the array is suitable for the identification of tDMRs.

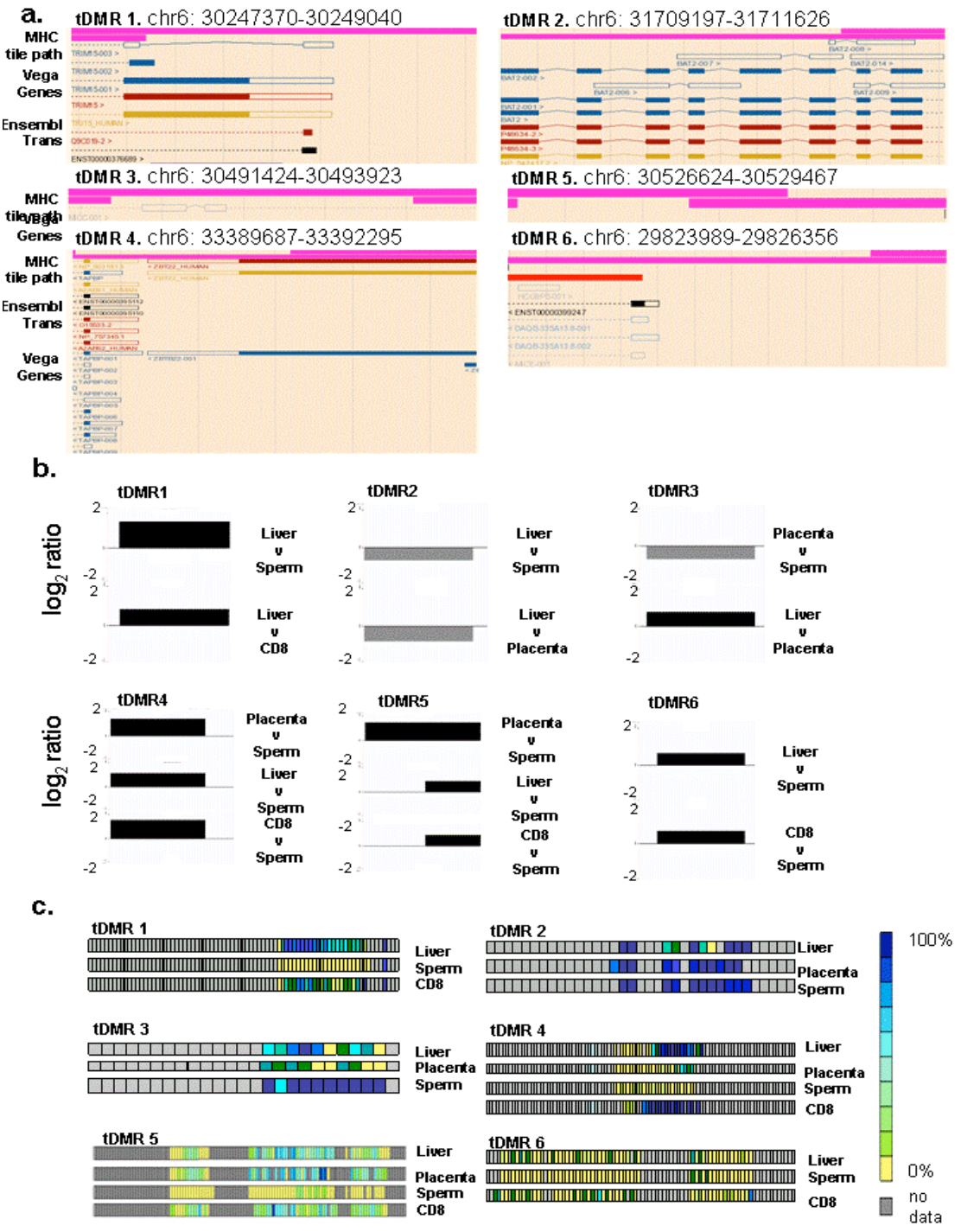

Figure 4.4 **tDMR validation.** Six tDMRs were randomly selected and subjected to bisulphite sequencing analysis. a. Genomic location and associated Ensembl annotation of the six tDMRs. The given chromosome 6 coordinates refer to the tiles (pink track) involved in the formation of these tDMRs. b. tDMR status based on pair-wise comparisons of the $\log_2$ MeDIP enrichment ratios of the indicated tissues/cell types. Black boxes represent tDMRs that are more methylated in sample 1 of the comparison and grey boxes represent tDMRs that are more methylated in sample 2 of the comparison. c. Absolute DNA methylation values of individual CpG sites in tDMRs based on bisulphite sequencing analysis. Because of assay and or technical limitations, bisulphite data could only be obtained for about 50% of the CpG

sites involved in the putative tDMRs. Each square represents a CpG site. The colour code indicates methylation values as calculated by ESME (section 2.2.3). Grey squares indicate CpG sites for which no data could be obtained. Based on this analysis, bisulphite data essentially agree with array data in all cases. It should be noted that I have not performed a systematic analysis defining the smallest size of a DMR that can be identified using the MeDIP-MHC array approach. Therefore, it is not certain if the three CpG sites that appear to be less methylated in liver-tDMR2 are sufficient for detection. It is possible that additional CpG sites are hypomethylated in liver (tDMR2) but bisulphite sequencing analysis was not successful for all CpG sites within this tDMR. Correlation of tDMRs identified by this study with tDMRs identified by MeDIP-chip (Nimblegen arrays - 50bp resolution) (Rakyan et al., 2008) will be informative in determining the minimum number of differentially methylated CpG sites to determine a tDMR. At the time this thesis was written there data were not available.

4.5.2 Correlation with HEP data

As part of the HEP study, a total of 253 unique amplicons corresponding to regulatory exonic and intronic regions associated with 90 MHC-genes were analysed for DNA methylation levels in multiple tissues and cell types (Eckhardt et al., 2006; Rakyan et al., 2004). Of these, 57 amplicons were from liver, sperm, placenta and $CD8^+$ T lymphocytes, the tissues/cell types used here. As it was noted in the previous section and in chapter 3, directly correlating methylation levels of these 57 values with the corresponding MeDIP-MHC tiling array data it is not possible. For this reason I only compared the 55 non-redundant tDMRs (see section 4.7) identified by my analysis with the tDMRs identified by the HEP. There was only one HEP tDMR overlapping with a tDMR identified by my analysis (figure 4.5). Based on MeDIP-MHC array data, this region (chr6:33,389,694-33,391,696) is less methylated in sperm compared to the other samples (figure 4.5a) and this agrees with the HEP values (figure 4.5b).

Eleven additional tDMRs were identified by the HEP within the four samples tested in this study. These tDMRs failed to be identified by the MeDIP-MHC tiling array approach probably due to the low resolution (2kb) of the MHC tiling array. Hence, it is possible that the MeDIP-MHC tiling array approach is not sufficient to detect DMRs smaller than 300 bp (300 bp is the average size of bisulphite sequencing amplicons;

section 2.2.3). On the other hand with the MeDIP-MHC tiling array approach I have managed to identify 54 additional tDMRs that were not reported by the HEP study. This may reflect the lower coverage of the MHC region by the HEP (2.5%) compared to my study (97%).

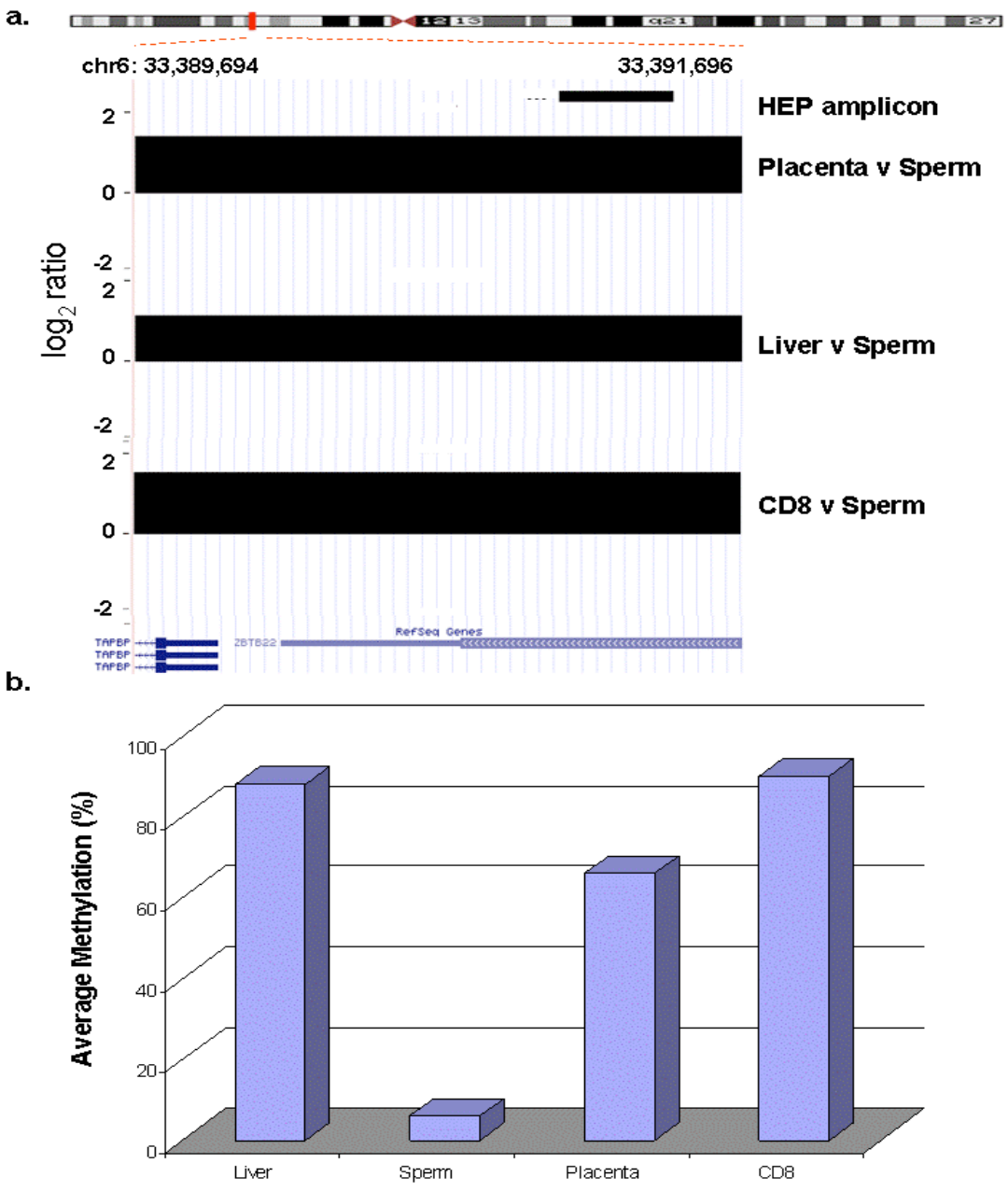

Figure 4.5 **Example of a tDMR identified by both HEP and MeDIP-MHC tiling array studies.** Comparisons of methylation profiles between samples (liver, placenta, sperm and CD8) identified a tDMR common to both studies. a. tDMR status based on pair-wise

comparisons of the $\log_2$ MeDIP enrichment ratios of the indicated tissues/cell types. Black boxes represent a tDMR that is more methylated in sample 1 of the comparison. b. Average methylation values based on HEP data. Absolute methylation levels of each CpG within the HEP amplicon (HEP amplicon ID: 536) were calculated using ESME (Lewin et al., 2004). Average methylation values for all CpGs in each of the four samples are indicated. Sperm is clearly less methylated compared to the other samples.

4.6 Correlation of tDMRs with expression data

I correlated the tDMRs with gene expression using data publicly available from the Genomics Institute of the Novartis Research Foundation Gene Expression Atlas database. This database contains whole-genome mRNA expression data obtained using human U95A Affymetrix microarray chips and mRNA extracted from a number of tissues, including liver, placenta and $CD8^+$ T lymphocytes (sperm was not included in this database) (Su et al., 2002). I identified the probes on the U95A Affymetrix which corresponding MHC loci overlapping with tDMRs according to the liver versus placenta, liver versus $CD8^+$ T lymphocytes and $CD8^+$ T lymphocytes versus placenta comparisons described above. Seven such probes were identified and the genomic features of the corresponding tDMRs are shown in Table 4.1 (see below). One of the probes (Affymetrix ID 40766_at that corresponds to C4A and C4B transcripts) shows a high inverse correlation between expression and methylation at these loci (Figure 4.6). Both loci are highly expressed and hypomethylated in the liver.

4.7 Non-redundant tDMRs

35 out of the 90 identified putative tDMRs were observed in more than one comparison (Figure 4.3; Appendix Table 4.1). Hence, there are 55 loci (average size 2kb), within the MHC region, that according to this study show tissue-specific methylation levels. I define these 55 loci as non-redundant tDMRs (to reflect the non-redundancy at the sequence level) and show their genomic locations in Figure 4.7a and Table 4.1. Based on this definition, about 3% of the MHC loci (average size 2kb)

show tissue specific methylation patterns. This is lower than what was found in the HEP study. According to HEP, 10% of the MHC loci analysed were characterised as tDMRs although only 2.5% of the MHC was tested. This difference can be due to: (i). array resolution and may indicate that there are additional tDMRs which the MeDIP-MHC tiling array approach failed to identify; or (ii). the eight additional samples tested by the HEP study (Eckhardt et al., 2006).

The C4 complement region is the region within the MHC with the highest density of non-redundant tDMRs (18) (Figure 4.7b). As discussed in the previous section, these tDMRs show inverse correlation with C4A and C4B expression patterns.

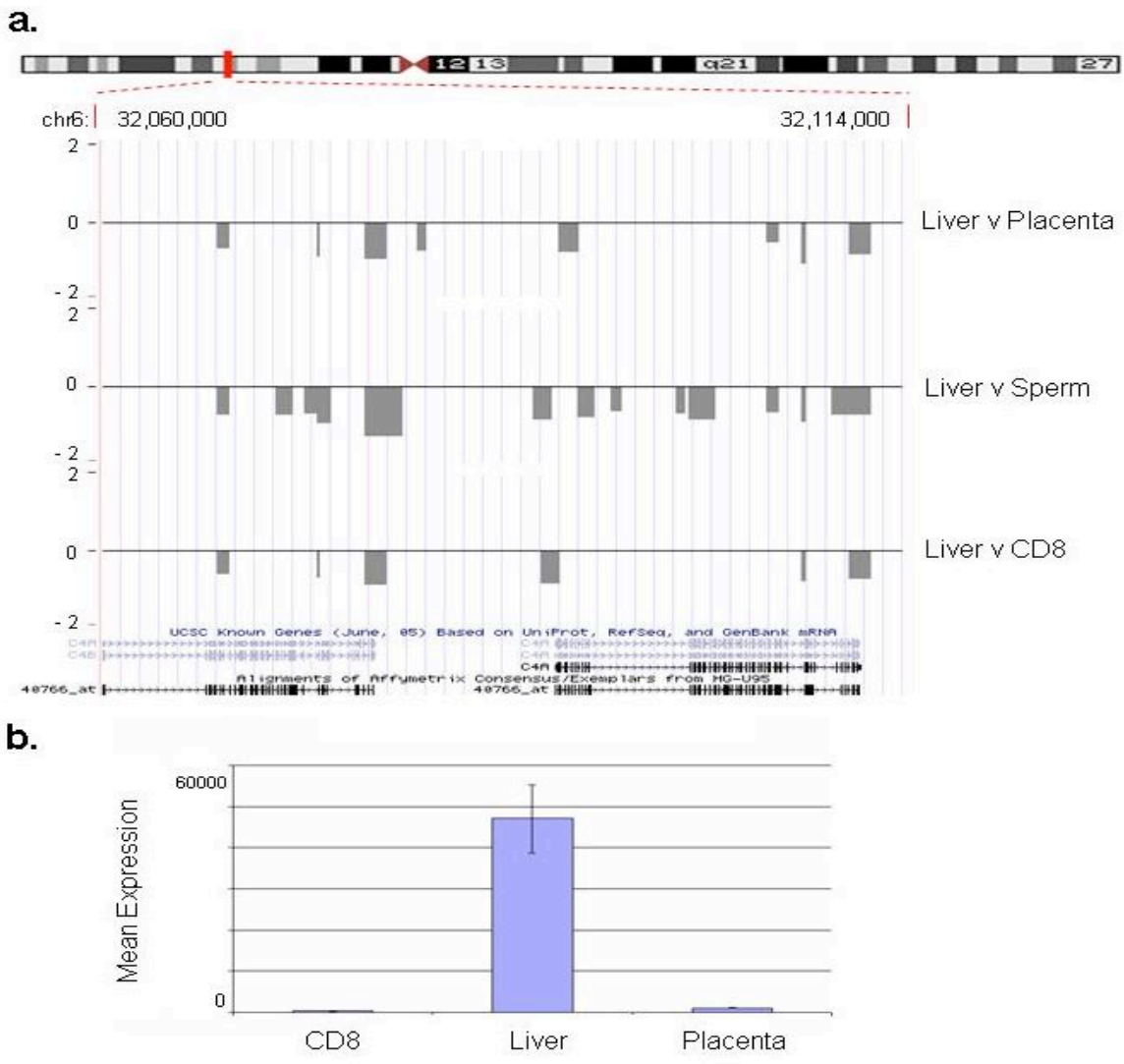

Figure 4.6. **Example of tDMRs correlating with tissue-specific gene expression.** a) tDMRs within the region encoding the C4A and C4B genes. Vertical axis shows the $\log_2$ ratio

of the two corresponding methylation profiles. Grey lines indicate regions (average size 2 kb) that are less methylated in liver compared to the other samples (placenta, sperm, CD8). Known genes and Affy_U95 expression array probes within this region are also shown. b). Expression of C4A and C4B. Graph shows the mean expression values of the probe corresponding to C4A and C4B (Affy_ID: 40776_at) transcripts in three samples tested: CD8, liver, placenta. C4A and C4B transcripts are highly expressed in liver tissue only. Data were taken from the GNF SymAtlas.

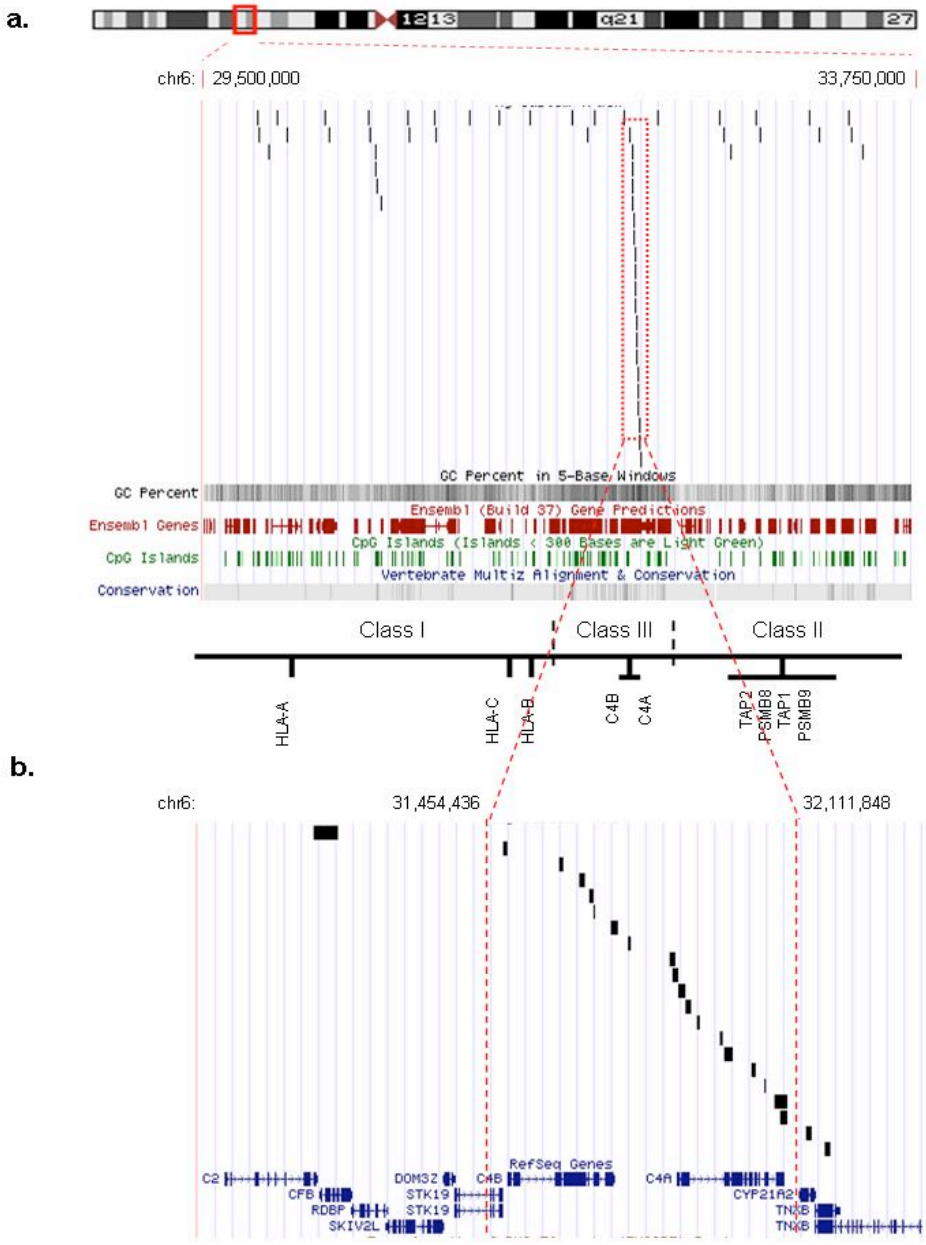

Figure 4.7 **Non-redundant tDMRs within the MHC region**. a. Screen-shot showing the locations of 55 non-redundant tDMRs identified in the MHC region after uploading of the data to the UCSC genome browser. Each vertical black line represents a putative tDMR. The high density of 18 tDMRs within the C4A and C4B complement region is clearly visible (boxed with

red doted line). Tracks showing C+G content, Ensembl genes, CpG islands and conservation are also shown. b. Enlargement of the C4A and C4B complement region showing the 18 overlapping or adjacent tDMRs (delimited by red dotted lines) which could be part of one large tDMR spanning the entire C4 complement region.

4.8 Genomic features of non-redundant tDMRs

To characterize the potential functionality of the 55 non-redundant tDMRs reported in the previous section, I analyzed them for a number of genomic features using the ENSEMBL functional build (Hubbard et al., 2007), as described in section 2.2.11. The result of this analysis is summarized in Table 4.1 and figure 4.8. I found the majority (39) of these tDMRs to map to intragenic regions and the minority (16) to map to intergenic regions. While repetitive elements were overrepresented within the intergenic tDMRs (44%), DNAse I sites and evolutionary conserved elements (ECRs) were overrepresented within the intragenic tDMRs (15%). Furthermore, only 2% of the tDMRs contained transcription start sites (TSS) and about 7% CpG islands and RNA polymerase II binding sites. In all, 21% of the tDMRs contained features significantly ($P < 0.05$) associated with regulation, such as CpG islands, DNase1 and RNA polII binding sites, TSSs and ECRs. Although only few other epigenetic data are yet publicly available for the MHC, I also analyzed the tDMRs for features associated with epigenetic function. Based on this analysis, 6 (11%) tDMRs have insulator protein (CTCF) binding sites, 13 correlated with the transcription-activating histone marks (H3K4me2, H3K36me3, H3K4me3 and H3K4me1) and two with the transcription-silencing mark H4K20me1. Interestingly, 54% of the H3K4me3 sites overlapping with both intragenic and intergenic tDMRs appeared to be close to DNaseI sites. Presence of both H3K4me3 and DNaseI sites indicates promoter regions. Finally, two tDMRs were associated with the histone variant H2AZ.

	chr6 coordinates (NCBI_35)	TSS	CTCF	H4K20me1	PolII	H3K4me2	H3K36me3	H3K4me3	DnaseI	H3K4me1	CpG island	ECR	H2AZ	repeats %	CpG%
1	29823989-29826356		x					x	x		x		x	28.63	2.94
2	30000805-30003606				x			x	x					12.6	9.28
*3	30228982-30231712													26.44	2.64
*4	30247370-30249040		x					x	x		x			4.73	9.1
*5	30565890-30568365			x	x		x	x						11.95	4.77
6	30721858-30724158							x					x	5.91	10.52
7	30731648-30734384													42.71	2.27
8	30891136-30893651													95.08	5.24
9	31709197-31711626											x		79.93	5.01
*10	31803609-31806450		x					x	x			x		0	2.88
11	31841070-31843352											x		0	11.05
12	32020686-32023216											x		18.4	5.61
13	32056738-32058031	x												6.57	3.935
*14	32067481-32068550													0	3.09
*15	32071709-32072864													0	5.61
16	32073608-32074514													0	5.02
17	32074474-32074660													13.67	3.97
*18	32077678-32079121													0	5.35
*19	32081199-32081780													19.53	5.4
20	32088659-32090434													0	3.685
*21	32088718-32090526													0	3.41
*22	32090749-32092076													1.96	4.22
23	32092057-32093147													0	2.38
24	32094350-32095101													100	1.33
25	32098656-32099323													100	3.59
26	32099573-32100214													0	3.875
*27	32104734-32105602													0	5.29
*28	32107212-32107398													0	5.35
29	32109195-32110435													9.995	5.6
*30	32110416-32111859													19.53	5.4
31	32115381-32116535											x		0	7.27
32	32119000-32120024											x		0	7.61
33	32223988-32226638							x			x			4.19	11.09
34	32659407-32660508							x	x		x			9	5
35	32817677-32820582													20.44	2.96
36	32836042-32838492													9.42	7.26
37	33192620-33193912		x											32.79	6.5
*38	33372651-33375048			x	x	x	x	x	x	x		x		10.93	8.76
39	33389687-33392295				x			x				x		2.3	7.51
40	29830203-29832660													6.08	7.77
41	29889483-29892066													21.2	4.15
42	29937894-29939594													38.78	2.48
43	30484481-30486798													96.59	1.04
44	30491424-30493923													1.4	2
45	30526624-30528439							x	x					3.54	7.33
46	30527803-30529467		x					x						3.54	6.73
47	30534798-30537070													42.42	1.26
48	30881555-30884300													98.55	4.27
49	31092038-31094660													74.72	7.51
50	31270669-31273172		x					x						4.59	2.75
51	31454436-31456982													8.59	5.84
*52	32590480-32591619													44.47	2.11
53	32622631-32625110													91.09	5.97
54	33132309-33134479								x					24.37	1.01
55	33450625-33452501													84.66	2.88

Table 4.1. **Genomic features of non-redundant tDMRs.** A total number of 55 non-redundant putative tDMRs (see text for definition – section 4.7) were identified. tDMRs are divided into 2 groups: intragenic and intergenic and their co-ordinates on chromosome 6 are provided. Enrichment of genomic features, including CpG islands, DNAseI sites, TSSs, ECRs, CTCF binding sites, RNA PolII binding sites, H4K20me1, H3K4me2, H3K4me3, H3K36me3 and

H2AZ was tested and marked by symbol 'x' if enrichment was statistically significant ($P < 0.05$). Percent CpG and repeat density were also determined and are shown for each tDMR. tDMRs 14 – 30 (intragenic) and 12 (intergenic) are mapping to the region encoding for C4A and C4B genes. Asterisks indicate the tDMRs that overlap with Affy_U95 expression array probes.

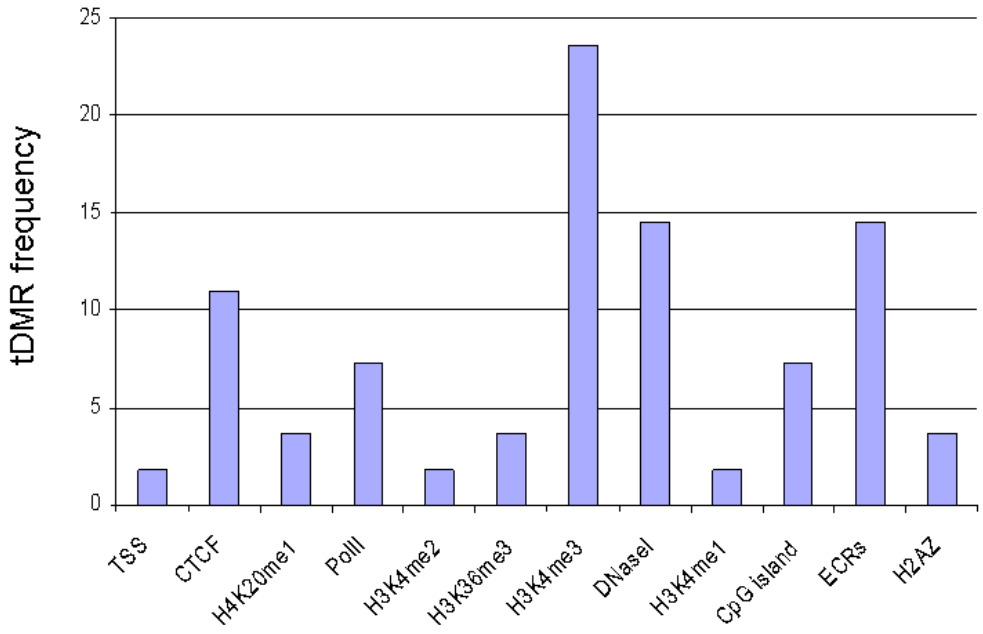

Figure 4.8. **Genomic features of putative tDMRs.** Proportion of putative tDMRs overlapping with genomic features. Histone mark H3K4me3 has the highest frequency whereas TSS, H3K4me2 and H3K4me1 have the lowest.

4.9 Discussion

I used the MHC-tiling array for DNA methylation profiling of four samples previously used for the HEP study: two tissues (liver and placenta), $CD8^+$ T lymphocytes and sperm. Comparison of these profiles allowed me to identify 55 putative, non-redundant tDMRs (90 in total). From these, I randomly selected 10% (6 tDMRs) for validation by an independent method. In all cases, tDMR status could be confirmed, indicating that the array is suitable for DNA methylation analysis and DMR identification. While the analysis carried out here is informative with respect to differential methylation between samples, it did not allow assigning absolute DNA methylation values to each tDMR. This is not a shortcoming of the array but a

limitation of the MeDIP assay which is highly dependent on CpG density as discussed in chapter 3 and illustrated in figure 3.7. Therefore, it was not possible to directly compare my data to the HEP data which, in any case, only cover about 2.5% of the MHC. Only one tDMR was identified by both studies. The on-going development of a novel algorithm employing a Bayesian de-convolution strategy to normalize MeDIP array data for CpG density is likely to overcome this current limitation in the near future (Down et al., 2008). For the same reason as mentioned above, the limited number of samples did not allow me to analyse the data for inter-individual variation which was observed in the HEP (Rakyan et al., 2004) and other studies (Flanagan et al., 2006).

I also correlated gene-associated tDMRs with expression data of the cognate genes available from the GNF SymAtlas. I found a strong correlation within the region encoding, for instance, the fourth component of the human complement (C4). C4 is an essential factor of the innate immunity and consists of two isoforms (C4A and C4B) that differ only in five nucleotides (Szilagyi et al., 2006). C4A and C4B are examples of copy number variants (CNVs) in the human genome. I show that regions within the 5'-UTR, 3'-UTR and the gene body of C4A and C4B are less methylated in liver than in sperm, placenta and $CD8^+$ T lymphocytes. As these two genes are expressed only in liver, it is possible that DNA methylation is the underlying mechanism controlling their expression. At this point, sensitivity and specificity should also be considered. While sensitivity is not an issue in this case (the experimental design normalizes for the genotype of the sample DNA), specificity is. As neither my array nor the Affymetrix U95 array can discriminate between C4A and C4B (which are more than 99% identical), it was not possible to ascertain whether or not these two loci are differentially methylated in this case. Selective hypermethylation is a known mechanism for silencing of duplicated genes (Rodin and Riggs, 2003).

Finally, genomic features associated with the 55 putative tDMRs were identified. Interestingly, only 21% of the tDMRs overlap with known genomic features. It is

possible that the rest of the tDMRs either do not have any genomic function or they are associated with novel genomic features and control elements that may be interesting to investigate further.

4.10 Conclusion

Using MeDIP, I have demonstrated the application of the MHC tiling array for DNA methylation profiling and the identification of tissue-specific differentially methylated regions (tDMRs). Based on the analysis of two tissues and two cell types, I identified 90 tDMRs within the MHC and described their characterisation. Its successful application for DNA methylation profiling indicates that this array represents a useful tool for molecular analyses of the MHC in the context of medical genomics. In the following chapter I describe its application for the investigation of a MHC class I^- phenotype which is commonly associated with cancer (Seliger et al., 2002; The International HapMap Project, 2003).

Chapter 5

Phenotype-specific DMR (pDMR) screen

5.1 Introduction

The MHC is associated with many complex diseases including infectious, autoimmune and inflammatory diseases as well as cancer. In many cases, their aetiologies are polygenic and involve genetic, epigenetic and environmental factors (de Bakker et al., 2006; Garcia-Lora et al., 2003; Rioux and Abbas, 2005; Vyse and Todd, 1996). Although past studies have generated extensive data for the genetics of the MHC (Horton et al., 2008; Nejentsev et al., 2007; Stewart et al., 2004; Traherne et al., 2006) resulting in important contributions to medicine, further studies are necessary to better understand the causes of such diseases.

My main aim was to elucidate the role of differentially methylated regions (DMRs) (see chapter 1) within the MHC in the context of a phenotype that is associated with defects in the MHC class I processing and presentation pathway (Chang et al., 2003; Groothuis et al., 2005; Parham, 2005).

MHC class I molecules have two critical functions: 1. to bind small (8-10mer) peptides derived from protein antigens, and 2. to present bound peptides to T-cell receptors (Flutter and Gao, 2004; Held and Mariuzza, 2008). They are cell surface glycoproteins consisting of two subunits (figure 5.1): a highly polymorphic heavy chain (α-chain) encoded by one of the three classical MHC loci *HLA-A*, *HLA-B* and *HLA-C* and a non-polymorphic light chain (β–chain) called β2-microglobulin (B2M) encoded outside the MHC. Proper folding of MHC class I molecules requires the formation of three disulfide bonds, one in the α3 immunoglobulin domain, one in the α2 immunoglobulin domain and one in the β chain (figure 5.1).

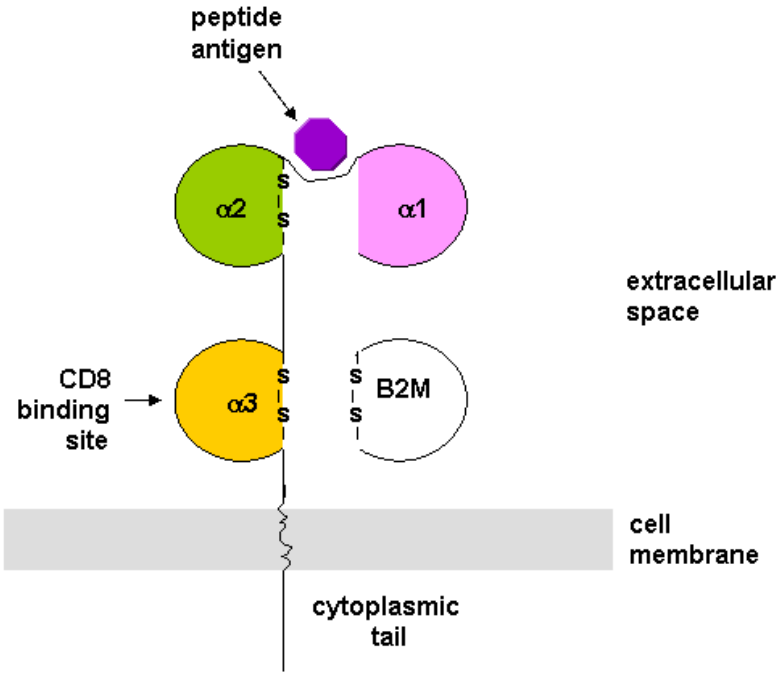

Figure 5.1. **MHC class I molecule.** Diagram of the MHC class I heavy chain associated with B2M and a peptide antigen presented on the cell surface. The heavy chain, also referred as α chain, is a 43kDa transmembrane glycoprotein consisting of three extracellular domains α1, α2 and α3. α1 and α2 are polymorphic and form a deep grove where the peptide antigen can bind. B2M which represents the light chain, has a molecular weight of 12 kDa and is non-polymorphic. The disulfide bonds (-S-S-) are also shown.

The peptide-MHC class I complexes are assembled in the endoplasmatic reticulum (ER) while going through a multifactorial pathway called the MHC class I pathway (Hewitt, 2003; Pamer and Cresswell, 1998). The latter involves at least eight components in addition to HLA-A, HLA-B, HLA-C and B2M: PSMB8, PSMB9, TAP1, TAP2 and TAPBP which are encoded within the MHC as well as the non-MHC encoded proteins ERp57, calnexin (CANX) and calreticulin (CALR) (figure 5.2). The components of the MHC class I pathway are discussed in more detail in sections 5.3 and 6.2.

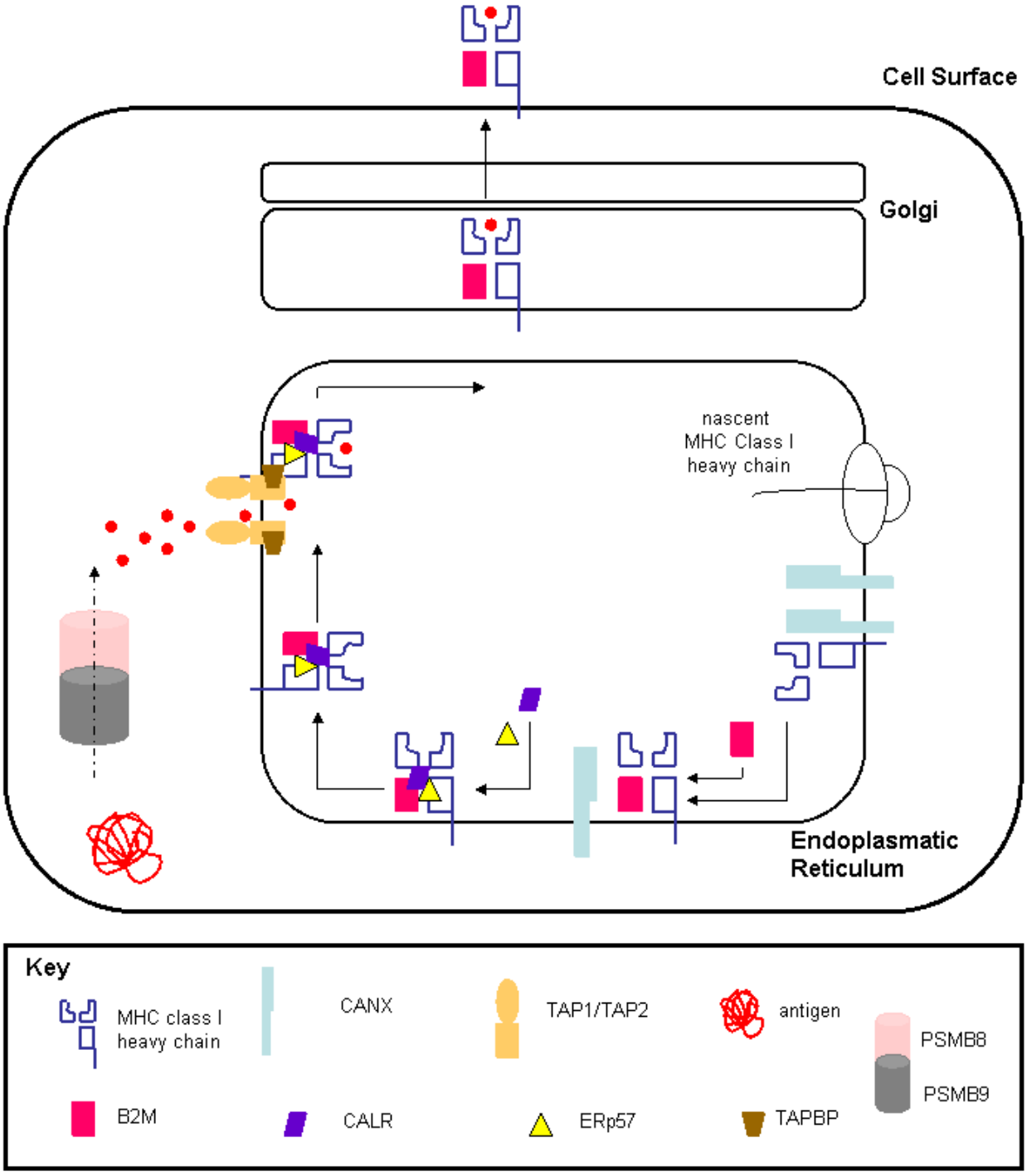

Figure 5.2 **MHC class I antigen presentation pathway.** Antigens are proteolytically processed in the cytosol by the proteasome (PSMB8/PSMB9). Peptides generated by the proteasome are translocated into the ER lumen by TAP. MHC class I molecules (heavy chain and associated B2M) fold and assemble in the ER lumen with the aid of the ER chaperones CANX, CALR and ERp57. The complex of MHC class I

molecules, chaperones, TAP and TAPBP facilitates peptide binding. Peptide-loaded MHC class I molecules dissociate from TAP and are transported through the secretory pathway to the cell surface.

In cases where any of the MHC class I pathway components are defective, intracellular MHC class I molecules (figure 5.1) can be subjected to unfolding and degradation resulting into MHC class I^- phenotypes (Hughes et al., 1997). Such phenotypes have been reported to be associated with many MHC related diseases including cancer where immune evasion can occur through repression of antigen presentation (Chang et al., 2003; de Visser et al., 2006). Although the MHC class I^- phenotype has been studied extensively, the underlying mechanism(s) remain unclear. Recent studies have implicated DNA methylation in the expression of MHC class I genes in cancer but their analysis was restricted to promoter regions only (Fonsatti et al., 2007; Fonsatti et al., 2003; Manning et al., 2008; Nie et al., 2001).

I aimed to pursue a more comprehensive study of the role of DNA methylation in the MHC class I pathway. For this, I used the samples described in section 5.2 and performed an analysis that can be divided into three parts:

Part 1. Expression analysis of the genes *HLA-A, HLA-B, HLA-C, TAP1, TAP2, PSMB8, PSMB9* and *TAPBP* which I call candidate genes (section 5.3). These genes are encoded within the MHC and are involved in the MHC class I antigen presentation pathway. The effect of inhibition of DNA methylation in the expression of these eight genes was also tested (section 5.4)

Part 2. Identification of differentially methylated regions (DMRs) between cell lines displaying the MHC class I^- phenotype (nine cancer cell lines) and two control cell lines (sections 5.5.1 and 5.5.2). To this end I used the MeDIP-MHC tiling array approach (chapter 3).

Part 3. Data generated under parts 1 and 2 were combined to identify:

(i). DMRs that can be associated with the MHC class I^- phenotype (section 5.5.3). I call these DMRs phenotype-specific DMRs (pDMRs).

(ii). DMRs overlapping with the coding regions of the eight candidate genes that may be hypermentylated as the result of low transcriptional levels (section 5.6). Low transcriptional activity has been reported to drive DNA hypermethylation in some instances (Bird, 2002; Meissner et al., 2008).

(iii) Prominent DMRs within the MHC region which, although not associated with the MHC class I^- phenotype, may be important for the regulation of MHC genes in general (section 5.7).

This analysis is described in more detail in the following sections.

5.2 Samples used for pDMR screen

For the pDMR screen I used samples with abnormal expression levels of one or more of the genes involved in the MHC class I antigen presentation pathway. I used cancer cell lines for two reasons: i. MHC class I^- phenotype is known to be associated with many cancer types; ii cancer cell lines were easy to obtain and work with. Based on published data (Blanchet et al., 1992) and availability, nine cancer cell lines were chosen for this screen. As positive controls for MHC class I pathway gene expression, two peripheral blood EBV-transformed cell lines (GM15510 and GM10851) were selected. Table 5.1 shows the characteristics of each of the cell lines chosen.

	Ethnicity	Age	Gender	Tissue	Disease	Levels of MHC class I expression
T47D		54	female	duct	carcinoma	low
578T	Caucasian	74	female	breast	carcinoma	
H69	Caucasian	55	male	lung	carcinoma	low
Colo-205	Caucasian	70	male	colon	adenocarcinoma	high
CCRF-CEM	Caucasian	4	female	blood	leukemia	low
MCF7	Caucasian	69	female	breast	adenocarcinoma	
MDA-MB-231	Caucasian	51	female	breast	adenocarcinoma	high
MDA-MB-361	Caucasian	40	female	breast	adenocarcinoma	intermediate
K562	Caucasian	53	female	bone marrow	leukemia	low
GM15510				blood	-	normal
GM10851	Caucasian	52	male	blood	-	normal

Table 5.1 **Characteristics of cell lines used in the pDMR screen.** The indicated expression status is based on published protein analysis (Blanchet et al., 1992). Empty boxes indicate that the corresponding information was not available.

MHC class I molecules are expressed in a wide range of tissues and cell types, including the tissues of origin of the cell lines selected here (Lechler, 2000). Although cancer cell lines are known to frequently display karyotypic variability (Roschke et al., 2003) this should not affect the methylation analysis as my experimental design (MeDIP-enriched versus total DNA) normalizes for the given genotype (chapter 3).

Finally, it should be noted that the two EBV transformed cell lines (GM15510 and GM10851), although normal with respect to the MHC class I^- phenotype, are expected to have modified methylation patterns compared to the primary cells from which they have been established. EBV virus has been shown to activate DNA methyltransferase activity by increasing the expression of DNMTs (Flanagan, 2007; Tsai et al., 2002).

5.3 Relative expression of MHC class I pathway genes encoded within the MHC

There are eight genes involved in the MHC class I pathway that are encoded within the MHC region: *HLA-A, HLA-B, HLA-C, TAP1, TAP2, PSMB8, PSMB9* and *TAPBP*. All eight genes are encoded within the MHC. Previous studies have shown that genes involved in the same pathway (e.g. members of the TGF-beta signalling pathway) as well as genes encoded within the same chromosomal band (e.g. 4Mb band of chromosome 2q.14.2) can be epigenetically silenced (Frigola et al., 2006; Hinshelwood et al., 2007). These studies support the notion that the eight genes investigated here maybe regulated concordantly by epigenetic mechanisms. These genes are discussed in more detail below:

HLA-A, HLA-B and *HLA-C* genes

Each of these genes encodes an α-chain of a class I molecule (figure 5.1). They are the most polymorphic human loci known to date (de Bakker et al., 2006; Horton et al., 2008; Traherne et al., 2006). It has been proposed previously that promoter methylation of these three loci may be involved in their down-regulation in cancer cells (Nie et al., 2001; Serrano et al., 2001).

TAP and *PSMB* genes

These genes are encoded within a tight cluster in the MHC class II region. The products of the two *TAP* genes, *TAP1* and *TAP2*, are members of the ATP-binding cassette (ABC) transporter superfamily (Townsend and Trowsdale, 1993). They form a complex in the endoplasmatic reticulum (ER) membrane that translocates peptide antigens from the cytoplasm into the lumen of the ER (figure 5.2) (Androlewicz and Cresswell, 1994; Kelly et al., 1992).

The *PSMB* genes, *PSMB8* and *PSMB9*, encode components of the proteasome (figure 5.2) (Gaczynska et al., 1993; Glynne et al., 1991). *PSMB9* has been implicated in proteolytic digestion of cytoplasmic proteins. Production of *PSMB8* and *PSMB9* components has been shown to alter the proteolytic activity of the proteasome to favour antigen peptides capable of binding to the peptide groove of MHC class I molecules (figures 5.1 and 5.2).

TAP1 and *PSMB9* share a bidirectional promoter (Wright et al., 1995). This is a minimal 593bp region which is sufficient for concurrent expression in both directions which implicates that these two genes are controlled simultaneously by common elements.

In cancer cells and human papilloma virus 16-associated tumours, epigenetic induction of MHC class I surface expression has been shown to be associated with the up-regulation of the following genes: *TAP1*, *TAP2*, *PSMB8* and *PSMB9* (Manning et al., 2008; Setiadi et al., 2007).

TAPBP

TAPBP is encoded within the class II region of the MHC. Its product acts as a chaperone that facilitates the association of MHC class I molecules with peptide antigens (figure 5.2) (Lauvau et

al., 1999). *TAPBP* has been shown to be epigenetically regulated in melanoma cells (Khan et al., 2008)

5.3.1 Expression analysis

According to published data MHC class I molecules show differential levels of expression and abundance at the surface of the cells I chose to use (Blanchet et al., 1992) (table 5.1). I analysed further the expression levels of all MHC encoded genes (eight genes) involved in the MHC class I pathway. To this end I performed quantitative real time PCR and calculated the difference in total mRNA levels of each of the eight genes between the cancer and the two normal EBV-transformed cell lines (shared controls). At this point it should be noted that all these genes have multiple isoforms. In order to simplify the analysis, primers were designed to capture all possible isoforms of each of the eight genes. Analysis of the data was done as described in section 2.2.4.3.

According to my data, *HLA-A, HLA-B, TAP1* and *PSMB8* were down-regulated in all cancer cell lines, in both biological replicates (figure 5.3), relative to the two controls (fold difference >1.5). *HLA-C* mRNA levels were close to normal in three cancer cell lines (CCRF-CEM, Colo-205 and MDA-MB-361; fold difference <1.5) and reduced in the rest six. *TAP2*, *PSMB9* and *TAPBP* levels were normal only in the T47D cell line and down regulated in the rest, apart from *PSMB9* which was the only gene that showed about 2-fold up-regulation in one cancer cell line (CCRF-CEM). Expression data are shown in figure 5.3 and are summarised in table 5.2.

With few exceptions, the eight MHC genes tested in this section seem to be co-ordinately down-regulated in almost all cancer cell lines tested. This finding agrees with previous publications (Johnsen et al., 1998; Meissner et al., 2005; Romero et al., 2005) and indicates that the eight MHC genes may share a common regulatory pathway. This is further supported by studies

showing that treatment of antigen presenting cells with the cytokines INF-γ or TNF-α induces coordinated changes at different steps of the MHC class I processing and presentation pathway (Dejardin et al., 1998). In addition, it has been shown previously that treatment of cancer cell lines with DNA methylation inhibitors resulted in up-regulation of MHC class I molecules, suggesting that DNA methylation plays a role in the regulation of MHC class I pathway genes (Fonsatti et al., 2007; Fonsatti et al., 2003; Nie et al., 2001).

Epigenetic modifications have the potential to target expression of multiple genes simultaneously. This can be done either by the epigenetic silencing or up-regulation of a common regulatory factor involved in expression of all genes that are part of the same pathway, or by simultaneous aberrant alterations of epigenetic marks at loci of multiple genes involved in the same pathway or encoded in the same chromosomal region (Frigola et al., 2006; Hinshelwood et al., 2007). I attempted to investigate the role of DNA methylation in the concordant silencing of genes involved in the MHC class I pathway as described in the following sections.

	HLA-A	***HLA-B***	***HLA-C***	***TAP1***	***TAP2***	***PSMB8***	***PSMB9***	***TAPBP***
T47D	**-**	**-**	**-**	**-**	**+/-**	**-**	**+/-**	**+/-**
MDA-MB-231	**-**	**-**	**-**	**-**	**-**	**-**	**-**	**-**
MDA-MB-361	**-**	**-**	**+/-**	**-**	**-**	**-**	**-**	**-**
CCRF-CEM	**-**	**-**	**+/-**	**-**	**-**	**-**	**+**	**-**
Colo-205	**-**	**-**	**+/-**	**-**	**-**	**-**	**-**	**-**
H69	**-**	**-**	**-**	**-**	**-**	**-**	**-**	**-**
578T	**-**	**-**	**-**	**-**	**-**	**-**	**-**	**-**
K562	**-**	**-**	**-**	**-**	**-**	**-**	**-**	**-**
MCF7	**-**	**-**	**-**	**-**	**-**	**-**	**-**	**-**

Table 5.2. **Summary of MHC encoded MHC class I pathway gene expression.** Relative expression levels were calculated for all cancer cell lines and each of the eight genes involved in the class I pathway compared to two normal control cell lines. Symbol – indicates reduced expression levels; + indicates upregulation and +/- denotes that the expression of the corresponding gene is similar in both cancer and

control cell lines. Only differences greater than 1.5 fold (in both biological replicates, figure 5.3) were considered to be significant.

Figure 5.3. **Relative expression of MHC encoded MHC class I pathway genes.** mRNA levels of *HLA-A, HLA-B, HLA-C, TAP1, TAP2, PSMB8, PSMB9* and *TAPBP* were determined by quantitative RT-PCR. After normalizing expression to *UBC* (section 2.2.4.3), the fold change in expression levels was calculated relative to the two normal EBV-transformed cell lines (shared controls). Figure shows data corresponding to two biological replicates. The mean of three technical replicates (for each biological replicate) is shown.

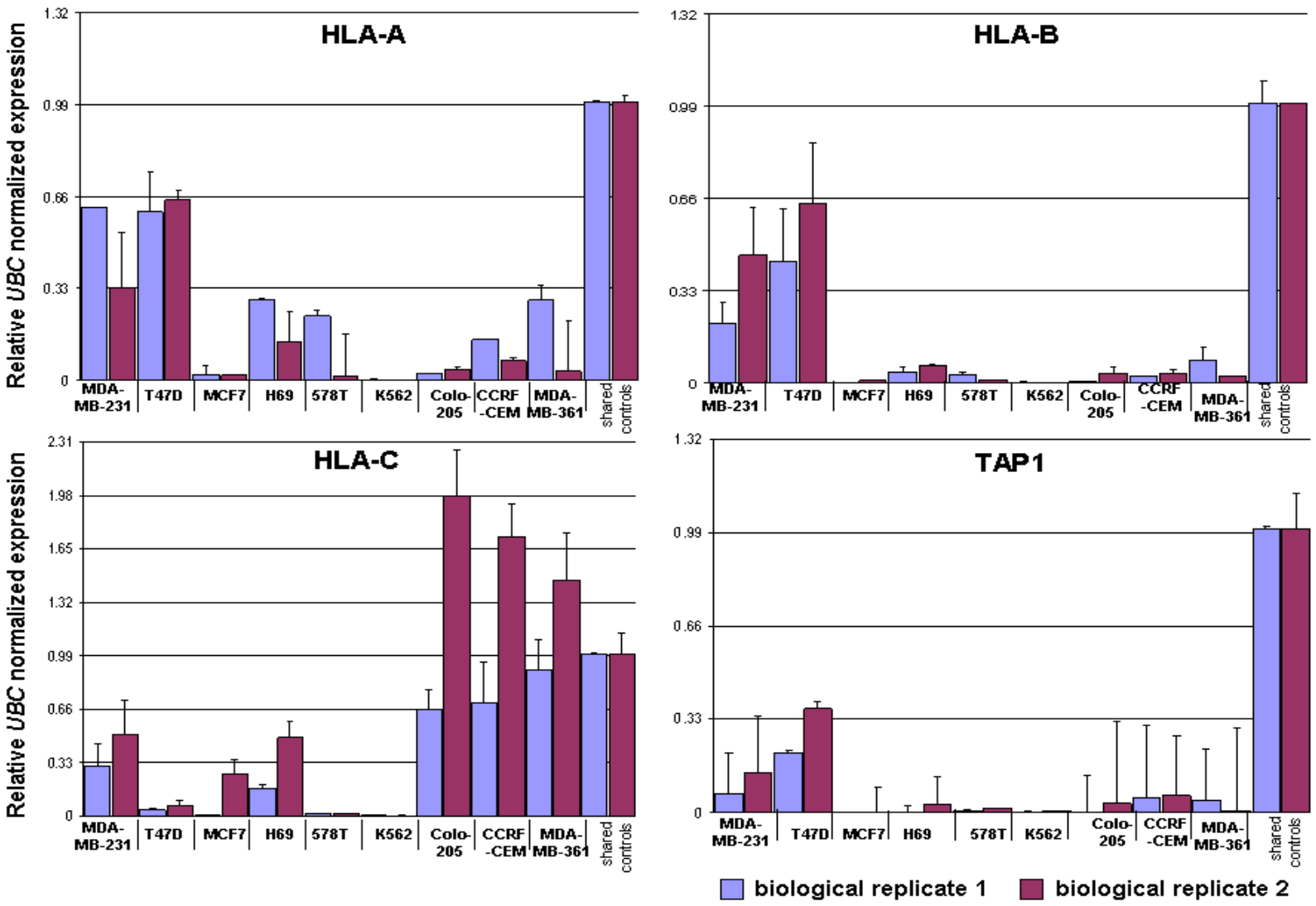
HLA-A
HLA-B
HLA-C
TAP1
Relative UBC normalized expression
1.32
0.99
0.66
0.33
0
2.31
1.98
1.65
MDA-MB-231
T47D
MCF7
H69
578T
K562
Colo-205
CCRF-CEM
MDA-MB-361
shared controls
biological replicate 1
biological replicate 2

Figure 5.3

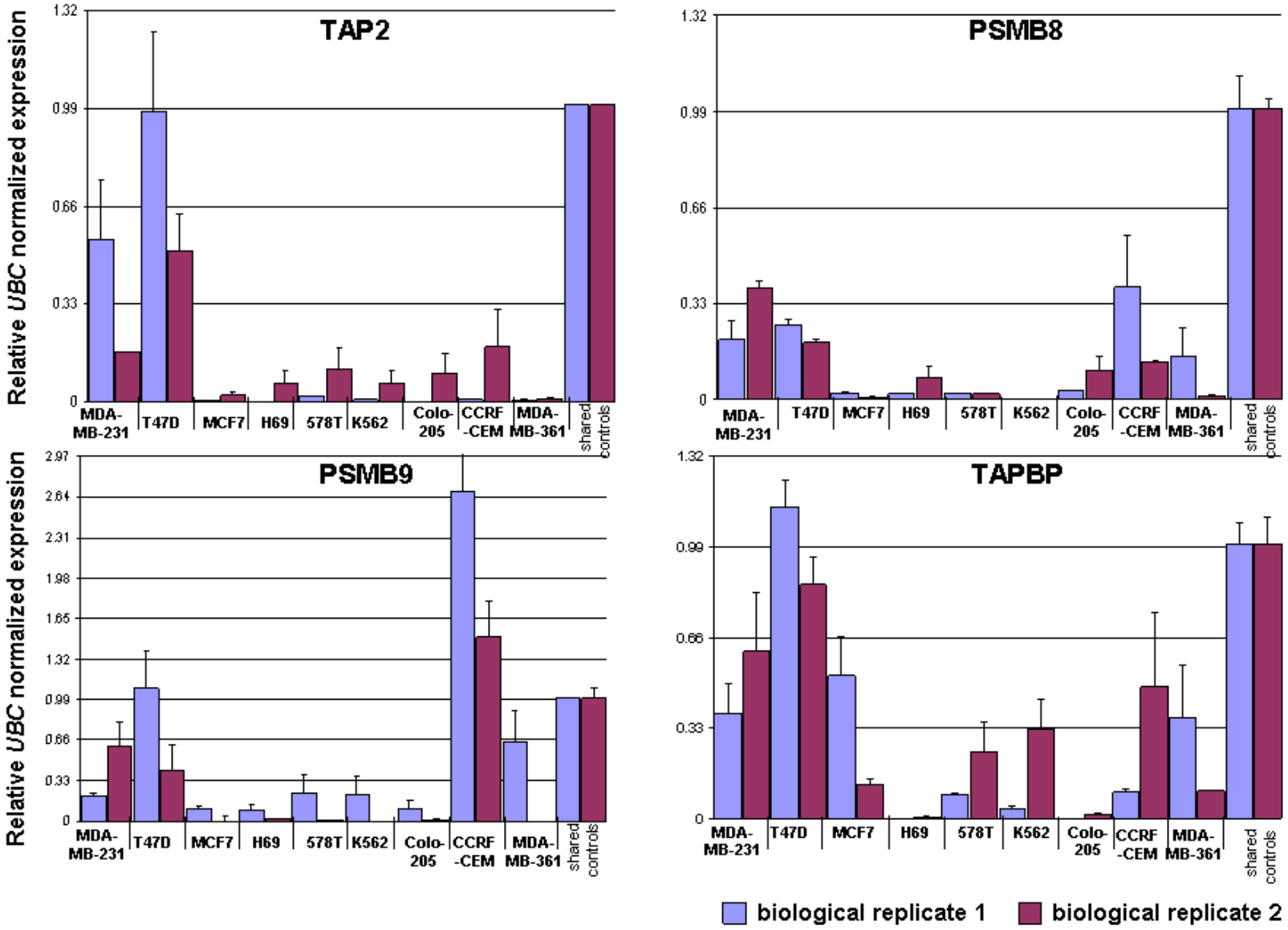
TAP2
PSMB8
PSMB9
TAPBP
Relative UBC normalized expression
1.32
0.99
0.66
0.33
0
2.97
2.64
2.31
1.98
1.65
MDA-MB-231
T47D
MCF7
H69
578T
K562
Colo-205
CCRF-CEM
MDA-MB-361
shared controls
biological replicate 1
biological replicate 2

Figure 5.3

5.4 Effect of DNA methylation inhibition on MHC encoded class I pathway genes

DNA methylation has been shown to co-ordinately change the expression of multiple genes in a chromosomal segment as well as genes involved in the same pathway (Frigola et al., 2006; Hinshelwood et al., 2007). The eight genes under investigation in this chapter are encoded within the same chromosomal band and are all involved in the same pathway, the MHC class I presentation pathway. According to my expression analysis (section 5.3) MHC-encoded MHC class I pathway genes are co-ordinately expressed.

I sought to investigate the effect of DNA methylation on the down-regulation of MHC class I pathway genes. For this I selected two cancer cell lines with the lowest expression of MHC class I pathway genes (MCF7 and 578T; figure 5.3) and treated them with increasing doses of the DNA methyltranferase inhibitor 5-aza-2'-deoxycytidine (5-aza-CdR) (sections 1.3.5 and 2.2.1.3.5). Real time qPCR analysis of MHC class I pathway gene expression revealed that 5-aza-CdR treatment can induce a marked increase of expression for most of the genes, in a dose-dependent manner (figure 5.4). In MCF7 cells, expression of all eight genes was up-regulated compared to untreated cells. The most dramatic effect was on the expression of the *PSMB8* gene (~6000-fold increase) whereas *TAPBP* and *TAP2* gene expression levels were the least affected (4-fold and 9-fold increase respectively) (figure5.4a). In 578T cells, methylation inhibition affected mainly the expression of *HLA-A* and *HLA-C* (20-fold increase) followed by *PSMB8* (6-fold increase). Treatment had no effect on the expression of the *TAP2* and *TAPBP* genes whereas for the rest of the genes, a small increase (4-fold) in mRNA levels was observed (figure 5.4b).

Although the degree of expression restoration of the MHC class I pathway genes varies between MCF7 and 578T cells, it is clear that 5-aza-CdR can co-ordinately up-regulate

genes involved in the pathway. Hence, this implicates a role for DNA methylation in the regulation of MHC class I genes.

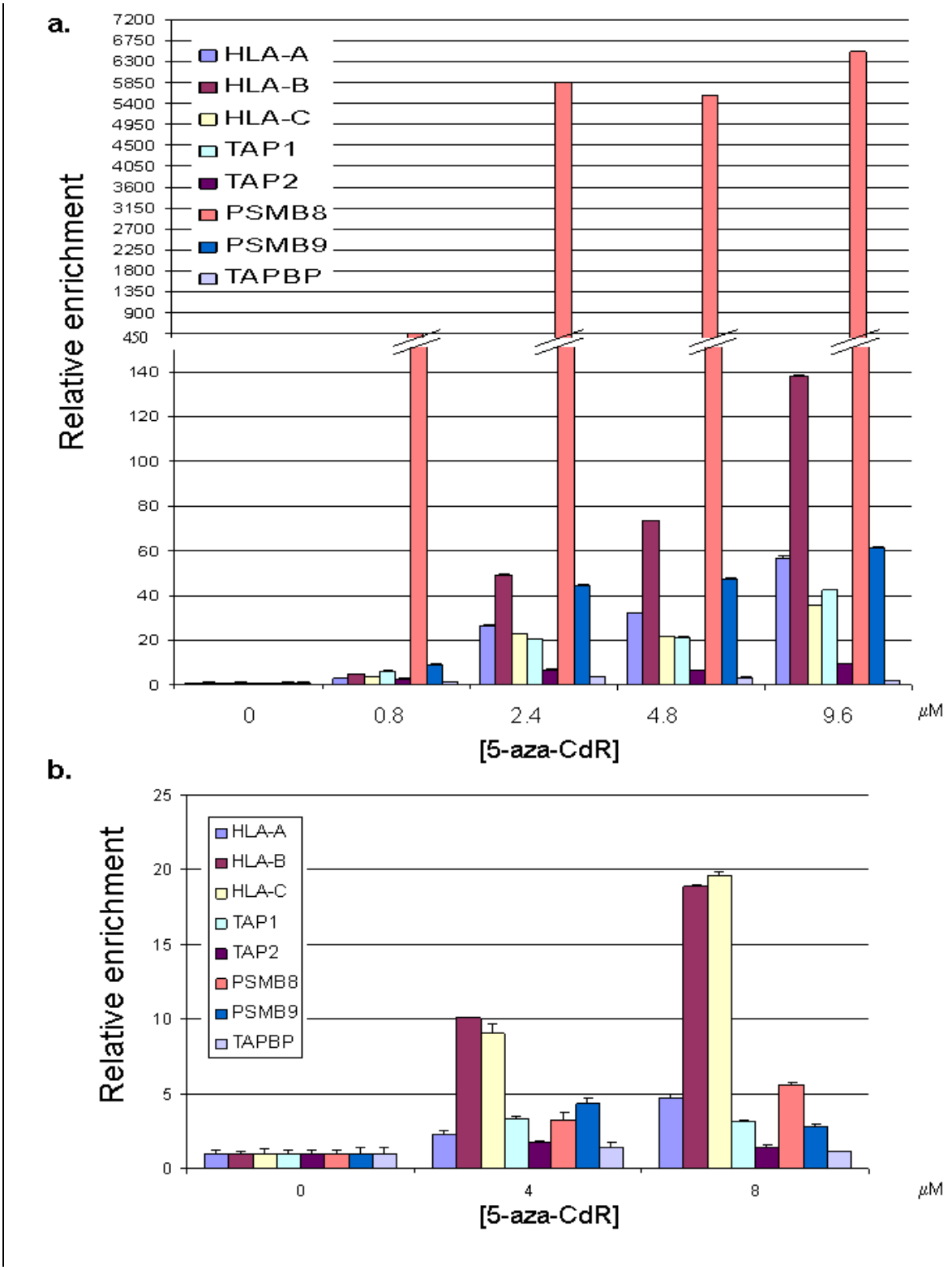

Figure 5.4. **Restoration of gene expression after DNA methylation inhibition in two cancer cell lines.** mRNA levels of *HLA-A, HLA-B, HLA-C, TAP1, TAP2, PSMB8, PSMB9* and *TAPBP* were determined in MCF7 (a) and 578T (b) in both untreated and 5-aza-CdR treated cells. After normalizing expression to *UBC*, the fold change in expression was calculated relative to untreated cells (0 μM 5-aza-CdR). The mean of six measurements (two biological replicates and three technical replicates for each) is shown in part a. The mean of three technical replicates is shown in part b.

At this point it is worth mentioning that, although the DNA demethylation capabilities of 5-aza-CdR are well characterised, this drug may exhibit alternative mechanisms of transcription reactivation. It has been shown for instance that 5-aza-CdR can induce expression of genes lacking CpG methylation (Scott et al., 2006; Soengas et al., 2001) and that it can be associated with H3K9 demethylation (Coombes et al., 2003; Fahrner et al., 2002; Nguyen et al., 2002). Also, as 5-aza-CdR is a global demethylation agent, 5-aza-CdR assays are not efficient to confirm that methylation of a specific genomic region affects expression of a gene. Therefore, the possibility that other epigenetic marks, as well as DNA methylation, and that demethylation of potential control regions outside the MHC may have an effect on MHC class I regulation should not be ignored.

Following verification of the role of DNA methylation in the concordant down-regulation of MHC class I pathway genes I sought to investigate further if aberrant DNA methylation patterns within the MHC region are involved in this phenotype.

5.5 MHC DMRs associated with the MHC class I$^-$ phenotype

The main aim of this chapter was to investigate if there are DMRs within the MHC that could be associated with the expression of MHC class I genes encoded within the MHC. To this end:

5.5.1 I generated methylation profiles for all eleven cell lines used here (table 5.1) by using the MeDIP-MHC tiling array approach (chapter 3).

5.5.2 I identified methylation differences between each of the nine cancer cell lines (table 5.1) and the shared controls. Methylation differences between two samples are referred to as DMRs.

5.5.3 I correlated the DMRs (5.5.2) with expression data based on the analysis described in section 5.3. DMRs that showed an association with expression data were called phenotype specific DMRs (pDMRs).

5.5.1 Generation of DNA methylation profiles within the MHC region

I generated methylation profiles for all eleven cell lines tested using the MHC tiling array in combination with MeDIP as described in chapter 3. In accordance to what was observed in chapter 4, the overall methylation profiles along the MHC are very similar in all 11 cell lines tested (figure 5.5). The profiles show similar patterns with the C+G content across the MHC region. Although MeDIP enrichment profiles do not allow absolute DNA methylation values to be called, they enable detection of relative methylation differences between samples (Keshet et al., 2006; Weber et al., 2005). These profiles were used to identify methylation differences between the shared control cell lines and the cancer cell lines tested here and subsequently for pDMR identification as described below.

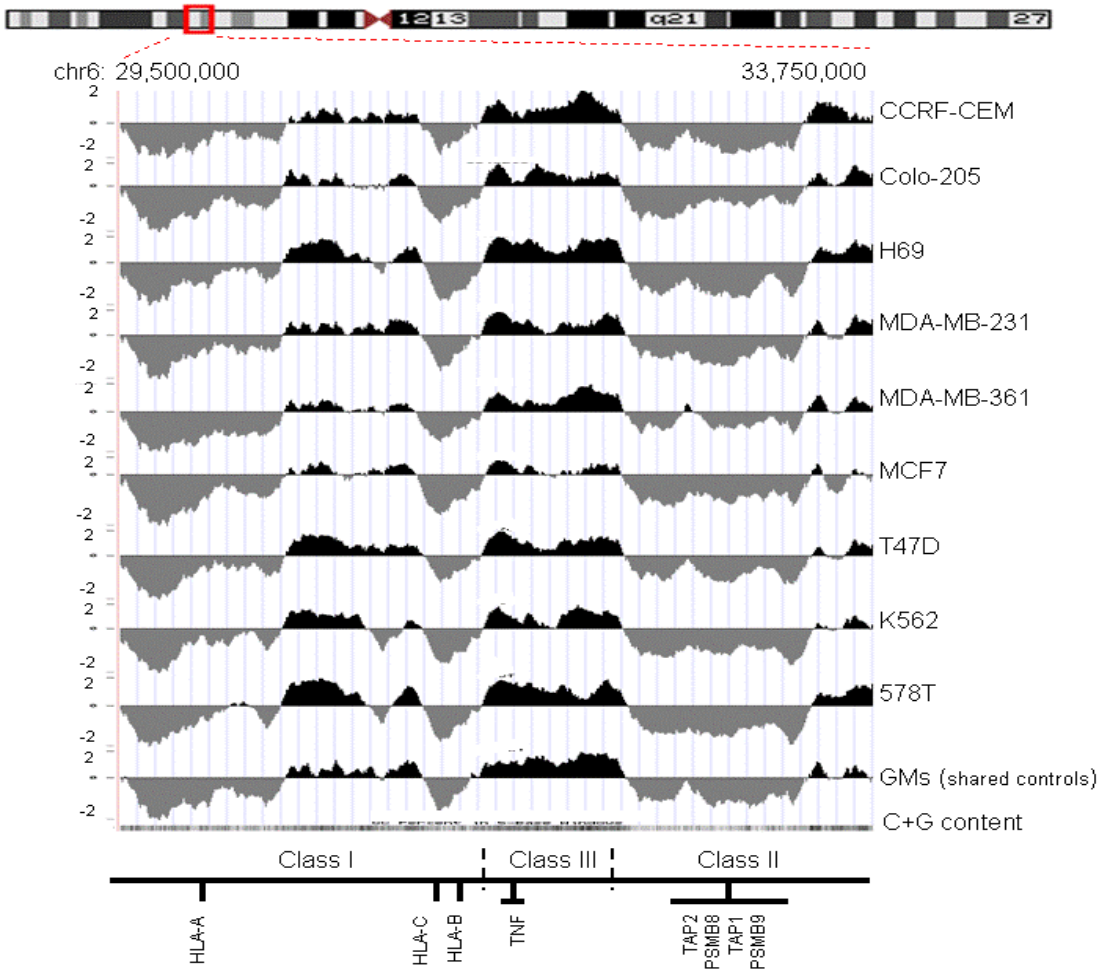

Figure 5.5 **DNA methylation profiles of the MHC.** For each of the 11 cell lines tested the $\log_2$ signal ratios (MeDIP/input) were uploaded as individual tracks to the UCSC genome browser using the 'smooth' function. For each sample the mean of two biological replicates was calculated. GMs-normal refers to the average values corresponding to the two control cell lines GM10851 and GM15510. Regions enriched or depleted in DNA methylation are shaded in black and grey, respectively. Also shown is a track of the C+G content (the darker the shading, the higher the C+G content). The approximate positions of the MHC class I, II and II subregions and some landmark genes are indicated.

5.5.2. DMRs between the cancer cell lines and shared controls

I identified differentially methylated regions (DMRs) between each of the nine cancer and the two normal EBV-transformed cell lines. The analysis for DMR identification was done in a similar manner as for tDMR identification (chapter 4).

At this point it is worth mentioning that the control cell lines originate from peripheral blood whereas the cancer cell lines originate from a variety of tissues (table 5.1). Hence, it should be expected that some of the DMRs are due to tissue-specific differences between the control and the corresponding cancer cell line. I reasoned that I should remove from the DMR list those DMRs that have already been characterised as tDMRs by the tDMR screen (chapter 4). Of the DMRs identified, 18 overlapped with tDMRs. These 18 DMRs were removed from further analysis. Their coordinates are given in appendix table 5.1. The genomic location of the remaining DMRs is shown in figure 5.6 (coordinates are in appendix table 5.2). A total of 552 putative DMRs were identified, of which 139 were present in multiple comparisons whereas 144 were identified only once. Hence 283 loci (average size 2kb) within the MHC region show methylation differences between the cancer cell lines and the two shared controls. I defined these 283 loci as non-redundant putative DMRs (to reflect the non-redundancy at the sequence level) in a similar manner as described in section 4.7 (non-redundant tDMRs). Figure 5.6 shows the location of the non-redundant DMRs as well as the 55 non-redundant tDMRs identified in chapter 4. The five fold difference between the number of the non-redundant DMRs and non-redundant tDMRs may be the outcome of more pair-wise comparisons (nine in the pDMR sceen and six in the tDMR) in the pDMR sceen.

The cell line with the most DMRs is MCF7 (141 DMRs) and the cell line with the least DMRs (43 DMRs) is T47D. The CCRF-CEM cell line, which is the only cancer cell line of the same tissue source as the shared controls (table 5.1), has 46 DMRs.

All of the 283 non-redundant DMRs are candidate methylation regulatory elements for the MHC class I^- phenotype. In the following section I filtered this list of DMRs further to identify those that show the highest co-occurrence with the phenotype under investigation.

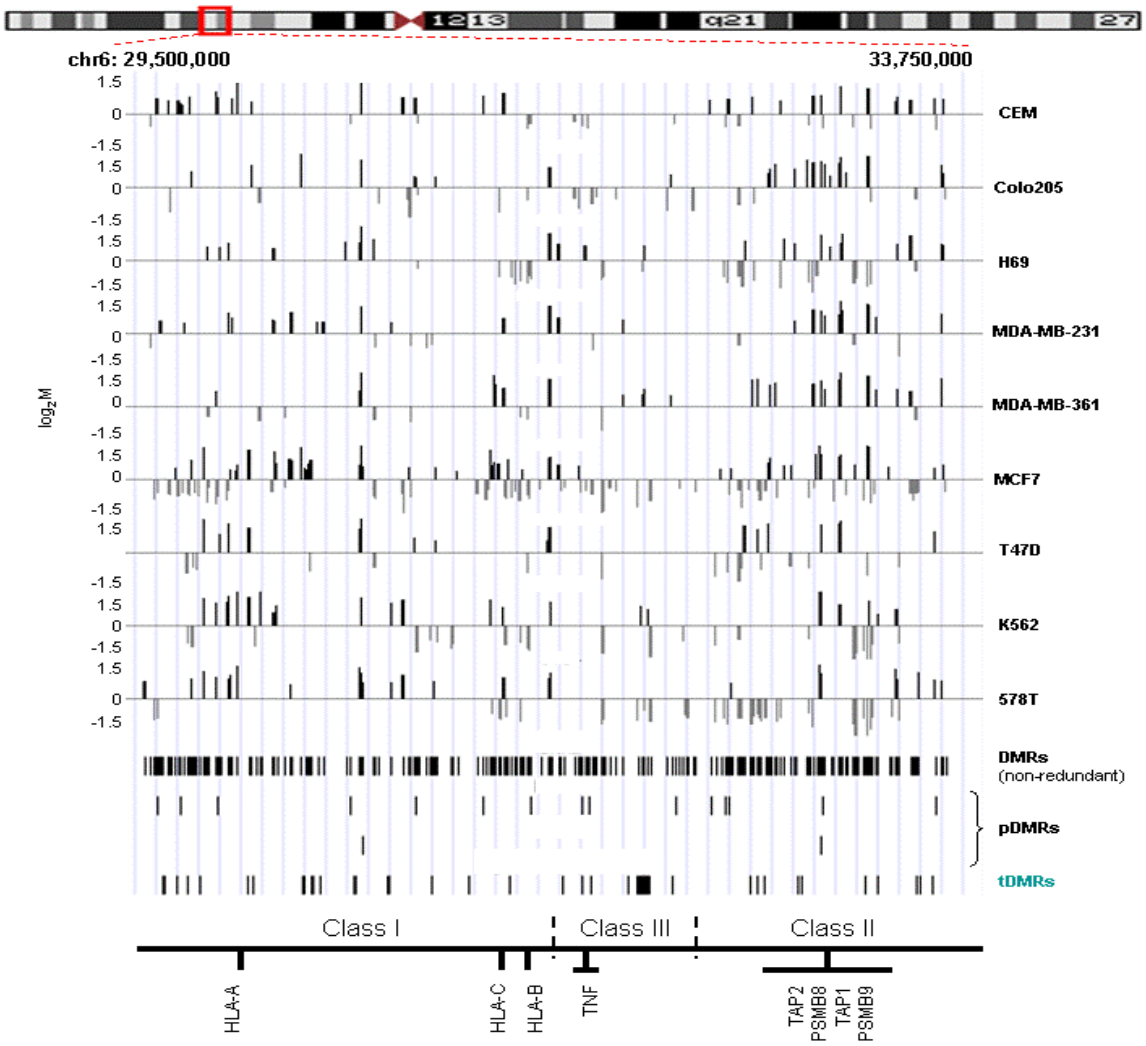

Figure 5.6 **DMRs identified between the cancer cell lines and shared controls**. Pair-wise comparisons (nine in total) of the MHC array-derived DNA methylation profiles were performed using t-statistics. A significance threshold p-value < 0.001 was used. Genomic location of DMRs identified for each pair-wise comparison (cancer cell line versus the mean values of the shared controls GM15510 and GM10851) are shown. The vertical axis shows the $\log_2$ ratio of the two corresponding methylation profiles (ie cancer cell line versus shared controls). Each line represents a DMR (average size 2kb). Black lines represent DMRs that are more methylated in cancer compared to the control cell lines (the identities of cancer cell lines within each comparison are given on the right) whereas grey lines represent less methylated DMRs. A track of the C+G content and the approximate positions of the MHC class I, II and II sub-regions and some landmark genes are also indicated. The genomic location of the 283 non-redundant DMRs (section 5.5.2) and 55 non-redundant tDMRs (section 4.7) are shown as black lines (average size 2kb). The pDMRs identified in section 5.5.3 are also shown. Upper track shows the 14 pDMRs

associated with *PSMB9* up-regulation whereas the lower track shows the two pDMRs associated with *HLA-A, HLA-B, PSMB8* and *TAP1* down-regulation.

5.5.3 pDMR identification

In the previous section I presented the DMRs between each of the nine cancer cell lines that display the MHC class I^- phenotype and shared normal control cell lines. In this section I analysed which of these DMRs can be highly linked with the MHC class I^- phenotype and hence called pDMRs.

This analysis was based on the expression analysis described in section 5.3. I aimed to identify the DMRs that could be connected with the expression of each of the eight genes involved in the MHC class I pathway and encoded within the MHC region (table 5.2; figure 5.3). The genes *HLA-A, HLA-B, TAP1* and *PSMB8* are down-regulated in all nine cancer cell lines compared to shared controls (>1.5 fold difference). I reasoned that MHC-DMRs linked with their expression should be present in all nine comparisons (figure 5.6). In a similar manner, *HLA-C* associated DMRs should be present in all but the CCRF-CEM, Colo-205 and MDA-MB-361 cell lines. *TAP2* and *TAPBP* DMRs should be present in all cell lines apart from T47D. Finally DMRs associated with *PSMB9* down-regulation should be present in MDA-MB-231, MDA-MB-361, Colo-205, H69, 578T, MCF7 and K562 comparisons. DMRs present only in CCRF-CEM comparison could be associated with *PSMB9* up-regulation (table 5.2).

5.5.3.1 pDMRs associated with *HLA-A, HLA-B, TAP1* and *PSMB8* expression

There are two putative pDMRs that can be associated with the expression of *HLA-A*, *HLA-B, TAP1* and *PSMB8* genes (figure 5.6). Interestingly, one of these DMRs overlaps with the bidirectional promoter of *TAP1* and *PSMB9* (figure 5.7a) (Wright et al., 1995). This pDMR is hypermethylated in all cancer cell lines compared to the shared controls and, because of its genomic location it can have a putative role in the regulation of

TAP1. Although this pDMR could also regulate the *PSMB9* gene, it seems that this is not the case as this pDMR is present in all cell lines, including those expressing *PSMB9* at normal levels (figure 5.3). The methylation status of the genomic region corresponding to this pDMR was verified further in all cell lines tested by bisulphite sequencing (figure 5.7b). These data show that about 10 CpG sites within this DMR are hypermethylated in all cancer cell lines. In the K562 cell line there are 20 additional CpG sites that are hypermethylated but these cannot be correlated with expression patterns (*TAP1* is downregulated in all cell lines, not only in K562 cells). About 36% of CpG sites within this pDMR were refractory for bisulphite sequencing analysis. Bisulphite sequencing analysis normally fails due to: i. failure in designing primers specific for bisulphite converted DNA (see section 1.3.6.1) and ii: poor quality of sequence traces corresponding to bisulphite converted DNA.

I attempted to verify further the role of the hypermethylation of the 10 CpG sites reported above. To this end I performed bisulphite sequencing analysis of DNA extracted from 5-aza-CdR treated MCF7 cells (section 5.4). This analysis revealed a 5-fold reduction in methylation levels of the 10 CpG sites after inhibition of DNA methylation (figure 5.7c). This result in combination with the expression analysis in 5-aza-CdR treated cells (section 5.4), where the expression of the *HLA-A, HLA-B, TAP1* and *PSMB8* genes is up-regulated (figure 5.4), indicates that methylation levels of these 10 CpG sites may be involved in the regulation of *HLA-A, HLA-B, PSMB8* and *TAP1* genes.

Interestingly, although these 10 CpG sites are located within the *TAP1*/*PSMB9* promoter, they do not overlap with any known control element within this region (figure 5.8). Instead they are located downstream of the start codon and TSS of *PSMB9*. It is possible that I have identified a new regulatory element within the promoter region. Functional analysis experiments, which are discussed in section 7.4.1, are required to verify further this possibility.

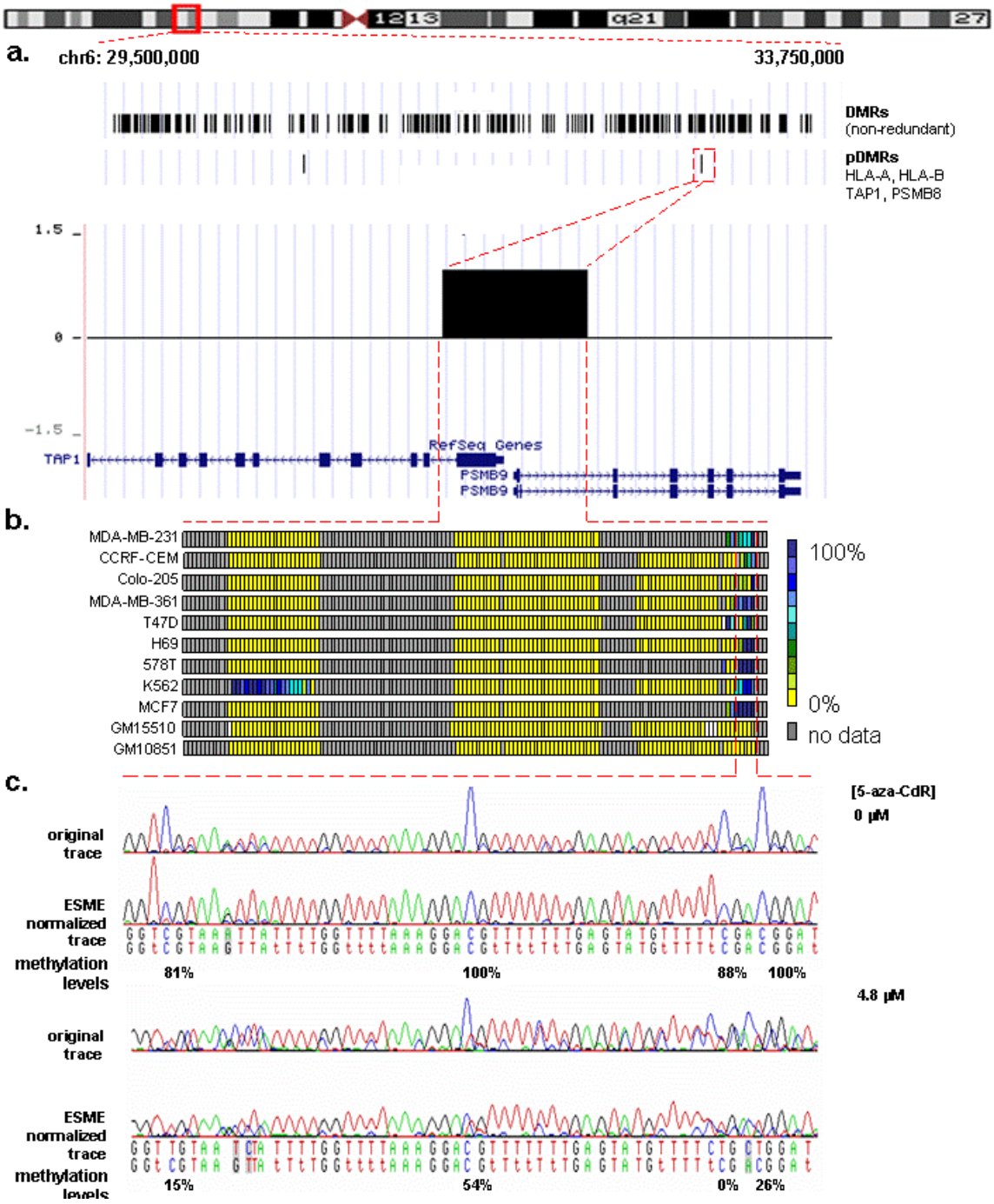

Figure 5.7. **A pDMR within the *TAP1*/*PSMB9* bidirectional promoter.** A pDMR within the *TAP1*/*PSMB9* promoter was associated with the down-regulation of *HLA-A, HLA-B, TAP1* and *PSMB8* but not *PSMB9*. According to MeDIP-MHC array data this pDMRs is hypermethylated in all cancer cell lines compared to the shared controls. a. Genomic location of the pDMR. b. The methylation patterns within this pDMR were verified by bisulphite sequencing. Each square represents a CpG site. The colour code indicates methylation percentage as calculated by ESME analysis (section 2.2.3). c. Effect of 5-aza-CdR. DNA extracted from MCF7 5-aza-CdR treated

and untreated cells, was subjected to bisulphite sequencing analysis. Methylation of the 10 CpG sites that were found to be hypermethylated (b) in cancer cell lines was tested. Traces corresponding to 5-aza-CdR treated and untreated samples as well as traces before and after ESME normalization (section 2.2.3.5) are shown. Concentration of 5-aza-CdR used is indicated. Upon 5-aza-treatment methylation values drop around 5-fold (on average). A representative part of the sequencing data generated is shown.

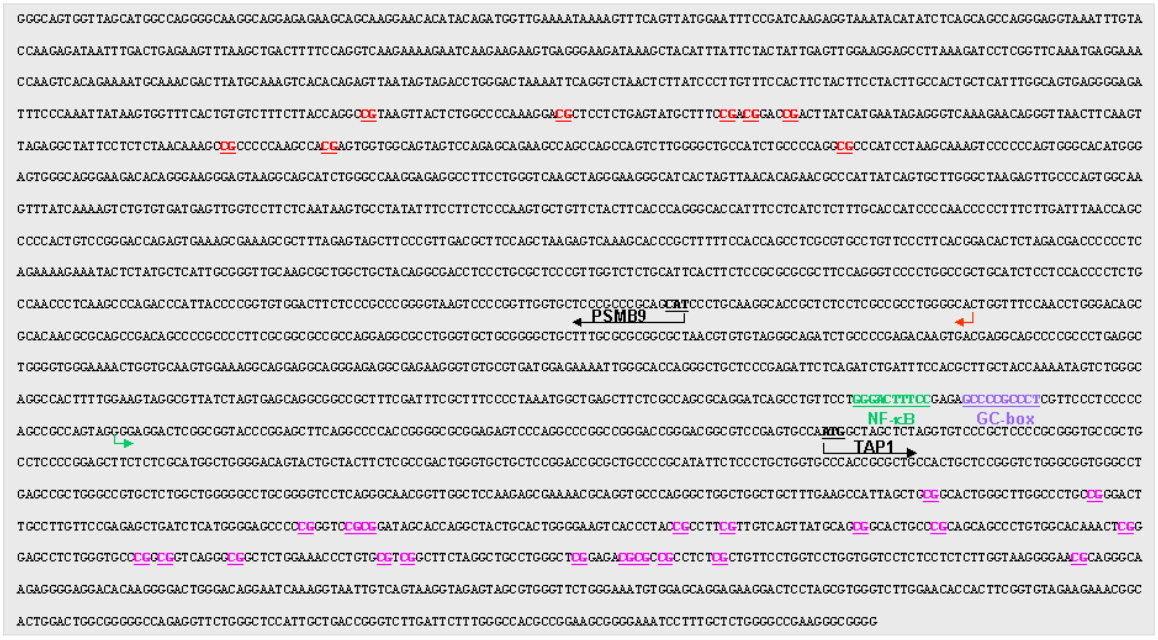

Figure 5.8. **Sequence of the DMR overlapping with the *TAP1*/*PSMB9* bidirectional promoter** The ATG translation start codons are indicated by a black arrow and the gene name. The most prominent transcription start sites are depicted by red and green arrows for PSMB9 and TAP1 respectively. Two functional transcription factor binding sites defined in Wright et al (Wright et al., 1995) are indicated. Green letters correspond to NF-kB and purple to GC-box binding sites. The ten CpG sites hypermethylated in all cancer cell lines are coloured red. The CpG sites hypermethylated only in the K562 cell line are coloured pink.

The second pDMR overlaps with the coding and 3'UTR regions of Nurim (NRM) which is an inner nuclear membrane (INM) protein (figure 5.9) (Holmer and Worman, 2001; Rolls et al., 1999). To date, there are no data implicating NRM in the MHC class I pathway indicating that I might have identified a novel control element for the expression of

members of the MHC class I pathway. However, further experiments are required to prove or refute this possibility.

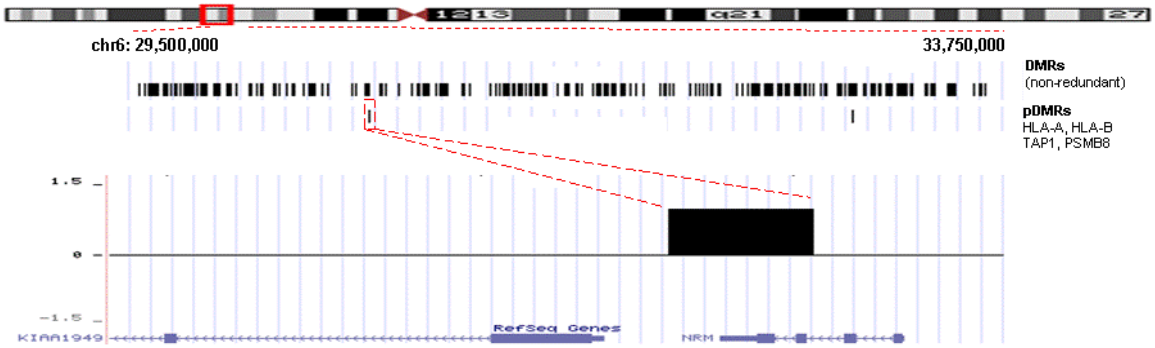

Figure 5.9. **pDMR associated with *HLA-A, HLA-B, TAP1* and *PSMB8* expression**. Pair-wise comparisons between each of the cancer cell lines and the two shared controls identified a putative pDMRs at the NMR loci in the MHC class I region. This pDMR is hypermethylated in all cancer cell lines compared to the shared controls. Tracks, also show the 283 non-redundant DMRs and the 2 pDMRs associated with HLA-A, HLA-B, PSMB8 and TAP1, were uploaded to the UCSC browser.

It is worth mentioning that none of these two pDMRs can be connected directly with the expression of *HLA-A, HLA-B* and *PSMB8* genes but this does not exclude the possibility that they regulate the expression of these genes. It is known that transcriptional control elements can regulate expression of genes within a distance on the same chromosomal band or even on different chromosomes (figure 4.1) (Maston et al., 2006).

5.5.3.2. pDMRs associated with *TAP2, TAPBP, HLA-C* and *PSMB9* expression

According to this analysis there are no pDMRs within the MHC associated with the expression of *TAP2*, *TAPBP* and *HLA-C*. Based on data of 5-aza-CdR treatment (section 5.4), expression levels of *TAP2* and *TAPBP* were the least affected. Hence it is possible that DNA methylation is not involved in the regulation of these two genes and that is why no pDMR was found to be associated with them. On the other hand *HLA-C* has been shown to be up-regulated after 5-aza-CdR treatment. It is possible that due to array

resolution I was not able to detect all pDMRs, particularly small pDMRs. Alternatively, the expression of *HLA-C* may be controlled by other epigenetic marks, for example histone marks. 5-aza-CdR has already been associated with H3 lysine 9 methylation (Coombes et al., 2003; Fahrner et al., 2002; Nguyen et al., 2002). Mapping histone marks across the MHC by performing Chromatin Immunoprecipitation (ChIP) in combination with the MHC tiling array will be informative on this matter.

Finally, 14 DMRs were present only in the CCRF-CEM cell line (figure 5.10). CCRF-CEM is the only cancer cell line in this study that shows increased levels of *PSMB9* mRNA (figure 5.3). Hence these 14 DMRs can be connected with *PSMB9* up-regulation and hence can be characterised as pDMRs. Although all of the 14 pDMRs can be equally important, the one overlapping with the coding and 3'UTR region of the *PSMB9* gene is the most likely to control *PSMB9* up-regulation. A previous study has shown that 3'UTR hypomethylation is associated with gene silencing (Shann et al., 2008). However, it is possible that the combination of 3'UTR hypomethylation together with 5'UTR hypermethylation, which is the case for the *PSMB9* gene in the CCRF-CEM cell line, leads to transcription activation (figures 5.10).

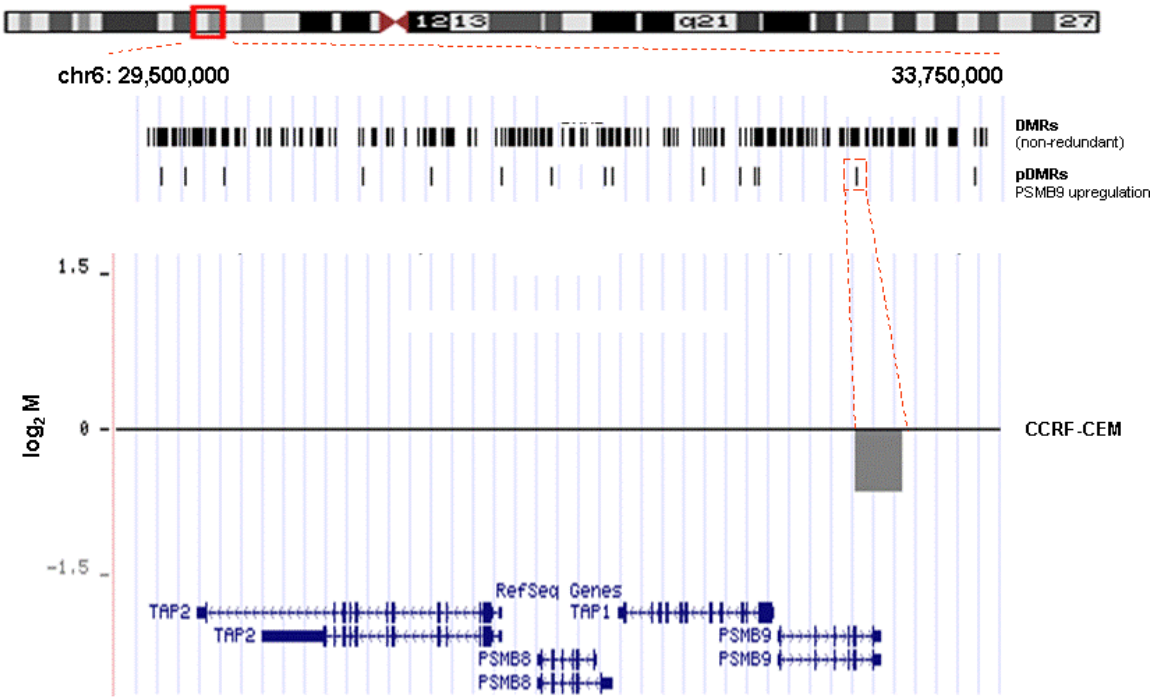

Figure 5.10. **pDMRs associated with *PSMB9* up-regulation.** 14 DMRs present only in the CCRF-CEM comparison were associated with *PSMB9* up-regulation. Of these the one overlapping the 3'UTR of *PSMB9* is the most likely to control expression of the gene. It seems to be less methylated in CCRF-CEM as shown in the lower part of the figure. RefSeq genes are also shown. Tracks showing the genomic location of DMRs were uploaded to the UCSC genome browser.

In summary, in this section I describe the identification of two pDMRs associated with the down-regulation of *HLA-A, HLA-B, TAP1* and *PSMB8* as well as of 14 pDMRs associated with the up-regulation of *PSMB9*. One interesting question arising from pDMR identification is the mechanism that drives their formation during the development of a phenotype, in this case the MHC class I^- phenotype. As it was discussed in the general introduction of this thesis (chapter 1), there is supporting evidence suggesting that DNA methylation is the result of low transcriptional activity. This implies that DNA methylation is a secondary event during the process of gene silencing (Bird, 2002; Clark and Melki, 2002; Turker, 2002).

In the following section I attempt to correlate increasing methylation levels with reduction of transcriptional activity.

5.6 DNA methylation and levels of transcriptional activity

It has been proposed that gene silencing is a gradual and evolving process that induces promoter DNA methylation at a very late stage of the transcriptional silencing process (Bird, 2002; Clark and Melki, 2002; Turker, 2002). This is consistent with recent data suggesting a “Use it or Lose it” model (Meissner et al., 2008). Based on this model, genes with low levels of transcriptional activity in a given cell type are susceptible to be locked into this state by DNA methylation. In an attempt to investigate this possibility further I identified all the DMRs (section 5.5.2) that overlap with the eight MHC encoded genes involved in the MHC class I pathway and I correlated them with the corresponding expression levels (section 5.3; figure 5.3). Although all candidate genes are down-regulated in almost all cases (figure 5.3), the level of down-regulation differs between cell lines.

Based on this analysis there is: (i). one DMR overlapping with the bidirectional promoter of *TAP1* and *PSMB9* which is present in all cell lines and hence cannot be correlated with differential expression levels. (ii). one DMR present within the *HLA-B* locus which is not correlated with expression levels and hence it is not discussed further within this thesis and (iii). a DMR overlapping with the promoter of *PSMB8* gene which is present in three cell lines: 578T, MCF7 and K562 (figure 5.11a). Interestingly these three cell lines are those with the lowest *PSMB8* expression levels compared to the rest (figures 5.3 and 5.11c). I tested this DMR further as described below.

5.6.1 DMRs overlapping with the PSMB8 promoter region

In three cancer cell lines (578T, K562, MCF7), a DMR was identified within the 5'UTR of the *PSMB8* gene (figure 5.11a). Bisulphite sequencing analysis confirmed that this region is heavily methylated in these three cell lines (figure 5.11b). As the *PSMB8* gene is down-regulated in all cancer cell lines (figures 5.3 and 5.11c) this DMR does not qualify as pDMR based on the analysis described in section 5.5.3. However it is important to note that 578T, K562 and MCF7 show the lowest expression levels of *PSMB8* compared to the rest of cancer cell lines (figure 5.11c) and this may be linked to the proposal that gene silencing is a gradual and evolving process that induces promoter DNA methylation (Clark and Melki, 2002; Meissner et al., 2008; Turker, 2002). Hence, I speculate that this can be the case for the silencing event of the *PSMB8* gene. Initially *PSMB8* silencing is the result of factor(s) other than DNA methylation. When transcription levels fall below a threshold (relative expression < 0.05) (figure 5.11c) induces an increase in local methylation and this could explain the high levels of methylation in the 578T, K562 and MCF7 cell lines. Treatment of MCF7 cells with 5-aza-CdR reduces methylation of the *PSMB8* DMR 5-fold (on average) (figure 5.11d) and this is in inverse correlation with the expression levels of the *PSMB8* gene in 5-aza-CdR treated cells (figure 5.4). Treatment of additional cell lines, other than MCF7, 578T and K562, with methylation inhibitors would be informative. The expectation is that treatment with 5-aza-CdR should not have an effect on the expression levels of the PSMB8 gene in cell lines lacking the DMR within the *PSMB8* 5'UTR.

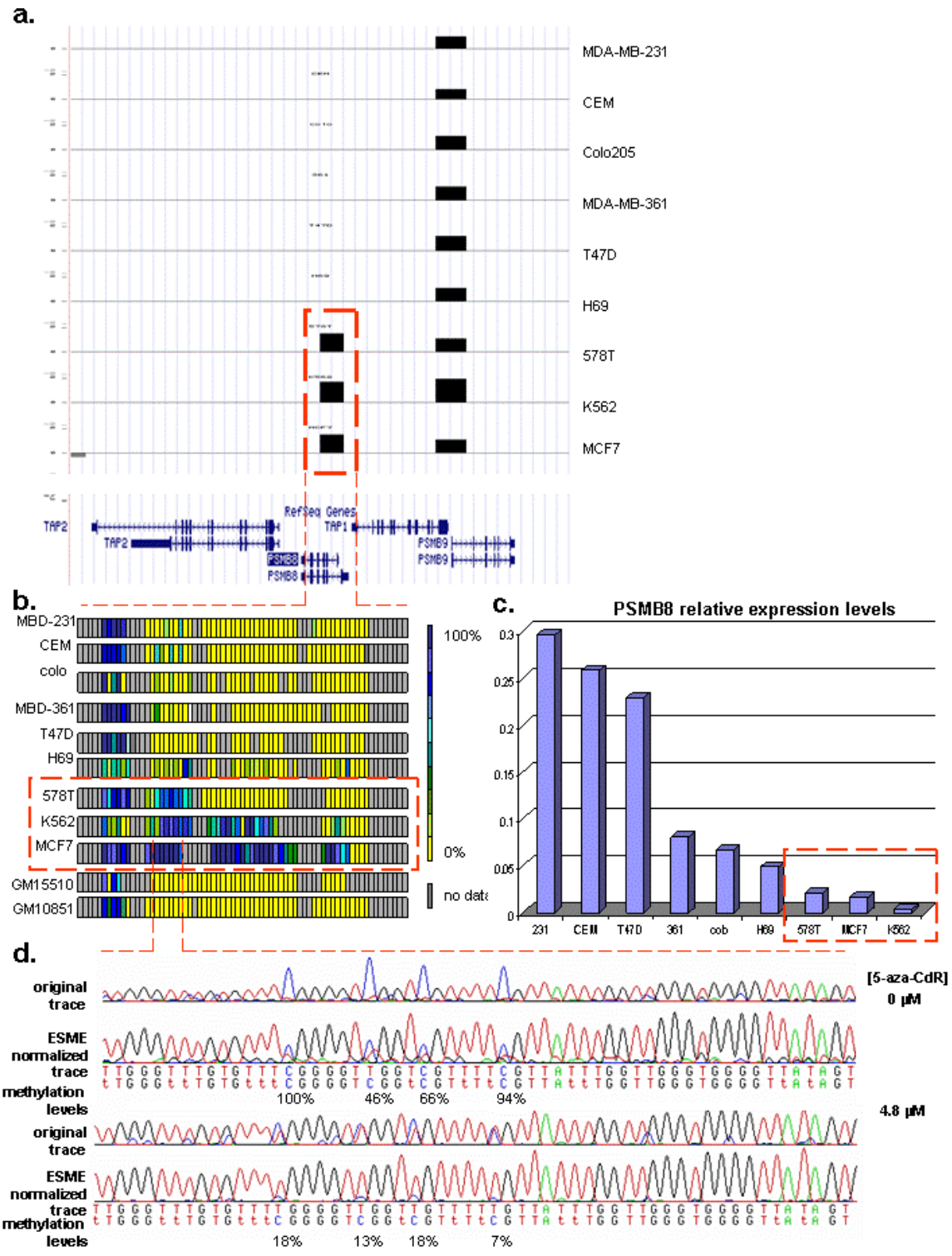

Figure 5.11 **DMRs within the PSMB8 promoter.** Pair-wise comparisons between the cancer and the shared control cells revealed a DMR within the *PSMB8* promoter in the cell lines 578T, K562 and MCF7.(a). DMRs identified by the MeDIP-MHC tiling array approach. The red box indicates the DMR within the *PSMB8* promoter. The pDMR within the *TAP1/PSMB9* promoter (discussed in

section 5.5.3.1; figure 5.7) is also shown. Tracks were uploaded to the UCSC browser. Vertical axis shows the $\log_2$ ratio of the cancer versus normal cell line profile. Identity of the corresponding cancer cell line is shown on the right. (b). DMR overlapping with *PSMB8* was validated further by bisulphite sequencing analysis. Each square represents a CpG site. The colour code indicates methylation percentage as calculated by ESME analysis. (c). Relative expression levels for *PSMB8* in the nine cancer cell lines (taken from figure 5.3). Red box indicates the three cell lines (K562, 578T, MCF7) with the lowest *PSMB8* levels (fold enrichment <0.05). Graph was reproduced using data shown in figure 5.3. (d).DNA extracted from MCF7 5-aza-CdR treated and untreated cells, was subjected to bisulphite sequencing analysis. Traces corresponding to 5-aza-CdR treated and untreated samples as well as traces before and after ESME normalization are shown. Concentration of 5-aza-CdR used is indicated. Upon 5-aza-CdR treatment methylation values dropped 5-fold. A representative part of the sequencing data generated is shown.

5.7 Prominent DMRs within the MHC region

One of the great advantages of the MeDIP-MHC tiling array approach compared to the bisulphite sequencing strategy, which followed by the HEP pilot study for the MHC region and covered only 2% of the MHC, is that it allows the unbiased methylation analysis of the complete MHC region, albeit at 2kb resolution. I wished to look for prominent DMRs within the MHC which, although they were not found to be associated with the MHC class I^- phenotype, may be important in the regulation of MHC genes in general.

To this end I used the list of DMRs that resulted by the analysis described in section 5.5.2 (pair-wise comparisons of DNA methylation profiles of cancer cell lines versus the shared controls) (appendix table 5.2) and I looked for DMRs present in the majority of comparisons. The most prominent DMRs were present in the tumour necrosis factor (TNF) cluster in the MHC class III region. These DMRs are discussed in the following sections.

5.7.1 The tumour necrosis factor cluster

The tumour necrosis factor (TNF) cluster contains genes for three cytokines (LTA, TNF-α and LTB) and is located in the MHC class III region (figure 1.1). These cytokines play multiple roles in the development and function of the immune system (Aggarwal et al., 2002; McDevitt et al., 2002). The regulation of expression of these genes is complex: transcription is controlled in a tissue- and stimulus-specific manner (Falvo et al., 2000; Falvo et al., 2000; Tsai et al., 1996). Recent evidence has shown that the *TNF-α* gene is epigenetically regulated. More specifically, it has been shown that in K562 cell (which is one of the cancer cell lines tested here), the promoter region of *TNF-α* is hyper-methylated (Sullivan et al., 2007). According to the same study K562 cells do not produce TNF-α upon lipopolysaccharide (LPS) treatment. LPS is one of the major inducers of TNF production both *in vivo* and *in vitro* (Dumitru et al., 2000).

The analysis conducted under section 5.5.2 revealed three DMRs within the TNF cluster, overlapping with the *LTA, TNF-α* and *LTB* genes. In the following sections I studied these DMRs further and, more specifically, I explored how they can be associated with the expression of the corresponding genes.

5.7.2 DMRs within the TNF cluster

According to the MHC array analysis (5.5.2) the gene body of *TNF-α* is hypermethylated in all cancer cell lines except CCRF-CEM. The *TNF-α* promoter region is hypermethylated in all but two cancer cell lines (K562 and CCRF-CEM). DMRs were also identified in some cell lines within the gene bodies of *LTA* and *LTB* (figure 5.12a). The DMRs identified within the TNF cluster were validated further by bisulphite sequencing (figure 5.12b), which agrees with the array data. The two EBV-transformed cell lines GM10851 and GM15510 (shared controls) appear to be unmethylated. CCRF-

CEM cells are either unmethylated or less methylated compared to the rest of the cancer cell lines within the regions tested. In addition, according to bisulphite sequencing data and previous studies the *TNF-α* promoter in K562 cells is hypermethylated. However the MeDIP-MHC approach failed to detect the corresponding DMR in these cells. This can be due to lower methylation levels in K562 cells compared to the other cancer cell lines (except CCRF-CEM). The lower methylation levels observed for K562 cells may not be sufficient to be detected by my experimental approach (MeDIP-MHC tiling array). Methylation values for the CpG sites within these DMRs, which were found to be refractory to bisulphite sequencing analysis, may be informative in this context

It was interesting to observe that the region overlapping with the *TNF-α* promoter-DMR contains the binding site for the transcription factor termed lipopolysaccharide-induced TNF-a factor (LITAF). LITAF is a regulatory element that has been shown to mediate LPS-induced *TNF-α* gene expression in THP-1 cells (Tang et al., 2003). Hence it is possible that the DMR identified within the promoter of TNF-α plays a role in the regulation of this gene. In a similar manner the additional DMRs identified within the TNF cluster, although they do not overlap with promoters of the *LTA* and *LTB* genes, may regulate their transcription.

In the following section I attempt to investigate how the three DMRs discussed herein may affect transcriptional levels of the corresponding genes.

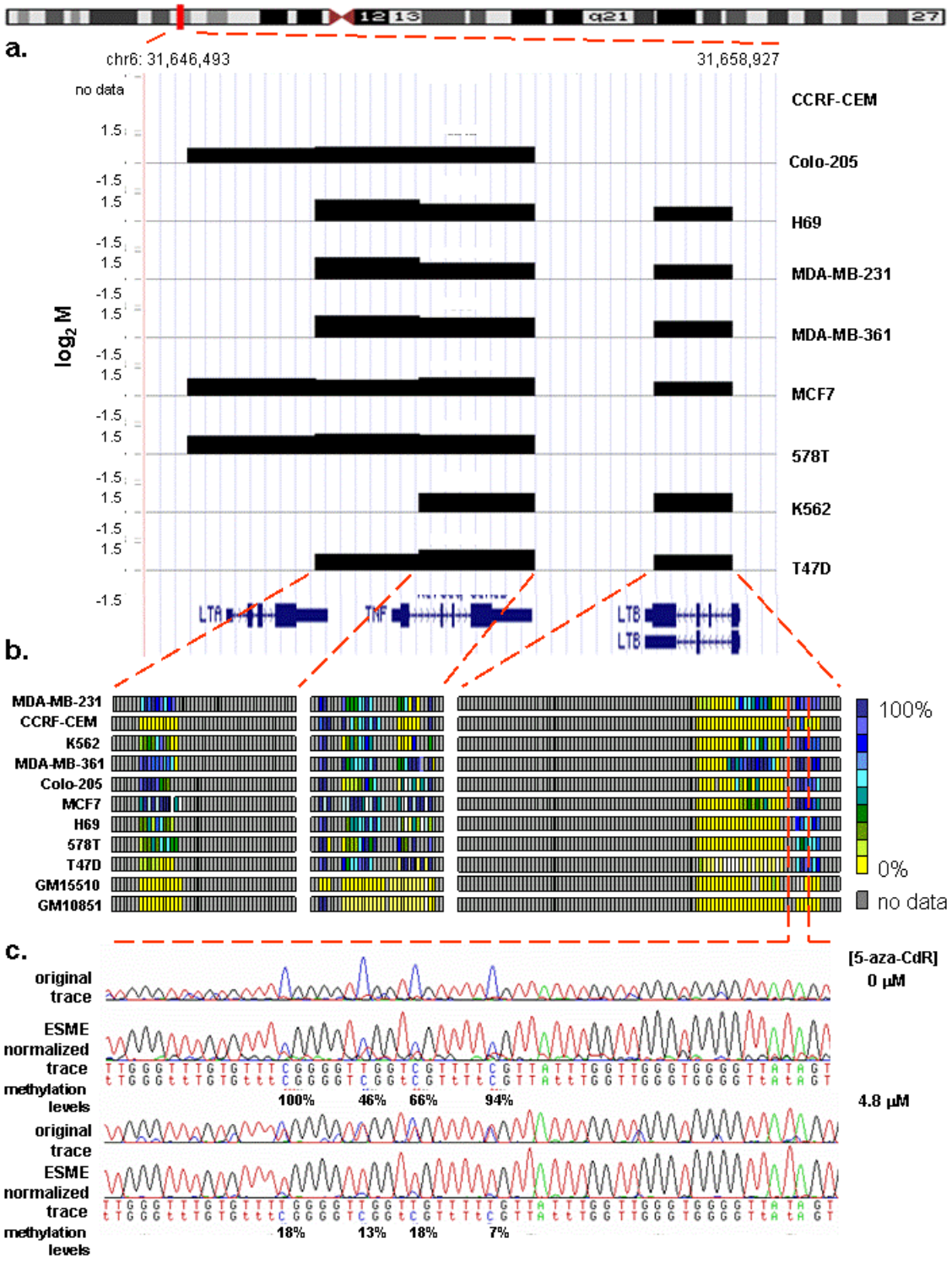

Figure 5.12. **DMRs within the TNF cluster.** Pair-wise comparisons between the cancer and control cell lines revealed four DMRs within the TNF cluster. a. Tracks were uploaded to the UCSC genome browser. Vertical axis shows the $\log_2$ ratio of the cancer versus normal cell line profile. b. DMRs overlapping with the *TNF-α* promoter, *TNF-α* gene body and *LTB* were validated

further by bisulphite sequencing analysis. Each square represents a CpG site. The colour code indicates methylation percentage as calculated by ESME analysis. c. Effect of 5-aza-CdR. DNA extracted from MCF7 5-aza-CdR treated and untreated cells, was subjected to bisulphite sequencing analysis. Traces corresponding to 5-aza-CdR treated and untreated samples as well as traces before and after ESME normalization are shown. Concentration of 5-aza-CdR used is indicated. Upon 5-aza-CdR-treatment, a 5-fold reduction (on average) in methylation levels was observed. A representative part of the sequencing data generated is shown.

5.8.3 Expression of TNF cluster genes and correlation with DMRs

To correlate the DMRs identified in the previous section with mRNA levels of the *LTA*, *LTB* and *TNF-α,* the expression of these genes in the cancer cell lines was compared to the shared controls. To this end, I performed real time qPCR using primer sets corresponding to *LTA, LTB* and *TNF-α* cDNAs respectively. Differences in expression between each of the cancer cell lines and the two shared controls were calculated as described in section 2.2.4. In all cancer cell lines all three genes were down-regulated (fold >1.5) compared to the two controls (figure 5.13)

Interestingly, the expression of *TNF-α* and *LTB* was about 4.5 fold higher in the CCRF-CEM line compared to the other cancer cell lines and this may explain the lower methylation levels in CCRF-CEM (figure 5.12a,b).

The correlation of low expression levels of genes encoded within the TNF cluster with the DMRs presented in the previous section suggests that DNA methylation may be a transcription regulator for these genes. In order to test this further, expression of *LTA*, *TNF-α* and *LTB* was determined in 5-aza-CdR treated MCF7 and 578T cells as it was done above for the MHC class I pathway genes (section 5.4). 5-aza-CdR was capable of inducing expression of *TNF-α, LTA* and *LTB* in both cell lines although the effect was

.

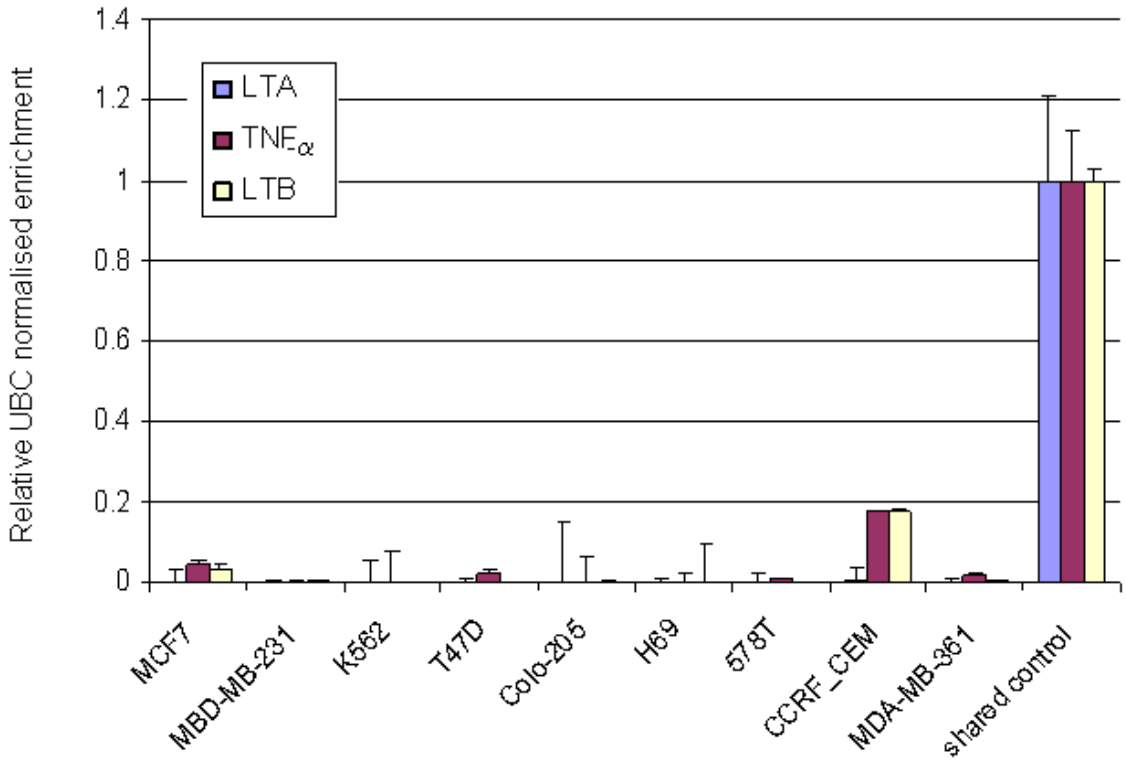

Figure 5.13. **Relative expression of TNF cluster genes.** mRNA levels of *LTA, TNF-α* and *LTB* were determined by quantitative RT-PCR. After normalizing expression to *UBC* (section 2.2.4.3) the fold change in expression levels was calculated relative to the two EBV transformed control cell lines (shared controls). Figure shows the mean of data corresponding to two biological replicates and three technical replicates of each (six measurements in total).

more significant in the MCF7 cell line (figure 5.14). In addition, bisulphite sequencing data corresponding to DNA extracted from 5-aza-CdR treated cells confirmed that methylation levels were decreased in the TNF cluster DMRs (figure 5.12c) follwing inhibition of DNA methylation.

At this point I would like to mention that TNF-α together with interferon-γ (IFN-γ) are two cytokines known to be involved in regulation of MHC class I molecules (Johnson, 2003; Johnson and Pober, 1994; Ohmori and Hamilton, 1995). In the next section, I discuss how methylation of the *TNF-α* promoter can be correlated with the expression of genes involved in the MHC class I pathway.

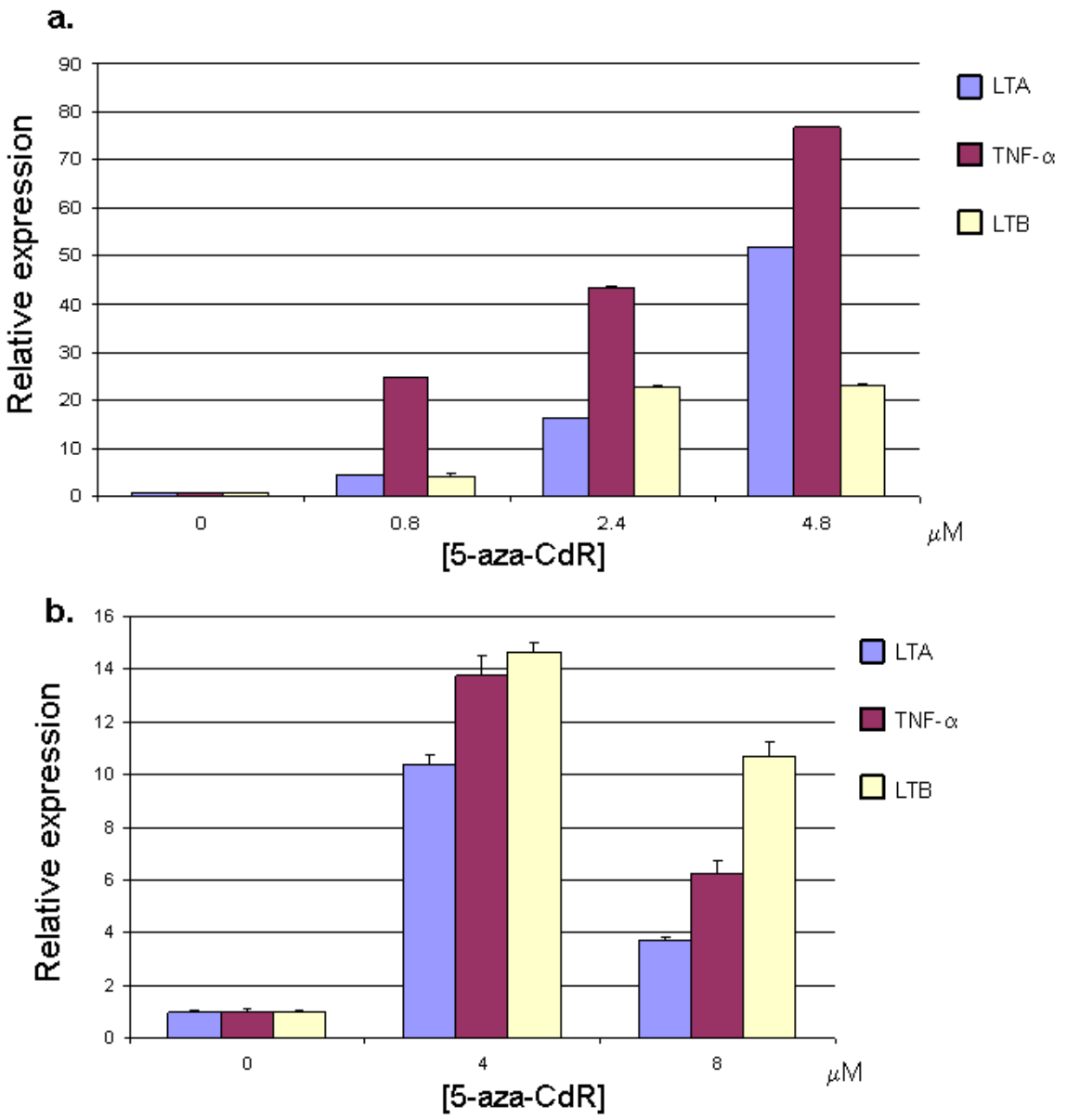

Figure 5.14 **TNF-cluster gene expression after DNA methylation inhibition in two cancer cell lines.** mRNA levels of *LTA, TNF-α* and *LTB* were determined in MCF7 (a) and 578T (b) in both untreated and 5-aza-CdR treated cells. After normalizing expression to *UBC*, the fold change in expression was calculated relative to untreated cells (0 μM 5-aza-CdR). The mean of six measurements (two biological replicates and three technical replicates for each) is shown in part a. The mean of three technical replicates is shown in part b.

5.8 Discussion

Previous studies provided supportive evidence for a role of DNA methylation in the regulation of genes involved in the MHC class I pathway (Fonsatti et al., 2007; Fonsatti et al., 2003; Nie et al., 2001). In this chapter I aimed to elucidate this further. Specifically, I attempted to test if DNA methylation within the MHC region is involved in the MHC class I^- phenotype. This is associated with many diseases. Hence elucidating the mechanism that leads to this phenotype can contribute to diagnosis and treatment.

My data confirmed the concordant down-regulation of the eight MHC class I pathway genes encoded within the MHC region in the nine cancer cell lines (displaying the MHC class I^- phenotype) used, compared to two shared controls (EBV-transformed cell lines). Treatment of two cancer cell lines (MCF7 and K562) with a DNA methyltransferase inhibitor (5-aza-CdR) revealed that changes in DNA methylation patterns in the cancer cell lines may lead to the concordant aberrant expression of the eight genes.

I used the MeDIP-MHC tiling path assay, which I developed, to investigate if there are any DNA methylation regulatory elements within the MHC region that may control the expression levels of the *HLA-A, HLA-B, HLA-C, TAP1, TAP2, TAPBP, PSMB8* and *PSMB9* genes. The advantage of this approach is that it allows for unbiased detection of DMRs within the complete MHC region. The MHC was one of the first genomic regions in which higher order chromatin architecture was shown to affect gene expression (Christova et al., 2007; Volpi et al., 2000). Consistent with this, a recent study using the tiling array I developed, has shown the existence of chromatin loops within the MHC which act as insulators for the transcription of MHC genes (Ottaviani, 2008). This indicates that the expression of MHC genes is not controlled solely by local control elements, but also by more distant regulatory elements (figure 4.1). Hence, it was important to expand this study beyond the methylation analysis of the eight loci implicated in the MHC class I pathway.

My analysis revealed 283 candidate DMRs that could be involved in the control of the expression of these genes. Correlation of these DMRs with relative expression levels of the eight candidate genes identified two DMRs that can be linked with *HLA-A, HLA-B, PSMB8* and *TAP1* down-regulation and 14 DMRs that can be linked with the up-regulation of *PSMB9*. I defined these DMRs phenotype-specific, pDMRs, to reflect their concordance with the phenotype under investigation.

Of the two pDMRs associated with *HLA-B, HLA-B, PSMB8* and *TAP1*, one is located within the *TAP1/PSMB9* bidirectional promoter and can be linked to the expression of the *TAP1* gene. Interestingly, it could not be associated with the expression of *PSMB9* because this pDMR was present in cell lines expressing this gene at normal levels (figures 5.3 and 5.7). It is possible that different elements within the promoter region control the two genes separately. More work has to be done to further elucidate this matter. Further bisulphite sequencing analysis, to reveal all the CpG sites with differential methylation patterns, and functional analysis (e.g. deleting the region with the promoter that contains the key CpG sites) will be informative. The second pDMR (NRM locus) cannot be linked directly to any of the genes of the MHC class I pathway (figure 5.9) but it may be part of a genomic loop that controls MHC genes. Chromatin loops have been associated with the MHC region (Ottaviani, 2008).

In a similar manner, although the 14 pDMRs associated with the PSMB9 up-regulation could not be linked directly with *PSMB9* expression (only one was located within its coding region) may be equally important for the regulation of the *PSMB9* gene.

My analysis did not reveal any pDMRs associated with *HLA-C, TAP2, TAPBP* and *PSMB9* down-regulation despite the fact the 5-aza-CdR treatment increases *HLA-C* and *PSMB9* expression in both cell lines tested (578T and MCF7) (figure 5.4). This can be explained by: i) the MHC tiling array resolution (2kb) (I have not performed any systematic analysis to define the number of CpG sites required to be differentially

methylated in order for a DMR to be detected), and ii). the possibility that other epigenetic marks (e.g. histone modification) may control the expression of these two genes. It has been shown that histone deacetylase inhibitors induce *TAP* and *TAPBP* genes (Khan et al., 2008).

The identification of a validated DMR within the *PSMB8* promoter in three cell lines (578T, K562 and MCF7) which show the lowest expression for *PSMB8* (enrichment < 0.05) allowed me to speculate that the hypermethylation observed may follow the silencing of the gene by other factors as it has been proposed by previous studies (Clark and Melki, 2002; Meissner et al., 2008; Turker, 2002). Hence, it is possible that the *PSMB8* promoter DMR is not the cause but rather the consequence of gene silencing. Treatment of cell lines other than MCF7, K562 and 578T with methylation inhibitors will be informative.

Finally three DMRs that could be correlated with expression of genes within the TNF cluster were identified, demonstrating the advantage of the unbiased MeDIP-MHC tiling array approach. This agrees with previous data showing the *TNF-*α expression to be controlled epigenetically (Sullivan et al., 2007). My data will be informative for future studies aiming to further elucidate the regulation of the *LTA, TNF-*α and *LTB* genes.

It is worth mentioning that TNF-α, together with IFN-γ, is a cytokine known to be an immune modifier acting on the MHC class I processing and presentation pathway by inducing expression of the *PSMB8, PSMB9, TAP1, TAP2* and MHC class I genes. A kB-like element within the promoter of these genes is responsible for the response upon TNF-α stimuli (Johnson and Pober, 1994). The connection of the DMRs within the TNF cluster and the MHC class I^- phenotype is discussed further in the final discussion (chapter 7) of this thesis.

5.9 Conclusion

A pDMR screen aiming to identify DMRs within the MHC region associated with the MHC class I^- phenotype was conducted. For this purpose the MeDIP-MHC tiling array approach was employed. In total 16 pDMRs were identified and validated further. The presence of a DMR within the *PSMB8* promoter in cells expressing this gene at the lowest level indicated that, in some cases, DNA methylation may be a secondary event during the process of gene silencing. Finally, three DMRs were identified within the TNF cluster, providing a broad basis for better understanding of how genes within this cluster are controlled. The data generated within this chapter will be of great value for future studies regarding MHC associated phenotypes.

Chapter 6

MHC class I pathway genes not encoded within the MHC

6.1 Introduction

To date there are at least 12 known genes whose products are involved in the MHC class I antigen presentation pathway. This was discussed in chapter 5. The aim of the pDMR screen (chapter 5) was to identify DMRs within the MHC region on the human chromosome 6 which can be associated with the MHC class I^- phenotype. However as four of the genes involved in the pathway are not encoded within the MHC region, there may be additional genomic regions (outside the MHC) for which methylation patterns may be important. In order to investigate this further I performed expression and DNA methylation analyses for these four genes: beta-2 microglobulin (*B2M*), *ERp57, calnexin* (*CANX*) and *calreticulin* (*CALR*). I studied these genes using the same cell lines as for the MHC encoded genes (chapter 5). The experimental approach employed in this chapter involved use of real time qPCR and bisulphite sequencing.

6.2 Non-MHC encoded MHC class I pathway components

B2M is an invariant small polypeptide chain referred to as the 'light' chain and is encoded on chromosome 15 at location 42,790,967 – 42,797,651. For stable expression on the cell surface, MHC class I molecules are always associated with B2M. In the absence of B2M, MHC class I molecules are not stably expressed on the cell surface (Hughes et al., 1997).

ERp57 is a member of the protein disulphide isomerase (PDI) family of thiol oxidoreductases (Garbi et al., 2007). Recent studies have shown that, together with TAPBP, it is an essential structural component required for the stable assembly of the MHC peptide-loading. ERp57 and TAPBP are involved in the formation of disulfide bonds of MHC class I molecules (figure 5.1) (Garbi et al., 2006; Kienast et al., 2007). *TAPBP* is encoded on chromosome 15 at location 41,825,882 – 41,852,093.

CARL is a calcium binding lectin that recognises N-linked glycans bearing a terminal glucose residue, an intermediate in oligosaccharide maturation, present on incompletely folded ER glycoproteins. CALR associates with MHC class I dimers and interacts poorly with free MHC class I heavy chains. *CALR* deletion results in low cell surface MHC class I expression (Culina et al., 2004). *CALR* is encoded on chromosome 19 at location 12,910,392 – 12,916,274.

CANX is an endoplasmatic reticulum (ER) lectin similar to CALR (Williams and Watts, 1995). One difference is that the latter can bind to newly synthesised MHC class I heavy chains as well. *CANX* is encoded on chromosome 5 at location 179,058,536-179,091,243.

.

6.3 Expression analysis of *B2M, ERp57, CRT* and *CANX genes*

Expression analysis of these four genes was done in the same way as for the MHC-encoded MHC class I pathway genes (section 5.3.1). According to this analysis *B2M* is the only gene that is down-regulated (fold >1.5) in all cancer cell lines. *ERp57, CALR* and *CANX* showed almost normal expression levels in most of the cell lines, except for few cases (three cell lines for *CALR* and *CANX* and one cell line for *ERp57*) where a up-regulation (fold > 1.5) was observed in some cell lines (figure 6.1).

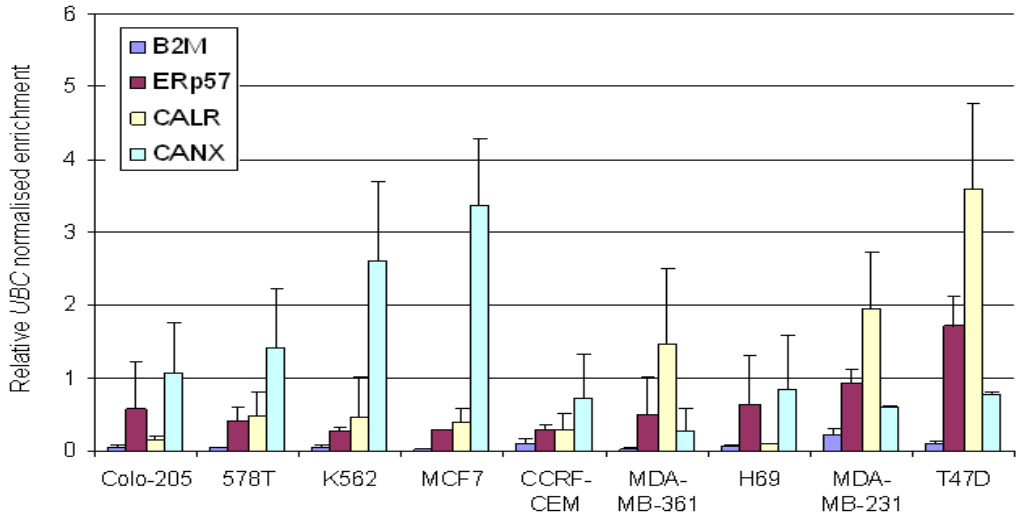

Figure 6.1. **Relative expression of non-MHC encoded MHC class I pathway genes.** mRNA levels of *B2M, ERp57, CALR* and *CANX* were determined by quantitative RT-PCR. After normalizing expression to UBC (section 2.2.2.4.3) the fold change in expression levels was calculated relative to the two control cell lines. Figure shows data corresponding to two biological replicates and three technical replicates of each (six measurement in total).

Expression analysis for these genes was also performed on mRNA extracted from MCF7 and 578T cells that were treated with 5-aza-CdR, as described in chapter 5 (section 5.4). Methylation inhibition affected only the expression of *B2M* in MCF7 cells. Specifically, expression of *B2M* increased in a 5-aza-CdR dose-depended manner up to 9-fold (figure 6.2). This effect is very similar to that corresponding to the *TAP2* gene (figure 5.4) in MCF7 cells.

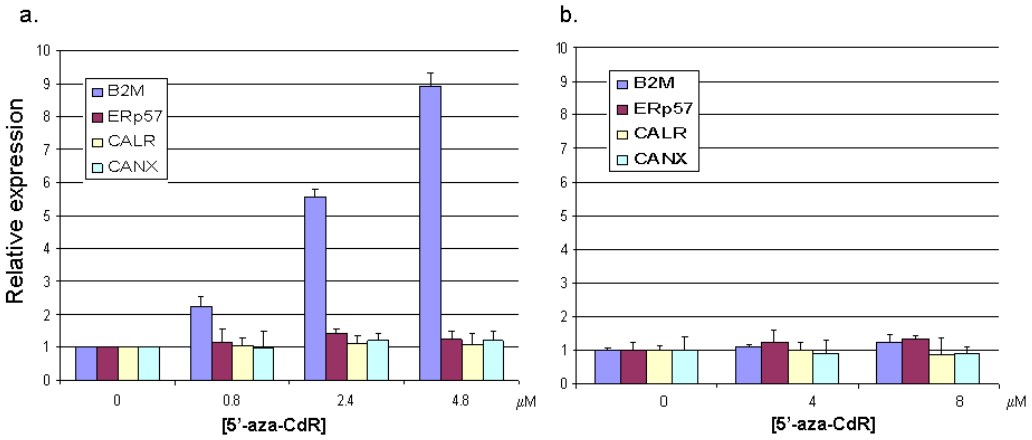

Figure 6.2: **Gene expression after DNA methylation inhibition in two cancer cell lines.** mRNA levels of *B2M, ERp57*, *CANX* and *CALR* were determined in MCF7 (a) and 578T (b) in both untreated and 5-aza-CdR treated cells. After normalizing expression to *UBC,* the fold change in expression was calculated relative to untreated cells. The mean of six measurements (two biological replicates and three technical replicates for each) is shown in part a. The mean of three technical replicates is shown in part b.

Hence, it is possible that DNA methylation is implicated only in *B2M* expression and only in MCF7 cells. As 5-aza-CdR treatment has no effect on *B2M* expression in 578T, it is likely that different cancer cell lines exploit different mechanisms to silence the same genes. Treating additional cell lines with the methylation inhibitor would be

informative. In an effort to elucidate this further I studied methylation across the encoding region of the *B2M* gene as described in the following section.

6.4 Methylation analysis of the *B2M* gene.

B2M is encoded within a 7kb region on chromosome 15 and has four exons (figure 6.3a). It has a CpG island covering about 200 bp of the 5'UTR, the first exon and about 500bp of intron 1. I aimed to generate bisulphite sequencing data for all CpG sites within the *B2M* gene. Methylation data for 20% of the CpG sites covering the whole gene were generated (figure 6.3b).

According to these data there are 3 CpGs in the 5'UTR and 8 CpGs at the end of intron 1 and beginning of exon 2, which are hypermethylated in all cancer cell lines compared to the shared controls. Their methylation status was tested after 5-aza-CdR treatment (see section 5.4) and in all cases methylation dropped to 20% (figure 6.3c). Although, the hypermethylation of these sites could be correlated with *B2M* expression, 5-aza-CdR treatment has no effect on B2M expression levels in 578T cells (figure 6.2). Hence, I cannot conclude that DNA methylation affects *B2M* expression.

However, it is worth noting the 9-fold increase of B2M mRNA levels following 5-aza-CdR treatment of MCF7 cells. Interestingly, this cell line is the only one that is hypermethylated close to the CpG island in intron 1 (figure 6.3a,b) and also has the lowest level of *B2M* expression compared to other cell lines (figure 6.1). A similar observation was made in chapter 5 for the *PSMB8* gene (section 5.6). It is possible that down-regulation of the *B2M* gene below a certain threshold leads to additional methylation, but treatment of additional cell lines with methylation inhibitors is necessary to verify this speculation.

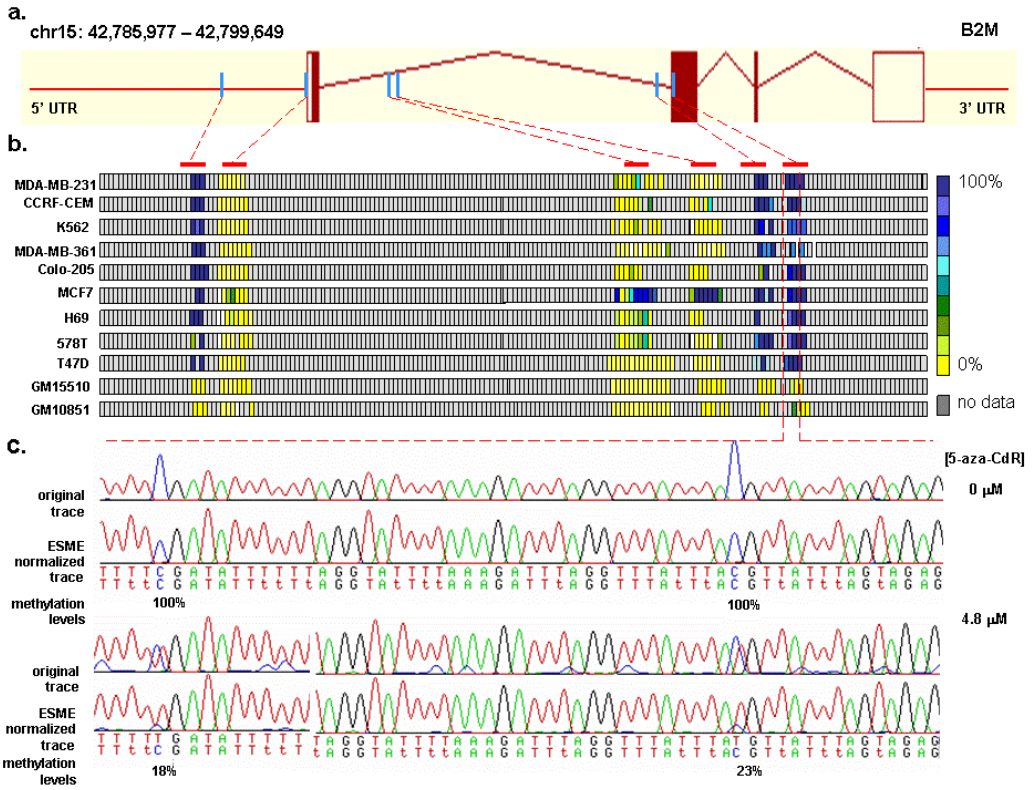

Figure 6.3. **Methylation analysis of the *B2M* gene**. Methylation analysis of six regions (average size 300-400bp) covering parts of the *B2M* gene was performed by bisulphite sequencing. (a). Diagram of the *B2M* gene. Regions (six in total) analysed by bisulphite sequencing are indicated by blue lines. (b). *B2M* methylation analysis data. Each square represents a CpG site. Total number of CpG sites within the *B2M* gene is shown. The colour code indicates methylation percentage as calculated by ESME analysis. (c). Methylation levels after 5-aza-CdR treatment. DNA extracted from MCF7 5-aza-CdR treated and untreated cells were subjected to bisulphite sequencing analysis. Data were analysed using ESME. Traces corresponding to 5-aza-CdR treated and untreated samples as well as traces before and after ESME normalization values are shown. Concentration of 5-aza-CdR used is indicated. Methylation values for each CpG are shown. This figure shows a representative part of the sequencing data generated corresponding for the amplicon in exon-2.

6.5 Discussion

In this chapter the four genes, *B2M*, *ERp57*, *CANX* and *CALR*, involved in the MHC pathway and encoded outside the MHC, were analysed. Expression analysis revealed that only *B2M* is down-regulated in the nine cancer cell lines tested. Treatment of two cell lines with DNA methylation inhibitors resulted in *B2M* up-regulation in only one (MCF7). Bisulphite sequencing analysis revealed methylation

differences between the cancer cell lines and the shared controls. However, because of no induction of expression in 578T cells after 5-aza-CdR treatment, methylation within the *B2M* gene could not be correlated with expression. The induction observed in MCF7 5-aza-CdR treated cells may be explained by an MCF7-specific silencing mechanism involving DNA methylation; different cancer cell lines may use different mechanisms for gene silencing.

ERp57, *CANX* and *CALR* did not show down-regulation in the cell lines studied here and did not respond to 5'-aza-CdR treatment. Hence their methylation status was not studied further. The slight up-regulation of these genes in some of the cell lines may contribute to the MHC class I^- phenotype. Further experiments including inhibition of expression of these genes and studying the effect on MHC class I^- phenotype will be informative.

6.6 Conclusion

B2M, *ERp57*, *CANX* and *CALR*, are genes encoded outside the MHC region, but their products are involved in the MHC class I pathway. Expression analysis revealed that only the *B2M* gene was down-regulated in the cell lines displaying the MHC class I^- phenotype.

Chapter 7

General Discussion

7.1 Introduction

In this chapter, data from chapters 3, 4, 5 and 6 are discussed in the context of recent studies concerning the epigenetics and regulation of MHC gene expression. A discussion on array-based assays for the identification of differentially methylated regions (DMRs) (chapter 3) is followed by discussions on the two DMR screens I performed (tDMR and pDMR screens) and are described in chapters 4, 5 and 6. Plans for future work following the work described in this thesis are also presented.

Finally, I introduce and discuss: (i). the phenomenon of Long Range Epigenetic Silencing (section 7.5), and (ii). the association between recombination hotspots and epigenetic events (section 7.6). These two concepts, although not discussed before in this thesis, are both relevant to the MHC region and should be considered for future MHC-related studies.

7.2 Array-based assay for DMR identification

I constructed a 2kb genomic tiling array of the entire MHC region. At the time of the array design, whole genome tiling arrays were constructed from PACs and BACs resulting in an approximate resolution of 100kb (Fiegler et al., 2006). Although commercial arrays are now available at much higher resolution (5 - 50mers), the MHC tiling array is still of great value today, as it can be used for multiple applications and is freely available from the Wellcome Trust Sanger Institute Microarray facility.

With respect to applications, the array is compatible with chromatin immunoprecipitation (ChIP), methylated DNA immunoprecipitation (MeDIP), array comparative genomic hybridization (aCGH) and expression analysis. It can be used to: (i). generate histone modification and DNA methylation maps, (ii). to study structural variation (CNVs) and (iii). to generate gene expression profiles and strand-specific transcript maps along the MHC. Hence, this platform in combination with the abundant data regarding single

nucleotide polymorphisms (SNPs) within the MHC, is a great resource for studying how genetic and epigenetic variation interact and how this interplay affects expression patterns which could eventually result in MHC-linked complex diseases.

This array has been used here for DNA methylation analysis and DMR identification and, by another group, for the identification of chromatin loops within the MHC (Ottaviani, 2008), underlining the multiple-purpose design of this array.

7.2.1 Future directions

Today, oligonucleotide tiling arrays with increasingly high probe densities and improved coverage, resolution and cost-effectiveness have enabled high-resolution studies of cytosine methylation when combined with MeDIP. Such arrays have already been used for the completion of the first high-resolution analysis of the *A. thaliana* methylome (Zhang et al., 2008). In addition, the development of a novel algorithm employing a Bayesian de-convolution strategy to normalize MeDIP array data can be expected to further increase the potential of high-resolution arrays for DNA methylation analysis (Down et al., 2008).

Hence, if I were to decide on my experimental approach today, I would have taken a different path. I would either develop a higher resolution array covering the MHC region or use deep sequencing of MeDIP- or bisulphite-treated DNA as it was described recently (Down et al., 2008; Meissner et al., 2008) and is discussed in the general introduction of this thesis (chapter 1).

In conclusion, the development of the MeDIP-MHC tiling array approach for DMR detection was highly innovative and demanding at the time it was established and remains to be a valuable resource for MHC-related studies.

7.3 tDMR screen

7.3.1 tDMRs within the MHC

Following the publication of the HEP pilot study (Rakyan et al., 2004) I performed the tDMR screen aiming to generate more comprehensive tissue-specific methylation data within the MHC. I identified 55 tDMRs, of which 54 were not identified by the HEP study, emphasizing the advantage of my unbiased assay covering the whole MHC region. However, I failed to identify 11 tDMRs reported by the HEP. The reason for this may be the limited resolution (2kb) of my MHC tiling array compared to bisulphite sequencing (1 bp resolution) used by the HEP. Today, this limitation could be overcome by higher resolution microarrays.

7.3.2 Genomic Features of tDMRs

Our understanding of the biological function of DNA methylation in mammals has been growing steadily over the last few years but is still far from complete. Identification of genomic regions with known and as yet unknown features that show differential methylation patterns is expected to give further functional insights into DNA methylation. To this end, a number of large-scale and genome-wide DNA methylation studies have been conducted aiming to identify DMRs in normal and disease-associated samples (Eckhardt et al., 2006; Keshet et al., 2006; Rakyan et al., 2008; Weber et al., 2005; Weber et al., 2007). One of the most striking findings of these studies is that DMRs are not always present in 5'UTRs or in close proximity to TSSs of genes, supporting the notion that DNA methylation has a functional role beyond the mere control of transcription through promoter methylation.

In this context and by using the annotation provided by the Ensembl genome browser, I extracted the genomic features overlapping with the 55 MHC loci characterised as

tDMRs. More specifically, I reported the genomic features mapping within the genomic boundaries of the tDMRs (average size 2kb).

In agreement with what has been reported in other studies, only one of the tDMRs identified within this study overlaps with a TSS and only two with RNA polII binding sites. Based on my analysis, H3 lysine 4 tri-methylation (H3K4me3) is the most highly correlated genomic feature with differential DNA methylation. According to a recent publication, DNA methylation is in strong inverse correlation with H3K4me3 (Meissner et al., 2008) indicating that histone marks may drive the formation of DNA methylation patterns. Generation of maps for histone marks across the MHC using the MHC tiling array may therefore be informative in this context and may give further insights into the interplay between histone marks and DNA methylation. Histone marks and DNA methylation are the two major components defining the epigenome.

7.3.3 Copy number variation and DNA methylation

As part of the analysis conducted for the tDMR screen (chapter 4), I correlated the tDMRs overlapping with MHC transcripts with the corresponding expression data available from the GNF atlas of gene expression. This analysis revealed that tDMRs within the *C4A* and *C4B* loci show inverse correlation with *C4A* and *C4B* expression levels, implicating DNA methylation in the mechanism regulating their expression.

C4A and *C4B* genes are located in the MHC class III region, show more that 99% sequence similarity and are examples of copy number variants (CNVs) in the human genome. In the Caucasian population 55% of the MHC haplotypes have the 2-locus C4A-C4B configuration and 45% have an unequal number of *C4A* and *C4B* genes. This indicates that MHC haplotypes are subjected to duplications/deletions within the region encoding for *C4A* and *C4B* loci (Blanchong et al., 2001).

Gene duplication is commonly regarded as the main evolutionary mechanism towards the gain of a new gene function (Jiang et al., 2007). It has been suggested that epigenetic silencing protects newly born duplications from degradation to pseudogenes (Rodin and Riggs, 2003), leading to functional divergence between duplicated genes. This is further supported by the notion that the frequency of young gene duplicates is higher in organism that have cytosine methylation (*H. sapiens, M. musculus* and *A. thaliana*) than in organisms that do not have methylated genomes (*S. cerevisiae*, *D. melanogaster*, and *C. elegans*) (Lynch and Conery, 2000).

Based on the above and on my data, I have reasoned that duplicated genes with otherwise normal expression levels may be silenced by DNA methylation. This is supported by association studies reporting that gene duplications are not always in positive correlation with gene expression (Stranger et al., 2007). In this context and in collaboration with Vardhman Rakyan, I have already generated methylation data for a number of samples used for the CNV project (Redon et al., 2006). Analysis and correlation of these data with the available CNV, HapMap (SNPs) and expression data for these samples is expected to provide great insights into how DMRs, CNVs and SNPs interact to form complex phenotypes. In addition, this analysis may provide further insights into the evolutionary mechanism that lead to the generation of new genes by duplication.

7.3.4 Future directions

While acknowledging the progress that has been made in DNA methylation profiling technology, the tDMR screen (using the MeDIP-MHC tiling array approach) can be followed up by additional experiments as described below:

i. Recently the term ‘population epigenetics’ was introduced (Richards, 2008) underlining one of the greatest challenges in the field of epigenetics at moment: the determination of

the proportion of natural epigenetic variation in the human population. Understanding the significance of epigenetic polymorphism requires: (i). systematic approaches cataloguing epigenetic variation across the genome, including cytosine methylation and histone tail modifications and (ii). association of epigenetic variability with changes in local gene expression. Analyses of samples from different human populations, different tissues and cell types as well as from different phenotypes are necessary.

In this context, I would analyse additional tissue types and biological samples. This will allow the identification of additional tDMRs and the estimation of inter-individual variability in DNA methylation levels which has been reported for the MHC region (Rakyan et al., 2004) as well as in germ cells (Flanagan et al., 2006) and repetitive elements (Sandovici et al., 2005).

At this point I would like to mention that currently there are a lot of large collaborative projects both in the USA and in Europe that aim to determine and elucidate the significance of epigenetic variation in the human population (Jones and Martienssen, 2005; Qiu, 2006).

ii. Although most of the genes in the MHC class I and III regions are expressed in all somatic cell types, MHC class II gene expression is largely restricted to antigen presenting cells. Cytokines such as IFN-γ can induce expression of classical MHC class II genes and up-regulate genes in the MHC class I and III regions (Boehm et al., 1997; Rohn et al., 1996). It is also known that epigenetic events, including histone marks and non-coding RNAs (Wright and Ting, 2006), can control MHC class II gene expression. These epigenetic events were shown to be induced by IFN-γ (Morris et al., 2002; Pattenden et al., 2002). It would be interesting to investigate further the role of DNA methylation in the selective expression of MHC class II molecules and how DNA methylation patterns change upon treatment with cytokines. To this end, it would be informative to apply the MeDIP-MHC tiling array approach to cell lines either expressing

or not expressing the classical MHC class II genes (*HLA-DP*, *-DQ*, and *-DR*), aiming to identify DMRs associated with MHC class II expression.

7.4 pDMR screen

7.4.1 pDMRs within the MHC

I identified two pDMRs that could be associated with the MHC class I^- phenotype. Of those only one was found to be overlapping with two of the genes involved in the MHC class I antigen and presentation pathway. This pDMR maps to the bidirectional promoter of the *TAP1/PSMB9* genes. Interestingly, this pDMR could not be associated with *PSMB9* down-regulation as it is also present in cell lines expressing this gene. Therefore, this pDMR is likely to be associated with the *TAP1* gene only. In addition, it was found to be associated with the down-regulation of the *HLA-A, HLA-B* and *PSMB8* gene expression levels. A second pDMR (within the *NMR* locus) was also associated with the down-regulation of these four genes: *HLA-A, HLA-B, TAP1* and *PSMB8*.

Although the association is high, proving the functional connection between the two pDMRs and the expression of the four genes is complicated due to our limited knowledge regarding the functional role of DNA methylation. It is possible that hypermethylation blocks a distant control element for *HLA-A, HLA-B, TAP1* and *PSMB8* genes (figure 4.1). This is possible to occur in a genomic region like the MHC where chromatin loops are known to be associated with transcriptional regulation (Ottaviani, 2008). Deletion of the two regions containing the two pDMRs and subsequent expression analysis would be an experimental approach to investigate this possibility. In addition chromatin conformation capture (3C) assay (Dekker et al., 2002) can be employed to test the interaction of distant regions within the MHC. This approach has been used previously to show that DMRs within the imprinted genes Igf2 and H19 interact (Murrell et al., 2004). The regulatory role of these pDMRs could be further

verified by experiments looking for factors binding to these regions. A DNase footprinting assay would detect any DNA-protein interactions within the corresponding regions. Subsequent mass-spectrometric analysis could be use to reveal the identity of these proteins. Finally, additional bisulphite sequencing analysis may also be necessary to identify the exact CpG sites within these pDMRs that undergo differential methylation.

Interestingly, no pDMRs were identified within the coding regions of *HLA-A, -B* and *–C* genes. According to a previous publication, the promoters of these three genes are hypermethylated in human oesophageal squamous cell carcinomas (Nie et al., 2001) that display the HLA class I^- phenotype. The authors of this paper claimed that hypermethylation of the promoter regions of the *HLA-A, HLA-B* and *HLA-C* genes is a major mechanism of transcriptional inactivation. This deviation can be explained by: (i). the fact that DNA hypermethylation of MHC class I genes is a specific characteristic of oesophageal squamous cells (not tested here); (ii). the low MHC tiling array resolution (2kb); and (iii). the high sequence similarity (>80%) between MHC class I genes; it is possible that co-hybridization of highly similar DNA molecules is masking the effect of differential methylation. I have attempted to perform methylation analysis of the promoters of *HLA-A, -B*, and *–C* genes but was not successful in designing bisulphite primers that were locus-specific; MHC class I loci are highly polymorphic.

7.4.2 DMRs within the TNF cluster

I have identified three DMRs within the TNF cluster that can be associated with the expression of *LTA, LTB* and *TNF-α* genes. This agrees with previous data showing that *TNF-α* expression is controlled epigenetically (Sullivan et al., 2007). I showed that in addition to the *TNF-α* promoter, the gene bodies of *TNF-α*, *LTB* and *LTA* were hypermethylated in the majority of the cell lines tested. Hypermethylation of multiple loci within the TNF cluster can happen either simultaneously or it can follow a spreading

model for DNA methylation (Clark and Melki, 2002; Turker, 2002). Based on this model, hypermethylation of the TNF cluster can be a two-step process. Initially, CpG sites within the 5'UTR of *TNF-α* may be hypermethylated by *de novo* methylation (5m-CpG seeds). Subsequently, these 5m-CpG seeds may act as foci for methylation spreading to distal 5' and 3' CpG sites, resulting in the observed hypermethylation of the TNF-α, LTA and LTB gene bodies. Additional functional studies are required to verify this model.

Interestingly, the DMRs within the TNF-α loci are also associated with the HLA class I^- phenotype. TNF-α, together with IFN-γ, is a cytokine known to be an immune modifier acting on the MHC class I processing and presentation pathway by inducing expression of the *PSMB8, PSMB9, TAP1, TAP2* and MHC class I genes. A kB-like element within the promoter of these genes is responsible for the response upon TNF-α stimulation. *TAPBP* and *B2M* are known not to respond to TNF-α (Dovhey et al., 2000; Johnson, 2003; Johnson and Pober, 1994).

It is possible that the up-regulation I observed in MHC class I gene expression levels after 5-aza-CdR treatment is the result of demethylation of the TNF cluster and subsequent up-regulation of *TNF-α*. This speculation is supported by the fact that *B2M* and *TAPBP* do not respond significantly to 5-aza-CdR treatment. However as *HLA-C, PSMB9* and *TAP2* show normal expression levels in some cell lines with reduced *TNF-α* expression, further experiments are required before I can draw a conclusion. Also, there is one cell line (CCRF-CEM) that shows up-regulation of the *PSMB9* gene; interestingly CCRF-CEM displays higher levels of *TNF-α* gene expression compared to the other cell lines tested here.

It has been reported that TNF-α acts in synergy with interferons for the transcriptional activation of the MHC class I heavy and light chain genes (Johnson and Pober, 1994). Hence, it should be expected that in the absence of *TNF-α* (as it is the case for the cell

lines tested here) other cytokines would be sufficient to stimulate MHC class I expression and presentation. One such cytokine is IFN-γ which is the most prominent inducer of MHC class I expression.

It would have been interesting to analyse the expression levels of *IFN-γ* in the cell lines tested here. Recent evidence implicates epigenetics in the regulation of *IFN-γ* expression as well (Schoenborn et al., 2007; Spilianakis and Flavell, 2007) indicating that the two cytokines, TNF-α and IFN-γ, may be down-regulated simultaneously by DNA hypermethylation. Methylation analysis of the *IFN-γ* gene in the cell lines tested here should clarify this matter.

Finally, previous studies using MCF7, T47D and MDA-MB-231 cells (cell lines tested here) have shown that stimulation of MHC class I molecules was induced by IFN-γ or TNF-α (Dejardin et al., 1998) treatment. Hence, it is possible that low expression of the two cytokines (possibly due to promoter hypermethylation) in combination with pDMRs or other epigenetic modifications in the MHC region result in the MHC class I^- phenotype. It may be informative to treat the cancer cell lines tested here with TNF-α and IFN-γ . If my speculation is correct, this treatment should have similar effects as 5-aza-CdR on the expression levels of my candidate genes. Combined treatment with 5-aza-CdR and TNF-α/IFN-γ should result in an additive effect on expression levels of genes involved in the MHC class I pathway.

7.4.3 Transcriptional silencing and DNA hypermethylation

It has been proposed that gene silencing is the critical precursor of DNA methylation, as it may change the dynamic interplay between *de novo* methylation and demethylation of

CpG islands and tilts the balance in favour of DNA hypermethylation (Clark and Melki, 2002; Turker, 2002). This model can be used to explain hypermethylation in the promoter regions of the *PSMB8* and *B2M* genes in the cell lines tested here that show the lowest expression levels for the corresponding genes. However, this is only a speculation made based on the presence of hypermethylated DMRs in cell lines with the lowest expression levels.

It would be interesting to follow up the impact of gene silencing to methylation patterns. This has already been done for a number of genes, including the *GSTP1* and *RASSF1A* (Song et al., 2002; Strunnikova et al., 2005) but further more systematic approaches are required to confirm the ability and the requirements for gene silencing to drive *de novo* methylation. This would give further mechanistic insights in *de novo* methylation that is observed in many diseases including cancer.

7.4.4 Future directions

The findings of the pDMR screen are consistent with the notion that DNA methylation is involved in the development of the MHC class I^- phenotype. In order to further support my findings, the following experiments could be performed:

(i). treatment of additional cell lines with and without the MHC class I^- phenotype with methylation inhibitors.

(ii). I would take advantage of recent developments in microarray technology and perform similar analysis using high-resolution (e.g. 50bp resolution) arrays, as it was discussed above. Using these array-platforms it may be possible to identify additional pDMRs and ease the effort to identify the exact CpG sites that undergo aberrant methylation in samples with the MHC class I^- phenotype.

(iii). study genetic variation (SNPs and CNVs) within the MHC region for the same samples tested under (ii). Meta-analysis of such genetic data with methylation data will

allow the identification of 'hepitypes' linked with MHC phenotypes. Hepitypes were introduced recently and refer to genetic haplotypes which when combined with specific methylation patterns (epitypes) may contribute to the development of a phenotype (Murrell et al., 2005). Sequence-dependent allele specific methylation patters (hepitypes) were recently identified in normal individuals (Kerkel et al., 2008) as well as in individuals with chronic lymphocytic leukaemia (CLL) (Raval et al., 2007). This analysis can also be implemented by expression analysis. Such meta-analysis can be expected to have great medical relevance for the diagnosis and treatment of MHC-linked diseases.

(iv) While the system and analysis described above is suitable to identify pDMRs and study their underlying mechanisms in cell lines, primary tissue samples will need to be analysed to confirm the involvement of such pDMRs in clinical samples displaying the same or similar phenotype.

7.5 Long Range Epigenetic Silencing

A recent study suggested that epigenetic changes in cancer are not always local but can be global encompassing large-scale chromosomal regions, resulting in concordant repression of large regions of DNA (Long Range Epigenetic Silencing – LRES) (Frigola et al., 2006). LRES was observant in a 4Mb band on chromosome 2q14.2. In a similar manner, LRES could be involved in the concordant silencing of multiple MHC (a 4Mb region on chromosome 6) loci. More comprehensive DNA methylation analysis, in combination with histone marks and expression profiling would be informative with respect to LRES within the MHC region.

7.6 Recombination hotspots and epigenetic events

Although not experimentally tested within this thesis, it has been shown that epigenetic events can be implicated in controlling events of recombination hotspots during meiosis. Meiotic recombination between highly similar duplicated sequences (non-allelic

homologous recombination, NAHR) generates deletions, duplications, inversions and translocations that frequently result in genomic disorders (Turner et al., 2008). It has been shown that in males, the presence of meiotic recombination hotspots is not influenced by genomic sequence but rather by distal regulatory elements or epigenetic events (Neumann and Jeffreys, 2006). The latter may control accessibility of these hotspots. The MHC class II region represents a prominent region where such hotspots have been detected (Kauppi et al., 2005).

Studying how epigenetic events within the MHC influence this phenomenon will be the basis for future studies regarding genomic disorders that are the result of genomic rearrangements as well as for studies aiming to elucidate the evolution of the MHC region.

7.7 Conclusion

This thesis describes the most comprehensive DNA methylation analysis of the human MHC region to date. I developed and used an unbiased array-based assay for the detection of differentially methylated regions (DMRs) that can be associated with particular tissues (tDMRs) and particular phenotypes (pDMRs). The study presented here, underlines the important role of epigenetic variation in phenotypic plasticity.

Current advances in epigenome mapping technologies and the various epigenome projects that have been established recently (Jones and Martienssen, 2005; Qiu, 2006) are expected to give critical insights into the interplay between the genotype, the epigenotype and the environment and serve as catalyst for future studies on human complex diseases.

Bibliography

Adorjan, P., Distler, J., Lipscher, E., Model, F., Muller, J., Pelet, C., Braun, A., Florl, A. R., Gutig, D., Grabs, G.*, et al.* (2002). Tumour class prediction and discovery by microarray-based DNA methylation analysis. Nucleic Acids Res *30*, e21.

Aggarwal, B. B., Shishodia, S., Ashikawa, K., and Bharti, A. C. (2002). The role of TNF and its family members in inflammation and cancer: lessons from gene deletion. Curr Drug Targets Inflamm Allergy *1*, 327-341.

Aguado, B. M., C.M.; Campbell, R.D.; (1996). Genes of the MHC class III region and the functions of the proteins they encode, In HLA and MHC: Genes, Molecules and Function, M. M. Browning, A.J., ed. (Bios Scientific Publishers Ltd, Oxford, UK), pp. 34-45.

Alfonso, C., and Karlsson, L. (2000). Nonclassical MHC class II molecules. Annu Rev Immunol *18*, 113-142.

Allis, C. D., Jenuwein, T., and Reinberg, D. (2007). Epigenetics (Cold Spring Harbor, N.Y.: Cold Spring Harbor Laboratory Press).

Andersson, G., Larhammar, D., Widmark, E., Servenius, B., Peterson, P. A., and Rask, (1987). Class II genes of the human major histocompatibility complex. Organization and evolutionary relationship of the DR beta genes. J Biol Chem *262*, 8748-8758.

Androlewicz, M. J. (1999). The role of tapasin in MHC class I antigen assembly. Immunol Res *20*, 79-88.

Androlewicz, M. J., and Cresswell, P. (1994). Human transporters associated with antigen processing possess a promiscuous peptide-binding site. Immunity *1*, 7-14.

Ballestar, E., Paz, M. F., Valle, L., Wei, S., Fraga, M. F., Espada, J., Cigudosa, J. C., Huang, T. H., and Esteller, M. (2003). Methyl-CpG binding proteins identify novel sites of epigenetic inactivation in human cancer. Embo J *22*, 6335-6345.

Ballestar, E., and Wolffe, A. P. (2001). Methyl-CpG-binding proteins. Targeting specific gene repression. Eur J Biochem *268*, 1-6.

Beck, S., Olek, A., and Walter, J. (1999). From genomics to epigenomics: a loftier view of life. Nat Biotechnol *17*, 1144.

Beck, S., and Rakyan, V. K. (2008). The methylome: approaches for global DNA methylation profiling. Trends Genet *24*, 231-237.

Beckmann, J. S., Estivill, X., and Antonarakis, S. E. (2007). Copy number variants and genetic traits: closer to the resolution of phenotypic to genotypic variability. Nat Rev Genet *8*, 639-646.

Berger, S. L. (2007). The complex language of chromatin regulation during transcription. Nature *447*, 407-412.

Bernstein, B. E., Meissner, A., and Lander, E. S. (2007). The mammalian epigenome. Cell *128*, 669-681.

Bertone, P., Gerstein, M., and Snyder, M. (2005). Applications of DNA tiling arrays to experimental genome annotation and regulatory pathway discovery. Chromosome Res *13*, 259-274.

Bestor, T. H. (2000). The DNA methyltransferases of mammals. Hum Mol Genet *9*, 2395-2402.

Bibikova, M., Chudin, E., Wu, B., Zhou, L., Garcia, E. W., Liu, Y., Shin, S., Plaia, T. W., Auerbach, J. M., Arking, D. E.*, et al.* (2006). Human embryonic stem cells have a unique epigenetic signature. Genome Res *16*, 1075-1083.

Bird, A. (2002). DNA methylation patterns and epigenetic memory. Genes Dev *16*, 6-21.

Blanchet, O., Bourge, J. F., Zinszner, H., Israel, A., Kourilsky, P., Dausset, J., Degos, L., and Paul, P. (1992). Altered binding of regulatory factors to HLA class I enhancer sequence in human tumor cell lines lacking class I antigen expression. Proc Natl Acad Sci U S A *89*, 3488-3492.

Blanchong, C. A., Chung, E. K., Rupert, K. L., Yang, Y., Yang, Z., Zhou, B., Moulds, J. M., and Yu, C. Y. (2001). Genetic, structural and functional diversities of human complement components C4A and C4B and their mouse homologues, Slp and C4. Int Immunopharmacol *1*, 365-392.

Boehm, U., Klamp, T., Groot, M., and Howard, J. C. (1997). Cellular responses to interferon-gamma. Annu Rev Immunol *15*, 749-795.

Brena, R. M., Huang, T. H., and Plass, C. (2006). Toward a human epigenome. Nat Genet *38*, 1359-1360.

Carrozza, M. J., Li, B., Florens, L., Suganuma, T., Swanson, S. K., Lee, K. K., Shia, W. J., Anderson, S., Yates, J., Washburn, M. P., and Workman, J. L. (2005). Histone H3 methylation by Set2 directs deacetylation of coding regions by Rpd3S to suppress spurious intragenic transcription. Cell *123*, 581-592.

Chang, C. C., Campoli, M., and Ferrone, S. (2003). HLA class I defects in malignant lesions: what have we learned? Keio J Med *52*, 220-229.

Chen, T., Hevi, S., Gay, F., Tsujimoto, N., He, T., Zhang, B., Ueda, Y., and Li, E. (2007). Complete inactivation of DNMT1 leads to mitotic catastrophe in human cancer cells. Nat Genet *39*, 391-396.

Christman, J. K. (2002). 5-Azacytidine and 5-aza-2'-deoxycytidine as inhibitors of DNA methylation: mechanistic studies and their implications for cancer therapy. Oncogene *21*, 5483-5495.

Christova, R., Jones, T., Wu, P. J., Bolzer, A., Costa-Pereira, A. P., Watling, D., Kerr, I. M., and Sheer, D. (2007). P-STAT1 mediates higher-order chromatin remodelling of the human MHC in response to IFNgamma. J Cell Sci *120*, 3262-3270.

Chung, E. K., Yang, Y., Rennebohm, R. M., Lokki, M. L., Higgins, G. C., Jones, K. N., Zhou, B., Blanchong, C. A., and Yu, C. Y. (2002). Genetic sophistication of human complement components C4A and C4B and RP-C4-CYP21-TNX (RCCX) modules in the major histocompatibility complex. Am J Hum Genet *71*, 823-837.

Clark, S. J., and Melki, J. (2002). DNA methylation and gene silencing in cancer: which is the guilty party? Oncogene *21*, 5380-5387.

Clark, S. J., Statham, A., Stirzaker, C., Molloy, P. L., and Frommer, M. (2006). DNA methylation: bisulphite modification and analysis. Nat Protoc *1*, 2353-2364.

Coombes, M. M., Briggs, K. L., Bone, J. R., Clayman, G. L., El-Naggar, A. K., and Dent, S. Y. (2003). Resetting the histone code at CDKN2A in HNSCC by inhibition of DNA methylation. Oncogene *22*, 8902-8911.

Costa, F. F. (2005). Non-coding RNAs: new players in eukaryotic biology. Gene *357*, 83-94.

Cross, S. H., and Bird, A. P. (1995). CpG islands and genes. Curr Opin Genet Dev *5*, 309-314.

Culina, S., Lauvau, G., Gubler, B., and van Endert, P. M. (2004). Calreticulin promotes folding of functional human leukocyte antigen class I molecules in vitro. J Biol Chem *279*, 54210-54215.

de Bakker, P. I., McVean, G., Sabeti, P. C., Miretti, M. M., Green, T., Marchini, J., Ke, X., Monsuur, A. J., Whittaker, P., Delgado, M.*, et al.* (2006). A high-resolution HLA and SNP haplotype map for disease association studies in the extended human MHC. Nat Genet *38*, 1166-1172.

de Visser, K. E., Eichten, A., and Coussens, L. M. (2006). Paradoxical roles of the immune system during cancer development. Nat Rev Cancer *6*, 24-37.

Dejardin, E., Deregowski, V., Greimers, R., Cai, Z., Chouaib, S., Merville, M. P., and Bours, V. (1998). Regulation of major histocompatibility complex class I expression by NF-kappaB-related proteins in breast cancer cells. Oncogene *16*, 3299-3307.

Dekker, J., Rippe, K., Dekker, M., and Kleckner, N. (2002). Capturing chromosome conformation. Science *295*, 1306-1311.

Dhami, P., Coffey, A. J., Abbs, S., Vermeesch, J. R., Dumanski, J. P., Woodward, K. J., Andrews, R. M., Langford, C., and Vetrie, D. (2005). Exon array CGH: detection of copy-number changes at the resolution of individual exons in the human genome. Am J Hum Genet *76*, 750-762.

Dovhey, S. E., Ghosh, N. S., and Wright, K. L. (2000). Loss of interferon-gamma inducibility of TAP1 and LMP2 in a renal cell carcinoma cell line. Cancer Res *60*, 5789-5796.

Down, T. A., Rakyan, V. K., Turner, D. J., Flicek, P., Li, H., Kulesha, E., Graf, S., Johnson, N., Herrero, J., Tomazou, E. M.*, et al.* (2008). A Bayesian deconvolution strategy for immunoprecipitation-based DNA methylome analysis. Nat Biotechnol *26*, 779-785.

Dumitru, C. D., Ceci, J. D., Tsatsanis, C., Kontoyiannis, D., Stamatakis, K., Lin, J. H., Patriotis, C., Jenkins, N. A., Copeland, N. G., Kollias, G., and Tsichlis, P. N. (2000). TNF-alpha induction by LPS is regulated posttranscriptionally via a Tpl2/ERK-dependent pathway. Cell *103*, 1071-1083.

Eckhardt, F., Lewin, J., Cortese, R., Rakyan, V. K., Attwood, J., Burger, M., Burton, J., Cox, T. V., Davies, R., Down, T. A.*, et al.* (2006). DNA methylation profiling of human chromosomes 6, 20 and 22. Nat Genet *38*, 1378-1385.

Eden, A., Gaudet, F., Waghmare, A., and Jaenisch, R. (2003). Chromosomal instability and tumors promoted by DNA hypomethylation. Science *300*, 455.

Ehrlich, M., Gama-Sosa, M. A., Huang, L. H., Midgett, R. M., Kuo, K. C., McCune, R. A., and Gehrke, C. (1982). Amount and distribution of 5-methylcytosine in human DNA from different types of tissues of cells. Nucleic Acids Res *10*, 2709-2721.

Estecio, M. R., Yan, P. S., Ibrahim, A. E., Tellez, C. S., Shen, L., Huang, T. H., and Issa, J. P. (2007). High-throughput methylation profiling by MCA coupled to CpG island microarray. Genome Res *17*, 1529-1536.

Fahrner, J. A., Eguchi, S., Herman, J. G., and Baylin, S. B. (2002). Dependence of histone modifications and gene expression on DNA hypermethylation in cancer. Cancer Res *62*, 7213-7218.

Falvo, J. V., Brinkman, B. M., Tsytsykova, A. V., Tsai, E. Y., Yao, T. P., Kung, A. L., and Goldfeld, A. E. (2000). A stimulus-specific role for CREB-binding protein (CBP) in T cell receptor-activated tumor necrosis factor alpha gene expression. Proc Natl Acad Sci U S A *97*, 3925-3929.

Falvo, J. V., Uglialoro, A. M., Brinkman, B. M., Merika, M., Parekh, B. S., Tsai, E. Y., King, H. C., Morielli, A. D., Peralta, E. G., Maniatis, T.*, et al.* (2000). Stimulus-specific assembly of enhancer complexes on the tumor necrosis factor alpha gene promoter. Mol Cell Biol *20*, 2239-2247.

Farthing, C. R., Ficz, G., Ng, R. K., Chan, C. F., Andrews, S., Dean, W., Hemberger, M., and Reik, W. (2008). Global mapping of DNA methylation in mouse promoters reveals epigenetic reprogramming of pluripotency genes. PLoS Genet *4*, e1000116.

Feinberg, A. P. (2004). The epigenetics of cancer etiology. Semin Cancer Biol *14*, 427-432.

Feinberg, A. P. (2008). Epigenetics at the epicenter of modern medicine. Jama *299*, 1345-1350.

Fellay, J., Shianna, K. V., Ge, D., Colombo, S., Ledergerber, B., Weale, M., Zhang, K., Gumbs, C., Castagna, A., Cossarizza, A.*, et al.* (2007). A whole-genome association study of major determinants for host control of HIV-1. Science *317*, 944-947.

Fiegler, H., Redon, R., Andrews, D., Scott, C., Andrews, R., Carder, C., Clark, R., Dovey, O., Ellis, P., Feuk, L.*, et al.* (2006). Accurate and reliable high-throughput detection of copy number variation in the human genome. Genome Res *16*, 1566- 1574.

Finnegan, E. J., and Kovac, K. A. (2000). Plant DNA methyltransferases. Plant Mol Biol *43*, 189-201.

Flanagan, J. M., Popendikyte, V., Pozdniakovaite, N., Sobolev, M., Assadzadeh, A., Schumacher, A., Zangeneh, M., Lau, L., Virtanen, C., Wang, S. C., and Petronis, A. (2006). Intra- and interindividual epigenetic variation in human germ cells. Am J Hum Genet *79*, 67-84.

Flutter, B., and Gao, B. (2004). MHC class I antigen presentation--recently trimmed and well presented. Cell Mol Immunol *1*, 22-30.

Fonsatti, E., Nicolay, H. J., Sigalotti, L., Calabro, L., Pezzani, L., Colizzi, F., Altomonte, M., Guidoboni, M., Marincola, F. M., and Maio, M. (2007). Functional up-regulation of human leukocyte antigen class I antigens expression by 5-aza-2'-deoxycytidine in cutaneous melanoma: immunotherapeutic implications. Clin Cancer Res *13*, 3333-3338.

Fonsatti, E., Sigalotti, L., Coral, S., Colizzi, F., Altomonte, M., and Maio, M. (2003). Methylation-regulated expression of HLA class I antigens in melanoma. Int J Cancer *105*, 430-431; author reply 432-433.

Fraga, M. F., Ballestar, E., Paz, M. F., Ropero, S., Setien, F., Ballestar, M. L., Heine-Suner, D., Cigudosa, J. C., Urioste, M., Benitez, J.*, et al.* (2005). Epigenetic differences arise during the lifetime of monozygotic twins. Proc Natl Acad Sci U S A *102*, 10604-10609.

Frigola, J., Song, J., Stirzaker, C., Hinshelwood, R. A., Peinado, M. A., and Clark, S. J. (2006). Epigenetic remodeling in colorectal cancer results in coordinate gene suppression across an entire chromosome band. Nat Genet *38*, 540-549.

Frommer, M., McDonald, L. E., Millar, D. S., Collis, C. M., Watt, F., Grigg, G. W., Molloy, P. L., and Paul, C. L. (1992). A genomic sequencing protocol that yields a positive display of 5-methylcytosine residues in individual DNA strands. Proc Natl Acad Sci U S A *89*, 1827-1831.

Futscher, B. W., Oshiro, M. M., Wozniak, R. J., Holtan, N., Hanigan, C. L., Duan, H., and Domann, F. E. (2002). Role for DNA methylation in the control of cell type specific maspin expression. Nat Genet *31*, 175-179.

Gaczynska, M., Rock, K. L., and Goldberg, A. L. (1993). Role of proteasomes in antigen presentation. Enzyme Protein *47*, 354-369.

Gal-Yam, E. N., Saito, Y., Egger, G., and Jones, P. A. (2008). Cancer epigenetics: modifications, screening, and therapy. Annu Rev Med *59*, 267-280.

Garbi, N., Hammerling, G., and Tanaka, S. (2007). Interaction of ERp57 and tapasin in the generation of MHC class I-peptide complexes. Curr Opin Immunol *19*, 99-105.

Garbi, N., Tanaka, S., Momburg, F., and Hammerling, G. J. (2006). Impaired assembly of the major histocompatibility complex class I peptide-loading complex in mice deficient in the oxidoreductase ERp57. Nat Immunol *7*, 93-102.

Garcia-Lora, A., Algarra, I., and Garrido, F. (2003). MHC class I antigens, immune surveillance, and tumor immune escape. J Cell Physiol *195*, 346-355.

Gentleman, R. C., Carey, V. J., Bates, D. M., Bolstad, B., Dettling, M., Dudoit, S., Ellis, B., Gautier, L., Ge, Y., Gentry, J.*, et al.* (2004). Bioconductor: open software development for computational biology and bioinformatics. Genome Biol *5*, R80.

Geraghty, D. E. (1993). Structure of the HLA class I region and expression of its resident genes. Curr Opin Immunol *5*, 3-7.

Gitan, R. S., Shi, H., Chen, C. M., Yan, P. S., and Huang, T. H. (2002). Methylation-specific oligonucleotide microarray: a new potential for high-throughput methylation analysis. Genome Res *12*, 158-164.

Gleimer, M., and Parham, P. (2003). Stress management: MHC class I and class I-like molecules as reporters of cellular stress. Immunity *19*, 469-477.

Glynne, R., Powis, S. H., Beck, S., Kelly, A., Kerr, L. A., and Trowsdale, J. (1991). A proteasome-related gene between the two ABC transporter loci in the class II region of the human MHC. Nature *353*, 357-360.

Goll, M. G., and Bestor, T. H. (2005). Eukaryotic cytosine methyltransferases. Annu Rev Biochem *74*, 481-514.

Grandjean, V., Yaman, R., Cuzin, F., and Rassoulzadegan, M. (2007). Inheritance of an Epigenetic Mark: The CpG DNA Methyltransferase 1 Is Required for De Novo Establishment of a Complex Pattern of Non-CpG Methylation. PLoS ONE *2*, e1136.

Groothuis, T. A., Griekspoor, A. C., Neijssen, J. J., Herberts, C. A., and Neefjes, J. J. (2005). MHC class I alleles and their exploration of the antigen-processing machinery. Immunol Rev *207*, 60-76.

Gruss, H. J., and Dower, S. K. (1995). The TNF ligand superfamily and its relevance for human diseases. Cytokines Mol Ther *1*, 75-105.

Hatchwell, E., and Greally, J. M. (2007). The potential role of epigenomic dysregulation in complex human disease. Trends Genet *23*, 588-595.

Held, W., and Mariuzza, R. A. (2008). Cis interactions of immunoreceptors with MHC and non-MHC ligands. Nat Rev Immunol *8*, 269-278.

Hellman, A., and Chess, A. (2007). Gene body-specific methylation on the active X chromosome. Science *315*, 1141-1143.

Hewitt, E. W. (2003). The MHC class I antigen presentation pathway: strategies for viral immune evasion. Immunology *110*, 163-169.

Hinshelwood, R. A., Huschtscha, L. I., Melki, J., Stirzaker, C., Abdipranoto, A., Vissel, B., Ravasi, T., Wells, C. A., Hume, D. A., Reddel, R. R., and Clark, S. J. (2007). Concordant epigenetic silencing of transforming growth factor-beta signaling pathway genes occurs early in breast carcinogenesis. Cancer Res *67*, 11517-11527.

Hoffmann, A. A., and Willi, Y. (2008). Detecting genetic responses to environmental change. Nat Rev Genet *9*, 421-432.

Hoheisel, J. D. (2006). Microarray technology: beyond transcript profiling and genotype analysis. Nat Rev Genet *7*, 200-210.

Holliday, R., and Pugh, J. E. (1975). DNA modification mechanisms and gene activity during development. Science *187*, 226-232.

Holmer, L., and Worman, H. J. (2001). Inner nuclear membrane proteins: functions and targeting. Cell Mol Life Sci *58*, 1741-1747.

Horton, R., Gibson, R., Coggill, P., Miretti, M., Allcock, R. J., Almeida, J., Forbes, S., Gilbert, J. G., Halls, K., Harrow, J. L.*, et al.* (2008). Variation analysis and gene annotation of eight MHC haplotypes: the MHC Haplotype Project. Immunogenetics *60*, 1-18.

Horton, R., Wilming, L., Rand, V., Lovering, R. C., Bruford, E. A., Khodiyar, V. K., Lush, M. J., Povey, S., Talbot, C. C., Jr., Wright, M. W.*, et al.* (2004). Gene map of the extended human MHC. Nat Rev Genet *5*, 889-899.

Hubbard, T. J., Aken, B. L., Beal, K., Ballester, B., Caccamo, M., Chen, Y., Clarke, L., Coates, G., Cunningham, F., Cutts, T.*, et al.* (2007). Ensembl 2007. Nucleic Acids Res *35*, D610-617.

Hughes, E. A., Hammond, C., and Cresswell, P. (1997). Misfolded major histocompatibility complex class I heavy chains are translocated into the cytoplasm and degraded by the proteasome. Proc Natl Acad Sci U S A *94*, 1896-1901.

Illingworth, R., Kerr, A., Desousa, D., Jorgensen, H., Ellis, P., Stalker, J., Jackson, D., Clee, C., Plumb, R., Rogers, J.*, et al.* (2008). A novel CpG island set identifies tissue-specific methylation at developmental gene loci. PLoS Biol *6*, e22.

Jaenisch, R., and Bird, A. (2003). Epigenetic regulation of gene expression: how the genome integrates intrinsic and environmental signals. Nat Genet *33 Suppl*, 245-254.

Jiang, Z., Tang, H., Ventura, M., Cardone, M. F., Marques-Bonet, T., She, X., Pevzner, P. A., and Eichler, E. E. (2007). Ancestral reconstruction of segmental duplications reveals punctuated cores of human genome evolution. Nat Genet *39*, 1361-1368.

Johnsen, A., France, J., Sy, M. S., and Harding, C. V. (1998). Down-regulation of the transporter for antigen presentation, proteasome subunits, and class I major histocompatibility complex in tumor cell lines. Cancer Res *58*, 3660-3667.

Johnson, D. R. (2003). Locus-specific constitutive and cytokine-induced HLA class I gene expression. J Immunol *170*, 1894-1902.

Johnson, D. R., and Pober, J. S. (1994). HLA class I heavy-chain gene promoter elements mediating synergy between tumor necrosis factor and interferons. Mol Cell Biol *14*, 1322-1332.

Jones, P. A., and Baylin, S. B. (2002). The fundamental role of epigenetic events in cancer. Nat Rev Genet *3*, 415-428.

Jones, P. A., and Martienssen, R. (2005). A blueprint for a Human Epigenome Project: the AACR Human Epigenome Workshop. Cancer Res *65*, 11241-11246.

Jones, P. A., and Taylor, S. M. (1980). Cellular differentiation, cytidine analogs and DNA methylation. Cell *20*, 85-93.

Kaminskas, E., Farrell, A., Abraham, S., Baird, A., Hsieh, L. S., Lee, S. L., Leighton, J. K., Patel, H., Rahman, A., Sridhara, R.*, et al.* (2005). Approval summary: azacitidine for treatment of myelodysplastic syndrome subtypes. Clin Cancer Res *11*, 3604-3608.

Kantarjian, H., Oki, Y., Garcia-Manero, G., Huang, X., O'Brien, S., Cortes, J., Faderl, S., Bueso-Ramos, C., Ravandi, F., Estrov, Z.*, et al.* (2007). Results of a randomized study of 3 schedules of low-dose decitabine in higher-risk myelodysplastic syndrome and chronic myelomonocytic leukemia. Blood *109*, 52-57.

Kauppi, L., Stumpf, M. P., and Jeffreys, A. J. (2005). Localized breakdown in linkage disequilibrium does not always predict sperm crossover hot spots in the human MHC class II region. Genomics *86*, 13-24.

Kelly, A., Powis, S. H., Kerr, L. A., Mockridge, I., Elliott, T., Bastin, J., Uchanska-Ziegler, B., Ziegler, A., Trowsdale, J., and Townsend, A. (1992). Assembly and function of the two ABC transporter proteins encoded in the human major histocompatibility complex. Nature *355*, 641-644.

Kerkel, K., Spadola, A., Yuan, E., Kosek, J., Jiang, L., Hod, E., Li, K., Murty, V. V., Schupf, N., Vilain, E.*, et al.* (2008). Genomic surveys by methylation-sensitive

SNP analysis identify sequence-dependent allele-specific DNA methylation. Nat Genet *40*, 904-908.

Keshet, I., Schlesinger, Y., Farkash, S., Rand, E., Hecht, M., Segal, E., Pikarski, E., Young, R. A., Niveleau, A., Cedar, H., and Simon, I. (2006). Evidence for an instructive mechanism of de novo methylation in cancer cells. Nat Genet *38*, 149-153.

Khan, A. N., Gregorie, C. J., and Tomasi, T. B. (2008). Histone deacetylase inhibitors induce TAP, LMP, Tapasin genes and MHC class I antigen presentation by melanoma cells. Cancer Immunol Immunother *57*, 647-654.

Khulan, B., Thompson, R. F., Ye, K., Fazzari, M. J., Suzuki, M., Stasiek, E., Figueroa, M. E., Glass, J. L., Chen, Q., Montagna, C.*, et al.* (2006). Comparative isoschizomer profiling of cytosine methylation: the HELP assay. Genome Res *16*, 1046-1055.

Kiberstis, R. (2002). It's not Just the Genes. Science *296*, 685.

Kienast, A., Preuss, M., Winkler, M., and Dick, T. P. (2007). Redox regulation of peptide receptivity of major histocompatibility complex class I molecules by ERp57 and tapasin. Nat Immunol *8*, 864-872.

Kioussis, D. (2005). Gene regulation: kissing chromosomes. Nature *435*, 579-580.

Klose, R. J., and Bird, A. P. (2006). Genomic DNA methylation: the mark and its mediators. Trends Biochem Sci *31*, 89-97.

Kouzarides, T. (2007). Chromatin modifications and their function. Cell *128*, 693-705.

Lander, E. S., and Schork, N. J. (1994). Genetic dissection of complex traits. Science *265*, 2037-2048.

Lauvau, G., Gubler, B., Cohen, H., Daniel, S., Caillat-Zucman, S., and van Endert, P. M. (1999). Tapasin enhances assembly of transporters associated with antigen processing-dependent and -independent peptides with HLA-A2 and HLA-B27 expressed in insect cells. J Biol Chem *274*, 31349-31358.

Lawlor, D. A., Warren, E., Ward, F. E., and Parham, P. (1990). Comparison of class I MHC alleles in humans and apes. Immunol Rev *113*, 147-185.

Le Bouteiller, P. (1994). HLA class I chromosomal region, genes, and products: facts and questions. Crit Rev Immunol *14*, 89-129.

Lechler, R. Warrens, A.; (2000). HLA in Health and Disease, second edn: Academic Press).

Lehner, P. J., and Trowsdale, J. (1998). Antigen presentation: coming out gracefully. Curr Biol *8*, R605-608.

Lewin, J., Schmitt, A. O., Adorjan, P., Hildmann, T., and Piepenbrock, C. (2004). Quantitative DNA methylation analysis based on four-dye trace data from direct sequencing of PCR amplificates. Bioinformatics *20*, 3005-3012.

Lewis, A., and Murrell, A. (2004). Genomic imprinting: CTCF protects the boundaries. Curr Biol *14*, R284-286.

Li, L. H., Olin, E. J., Buskirk, H. H., and Reineke, L. M. (1970). Cytotoxicity and mode of action of 5-azacytidine on L1210 leukemia. Cancer Res *30*, 2760-2769.

Lippman, Z., Gendrel, A. V., Black, M., Vaughn, M. W., Dedhia, N., McCombie, W. R., Lavine, K., Mittal, V., May, B., Kasschau, K. D*., et al.* (2004). Role of transposable elements in heterochromatin and epigenetic control. Nature *430*, 471-476.

Lister, R., O'Malley, R. C., Tonti-Filippini, J., Gregory, B. D., Berry, C. C., Millar, A. H., and Ecker, J. R. (2008). Highly integrated single-base resolution maps of the epigenome in Arabidopsis. Cell *133*, 523-536.

Loke, Y. W., and King, A. (1991). Recent developments in the human maternal-fetal immune interaction. Curr Opin Immunol *3*, 762-766.

Lynch, M., and Conery, J. S. (2000). The evolutionary fate and consequences of duplicate genes. Science *290*, 1151-1155.

Maio, M., Coral, S., Fratta, E., Altomonte, M., and Sigalotti, L. (2003). Epigenetic targets for immune intervention in human malignancies. Oncogene *22*, 6484-6488.

Manning, J., Indrova, M., Lubyova, B., Pribylova, H., Bieblova, J., Hejnar, J., Simova, J., Jandlova, T., Bubenik, J., and Reinis, M. (2008). Induction of MHC class I molecule cell surface expression and epigenetic activation of antigen-processing machinery components in a murine model for human papilloma virus 16-associated tumours. Immunology *123*, 218-227.

Marsh, S. G. E., Parham, P and Barber, L.D. (2000). The HLA factsbook (San Diego, California: Academic Press).

Marx, K. A., Allen, J. R., and Hearst, J. E. (1976). Characterization of the repetitious human DNA families. Biochim Biophys Acta *425*, 129-147.

Maston, G. A., Evans, S. K., and Green, M. R. (2006). Transcriptional regulatory elements in the human genome. Annu Rev Genomics Hum Genet *7*, 29-59.

McDevitt, H., Munson, S., Ettinger, R., and Wu, A. (2002). Multiple roles for tumor necrosis factor-alpha and lymphotoxin alpha/beta in immunity and autoimmunity. Arthritis Res *4 Suppl 3*, S141-152.

Meissner, A., Gnirke, A., Bell, G. W., Ramsahoye, B., Lander, E. S., and Jaenisch, R. (2005). Reduced representation bisulfite sequencing for comparative high-resolution DNA methylation analysis. Nucleic Acids Res *33*, 5868-5877.

Meissner, A., Mikkelsen, T. S., Gu, H., Wernig, M., Hanna, J., Sivachenko, A., Zhang, X., Bernstein, B. E., Nusbaum, C., Jaffe, D. B.*, et al.* (2008). Genome-scale DNA methylation maps of pluripotent and differentiated cells. Nature.

Meissner, M., Reichert, T. E., Kunkel, M., Gooding, W., Whiteside, T. L., Ferrone, S., and Seliger, B. (2005). Defects in the human leukocyte antigen class I antigen processing machinery in head and neck squamous cell carcinoma: association with clinical outcome. Clin Cancer Res *11*, 2552-2560.

Mendel, G. (1950). Gregor Mendel's letters to Carl Nageli, 1866-1873. Genetics *35*, 1-29.

Mendenhall, E. M., and Bernstein, B. E. (2008). Chromatin state maps: new technologies, new insights. Curr Opin Genet Dev *18*, 109-115.

Mockler, T. C., Chan, S., Sundaresan, A., Chen, H., Jacobsen, S. E., and Ecker, J. R. (2005). Applications of DNA tiling arrays for whole-genome analysis. Genomics *85*, 1-15.

Mohn, F., Weber, M., Rebhan, M., Roloff, T. C., Richter, J., Stadler, M. B., Bibel, M., and Schubeler, D. (2008). Lineage-Specific Polycomb Targets and De Novo DNA Methylation Define Restriction and Potential of Neuronal Progenitors. Mol Cell.

Morris, A. C., Beresford, G. W., Mooney, M. R., and Boss, J. M. (2002). Kinetics of a gamma interferon response: expression and assembly of CIITA promoter IV and inhibition by methylation. Mol Cell Biol *22*, 4781-4791.

Mungall, A. J., Palmer, S. A., Sims, S. K., Edwards, C. A., Ashurst, J. L., Wilming, L., Jones, M. C., Horton, R., Hunt, S. E., Scott, C. E.*, et al.* (2003). The DNA sequence and analysis of human chromosome 6. Nature *425*, 805-811.

Murrell, A., Heeson, S., Cooper, W. N., Douglas, E., Apostolidou, S., Moore, G. E., Maher, E. R., and Reik, W. (2004). An association between variants in the IGF2 gene and Beckwith-Wiedemann syndrome: interaction between genotype and epigenotype. Hum Mol Genet *13*, 247-255.

Murrell, A., Rakyan, V. K., and Beck, S. (2005). From genome to epigenome. Hum Mol Genet *14 Spec No 1*, R3-R10.

Murrell, A., Heeson, S., and Reik, W. (2004). Interaction between differentially methylated regions partitions the imprinted genes Igf2 and H19 into parent-specific chromatin loops. Nat Genet *36*, 889-893.

Nejentsev, S., Howson, J. M., Walker, N. M., Szeszko, J., Field, S. F., Stevens, H. E., Reynolds, P., Hardy, M., King, E., Masters, J.*, et al.* (2007). Localization of type 1 diabetes susceptibility to the MHC class I genes HLA-B and HLA-A. Nature *450*, 887-892.

Neumann, R., and Jeffreys, A. J. (2006). Polymorphism in the activity of human crossover hotspots independent of local DNA sequence variation. Hum Mol Genet *15*, 1401-1411.

Nguyen, C. T., Weisenberger, D. J., Velicescu, M., Gonzales, F. A., Lin, J. C., Liang, G., and Jones, P. A. (2002). Histone H3-lysine 9 methylation is associated with aberrant gene silencing in cancer cells and is rapidly reversed by 5-aza-2'-deoxycytidine. Cancer Res *62*, 6456-6461.

Nie, Y., Yang, G., Song, Y., Zhao, X., So, C., Liao, J., Wang, L. D., and Yang, C. S. (2001). DNA hypermethylation is a mechanism for loss of expression of the HLA class I genes in human esophageal squamous cell carcinomas. Carcinogenesis *22*, 1615-1623.

Novik, K. L., Nimmrich, I., Genc, B., Maier, S., Piepenbrock, C., Olek, A., and Beck, S. (2002). Epigenomics: genome-wide study of methylation phenomena. Curr Issues Mol Biol *4*, 111-128.

Oberley, M. J., Tsao, J., Yau, P., and Farnham, P. J. (2004). High-throughput screening of chromatin immunoprecipitates using CpG-island microarrays. Methods Enzymol *376*, 315-334.

Ohmori, Y., and Hamilton, T. A. (1995). The interferon-stimulated response element and a kappa B site mediate synergistic induction of murine IP-10 gene transcription by IFN-gamma and TNF-alpha. J Immunol *154*, 5235-5244.

Ottaviani, D., Lever, E., Takousis, P., and Sheer, D. (2008). Anchoring the genome. Genome Biol *9*, 201.

Ottaviani, D. L., E.; Mitter, R.; Jones, T.; Forshew, T.; Tomazou, EM.; Rakyan, VR.; Beck, S.; Krawetz, SA.; Platts, AE.; Segarane, B.; Sheer, D. (2008). Recruitment of Genome Anchors to the Nuclear Matrix: a Novel Mechanism for Regulationg Expression of the Human MHC?

Pamer, E., and Cresswell, P. (1998). Mechanisms of MHC class I--restricted antigen processing. Annu Rev Immunol *16*, 323-358.

Parham, P. (1996). Immunology: keeping mother at bay. Curr Biol *6*, 638-641.

Parham, P. (2005). MHC class I molecules and KIRs in human history, health and survival. Nat Rev Immunol *5*, 201-214.

Pattenden, S. G., Klose, R., Karaskov, E., and Bremner, R. (2002). Interferon-gamma-induced chromatin remodeling at the CIITA locus is BRG1 dependent. Embo J *21*, 1978-1986.

Qiu, J. (2006). Epigenetics: unfinished symphony. Nature *441*, 143-145.

Rakyan, V., Down, T., Thorne, N., Flicek, P., Kulesha, E., Graf, S., Tomazou, E., Backdahl, L., Johnson, N., Herberth, M.*, et al.* (2008). An integrated resource for genome-wide identification and analysis of human tissue-specific differentially methylated regions (tDMRs). Genome Res.

Rakyan, V. K., and Beck, S. (2006). Epigenetic variation and inheritance in mammals. Curr Opin Genet Dev *16*, 573-577.

Rakyan, V. K., Hildmann, T., Novik, K. L., Lewin, J., Tost, J., Cox, A. V., Andrews, T. D., Howe, K. L., Otto, T., Olek, A.*, et al.* (2004). DNA methylation profiling of the human major histocompatibility complex: a pilot study for the human epigenome project. PLoS Biol *2*, e405.

Ramsahoye, B. H., Biniszkiewicz, D., Lyko, F., Clark, V., Bird, A. P., and Jaenisch, R. (2000). Non-CpG methylation is prevalent in embryonic stem cells and may be mediated by DNA methyltransferase 3a. Proc Natl Acad Sci U S A *97*, 5237-5242.

Raval, A., Tanner, S. M., Byrd, J. C., Angerman, E. B., Perko, J. D., Chen, S. S., Hackanson, B., Grever, M. R., Lucas, D. M., Matkovic, J. J.*, et al.* (2007). Downregulation of death-associated protein kinase 1 (DAPK1) in chronic lymphocytic leukemia. Cell *129*, 879-890.

Redon, R., Ishikawa, S., Fitch, K. R., Feuk, L., Perry, G. H., Andrews, T. D., Fiegler, H., Shapero, M. H., Carson, A. R., Chen, W.*, et al.* (2006). Global variation in copy number in the human genome. Nature *444*, 444-454.

Reik, W., Dean, W., and Walter, J. (2001). Epigenetic reprogramming in mammalian development. Science *293*, 1089-1093.

Reinders, J., Delucinge Vivier, C., Theiler, G., Chollet, D., Descombes, P., and Paszkowski, J. (2008). Genome-wide, high-resolution DNA methylation profiling using bisulfite-mediated cytosine conversion. Genome Res *18*, 469-476.

Repsilber, D., and Ziegler, A. (2005). Two-color microarray experiments. Technology and sources of variance. Methods Inf Med *44*, 400-404.

Richards, E. J. (2008). Population epigenetics. Curr Opin Genet Dev *18*, 221-226.

Riggs, A. D. (1975). X inactivation, differentiation, and DNA methylation. Cytogenet Cell Genet *14*, 9-25.

Rioux, J. D., and Abbas, A. K. (2005). Paths to understanding the genetic basis of autoimmune disease. Nature *435*, 584-589.

Robertson, K. D. (2005). DNA methylation and human disease. Nat Rev Genet *6*, 597-610.

Robinson, J., Waller, M. J., Parham, P., de Groot, N., Bontrop, R., Kennedy, L. J., Stoehr, P., and Marsh, S. G. (2003). IMGT/HLA and IMGT/MHC: sequence databases for the study of the major histocompatibility complex. Nucleic Acids Res *31*, 311-314.

Rodin, S. N., and Riggs, A. D. (2003). Epigenetic silencing may aid evolution by gene duplication. J Mol Evol *56*, 718-729.

Rohn, W. M., Lee, Y. J., and Benveniste, E. N. (1996). Regulation of class II MHC expression. Crit Rev Immunol *16*, 311-330.

Rollins, R. A., Haghighi, F., Edwards, J. R., Das, R., Zhang, M. Q., Ju, J., and Bestor, T. H. (2006). Large-scale structure of genomic methylation patterns. Genome Res *16*, 157-163.

Rolls, M. M., Stein, P. A., Taylor, S. S., Ha, E., McKeon, F., and Rapoport, T. A. (1999). A visual screen of a GFP-fusion library identifies a new type of nuclear envelope membrane protein. J Cell Biol *146*, 29-44.

Romero, J. M., Jimenez, P., Cabrera, T., Cozar, J. M., Pedrinaci, S., Tallada, M., Garrido, F., and Ruiz-Cabello, F. (2005). Coordinated downregulation of the antigen presentation machinery and HLA class I/beta2-microglobulin complex is responsible for HLA-ABC loss in bladder cancer. Int J Cancer *113*, 605-610.

Roschke, A. V., Tonon, G., Gehlhaus, K. S., McTyre, N., Bussey, K. J., Lababidi, S., Scudiero, D. A., Weinstein, J. N., and Kirsch, I. R. (2003). Karyotypic complexity of the NCI-60 drug-screening panel. Cancer Res *63*, 8634-8647.

Rozen, S., and Skaletsky, H. (2000). Primer3 on the WWW for general users and for biologist programmers. Methods Mol Biol *132*, 365-386.

Sandovici, I., Kassovska-Bratinova, S., Loredo-Osti, J. C., Leppert, M., Suarez, A., Stewart, R., Bautista, F. D., Schiraldi, M., and Sapienza, C. (2005). Interindividual variability and parent of origin DNA methylation differences at specific human Alu elements. Hum Mol Genet *14*, 2135-2143.

Sanger, F., Nicklen, S., and Coulson, A. R. (1977). DNA sequencing with chain-terminating inhibitors. Proc Natl Acad Sci U S A *74*, 5463-5467.

Santos, F., Hendrich, B., Reik, W., and Dean, W. (2002). Dynamic reprogramming of DNA methylation in the early mouse embryo. Dev Biol *241*, 172-182.

Schoenborn, J. R., Dorschner, M. O., Sekimata, M., Santer, D. M., Shnyreva, M., Fitzpatrick, D. R., Stamatoyannopoulos, J. A., and Wilson, C. B. (2007). Comprehensive epigenetic profiling identifies multiple distal regulatory elements directing transcription of the gene encoding interferon-gamma. Nat Immunol *8*, 732-742.

Scott, S. A., Dong, W. F., Ichinohasama, R., Hirsch, C., Sheridan, D., Sanche, S. E., Geyer, C. R., and Decoteau, J. F. (2006). 5-Aza-2'-deoxycytidine (decitabine) can relieve p21WAF1 repression in human acute myeloid leukemia by a mechanism involving release of histone deacetylase 1 (HDAC1) without requiring p21WAF1 promoter demethylation. Leuk Res *30*, 69-76.

Seliger, B., Cabrera, T., Garrido, F., and Ferrone, S. (2002). HLA class I antigen abnormalities and immune escape by malignant cells. Semin Cancer Biol *12*, 3-13.

Serrano, A., Tanzarella, S., Lionello, I., Mendez, R., Traversari, C., Ruiz-Cabello, F., and Garrido, F. (2001). Rexpression of HLA class I antigens and restoration of antigen-specific CTL response in melanoma cells following 5-aza-2'-deoxycytidine treatment. Int J Cancer *94*, 243-251.

Shann, Y. J., Cheng, C., Chiao, C. H., Chen, D. T., Li, P. H., and Hsu, M. T. (2008). Genome-wide mapping and characterization of hypomethylated sites in human tissues and breast cancer cell lines. Genome Res *18*, 791-801.

Shiota, K. (2004). DNA methylation profiles of CpG islands for cellular differentiation and development in mammals. Cytogenet Genome Res *105*, 325-334.

Smyth, G. K. (2004). Linear models and empirical bayes methods for assessing differential expression in microarray experiments. Stat Appl Genet Mol Biol *3*, Article3.

Smyth, G. K. (2005). Limma: linear models for microarray data, In Bioinformatics and Computational Biology Solutions using R and Bioconductor., V. C. R. Gentleman, S. Dudoit, R. Irizarry, W. Huber, ed. (New York: Springer), pp. 397-420.

Smyth, G. K., and Speed, T. (2003). Normalization of cDNA microarray data. Methods *31*, 265-273.

Soengas, M. S., Capodieci, P., Polsky, D., Mora, J., Esteller, M., Opitz-Araya, X., McCombie, R., Herman, J. G., Gerald, W. L., Lazebnik, Y. A.*, et al.* (2001). Inactivation of the apoptosis effector Apaf-1 in malignant melanoma. Nature *409*, 207-211.

Song, J. Z., Stirzaker, C., Harrison, J., Melki, J. R., and Clark, S. J. (2002). Hypermethylation trigger of the glutathione-S-transferase gene (GSTP1) in prostate cancer cells. Oncogene *21*, 1048-1061.

Spilianakis, C. G., and Flavell, R. A. (2007). Epigenetic regulation of Ifng expression. Nat Immunol *8*, 681-683.

Stephens, H. A. (2001). MICA and MICB genes: can the enigma of their polymorphism be resolved? Trends Immunol *22*, 378-385.

Stern-Ginossar, N., Elefant, N., Zimmermann, A., Wolf, D. G., Saleh, N., Biton, M., Horwitz, E., Prokocimer, Z., Prichard, M., Hahn, G.*, et al.* (2007). Host immune system gene targeting by a viral miRNA. Science *317*, 376-381.

Stewart, C. A., Horton, R., Allcock, R. J., Ashurst, J. L., Atrazhev, A. M., Coggill, P., Dunham, I., Forbes, S., Halls, K., Howson, J. M.*, et al.* (2004). Complete MHC haplotype sequencing for common disease gene mapping. Genome Res *14*, 1176- 1187.

Stirzaker, C., Song, J. Z., Davidson, B., and Clark, S. J. (2004). Transcriptional gene silencing promotes DNA hypermethylation through a sequential change in chromatin modifications in cancer cells. Cancer Res *64*, 3871-3877.

Stranger, B. E., Forrest, M. S., Dunning, M., Ingle, C. E., Beazley, C., Thorne, N., Redon, R., Bird, C. P., de Grassi, A., Lee, C.*, et al.* (2007). Relative impact of nucleotide and copy number variation on gene expression phenotypes. Science *315*, 848-853.

Strunnikova, M., Schagdarsurengin, U., Kehlen, A., Garbe, J. C., Stampfer, M. R., and Dammann, R. (2005). Chromatin inactivation precedes de novo DNA methylation during the progressive epigenetic silencing of the RASSF1A promoter. Mol Cell Biol *25*, 3923-3933.

Su, A. I., Cooke, M. P., Ching, K. A., Hakak, Y., Walker, J. R., Wiltshire, T., Orth, A. P., Vega, R. G., Sapinoso, L. M., Moqrich, A.*, et al.* (2002). Large-scale analysis of the human and mouse transcriptomes. Proc Natl Acad Sci U S A *99*, 4465-4470.

Sullivan, K. E., Reddy, A. B., Dietzmann, K., Suriano, A. R., Kocieda, V. P., Stewart, M., and Bhatia, M. (2007). Epigenetic regulation of tumor necrosis factor alpha. Mol Cell Biol *27*, 5147-5160.

Suzuki, K., Suzuki, I., Leodolter, A., Alonso, S., Horiuchi, S., Yamashita, K., and Perucho, M. (2006). Global DNA demethylation in gastrointestinal cancer is age dependent and precedes genomic damage. Cancer Cell *9*, 199-207.

Szilagyi, A., Blasko, B., Szilassy, D., Fust, G., Sasvari-Szekely, M., and Ronai, Z. (2006). Real-time PCR quantification of human complement C4A and C4B genes. BMC Genet *7*, 1.

Tang, X., Fenton, M. J., and Amar, S. (2003). Identification and functional characterization of a novel binding site on TNF-alpha promoter. Proc Natl Acad Sci U S A *100*, 4096-4101.

The International HapMap Project (2003). The International HapMap Project. Nature *426*, 789-796.

Thorne NP, M. J., Rakyan VK, Ibrahim AEK, Massie C, Curtis C, Brenton JD, Murrell A, Tavare S (2006). DNA methylation arrays: Methods and Analysis, In Microarray Innovations - Technology and Experimentation.

Townsend, A., and Trowsdale, J. (1993). The transporters associated with antigen presentation. Semin Cell Biol *4*, 53-61.

Traherne, J. A., Horton, R., Roberts, A. N., Miretti, M. M., Hurles, M. E., Stewart, C. A., Ashurst, J. L., Atrazhev, A. M., Coggill, P., Palmer, S.*, et al.* (2006). Genetic analysis of completely sequenced disease-associated MHC haplotypes identifies shuffling of segments in recent human history. PLoS Genet *2*, e9.

Tsai, E. Y., Jain, J., Pesavento, P. A., Rao, A., and Goldfeld, A. E. (1996). Tumor necrosis factor alpha gene regulation in activated T cells involves ATF-2/Jun and NFATp. Mol Cell Biol *16*, 459-467.

Turker, M. S. (2002). Gene silencing in mammalian cells and the spread of DNA methylation. Oncogene *21*, 5388-5393.

Turner, D. J., Miretti, M., Rajan, D., Fiegler, H., Carter, N. P., Blayney, M. L., Beck, S., and Hurles, M. E. (2008). Germline rates of de novo meiotic deletions and duplications causing several genomic disorders. Nat Genet *40*, 90-95.

van Endert, P. M. (1999). Genes regulating MHC class I processing of antigen. Curr Opin Immunol *11*, 82-88.

van Vliet, J., Oates, N. A., and Whitelaw, E. (2007). Epigenetic mechanisms in the context of complex diseases. Cell Mol Life Sci *64*, 1531-1538.

Vandesompele, J., De Preter, K., Pattyn, F., Poppe, B., Van Roy, N., De Paepe, A., and Speleman, F. (2002). Accurate normalization of real-time quantitative RT-PCR data by geometric averaging of multiple internal control genes. Genome Biol *3*, RESEARCH0034.

Volpi, E. V., Chevret, E., Jones, T., Vatcheva, R., Williamson, J., Beck, S., Campbell, R. D., Goldsworthy, M., Powis, S. H., Ragoussis, J*., et al.* (2000). Large-scale chromatin organization of the major histocompatibility complex and other regions of human chromosome 6 and its response to interferon in interphase nuclei. J Cell Sci *113 (Pt 9)*, 1565-1576.

Vyse, T. J., and Todd, J. A. (1996). Genetic analysis of autoimmune disease. Cell *85*, 311-318.

Waddington, C. (1942). The epigenotype. Endeavour *1*, 18-20.

Walsh, C. P., and Bestor, T. H. (1999). Cytosine methylation and mammalian development. Genes Dev *13*, 26-34.

Walsh, C. P., Chaillet, J. R., and Bestor, T. H. (1998). Transcription of IAP endogenous retroviruses is constrained by cytosine methylation. Nat Genet *20*, 116-117.

Wang, W. Y., Barratt, B. J., Clayton, D. G., and Todd, J. A. (2005). Genome-wide association studies: theoretical and practical concerns. Nat Rev Genet *6*, 109-118.

Warnecke, P. M., and Clark, S. J. (1999). DNA methylation profile of the mouse skeletal alpha-actin promoter during development and differentiation. Mol Cell Biol *19*, 164-172.

Watt, F., and Molloy, P. L. (1988). Cytosine methylation prevents binding to DNA of a HeLa cell transcription factor required for optimal expression of the adenovirus major late promoter. Genes Dev *2*, 1136-1143.

Weaver, I. C., Cervoni, N., Champagne, F. A., D'Alessio, A. C., Sharma, S., Seckl, J. R., Dymov, S., Szyf, M., and Meaney, M. J. (2004). Epigenetic programming by maternal behavior. Nat Neurosci *7*, 847-854.

Weber, M., Davies, J. J., Wittig, D., Oakeley, E. J., Haase, M., Lam, W. L., and Schubeler, D. (2005). Chromosome-wide and promoter-specific analyses identify sites of differential DNA methylation in normal and transformed human cells. Nat Genet *37*, 853-862.

Weber, M., Hellmann, I., Stadler, M. B., Ramos, L., Paabo, S., Rebhan, M., and Schubeler, D. (2007). Distribution, silencing potential and evolutionary impact of promoter DNA methylation in the human genome. Nat Genet *39*, 457-466.

Weber, M., and Schubeler, D. (2007). Genomic patterns of DNA methylation: targets and function of an epigenetic mark. Curr Opin Cell Biol *19*, 273-280.

Williams, D. B., and Watts, T. H. (1995). Molecular chaperones in antigen presentation. Curr Opin Immunol *7*, 77-84.

Wright, K. L., and Ting, J. P. (2006). Epigenetic regulation of MHC-II and CIITA genes. Trends Immunol *27*, 405-412.

Wright, K. L., White, L. C., Kelly, A., Beck, S., Trowsdale, J., and Ting, J. P. (1995). Coordinate regulation of the human TAP1 and LMP2 genes from a shared bidirectional promoter. J Exp Med *181*, 1459-1471.

WTCCC (2007). Genome-wide association study of 14,000 cases of seven common diseases and 3,000 shared controls. Nature *447*, 661-678.

Xu, G. L., Bestor, T. H., Bourc'his, D., Hsieh, C. L., Tommerup, N., Bugge, M., Hulten, M., Qu, X., Russo, J. J., and Viegas-Pequignot, E. (1999). Chromosome instability and immunodeficiency syndrome caused by mutations in a DNA methyltransferase gene. Nature *402*, 187-191.

Yang, Y. H., and Thorne, N.P. (2003). Normalization for two- color cDNA microarray data., In Science and Statistics: A Festschrift for Terry Speed, D. R. Goldstein, ed.,pp. 403-418.

Yang, Z., Mendoza, A. R., Welch, T. R., Zipf, W. B., and Yu, C. Y. (1999). Modular variations of the human major histocompatibility complex class III genes for serine/threonine kinase RP, complement component C4, steroid 21-hydroxylase CYP21, and tenascin TNX (the RCCX module). A mechanism for gene deletions and disease associations. J Biol Chem *274*, 12147-12156.

Yazaki, J., Gregory, B. D., and Ecker, J. R. (2007). Mapping the genome landscape using tiling array technology. Curr Opin Plant Biol *10*, 534-542.

Yoo, C. B., and Jones, P. A. (2006). Epigenetic therapy of cancer: past, present and future. Nat Rev Drug Discov *5*, 37-50.

Zhang, X., Shiu, S., Cal, A., and Borevitz, J. O. (2008). Global analysis of genetic, epigenetic and transcriptional polymorphisms in Arabidopsis thaliana using whole genome tiling arrays. PLoS Genet *4*, e1000032.

Zhang, X., Yazaki, J., Sundaresan, A., Cokus, S., Chan, S. W., Chen, H., Henderson, I. R., Shinn, P., Pellegrini, M., Jacobsen, S. E., and Ecker, J. R. (2006). Genome-wide high-resolution mapping and functional analysis of DNA methylation in arabidopsis. Cell *126*, 1189-1201.

Zika, E., and Ting, J. P. (2005). Epigenetic control of MHC-II: interplay between CIITA and histone-modifying enzymes. Curr Opin Immunol *17*, 58-64.

Zilberman, D., Gehring, M., Tran, R. K., Ballinger, T., and Henikoff, S. (2007). Genome-wide analysis of Arabidopsis thaliana DNA methylation uncovers an interdependence between methylation and transcription. Nat Genet *39*, 61-69.

Zilberman, D., and Henikoff, S. (2007). Genome-wide analysis of DNA methylation patterns. Development *134*, 3959-3965.

Appendix

Table 2.1

section			
2.1.1	**MHC tiling array primers**		
2.1.1.1	*gaps*		
	primer name	**forward primer**	**reverse primer**
	stSG1159307	TGGTCATGGGCTGTCTGTAA	CTGTGCCATCTCTTTCCTGC
	stSG1159309	TTGGTTCTGTGAGCAGCATC	AGCCAGTCTCTCAGCTCTGC
	stSG1159310	GTGGGAAGGGAGAGAGGTTC	ACATCAGGCAACGTAGACCC
	stSG1159311	TCTGATTGGTCCAAGGAAGG	TGATGCTCTTGTTCAGGTCG
	stSG1159312	GCCTTGTCTTTCTCCTGCAC	GACTTCGCTCTGACACCTCC
	stSG1159313	GGAGGTGTCAGAGCGAAGTC	TGAGAATGGACAAGGAAGGG
	stSG1159314	TCTCCAGGTATCTGCAGGCT	AAAGACCTGCAAGAAAGGCA
	stSG1159315	TGCCTTTCTTGCAGGTCTTT	TCTTCTTGCGCAGACTCTCA
	stSG1159316	TGAGAGTCTGCGCAAGAAGA	AATGGCTGGAGGTAGAGGGT
	stSG1159317	GGCAGGCTGTAGTCCTGTGT	CCATCAGGGATCATATTGGG
	stSG1159318	CCCAATATGATCCCTGATGG	TCAACACAAAGGCTGTGAGC
	stSG1159319	AGGCTCACAGCCTTTGTGTT	TGGTCTGAGGACTACCCACC
	stSG1159320	GGTGGGTAGTCCTCAGACCA	CTGAGGTGTCTGCCTCCTTC
	stSG1159321	GAAGGAGGCAGACACCTCAG	TCTGGTGCCATACCTAAGGG
	stSG1159322	ATCCTGTAGCCCAGGGAGAT	GTGTACTCGACGTGGCCTTT
	stSG1159323	TCCTGGACATGAAGAACACG	TACTCAGTAAACCCGGTGCC
	stSG1159324	AGATGAGGCAGGAAGGGACT	AGCCACCACACCTTTCTCAC
	stSG1159325	GTGAGAAAGGTGTGGTGGCT	TCGGAACTTCCTTCCTCAGA
	stSG1159326	GAAGTTCCGAAGGAGGGAAC	TTCCAGATGGTCAGGTCCTC
	stSG1159327	GAGGACCTGACCATCTGGAA	ACAGACGCGGAGTCATCTCT
	stSG1159328	AGAGATGACTCCGCGTCTGT	GGTCCCACTGGACTGACACT
	stSG1159329	AGTGTCAGTCCAGTGGGACC	ATCACCCATCGAGAAGCAAG
	stSG1159330	AAAGGTCAGGGTTGCATTTC	TTCCTCAATGGTCCTCTTGG
	stSG1159331	CCAAGAGGACCATTGAGGAA	CACCCTGAGAAAGGGAATCA
	stSG1159332	TGGACGTGATTCCCTTTCTC	CCACATACCAGGCCAGAACT
	stSG1159333	AGTTCTGGCCTGGTATGTGG	GGTAAGCAGAGGCTGTGAGG
	stSG1159334	CCTCACAGCCTCTGCTTACC	CCTTGTCCTCCACACCAACT
	stSG1159335	AGTTGGTGTGGAGGACAAGG	ATCTGCAGAGCGACTTCCAT
	stSG1159336	GAAGTCGCTCTGCAGATTCC	CTCTCAGAAGGGAGCACCAC
	stSG1159337	TGAGCTTGAGGAGTGTGGTG	GTGCAGGAGAAAGACAAGGC
	stSG1159338	ATTCTCCCTGTGGAGTGGTG	GACTTCGCTCTGACACCTCC

	stSG1159339	GGAGGTGTCAGAGCGAAGTC	TGAGAATGGACAAGGAAGGG
	stSG1159340	CCCTTCCTTGTCCATTCTCA	CAACACATGTCCACTGGAGG
	stSG1159341	TCGTTCTGCTCATTCCTTCA	CCAAACACCACAAATAAGCCA
	stSG1159342	AGACAGGAATACGGCAGCCT	GGTCAGGTGCGAATAGGGTA
	stSG1159343	GTGACTGCAATAAGGCCCAT	GGTGCCAACAACCTTAACAA
	stSG1159344	AGACAGGAATACGGCAGCCT	GGTCAGGTGCGAATAGGGTA
	stSG1159345	AGACAGGAATACGGCAGCCT	GGTCAGGTGCGAATAGGGTA
	stSG1159346	TGGGCTCCAGAGCAAACTTA	CCGAGGCCATGAAAGAGTTA
	stSG1159347	AGACAGGAATACGGCAGCCT	GGTCAGGTGCGAATAGGGTA
	stSG1159348	CGGTTGAATTACAGCGTTGA	CTTCCTACGGCAGCTCTTCA
	stSG1159349	AGACAGGAATACGGCAGCCT	GGTCAGGTGCGAATAGGGTA
	stSG1159350	CAGTGCGTCACAGGCATAAT	CACCTGCAAGACAAAGGACA
	stSG1159351	TGGGAGCTCACTGTCTTGTG	GGTCAGGTGCGAATAGGGTA
	stSG1159352	TCTCCAGGTATCTGCAGGCT	AAAGACCTGCAAGAAAGGCA
	stSG1159353	TGCCTTTCTTGCAGGTCTTT	TCTTCTTGCGCAGACTCTCA
	stSG1159354	TGAGAGTCTGCGCAAGAAGA	AATGGCTGGAGGTAGAGGGT
	stSG1159355	GGCAGGCTGTAGTCCTGTGT	CCATCAGGGATCATATTGGG
	stSG1159356	CCCAATATGATCCCTGATGG	CACCTGCATGCTCCTGTCTA
	stSG1159357	TAACTGGCTTCTGTCCCAGC	GCAGAAACGCCACTGAACTT
	stSG1159358	TCACAGCCTTTGTGACCATC	TGGTCTGAGGACTACCCACC
	stSG1159359	GGTGGGTAGTCCTCAGACCA	CTGAGGTGTCTGCCTCCTTC
	stSG1159360	GAAGGAGGCAGACACCTCAG	TCTGGTGCCATACCTAAGGG
	stSG1159361	ATCCTGTAGCCCAGGGAGAT	GTGTACTCGACGTGGCCTTT
	stSG1159362	TCCTGGACATGAAGAACACG	TACTCAGTAAACCCGGTGCC
	stSG1159363	AGATGAGGCAGGAAGGGACT	AGCCACCACACCTTTCTCAC
	stSG1159364	GTGAGAAAGGTGTGGTGGCT	TCGGAACTTCCTTCCTCAGA
	stSG1159365	GAAGTTCCGAAGGAGGGAAC	TTCCAGATGGTCAGGTCCTC
	stSG1159366	GAGGACCTGACCATCTGGAA	ACAGACGCGGAGTCATCTCT
	stSG1159367	AGAGATGACTCCGCGTCTGT	GGTCCCACTGGACTGACACT
	stSG1159368	AGTGTCAGTCCAGTGGGACC	TCAAGAAGCAAGGAAGGGAA
	stSG1159369	TTCCCTTCCTTGCTTCTTGA	CACCCTGAGAAAGGGAATCA
	stSG1159370	TGGACGTGATTCCCTTTCTC	CCACATACCAGGCCAGAACT
	stSG1159372	CCTCACAGCCTCTGCTTACC	CCTTGTCCTCCACACCAACT
	stSG1159373	AGTTGGTGTGGAGGACAAGG	ATCTGCAGAGCGACTTCCAT
	stSG1159374	GAAGTCGCTCTGCAGATTCC	AGTATGAGGACACGAACGGG
	stSG1159375	CCCGTTCGTGTCCTCATACT	GCTTGTGTGGGTTTCCTTGT

stSG1159376	ACAAGGAAACCCACACAAGC	TGCCTATGACTCAGCTCCCT
stSG1159377	AACAGGGCATGGACTACCTG	TCTGGTCAGCACCACAGAAC
stSG1159378	TGCTATGCATCTCTTGGCTG	ATTTGTCTGCATTTGACGGC
stSG1159380	ACAGAGGGCAGAAACACTGG	TTGAGTAGCGAGCTTCAGGG
stSG1159381	GACTTGCTGGCTGGTTTCTC	GGGACAGGGCTGTTCATCTA
stSG1159382	CATTCCACTGTGAGAGGGCT	CCCTGCCTTGATTCAAATGT
stSG1159383	ACATTTGAATCAAGGCAGGG	ACCTTGGTTGTCTCGTGTCC
stSG1159384	AGGACACGAGACAACCAAGG	GGCCATAGCTTTCACTGCTC
stSG1159385	CGGTCATTCCAATGTGTGAG	GAGAAACCAGCCAGCAAGTC
stSG1159386	TTTGGCTGTGTGTCTGCTTC	GGCATTGTTGTCTCCAGGTT
stSG1159387	AACCTGGAGACAACAATGCC	TTGGGATAATGTGAGGAGGC
stSG1159388	GCCTCCTCACATTATCCCAA	AGGTACCGGTAAAGCGTGTG
stSG1159389	TCCAGATATGAGGGTGGCTC	GCAGTCTGCTCACCATTGAA
controls		
primer name	**forward primer**	**reverse primer**
AF043430 H19 4661	ATTAATGCGCTGTGGCTGATGTGTAGTAG	GAGCCGAGGTGAGGGTCTGGAAATG
AF043430 H19 4600	CACCGCCGGCCGATTTTCTGTAA	ATCTCATCTCCCCCAACCCTCAATAGTGC
AF043430 H19 2142	AGCCCTGACCACCCCGACTCTGACCTTCTA	TGACTCGCCCCCTACCCACCAAATGAT
AF043430 H19 1632	TGGTGGGCACAGGTGAGAGGGAGGTA	GTTGGGCGGTTAGACGGGTTCAGACACT
M22373 IGF2 425	TTCCCCGCCGCCTCCTCTTCATCT	CCCGCCCGCCCCCGTCTTC
M22373 IGF2 2513	CCCCCACCTGGCGTCTCTGCTC	AACGCGGCGGGAAGGTCAAAGTCT
M22373 IGF2 3998	CTCCCGCCCCCAGACACCAATG	CTCACCCCTGCCACCCACCAACTG
M22373 IGF2 1653	GGCCTCCGGGGTGCTGGGTAACG	TGGGGGCAGGGGCAGAGGAAAAGA
U13802 IGF2 378	AGGCAGAGGGGGATAGAAGAGGGAAGGGGAAGGAA	CAGGGTGCGGGGAGAGCCAGTGTTGAAGTGAC
U90095 KvDMR1 68000	TCTCCTCAGCGCGGCCCTCCCC	ATTCGGGCCCTGACTCAGAACC
X03562 HSIGF2G 2122	CCGCCGGCGTTGTCACC	GGGGCGGGCCAGATGTTG
X03562 HSIGF2G 8103	CACCGTCCCCTGATTGCTCTACC	TCTGGGGCCCTTCTTTTCTCTTTG
X03562 HSIGF2G 5925	GACTTTGACCTTCCCGCCGCGTTTCTGAGCAC	TCTTCCGCCTTGAGCCGCCCGCCTGACCTGA
X03562 HSIGF2G 3280	CCTGGCCTCCGGGGTGCTGGGTAACGA	GCAAGGAGGGGGCCGAAGGGAAGGAACAG
X91880 IGF2RDMR2 652	GGGCAGCCGCGTGAACCT	AAGCCAAGCCCCCAACCTCGTAAC
X91880 IGF2RDMR2 307	CTGGCGGCTGGGTCGGGTTTTAT	TCGTGGGGGACATGGGGAGGTG
X91880 IGF2RDMR2 185	CAAAGTGGACCCGCCTGCCTGTG	GCCCGCCGGAACCCCTAAGACTC
Y13633 DMR0 826	AGGTGGGGGTGTTTGGAGGTGGAGGAGGCTTTCATA	CTCTCCCTGCCCCTCTCCCCTTCTTTGCCCTCTTTCGTCT
Y13633 DMR0 3273	CCCCAGCACCCCCAAAGAGGAGGAGAACCCACAACT	GGAGAACCCGCCCCCACCATGAAAAACAGC

	Y13633 DMR0 306	TGCATCCCCCATCCCATTCCCAGAGACAAACA	GAATATGAAAGCCTCCTCCACCTCCAAACACC
	Y13633 DMR0 2292	GCCTTGGGGTGGTCTGTGCTGTCTGGTGTG	ACTAGGTTGCCGAGGCTCCCGTCAT
	BRCA1	CTTCCTCTTCCGTCTCTTTCC	ATCTGTAATTCCCGCGCTTT
	MLH1	TGGTATACAAAGTCCCCCTCA	ACGAGGCTGAGCACGAATAC
	RARB2	GAGCAAACGAGTGCAGTCAA	CTCTGTGCGCCTTTCTGTCT
	GSTP1	CTCTCCCCTGCCCTGTGA	GGGAAGCCTTTCCCTCTTT
	PRM	CCACCTGACAAAAGCTCCAG	GGAAGCCAGGTTTGTGTGAT
	F	AATAATCCTTTTGTCTCTCCAC	TTCCCATCAGCATAAATAAGTA
	PREP30	GTTGGGTAGAATGTCCTGTA	GAATTCACCAACCAGTTATC
	HS1	AATGAATGAGCAGTCAAAC	CATGAAGATGGATGAATAAG
	HS3	GACACGAGGAAATAGTGTAGAT	TCTGAGTATTGGTGTGAGTAAA
	IRF1	CCTGCGTTCGGGAGATATAC	ACCGAGCAATCCAAACACTT
	GP1.1	TAGCCAGTTTTAGGAGGACA	GTTATTTTTGAGAAGTGGGATT
	GP2.1	CACGGTAATCTTAGGGAGAA	AGATGAAAAGTGGACAGTGG
	GP3.1	ATAACGGGACTGACTGAGTG	CTTTGTCCATCCAGTCCTAC
	GP4.1	TTTGTCCTGGAGAATTTCAT	GGCAAATAGCAGCTTTGTAT
	GP5.1	TGCATTTCTTGATTGGAATA	TGCAAGATCCATAGCAAAGT
	GP6.1	TCTTGCCTTATTCATGATCC	AGCAAGTTTCTCCATGTAAC
	GP8.1	TTCTTTGCTTTGTTCTCATT	GATTTTCCATTCCCTTTGTA
	GP11.2	TTCCTTGGAGTTAGAGGTTG	TCCAAGCTATTTGATTTCCA
	GP12.1	GTAAGAAAAATGGCCAAGAA	AGCTATGCAAGAGTTTCAATC
	LB4	GGCTGGCATGGACTTTCATTTCAG	GTGGAGGGATCTTTCTTAGACATC
	BG7	GCATTTAATGGGAAGGCAAA	GAATTCTTTGCCGAAATGGA
	GAPDH	CGGCTACTAGCGGTTTTACG	AAGAAGATGCGGCTGACTGT
2.1.2	**Bisulphite Sequencing Primers**		
2.1.2.1	*Chapter 4 - tDMR validation*		
	primer name	**forward primer**	**reverse primer**
	1Liver_1	gagaagtggTTTaatggTaggTtg	ccatctctcccttcctcctc
	1Liver_2	TttgggaaaaatTagggttttg	tcatcacccttcctctctAcatc
	1Liver_3	TtggTtTTtaggttggTtgttg	ccaAAaAcccatcttcacct
	1Liver_1	ggtggagaaTTtggTTtaggg	aaAcacaatctcaaacccatcc
	2Liver_2	tgggTtTtaagTTtgagggTTT	tcccaccctcactcacttct
	2Liver_3	ggggaatgtttTTaggaatTtg	ccttctctccacccaactca
	2Liver_4	tgagttgggtggagagaagg	cacaAtAcccaAaatccaAAttc
	3Placenta_1	ccccagggtaaggacagact	tcccattcccattAAAcaAAa

	3Placenta_2	tttgggaggggaataggagT	ctaAccctccccaAatcaca
	3Placenta_3	gggggTTtgTTtgtgTagTTT	AAtccctAaAcactAtAtccctAaAA
	3Placenta_4	tgagaggTtgggtgtTTagga	cacacccttccctAAccaat
	4Sperm_1	gggtggggTtTaaaggTTtt	tcccaccacacttactAtcttcc
	4Sperm_2	gaTtTtgggtggggaTTaga	aaAAccttctcccacaaAaAca
	5Sperm_1	TtTaggtggggTaTttggtga	cacaAccacctcctAaaAcca
	5Sperm_2	tgtggaTtgggtggtTaaaaa	cccaAccttccttccctAAA
	5Sperm_3	TTtgggTtgTTtggaaTTtg	ccaAccctcccctAtAAacc
	5Sperm_4	agggaatggagatggTaggg	tccactaAttAatcctccaacc
	5Sperm_5	gagggTtgggggaagTTtta	tcccctAccatctccattcc
	6Sperm_1	ggagaatgagTtggggatga	ccaAtctttctAaAAcccctAAA
	6Sperm_2	ggggTTtTagaaagaTtggtttg	ccctttttAcaccccaAAAa
	6Sperm_3	gaTTtggagaaTtttggTtgg	caaatctAAtcactAAccacataAcca
	6Sperm_4	gggtgatTaaaaggTTaaggaggT	AAAaAcccactttactAcaacactAA
2.1.2.2	*Chapter 5 - pDMR validation*		
	primer name	**forward primer**	**reverse primer**
	PSMB8_promoter_1	atggagTtttgggagagaagg	tcaAcccacaAaattcttcca
	PSMB8_promoter_2	ggggaatgatgggtTaagg	tAcaAttAAcccaAAacctAtttcca
	PSMB8_promoter_3	ttgtgtgtggaTaagggTagga	AacccaAAacactacaAtttctct
	PSMB8_promoter_4	gtgtgatggtTTtggtTTaggT	tccctAcatccctaAAAActtcc
	PSMB8_promoter_5	ggaagTTTTtagggatgTaggg	tttcccaaAacaccacacac
	TAP1/PSMB9_promoter_1	aatggagTTTagaaTTtTtggTTTT	ctAttcctAAtcctAAtAAtcctctcc
	TAP1/PSMB9_promoter_2	aaaagtggTTtgTTTagaTtattttgg	ctAAAAcactAAtttccaacctAAAac
	TAP1/PSMB9_promoter_3	TtgggTttgagggttggTag	cacccaAAAcaccatttcct
	TAP1/PSMB9_promoter_4	ggggTaTtggtttTTaaTTtgg	cctacttccaaaaAtAAcctAccc
	TAP1/PSMB9_promoter_5	agggTtggTtggTtgTtttg	tcccctAtAtcctcccctct
	TAP1/PSMB9_promoter_6	tTtgggTaggTTaTttttggaag	AaaAtaAcaAtactAtccccaAcca
	TAP1/PSMB9_promoter_7	ttggTagtgaggggagatttTT	cttccctAcccactcccatA
	TNF-α_1	TtggggagTagaggTtTagTaatga	ccctccccatAAaAccaAct
	TNF-α_2	ggttgagggtgtTtgaagga	cccctccacccatAtActcc
	TNF-α_3	ggagggagagagggagagg	ttttctctctcctcttcaAAatca
	TNF-α_4	tgatTTtgaagaggagagagaaaa	caAAccaAacaAAcaAccaA
	LTA_1	TaggggagagagggtggagT	Atccccaactttccaaatcc
	LTA_2	gggttggagggaaaagTtgt	aaAaAcctccaAAacctccaA
	LTA_3	Tttgggtgggagagtggat	ccccctAaaaacaaccctca
	LTB_1	gTttgggaTttTtggggaag	ActcccaActAcccacctca

	LTB_2	ggatggggagTTtggattTT	ccccttAtAtctcctctcctcttc		
2.1.2.3	*Chapter 6 - B2m primers*				
	primer name	**forward primer**	**reverse primer**		
	B2m_1	aTTaggTattgtgggaggTtTtT	AcatctAccttAAacccaAccaa		
	B2m_2	TtgaagggataTaagaagTaagaaagg	caAActAAaAAcacattaaAActAccc		
	B2m_3	tgtgTTaaggaTtttatgtgTtttg	cccaacccctcatAttttc		
	B2m_4	TTtggTTaaTatggtgaagTTtgg	tcctcaacaAtcttAAtaaccatctt		
	B2m_5	ggtaTaaagtTagagaggggtTtgg	tctcattccattAcccaAActAAa		
	B2m_6	ttTaaaatggaggtggTttgtt	tccacttttcaattctctctcc		
2.1.3	**RT qPCR Primers**				
2.1.3.1	*MeDIP validation*				
	primer name	**forward primer**	**reverse primer**	**Methylation status**	**%CpG**
	11185.0	CGCTTTGTTTCTGCTCCTTT	GCAACTCTGATGCACCTCAA	methylated	0.7
	11821	TGACAGCCTGTGAGAGCAAG	AGCGAAGCCAGTCTATCAGC	methylated	1.4
	6583	CACTCACCGTCCAGCTATCA	CTCCCTGACCTCCATCTTCA	methylated	2.1
	11851	CCAAGAGGGCTCCCTAGAAG	ATTTGGAAGGGACCTTGCTT	methylated	2.9
	6165.0	CCCTCAGTTCCTACCTCCAA	AGTTACGTGGACTCGGCAAT	methylated	3.8
	4994.0	GGGAATATAAGGAGCGCACA	TCGGTTAAAACGGTCAGGTC	methylated	4.9
	9066.0	GCGTAATGAGTGTGGGGATT	GAGGACGCCTTTGTCATTGT	unmethylated	2.5
	8804.0	CGAGGCGTGAGTTATTCCTG	CTCTTGTGGCTGAGCTCCTT	unmethylated	2.9
	5132.0	AAGGTGCCCAATTCAAGGTA	CTTCCCCACCAGTCTTGAAA	unmethylated	4.0
	13663.0	CCGCCATCATGCTCTAATTT	AACGAGCTAGGATTGGCTGA	unmethylated	4.9
	9710.0	TTCAGCAGGTCCTCTGGAGT	CTGGACACAGCTGATGGGTA	unmethylated	5.9
	13478.0	TGAGAGCGGATGACAGATTG	GGTCCCTCCCTTTTCTGTCT	unmethylated	7.2
2.1.3.2	*Expression Analysis*				
2.1.3.2.1	Chapter 5 - MHC genes				
	primer name	**forward primer**	**reverse primer**		
	HLA-A	CGTGATGTGGAGGAGGAAGA	AAGCTGTGAGGGACACATCA		
	HLA-B	ACCAGAGCGAGGCCGGG	GTGTCCGCSCGGTCCAG		
	HLA-C	CGCGCGGAGTCCRAGAGG	GTGTCCGCSCGGTCCAG		
	TAP1	CACTTGCAGGGAGAGGTGTT	ATCACTCAGGGTGGACGTGT		
	TAP2	GGCTGCTTCACCTACACCAT	TGAGTTCAGCTCCCCTGTCT		
	TAPBP	GCTTCATGGCTGAGGAGGT	CACGAACCAACACTCGATCA		
	PSMB8	CTGGCTGTGCAGCAGACTGT	GCTGCCGACACTGAAATACGT		
	PSMB9	GAGGAACCTCCACTTGTTTTGG	CCCAGCCAGCTACCATGAGA		

	LTA	CCACCCTACACCTCCTCCTT	GCAGTGAGTTCTGCTTGCTG
	TNF-α	CCCCAGGGACCTCTCTCTAA	CAGCTTGAGGGTTTGCTACA
	LTB	GAGGACTGGTAACGGAGACG	GGGCTGAGATCTGTTTCTGG
	UBC_control	ATTTGGGTCGCGGTTCTTG	TGCCTTGACATTCTCGATGGT
2.1.3.2.2	Chapter 6 - non-MHC genes		
	primer name	**forward primer**	**reverse primer**
	B2M	TGACTTTGTCACAGCCCAAG	AGCAAGCAAGCAGAATTTGG
	ERp57	AGCAAAGGTTGATTGCACTG	AGCACCTGCTTCTTCACCAT
	CANX	TGAAGAAGATGGTGGCACTG	CGTGGCTTTCTGTTTCTTGG
	CALR	GAGCATATCCCTGACCCTGA	GGCTTCCACTCACCCTTGTA
	UBC_control	ATTTGGGTCGCGGTTCTTG	TGCCTTGACATTCTCGATGGT

Table 2.1 **Primer sets used within this thesis.**

Table 2.2

	Clone Name	chr6 coordinates (NCBI35)		Clone Name	chr6 coordinates (NCBI35)
1	6S17_2-317p19.q1kw	29739385-29741249	**875**	S6A_2-533c24.p1kw	31705175-31707477
2	S6A_2-77l14.p1kk	29741918-29744577	**876**	S6C_2-154e07.q1kw	31706699-31708924
3	6S17_2-612l05.q1ka	29744676-29747250	**877**	S6A_2-336g08.p1k	31709197-31711626
4	6S17_2-476d07.q1kw	29746874-29749870	**878**	S6C_2-738i03.p1kw	31711062-31712741
5	S6A_2-58b24.q1kk	29749779-29752306	**879**	S6C_2-735b07.q1kw	31712696-31715591
6	6S17_2-791d16.p1kw	29751462-29754255	**880**	6S17_2-603k01.p1kw	31714908-31717675
7	S6C_2-527b07.p1ka	29753458-29755924	**881**	S6A_3-6j09.q1kkw	31717156-31720176
8	6S17_2-247p20.p1kw	29755213-29757127	**882**	6S17_2-275j11.q1kw	31720109-31723033
9	S6C_2-310l18.p1kw	29757489-29760285	**883**	S6A_2-443n24.q1kw	31722899-31725309
10	S6A_2-161l04.q1k	29760268-29762334	**884**	S6A_2-434p15.p1kw	31725313-31727536
11	S6A_2-44e16.q1k	29761508-29764267	**885**	S6A_2-232f15.q1k	31727324-31729280
12	6S17_2-225m22.p1kw	29764237-29767111	**886**	S6C_2-315c16.p1kw	31729834-31732303
13	S6A_2-550n14.q1kw	29766552-29768946	**887**	S6A_2-499p23.q1kw	31732290-31734492
14	S6C_2-295c12.p1kw	29767842-29770217	**888**	S6A_2-708j08.p1kw	31734575-31736864
15	S6A_2-271c01.p1k	29770200-29772534	**889**	6S17_2-353f04.p1kw	31736665-31737878
16	S6A_2-31n18.p1k	29772399-29775033	**890**	6S17_2-336l18.q1kw	31738344-31740752
17	S6C_2-342g03.p1kw	29774950-29777612	**891**	S6A_2-107j06.q1k	31740853-31742657
18	S6C_2-600c01.q1kw	29777595-29779994	**892**	S6A_2-617d06.p1kw	31743642-31745854
19	6S17_2-677d21.q1kw	29779522-29782053	**893**	S6A_2-269c19.q1k	31745824-31748295
20	6S17_2-432b11.q1kw	29781700-29784102	**894**	S6A_2-619o04.p1kw	31748193-31750716
21	S6C_2-33f20.q1kkw	29784008-29786547	**895**	S6A_2-529c07.q1kw	31750913-31753578
22	S6A_2-388e21.q1kw	29786066-29788536	**896**	S6C_2-650e15.q1kw	31753446-31755818
23	S6A_2-84i07.p1kk	29788550-29790980	**897**	S6C_2-188o10.q1kw	31755675-31758033
24	6S17_2-561c08.p1kw	29790708-29792696	**898**	S6A_2-369h15.p1kw	31757550-31760177
25	S6C_3-101a09.p1kw	29792469-29798300	**899**	S6C_2-82n19.p1kkw	31759922-31762901
26	S6C_2-557i06.p1kw	29797138-29799948	**900**	S6A_2-407f17.p1kw	31762769-31765478
27	stSG1159305	29799299-29800711	**901**	6S17_2-406p23.q1kw	31765370-31767911
28	S6A_2-697f03.q1kw	29800446-29802662	**902**	S6C_2-684o06.q1ka	31767892-31770216
29	S6A_2-592e18.q1kw	29802604-29804427	**903**	6S17_2-119b24.q1k	31770162-31772565
30	6S17_2-714f01.q1kw	29804125-29806216	**904**	S6C_2-471o13.q1kw	31772684-31775546
31	S6C_2-296i15.p1kw	29805657-29808379	**905**	6S17_2-276f22.p1kw	31775197-31778030
32	S6A_2-424g15.q1kw	29807664-29809837	**906**	S6C_3-146h06.q1kw	31777395-31779445
33	S6C_2-497m09.q1kw	29808891-29811370	**907**	S6C_2-111d08.q1kw	31779822-31782451
34	S6A_2-372b12.q1kw	29811013-29813380	**908**	6S17_2-66h05.p1kkw	31782028-31784830
35	6S17_2-614l12.p1ka	29812577-29815102	**909**	S6C_2-728o04.p1kw	31784795-31786680
36	S6C_2-242e07.p1kw	29814777-29817114	**910**	S6A_2-100c11.p1k	31786563-31788682
37	S6C_2-704i08.p1kw	29817132-29819812	**911**	S6C_2-94g11.p1kkw	31789216-31792018
38	6S17_2-471h23.q1kw	29819808-29822523	**912**	S6A_2-400k18.p1kw	31791865-31794379
39	S6C_2-722b13.p1kw	29821557-29823518	**913**	6S17_2-5n02.q1k1k	31794386-31796755
40	stSG1159306	29823382-29824715	**914**	6S17_2-59h04.p1kkw	31796596-31799113
41	S6A_2-373m17.p1kw	29823989-29826356	**915**	S6C_2-176p07.q1kw	31799483-31801330
42	S6A_2-336c03.p1k	29825952-29827714	**916**	S6A_2-474a15.q1kw	31801630-31803851
43	S6A_2-701f10.p1kw	29828204-29830400	**917**	S6C_2-469h10.p1kw	31803609-31806450
44	S6C_2-599m15.q1kw	29830203-29832660	**918**	S6A_2-453n01.p1kw	31806374-31808611
45	S6A_2-407n04.p1kw	29831649-29833322	**919**	6S17_2-345d19.p1kw	31809088-31811582
46	6S17_2-685h21.p1ka	29832961-29834787	**920**	S6A_2-4a08.q1k	31811489-31813785
47	stSG1159307	29834734-29836045	**921**	6S17_2-490o08.p1ka	31813686-31816211

48	6S17_2-304c03.p1kw	29835737-29838100	**922**	6S17_2-172f10.p1kw	31815961-31818685
49	6S17_2-520o23.p1kw	29837818-29840729	**923**	S6A_2-159m03.q1k	31818595-31821046
50	S6C_2-413g09.p1kw	29840342-29842808	**924**	6S17_2-594d22.q1kw	31820798-31823180
51	S6A_2-213d23.p1k	29842501-29844941	**925**	S6C_2-560j06.p1kw	31822009-31824451
52	S6C_2-540l12.p1kw	29845156-29847476	**926**	6S17_2-433c06.q1kw	31824052-31827057
53	S6C_2-650j23.q1kw	29847589-29849374	**927**	S6C_2-139h02.q1kw	31826313-31828991
54	6S17_2-597i23.q1kw	29849827-29852415	**928**	S6C_2-317k02.p1kw	31828576-31830902
55	S6A_2-349p03.p1kw	29852518-29854940	**929**	S6C_2-47j02.p1kkw	31830687-31833596
56	S6A_2-716f16.p1kw	29854767-29857057	**930**	6S17_2-589a11.q1kw	31833435-31836123
57	S6A_3-13f15.q1kw	29857045-29859021	**931**	S6A_2-645c14.p1kw	31835995-31838462
58	S6A_2-18j08.p1k	29859685-29861731	**932**	S6C_2-19k18.p1kkw	31838392-31840676
59	S6A_2-149a10.p1kw	29861411-29863644	**933**	S6A_2-367m01.p1kw	31841070-31843352
60	6S17_2-491n23.p1ka	29863681-29866461	**934**	6S17_2-45g23.q1kkw	31843318-31845787
61	S6A_2-282b18.q1k	29865282-29867840	**935**	S6A_2-19m07.q1k	31845227-31847566
62	S6C_2-484b07.q1kw	29867463-29870199	**936**	6S17_2-18c07.p1kkw	31846972-31849912
63	6S17_2-263k01.p1kw	29870027-29872891	**937**	S6C_2-630p01.p1kw	31849432-31852366
64	6S17_2-316o20.p1kw	29872823-29875035	**938**	S6C_2-278j09.q1kw	31852239-31855038
65	6S17_2-23i13.q1kkw	29874986-29877591	**939**	S6A_2-572p22.p1kw	31854646-31857207
66	6S17_2-525l10.q1kw	29877078-29879862	**940**	S6C_2-131i07.p1kw	31856985-31859439
67	S6A_2-379e14.p1kw	29879486-29881787	**941**	S6C_2-561l12.p1kw	31859370-31862320
68	6S17_2-530o06.p1ka	29882039-29884543	**942**	S6C_2-529b19.p1kw	31862110-31863937
69	S6A_2-211a07.p1k	29884167-29886552	**943**	6S17_2-481i16.p1kw	31865033-31867206
70	S6C_2-205j21.q1kw	29886939-29889520	**944**	S6A_2-401f24.q1kw	31867881-31870208
71	S6A_2-50m21.p1k	29889483-29892066	**945**	S6C_2-92c15.p1kkw	31870354-31872942
72	S6C_2-749j17.p1kw	29891828-29893645	**946**	S6A_2-464a03.p1kw	31870975-31873642
73	S6C_2-381a21.q1kw	29894385-29896949	**947**	S6A_2-199g12.p1k	31873532-31875332
74	S6A_2-381f21.q1kw	29896602-29899084	**948**	S6C_2-230l20.q1kw	31875927-31878341
75	6S17_2-523e17.p1kw	29899083-29901168	**949**	S6C_2-207b12.p1kw	31878381-31880253
76	6S17_2-347m18.q1kw	29901199-29903435	**950**	S6C_2-184p08.p1kw	31880395-31882817
77	S6C_2-321i11.q1kw	29903484-29906081	**951**	S6C_2-577e08.p1kw	31882344-31884920
78	S6A_2-756f06.q1kw	29906069-29908224	**952**	6S17_2-2n16.p1k1kw	31884919-31887772
79	stSG1159308	29907592-29909062	**953**	S6C_2-562l23.q1kw	31887755-31890158
80	6S17_2-333l22.p1kw	29908506-29911028	**954**	6S17_2-698l07.p1ka	31889902-31892575
81	S6C_3-142l19.p1kw	29910920-29914161	**955**	S6A_2-607b18.p1kw	31892543-31894559
82	S6A_2-752d23.q1kw	29913643-29915459	**956**	6S17_2-747i14.p1kw	31894534-31897087
83	S6A_3-4c06.p1kkw	29915448-29918152	**957**	S6C_2-251l05.q1kw	31896891-31898751
84	6S17_2-379c19.p1kw	29917144-29919923	**958**	S6A_3-74b09.p1kw	31899148-31902281
85	6S17_2-173d18.p1kw	29919898-29922654	**959**	S6C_2-242l24.q1kw	31901568-31903345
86	S6A_2-427m23.q1kw	29921905-29924681	**960**	S6A_2-223f06.q1k	31902447-31904569
87	S6A_2-305d19.q1k	29924579-29926851	**961**	stSG1159311	31903338-31904796
88	S6A_2-190a09.q1k	29926829-29929043	**962**	S6C_2-35n12.q1kkw	31904599-31907111
89	S6A_2-71a13.p1kk	29929108-29931705	**963**	6S17_2-281c12.q1kw	31905838-31908522
90	S6A_2-489k11.p1kw	29931599-29934065	**964**	S6A_2-502o09.p1kw	31908201-31910216
91	S6A_2-134k22.p1k	29933548-29935949	**965**	S6A_2-85a14.p1kk	31910172-31912771
92	6S17_2-201c14.p1kw	29935654-29938224	**966**	S6C_2-456j01.q1kw	31912703-31915282
93	6S17_2-580e24.p1kw	29937894-29939594	**967**	S6C_2-477a23.q1kw	31914590-31917011
94	6S17_2-34c02.p1kkw	29939562-29942347	**968**	6S17_2-512f15.p1ka	31916858-31919434
95	S6C_2-189h20.q1kw	29942189-29945148	**969**	S6C_2-40h05.p1kkw	31919393-31921980
96	6S17_2-403h19.q1kw	29945051-29947511	**970**	S6A_2-496h10.q1kw	31922562-31924805

97	S6A_2-66m22.q1k	29947487-29949977	**971**	S6A_2-237d22.p1k	31924942-31927455
98	6S17_2-637n22.p1kw	29949751-29952328	**972**	S6C_2-639k15.q1kw	31927428-31929146
99	S6C_2-233b21.p1kw	29952327-29954750	**973**	S6C_2-546o07.p1kw	31929098-31930771
100	S6C_2-77l13.q1kkw	29954618-29957153	**974**	S6A_2-536g11.q1kw	31930621-31933345
101	6S17_2-192f09.p1kw	29956443-29958865	**975**	S6C_3-147l15.q1kw	31933254-31936222
102	S6C_2-330d20.q1kw	29958784-29961560	**976**	S6A_3-65a04.p1kw	31936004-31939194
103	S6C_2-256g20.p1kw	29960874-29962955	**977**	6S17_2-665b10.p1ka	31938977-31941560
104	S6C_2-721i02.q1kw	29963000-29965350	**978**	S6A_2-486e01.p1kw	31941503-31943380
105	S6A_2-434k14.p1kw	29965444-29967775	**979**	S6A_2-16n19.q1k	31943558-31945978
106	S6C_2-482e09.p1kw	29967686-29969637	**980**	S6A_2-221i07.p1k	31945923-31948419
107	S6C_3-160e10.p1kw	29970136-29973125	**981**	S6C_2-497f24.q1kw	31948132-31950874
108	S6C_2-547i03.p1kw	29972904-29975600	**982**	6S17_2-700l22.q1kw	31950162-31952297
109	6S17_2-9m02.p1k1kw	29975451-29978299	**983**	S6C_2-361i24.p1kw	31951943-31953812
110	S6C_2-661p16.p1kw	29977965-29979873	**984**	6S17_2-710n11.p1kw	31953112-31955256
111	6S17_2-553o14.p1kw	29980107-29982593	**985**	6S17_2-715d06.q1kw	31955316-31957399
112	S6C_2-479j22.p1kw	29982740-29984644	**986**	S6C_2-588b18.q1kw	31957685-31960197
113	S6A_2-137k10.p1k	29983949-29986575	**987**	S6A_2-740e20.q1kw	31960172-31962699
114	6S17_2-344k12.p1kw	29986165-29989239	**988**	6S17_2-150b10.p1kw	31962270-31964146
115	6S17_2-264k07.q1kw	29989170-29991827	**989**	S6C_2-140g11.p1kw	31963191-31965805
116	S6A_2-6f10.p1kk	29991719-29994153	**990**	S6A_2-237p20.p1k	31965780-31967586
117	S6A_2-251f13.q1k	29993954-29996553	**991**	S6C_2-285j22.q1kw	31967460-31969965
118	S6C_2-617g14.q1kw	29996470-29998921	**992**	S6A_2-207e13.q1k	31969747-31971815
119	S6A_2-435c02.q1kw	29997684-29999912	**993**	S6A_2-110g08.p1k	31970722-31973699
120	6S17_2-703n06.q1kw	29999473-30001868	**994**	6S17_2-385k11.p1kw	31973209-31975528
121	S6C_2-161i01.q1kw	30000805-30003606	**995**	S6A_2-139d11.p1k	31975147-31977228
122	S6C_2-282i03.p1kw	30003664-30006525	**996**	6S17_2-198p02.q1kw	31976280-31979189
123	6S17_2-239i01.p1kw	30006173-30009006	**997**	S6C_2-48n21.q1kkw	31978958-31981348
124	S6A_2-35b03.p1kk	30007795-30009507	**998**	S6C_2-493g17.q1kw	31980740-31983206
125	6S17_2-9k16.q1k1k	30011212-30013747	**999**	S6C_2-183h11.q1kw	31983076-31985681
126	6S17_2-332a14.p1kw	30014008-30016512	**1000**	S6A_2-452h04.q1kw	31985622-31987748
127	6S17_2-521h21.p1kw	30016538-30019300	**1001**	6S17_2-131e15.p1kw	31987695-31990289
128	S6A_2-507g02.q1kw	30018788-30021193	**1002**	S6A_2-108k06.p1k	31990195-31993322
129	6S17_2-435e01.q1kw	30020915-30023760	**1003**	6S17_2-191e08.q1kw	31993048-31995603
130	S6C_2-417b10.q1kw	30023644-30025314	**1004**	6S17_2-707l19.q1kw	31995564-31998405
131	6S17_2-646f18.q1kw	30026610-30029371	**1005**	S6A_2-528m10.q1kw	31997990-32000159
132	6S17_2-587a07.q1kw	30028877-30031724	**1006**	S6C_2-503j20.p1kw	31999961-32002282
133	S6A_3-71b23.q1k	30031448-30034797	**1007**	S6C_2-625b21.p1kw	32002259-32004084
134	S6A_2-673h09.q1kw	30034394-30036661	**1008**	6S17_2-806b06.p1kw	32004149-32006374
135	6S17_2-432c04.p1kw	30036629-30039288	**1009**	S6C_3-107l20.p1kw	32006253-32009766
136	S6A_2-590e16.p1kw	30038988-30040493	**1010**	S6A_2-519g18.q1kw	32009459-32011854
137	6S17_2-244b17.p1kw	30041663-30044107	**1011**	S6C_3-107f16.q1kw	32011193-32014262
138	6S17_2-205k15.p1kw	30044313-30047010	**1012**	S6C_2-523d11.p1kw	32014233-32016871
139	S6C_2-210c04.q1kw	30046908-30048715	**1013**	S6A_2-15f08.p1k	32016305-32018444
140	S6C_2-735d12.p1kw	30048336-30050918	**1014**	S6C_2-386k10.q1kw	32018292-32020105
141	6S17_2-191a21.q1kw	30050854-30053711	**1015**	6S17_2-553a14.q1kw	32020686-32023216
142	S6C_2-63n09.p1kkw	30053351-30055956	**1016**	S6C_2-408j22.q1kw	32022930-32025728
143	6S17_2-776k15.p1kw	30055493-30057919	**1017**	6S17_2-764f16.p1kw	32024913-32027262
144	S6C_2-193l16.q1kw	30057565-30060238	**1018**	6S17_2-330n20.p1kw	32027399-32030336
145	S6C_2-443n10.q1kw	30060205-30062801	**1019**	S6C_2-695j09.p1kw	32029888-32032163

146	S6C_2-241l02.p1kw	30062253-30064589	**1020**	S6C_2-683n19.p1kw	32031928-32033887
147	S6C_2-215k01.p1kw	30063822-30066274	**1021**	S6C_2-562a03.p1kw	32033879-32036689
148	S6A_2-483o03.q1kw	30065589-30067967	**1022**	S6C_2-291b04.p1kw	32036564-32038255
149	6S17_2-607h11.q1ka	30067834-30070174	**1023**	S6A_2-454d05.p1kw	32037890-32040336
150	S6A_2-113n19.p1k	30070105-30072143	**1024**	S6A_2-623d01.q1kw	32040029-32042313
151	S6A_2-222f14.q1k	30071694-30074112	**1025**	S6A_2-446k08.p1kw	32042356-32044607
152	S6A_2-708k14.q1kw	30073667-30076374	**1026**	S6C_2-8e19.q1k1kw	32044562-32047306
153	6S17_2-692c18.q1ka	30076294-30078914	**1027**	6S17_2-173p20.p1kw	32046987-32049475
154	S6A_2-377g19.q1kw	30078444-30080712	**1028**	6S17_2-657o24.p1ka	32049370-32051317
155	S6C_2-252b19.q1kw	30081271-30083717	**1029**	S6A_2-673d15.p1kw	32051147-32053485
156	S6A_2-302b02.p1k	30083166-30085450	**1030**	S6A_2-88d04.q1kk	32053428-32055086
157	S6C_2-707j22.q1kw	30085288-30087916	**1031**	6S17_2-214n05.p1kw	32055443-32057238
158	6S17_2-788a04.p1kw	30087895-30090090	**1032**	stSG1159312	32056738-32058031
159	S6A_2-712a01.q1kw	30090312-30092624	**1033**	stSG1159313	32058012-32059339
160	S6C_2-669c06.p1kw	30092417-30094888	**1034**	6S17_2-70j17.q1kkw	32059160-32061208
161	S6C_2-235c10.q1kw	30094409-30096974	**1035**	S6C_2-742l01.p1kw	32061007-32063565
162	S6A_3-77e12.p1kw	30096934-30100100	**1036**	S6C_2-173b09.p1kw	32063457-32066073
163	6S17_2-125k04.q1k	30099548-30101323	**1037**	S6A_2-106a16.q1k	32065839-32067620
164	S6A_2-671m22.q1kw	30101121-30103717	**1038**	S6C_3-114l23.q1k	32066328-32068070
165	6S17_2-596p06.p1ka	30103986-30106521	**1039**	stSG1159314	32067481-32068550
166	6S17_2-563e18.q1kw	30106463-30109071	**1040**	stSG1159315	32068538-32069345
167	S6C_2-29k02.q1kkw	30108625-30111062	**1041**	stSG1159316	32069326-32070786
168	S6C_2-41i07.p1kkw	30110866-30113454	**1042**	stSG1159317	32070658-32070921
169	S6A_2-140c24.p1k	30113400-30115997	**1043**	stSG1159318	32070902-32071730
170	S6C_2-163i14.q1kw	30115916-30118521	**1044**	stSG1159319	32071709-32072864
171	6S17_2-181o18.p1kw	30118308-30120829	**1045**	stSG1159320	32072845-32073627
172	S6C_2-728o08.q1kw	30120845-30122794	**1046**	stSG1159321	32073608-32074514
173	S6A_2-85n06.q1kk	30123120-30125633	**1047**	stSG1159322	32074474-32074660
174	S6C_2-25i17.q1kww	30125000-30127465	**1048**	stSG1159323	32074588-32075372
175	6S17_2-104d15.p1k	30127345-30129803	**1049**	stSG1159324	32075329-32075948
176	S6C_2-446o03.p1kw	30129527-30132152	**1050**	stSG1159325	32075929-32076466
177	S6C_2-529n06.q1kw	30131866-30134499	**1051**	stSG1159326	32076457-32077697
178	6S17_2-111f06.p1k	30134479-30136131	**1052**	stSG1159327	32077678-32079121
179	6S17_2-601m22.p1ka	30136810-30139268	**1053**	stSG1159328	32079102-32080248
180	S6A_2-326i01.q1k	30139608-30142021	**1054**	stSG1159329	32080229-32081243
181	S6C_2-547h11.p1kw	30141934-30144322	**1055**	stSG1159330	32081199-32081780
182	S6C_2-684k19.p1kw	30144275-30146744	**1056**	stSG1159331	32081761-32082669
183	6S17_2-214d05.p1kw	30146157-30148833	**1057**	stSG1159332	32082644-32083799
184	S6A_2-716g15.p1kw	30148736-30150453	**1058**	stSG1159333	32083780-32085032
185	S6A_2-155m13.p1k	30151190-30153032	**1059**	stSG1159334	32085013-32086284
186	S6C_2-651k20.q1kw	30152988-30155591	**1060**	stSG1159335	32086265-32087169
187	S6A_2-471l02.p1k	30155515-30157551	**1061**	stSG1159336	32087153-32088530
188	S6A_2-257e02.q1k	30157712-30159479	**1062**	stSG1159337	32088497-32089494
189	S6C_3-93m23.p1kkw	30159325-30162190	**1063**	S6C_2-542p17.q1kw	32088659-32090434
190	S6C_2-141e11.p1kw	30161540-30164048	**1064**	S6A_2-48e04.p1k	32088718-32090526
191	S6A_2-163f10.q1k	30163862-30166356	**1065**	stSG1159338	32090068-32090760
192	6S17_2-802h10.p1kw	30166781-30169111	**1066**	stSG1159339	32090749-32092076
193	S6A_2-135a12.p1kw	30168959-30171414	**1067**	stSG1159340	32092057-32093147
194	S6A_2-106c02.q1k	30170963-30172669	**1068**	stSG1159341	32093106-32093797

195	S6A_2-174l24.q1k	30173168-30175684	**1069**	stSG1159342	32093716-32094383
196	S6C_3-162p09.q1kw	30175610-30178761	**1070**	stSG1159343	32094350-32095101
197	6S17_2-550d16.q1kw	30178743-30181378	**1071**	stSG1159344	32094951-32095618
198	S6C_2-557f19.q1kw	30180952-30183761	**1072**	stSG1159345	32096186-32096853
199	S6A_2-223g14.q1k	30183196-30185757	**1073**	stSG1159346	32096816-32097444
200	S6A_2-453d07.p1kw	30185263-30187645	**1074**	stSG1159347	32097421-32098088
201	6S17_2-269i03.p1kw	30187022-30189582	**1075**	stSG1159348	32098047-32098810
202	S6C_2-652k08.q1kw	30189405-30191834	**1076**	stSG1159349	32098656-32099323
203	S6A_2-708n04.p1kw	30191811-30194015	**1077**	stSG1159350	32099221-32099687
204	S6A_2-262n22.q1k	30194032-30196444	**1078**	stSG1159351	32099573-32100214
205	S6C_2-144e19.q1kw	30196396-30199101	**1079**	stSG1159352	32100218-32101294
206	S6A_2-747p05.q1kw	30198825-30200967	**1080**	stSG1159353	32101275-32102082
207	S6C_2-601k13.q1kw	30200798-30203110	**1081**	stSG1159354	32102063-32103523
208	S6A_2-7i02.p1k	30203030-30205314	**1082**	stSG1159355	32103395-32103658
209	6S17_2-431l04.p1kw	30205018-30207995	**1083**	stSG1159356	32103639-32104607
210	S6A_2-311o21.p1k	30207839-30210162	**1084**	stSG1159357	32104529-32104838
211	S6A_2-673l12.q1kw	30209756-30211921	**1085**	stSG1159358	32104734-32105602
212	6S17_2-80f06.p1kkw	30211416-30214316	**1086**	stSG1159359	32105583-32106365
213	S6A_3-25j03.q1kw	30214249-30217124	**1087**	stSG1159360	32106346-32107252
214	S6C_2-485l19.q1kw	30217012-30218864	**1088**	stSG1159361	32107212-32107398
215	S6C_2-101e10.p1kw	30219223-30221767	**1089**	stSG1159362	32107326-32108110
216	S6A_2-563c04.q1kw	30221831-30223967	**1090**	stSG1159363	32108067-32108686
217	S6C_2-647k08.p1kw	30223796-30226544	**1091**	stSG1159364	32108667-32109204
218	S6A_2-534o13.q1kw	30226106-30228443	**1092**	stSG1159365	32109195-32110435
219	S6C_2-310e17.q1kw	30228982-30231712	**1093**	stSG1159366	32110416-32111859
220	6S17_2-583k01.q1kw	30231506-30234359	**1094**	stSG1159367	32111840-32112986
221	S6A_2-238l14.p1k	30233200-30235491	**1095**	stSG1159368	32112967-32113971
222	S6C_3-111o21.q1k	30235887-30239058	**1096**	stSG1159369	32113952-32115406
223	6S17_2-617i02.p1ka	30238940-30240972	**1097**	stSG1159370	32115381-32116535
224	S6A_2-466d22.q1k	30241241-30243458	**1098**	stSG1159371	32116516-32117768
225	S6C_2-724m20.p1kw	30243167-30246046	**1099**	stSG1159372	32117749-32119019
226	6S17_2-178p14.q1kw	30245610-30247676	**1100**	stSG1159373	32119000-32120024
227	S6A_2-454k03.p1kw	30247370-30249040	**1101**	stSG1159374	32120008-32120922
228	6S17_2-452n04.q1kw	30249896-30252535	**1102**	stSG1159375	32120903-32121897
229	S6A_2-227e24.q1k	30252097-30254580	**1103**	stSG1159376	32121878-32123038
230	S6C_2-300o04.q1kw	30254297-30256821	**1104**	S6C_2-161i04.q1kw	32122000-32123654
231	S6C_2-478b08.q1kw	30256578-30258948	**1105**	S6C_2-153b21.q1k	32122197-32124965
232	S6C_2-359b06.p1kw	30258897-30261696	**1106**	stSG1159377	32124830-32125663
233	6S17_2-382n04.q1kw	30261629-30264590	**1107**	S6A_2-6n18.q1kk	32125354-32127124
234	6S17_2-206g17.q1kw	30264102-30266980	**1108**	S6A_2-84l07.p1kk	32126619-32128476
235	S6A_2-558e01.p1kw	30266722-30268934	**1109**	S6A_3-30f14.p1kw	32127610-32130779
236	S6C_2-119k15.q1kw	30269344-30271071	**1110**	6S17_2-140h16.q1kw	32130633-32133573
237	S6C_3-158j05.q1kw	30271840-30274861	**1111**	6S17_2-794m01.q1kw	32133633-32134851
238	S6A_2-154j09.p1k	30274583-30276957	**1112**	6S17_2-719c06.p1kw	32134686-32136930
239	S6A_2-599k23.p1kw	30276880-30279160	**1113**	6S17_2-269a16.p1kw	32136836-32138862
240	S6A_2-651j12.p1kw	30279117-30281405	**1114**	S6C_2-524g20.q1kw	32138807-32141209
241	S6A_2-19f16.p1k	30281160-30283602	**1115**	S6A_2-670i15.p1kw	32141276-32143069
242	6S17_2-75k18.q1kkw	30283371-30285180	**1116**	6S17_2-750c21.p1kw	32143215-32145326
243	S6C_2-594k01.p1kw	30285428-30288361	**1117**	6S17_2-25g07.p1kkw	32145676-32148218

244	S6A_2-63e09.p1kk	30288220-30290560	**1118**	6S17_2-181f24.p1kw	32147563-32149995
245	S6A_2-273p03.p1k	30290402-30292798	**1119**	6S17_2-418g15.q1kw	32150241-32152796
246	6S17_2-131c02.p1kw	30293081-30295008	**1120**	6S17_2-174p13.q1kw	32152743-32155604
247	S6A_2-498c09.q1kw	30294868-30297043	**1121**	S6C_2-513n18.p1kw	32155253-32157618
248	S6C_2-163i17.q1kw	30296768-30299180	**1122**	S6C_2-291d22.p1kw	32157626-32160240
249	6S17_2-396e16.q1kw	30299219-30301983	**1123**	S6C_2-326j20.q1kw	32159820-32162689
250	S6C_2-199e05.p1kw	30301929-30304620	**1124**	6S17_2-434b21.p1kw	32162634-32165023
251	6S17_2-477i01.q1kw	30304335-30306759	**1125**	6S17_2-389b01.p1kw	32163006-32165743
252	6S17_2-236g22.p1kw	30306687-30309185	**1126**	S6A_2-108k20.p1k	32165679-32167479
253	S6C_2-320k13.p1kw	30309105-30311651	**1127**	S6C_3-164b14.q1kw	32167536-32170988
254	S6A_2-244f10.p1k	30310928-30313255	**1128**	S6A_2-188c20.q1k	32170830-32173166
255	S6A_2-226b24.p1k	30312424-30314809	**1129**	6S17_2-36b20.p1kkw	32172853-32175681
256	S6C_2-751c24.q1kw	30314787-30317588	**1130**	S6C_2-26m20.q1kkw	32175385-32178187
257	S6C_2-603l10.q1kw	30317074-30319753	**1131**	S6C_2-690h09.p1kw	32178090-32180099
258	S6C_2-383m11.q1kw	30318304-30320534	**1132**	6S17_2-113k10.p1k	32179518-32182024
259	S6A_3-82k19.p1kw	30319881-30322996	**1133**	S6C_2-332n21.q1kw	32181677-32184316
260	S6C_2-385l07.p1kw	30322904-30325267	**1134**	6S17_2-285k20.p1kw	32184266-32186875
261	S6A_3-71j14.p1kw	30324946-30327580	**1135**	S6A_2-287j14.q1k	32186657-32188872
262	S6A_2-262l08.q1k	30326343-30328780	**1136**	6S17_2-451g19.q1kw	32188704-32191189
263	S6A_3-80j02.q1kw	30328752-30331413	**1137**	6S17_2-170n17.p1kw	32191153-32193966
264	S6A_2-137k04.p1k	30331401-30333872	**1138**	6S17_2-598d07.p1kw	32193954-32196840
265	6S17_2-206p12.q1kw	30333824-30336492	**1139**	S6C_2-31n14.q1kkw	32196380-32199082
266	6S17_2-399g08.q1kw	30336443-30339254	**1140**	S6A_2-583m19.p1kw	32198195-32200755
267	6S17_2-715k20.p1kw	30339215-30341370	**1141**	S6C_2-429i16.q1kw	32200537-32203354
268	S6C_2-47o13.q1kkw	30341155-30343559	**1142**	S6A_2-366o15.p1k	32203258-32205842
269	S6C_2-197e05.q1kw	30343050-30345405	**1143**	6S17_2-337k22.p1kw	32205637-32208043
270	S6C_2-119a05.q1kw	30345571-30347925	**1144**	S6C_2-108m04.q1kw	32207678-32210016
271	S6A_2-236p14.p1k	30347804-30350169	**1145**	S6A_2-276j12.q1k	32209653-32211785
272	S6A_2-724m04.q1kw	30350008-30351777	**1146**	S6C_2-317i18.p1kw	32212464-32215038
273	S6C_2-725k15.q1kw	30351301-30353113	**1147**	S6C_2-457p24.p1kw	32215006-32217687
274	S6A_2-48p07.p1k	30353431-30355824	**1148**	6S17_2-378o15.q1kw	32217561-32220047
275	S6A_2-218p05.p1k	30355557-30357404	**1149**	6S17_2-370g20.p1kw	32220043-32222067
276	6S17_2-333c06.q1kw	30356186-30358959	**1150**	S6A_2-42g10.p1k	32222119-32224613
277	S6C_2-227g08.q1kw	30358915-30361227	**1151**	6S17_2-451l18.q1kw	32223988-32226638
278	S6C_2-769l13.q1kw	30360627-30363086	**1152**	6S17_2-321d11.p1kw	32226074-32228304
279	S6A_2-577p21.p1kw	30363052-30365623	**1153**	6S17_2-277b13.q1kw	32228428-32231227
280	S6C_3-110n15.q1kw	30365212-30368158	**1154**	S6A_2-277j06.q1k	32231190-32233498
281	S6C_2-106a18.q1kw	30368063-30370782	**1155**	6S17_2-351k16.p1kw	32232939-32234889
282	S6A_2-338l12.p1kw	30368214-30370831	**1156**	S6C_2-546c20.q1kw	32235275-32238140
283	stSG1159309	30370522-30371723	**1157**	S6A_2-139f17.q1k	32238133-32240410
284	6S17_2-527n01.p1kw	30371106-30373524	**1158**	S6A_2-573a20.p1kw	32240369-32242019
285	S6A_2-305e12.p1k	30373125-30373916	**1159**	6S17_2-440g13.p1kw	32241499-32244364
286	S6A_2-526m17.p1kw	30375512-30377983	**1160**	S6A_2-174l16.q1k	32244192-32246383
287	S6C_2-467d24.q1kw	30377836-30380380	**1161**	S6C_3-168j03.q1kw	32246419-32248999
288	S6C_2-131c20.p1kw	30380190-30382789	**1162**	S6A_2-551j22.p1kw	32248564-32250364
289	6S17_2-605k15.p1ka	30382810-30384600	**1163**	S6A_2-393o01.q1kw	32249781-32252103
290	S6C_2-208j05.q1kw	30383972-30386726	**1164**	S6A_2-379m24.q1kw	32252077-32253933
291	S6A_3-11i22.p1kw	30386439-30389440	**1165**	6S17_2-322m15.q1kw	32254579-32257632
292	S6C_3-105o09.q1kw	30389144-30392634	**1166**	S6A_2-691m15.p1kw	32257314-32259506

293	6S17_2-620j16.p1ka	30391810-30393924	**1167**	6S17_2-22e07.p1kkw	32259227-32261868
294	S6A_2-608o13.p1kw	30393899-30396193	**1168**	S6A_2-131p01.q1k	32261170-32263480
295	S6C_2-511c09.q1kw	30396832-30399470	**1169**	6S17_2-105o14.q1k	32262484-32264924
296	S6A_2-711o21.p1kw	30399467-30401924	**1170**	S6A_2-48g01.p1k	32264851-32267175
297	S6A_2-604p02.p1kw	30401869-30404481	**1171**	6S17_2-340o16.p1kw	32267130-32269967
298	S6C_2-269h18.q1kw	30404296-30406670	**1172**	6S17_2-345g09.p1kw	32269887-32272253
299	6S17_2-556i24.p1kw	30406289-30409007	**1173**	6S17_2-803o14.p1kw	32272047-32274520
300	S6C_2-166n15.q1kw	30408482-30410987	**1174**	S6A_2-470g09.p1k	32274363-32277053
301	S6A_2-610k24.p1kw	30411277-30413752	**1175**	6S17_2-652k23.q1ka	32276844-32278786
302	6S17_2-62e06.p1kkw	30413558-30415846	**1176**	S6A_2-352g13.q1kw	32278686-32281326
303	S6C_2-681h24.p1kw	30415752-30417462	**1177**	S6C_2-650o01.p1kw	32280664-32283173
304	S6A_2-668c19.q1kw	30417193-30419689	**1178**	S6A_2-165l21.p1k	32283065-32285225
305	S6A_2-720i16.q1kw	30419279-30421497	**1179**	S6A_2-537g07.p1kw	32285571-32288206
306	S6C_3-93e16.q1kkw	30421568-30424503	**1180**	S6A_2-528m17.q1kw	32288063-32290295
307	S6A_2-446h15.p1kw	30424262-30426665	**1181**	S6C_2-377n05.p1kw	32289254-32291325
308	S6C_2-287d19.p1kw	30426212-30428064	**1182**	6S17_2-162f10.q1kw	32291705-32294316
309	6S17_2-624p03.p1kw	30428243-30430343	**1183**	6S17_2-700n22.p1ka	32293344-32295765
310	S6C_3-117a10.q1k	30430493-30433527	**1184**	S6A_2-394m04.q1kw	32295755-32298096
311	S6A_2-403c13.p1kw	30433512-30435982	**1185**	6S17_2-601o04.q1ka	32298082-32300874
312	S6A_2-489p05.q1kw	30435458-30437915	**1186**	S6C_2-492i22.q1kw	32300820-32303714
313	6S17_2-377o10.q1kw	30437860-30440596	**1187**	S6C_2-464c15.q1kw	32303650-32306151
314	S6A_2-470b19.p1k	30440595-30442886	**1188**	S6C_2-657n17.p1kw	32305696-32308227
315	S6A_2-436n08.p1kw	30442776-30445345	**1189**	6S17_2-701n21.q1ka	32308325-32311173
316	6S17_2-550i06.p1kw	30445574-30448407	**1190**	S6A_2-227l07.q1k	32311037-32313141
317	S6A_2-137p02.q1k	30448175-30450582	**1191**	S6C_2-608i13.q1kw	32312649-32315293
318	S6A_2-504i01.p1kw	30450571-30453097	**1192**	S6A_2-693f20.q1kw	32314880-32317419
319	S6C_2-253n01.q1kw	30453257-30455963	**1193**	6S17_2-391g13.p1kw	32317222-32319880
320	S6A_2-700h17.p1kw	30455483-30457800	**1194**	S6A_2-15g14.p1k	32319487-32321971
321	6S17_2-654k24.q1ka	30457324-30459145	**1195**	S6A_2-19o06.q1k	32321572-32324023
322	S6A_2-585p02.q1kw	30459362-30461425	**1196**	6S17_2-333n04.p1kw	32323976-32326426
323	S6A_2-363m19.p1k	30461074-30463679	**1197**	S6A_2-40b07.p1k	32326052-32327925
324	S6C_2-113b05.p1kw	30463598-30466352	**1198**	S6C_2-544p17.q1kw	32327905-32330164
325	S6A_2-235c01.q1k	30466391-30468882	**1199**	S6C_3-119l10.p1k	32330237-32333661
326	S6A_2-83e17.q1kk	30468512-30470936	**1200**	6S17_2-691p19.p1kw	32333324-32335035
327	S6A_2-630n19.q1kw	30470785-30472844	**1201**	S6A_2-306m22.p1k	32334902-32337196
328	S6C_2-232d09.q1kw	30472435-30474725	**1202**	S6C_2-53l16.q1kkw	32337055-32339933
329	S6A_2-726b11.p1kw	30474644-30477030	**1203**	6S17_2-388n01.q1kw	32339897-32342653
330	S6C_2-405j01.q1kw	30476804-30479649	**1204**	S6A_2-47b21.p1k	32342598-32344977
331	6S17_2-482b22.q1kw	30479563-30482385	**1205**	S6A_2-473c20.q1kw	32344991-32347210
332	6S17_2-715l07.q1kw	30482335-30484495	**1206**	S6C_2-329e03.p1kw	32347172-32349492
333	S6C_2-122d21.p1kw	30484481-30486798	**1207**	S6C_2-356p18.q1kw	32349911-32352716
334	S6A_2-364h11.q1k	30486590-30488863	**1208**	S6A_2-359j18.q1kw	32352121-32354558
335	S6A_2-614f15.p1kw	30489386-30491682	**1209**	6S17_2-453h05.p1kw	32354408-32357209
336	S6C_2-431j21.p1kw	30491424-30493923	**1210**	6S17_2-99c23.p1kk	32357072-32359919
337	S6A_2-750n07.q1kw	30493541-30495842	**1211**	S6C_2-186k14.p1kw	32359755-32362494
338	S6A_2-149i02.q1k	30495615-30497361	**1212**	S6C_2-671n06.q1kw	32362260-32364675
339	S6C_2-581h23.p1kw	30496479-30499147	**1213**	S6C_2-301f13.q1kw	32364646-32367027
340	S6A_2-507a06.q1kw	30498694-30501279	**1214**	S6C_3-121k16.q1kw	32367187-32370019
341	S6C_2-295l04.p1kw	30501127-30503780	**1215**	S6C_3-141l24.q1kw	32369513-32372579

342	S6C_2-25f21.q1kkw	30503512-30505932	**1216**	S6A_2-36i20.q1k	32372351-32375042
343	6S17_2-400l17.q1kw	30505856-30508413	**1217**	S6A_2-280d20.p1k	32375009-32376811
344	S6A_2-540o20.p1kw	30507610-30510119	**1218**	6S17_2-799l05.q1kw	32376862-32379701
345	6S17_2-477f16.q1kw	30509530-30512280	**1219**	S6C_2-670i02.p1kw	32379696-32381542
346	S6A_2-307k14.q1k	30512150-30514491	**1220**	S6A_2-462n13.p1kw	32381617-32384080
347	S6C_2-271f21.p1kw	30514250-30516917	**1221**	S6C_2-640n13.q1kw	32383418-32386054
348	6S17_2-716e10.p1kw	30516686-30519460	**1222**	6S17_2-49a24.q1kkw	32386043-32387227
349	S6C_2-285g11.p1kw	30519080-30521624	**1223**	6S17_2-294m12.p1kw	32387922-32390488
350	S6C_2-602b15.p1kw	30521587-30523578	**1224**	6S17_2-67f06.p1kkw	32390209-32393140
351	S6A_2-670e19.q1kw	30522628-30524632	**1225**	6S17_2-349k10.p1kw	32393119-32395967
352	S6A_3-70g05.p1k	30523998-30526686	**1226**	6S17_2-706c04.p1ka	32395956-32398655
353	S6C_3-122j09.p1kw	30526624-30528439	**1227**	S6C_2-461f12.p1kw	32398586-32401154
354	6S17_2-149n23.p1kw	30527803-30529467	**1228**	S6C_2-685o08.p1ka	32400808-32402021
355	S6A_2-288n24.p1k	30530465-30532499	**1229**	6S17_2-82j13.q1kk	32402691-32405190
356	S6C_2-583f04.q1kw	30532105-30534885	**1230**	S6A_2-518p02.q1kw	32404753-32407328
357	S6C_2-307h13.q1kw	30534798-30537070	**1231**	S6C_2-282n14.p1kw	32407198-32409584
358	S6A_2-231k06.q1k	30536189-30538357	**1232**	S6A_2-240h02.p1k	32409735-32412419
359	S6A_2-255b11.q1k	30537837-30539816	**1233**	S6C_2-22o07.p1kkw	32411660-32414241
360	S6A_2-272d08.q1k	30539289-30540956	**1234**	S6C_2-179h23.p1kw	32414203-32416787
361	6S17_2-465d24.q1kw	30541640-30543704	**1235**	6S17_2-786f06.p1kw	32416697-32418805
362	6S17_2-685m16.p1ka	30543626-30546580	**1236**	S6A_2-176i23.p1kw	32418544-32420769
363	S6A_3-54n20.q1kw	30546495-30548204	**1237**	S6A_2-64i05.p1kk	32419949-32422580
364	S6C_2-743g21.p1kw	30548127-30550788	**1238**	S6A_2-724i15.p1kw	32423326-32425860
365	6S17_2-544m01.q1kw	30550719-30553560	**1239**	S6A_2-200f17.p1k	32425489-32427795
366	S6C_2-179c19.q1kw	30553123-30554913	**1240**	S6C_2-566m04.p1kw	32427558-32430508
367	S6A_3-59l07.q1kw	30555778-30557696	**1241**	S6A_2-422n17.q1kw	32430334-32433086
368	S6A_2-24f07.q1k	30557295-30559029	**1242**	S6C_2-533m14.p1kw	32432791-32435294
369	6S17_2-304j10.q1kw	30559011-30561081	**1243**	6S17_2-218b15.p1kw	32434975-32437634
370	S6C_2-747i18.p1kw	30561209-30563657	**1244**	S6A_2-175p24.q1kw	32437597-32439662
371	S6C_2-464i11.p1kw	30562566-30564894	**1245**	S6A_2-233g24.q1k	32439560-32442112
372	S6C_2-611a24.p1kw	30563893-30565706	**1246**	S6A_2-560o19.p1kw	32441851-32444119
373	S6C_2-375i22.p1kw	30565890-30568365	**1247**	S6C_2-69e08.p1kkw	32444450-32446973
374	S6A_2-278m09.q1k	30568353-30570872	**1248**	S6C_2-220j13.q1kw	32446941-32449572
375	6S17_2-67k07.p1kkw	30570795-30573727	**1249**	S6C_2-569i07.q1kw	32449154-32450929
376	S6A_2-747m18.p1kw	30572905-30575560	**1250**	S6C_2-628h15.q1kw	32451114-32453613
377	S6C_2-172p23.q1kw	30575245-30577665	**1251**	6S17_2-698k06.q1kw	32453538-32456020
378	6S17_2-378i03.q1kw	30577899-30580927	**1252**	6S17_2-608m07.p1kw	32455394-32458106
379	S6C_2-513f11.p1kw	30580787-30583642	**1253**	S6C_2-696o02.q1kw	32457815-32460338
380	6S17_2-749c22.p1kw	30583516-30586461	**1254**	S6A_3-16c05.q1kw	32460037-32462779
381	S6A_3-62g20.q1kw	30586174-30588872	**1255**	S6A_2-705a07.p1kw	32462731-32465220
382	S6A_2-697m16.p1kw	30588870-30591425	**1256**	S6A_2-510h22.p1kw	32465117-32466918
383	6S17_2-641j23.q1ka	30591506-30594471	**1257**	S6C_3-172m09.q1kw	32467000-32470237
384	S6A_2-19p24.q1k	30593471-30595894	**1258**	S6C_2-469o13.q1kw	32469310-32471729
385	6S17_2-809d16.q1kw	30595623-30597651	**1259**	S6C_2-599m10.q1kw	32471036-32473567
386	6S17_2-180c13.p1kw	30598279-30600699	**1260**	6S17_2-529o09.q1ka	32473396-32476273
387	S6C_2-143j13.p1kw	30600787-30603165	**1261**	S6A_3-52o24.p1kw	32476215-32479059
388	S6C_2-338l08.q1kw	30603265-30606001	**1262**	S6A_2-80d09.p1kk	32478550-32480757
389	6S17_2-713f01.p1kw	30605872-30608344	**1263**	S6C_2-764n11.q1kw	32480829-32483469
390	S6A_2-430k18.p1kw	30608279-30610773	**1264**	S6C_2-725c15.q1kw	32483778-32485594

391	6S17_2-709l13.q1kw	30610759-30613495	**1265**	S6C_2-567l15.q1kw	32484275-32487774
392	6S17_2-276d01.p1kw	30613312-30615903	**1266**	S6A_2-69d24.p1kk	32487094-32489228
393	6S17_2-552g04.p1kw	30615039-30617134	**1267**	S6C_2-578i03.q1kw	32489023-32491841
394	S6A_2-639h21.p1kw	30615921-30618392	**1268**	6S17_2-455p07.q1kw	32491122-32493607
395	S6A_2-294e20.p1k	30618347-30620800	**1269**	6S17_2-144e24.q1kw	32493635-32496386
396	S6C_2-237l21.q1kw	30620979-30623383	**1270**	S6C_2-479j24.q1kw	32496153-32498835
397	6S17_2-36b13.p1kkw	30622725-30624634	**1271**	S6C_2-194k16.p1kw	32498517-32501144
398	6S17_2-802e14.p1kw	30624293-30626447	**1272**	S6A_2-58m09.q1kk	32501095-32503289
399	S6A_2-579n18.p1kw	30625905-30628399	**1273**	6S17_2-683h01.q1kw	32503289-32505783
400	S6C_3-159k18.p1kw	30628383-30631301	**1274**	6S17_2-536j18.p1ka	32505710-32507577
401	6S17_2-420n07.p1kw	30631236-30633764	**1275**	6S17_2-309p14.q1kw	32507665-32509609
402	S6A_2-303f10.p1k	30633576-30636156	**1276**	S6C_3-111f03.p1k	32509557-32512401
403	S6A_2-512f01.q1kw	30634913-30637265	**1277**	S6A_2-581h02.p1kw	32511421-32513544
404	S6C_2-451p19.q1kw	30637406-30640137	**1278**	S6A_2-701o11.q1kw	32513678-32516071
405	S6A_2-607l20.p1kw	30639961-30642497	**1279**	S6C_2-643b21.q1kw	32515863-32518446
406	S6C_2-73i20.p1kkw	30641900-30644649	**1280**	S6A_2-187g15.q1k	32518443-32520782
407	S6C_2-270i20.q1kw	30644018-30646431	**1281**	S6C_2-462h08.p1kw	32519353-32522182
408	6S17_2-165k19.p1kw	30646407-30648967	**1282**	S6A_2-635j03.q1kw	32521822-32523899
409	6S17_2-601g11.q1kw	30648853-30651217	**1283**	S6A_2-643f19.q1kw	32524176-32526297
410	S6C_2-448f23.p1kw	30651243-30653044	**1284**	6S17_2-287f10.q1kw	32526778-32528509
411	S6C_2-601l10.p1kw	30652902-30655245	**1285**	S6C_2-6n11.q1kkww	32529286-32531892
412	6S17_2-423g01.q1kw	30654388-30657128	**1286**	6S17_2-69c01.q1kkw	32531595-32534000
413	S6C_2-438f22.p1kw	30657126-30659083	**1287**	S6A_3-30g20.p1kw	32533849-32536651
414	S6A_2-181m21.q1k	30659373-30661831	**1288**	S6A_2-470m16.q1k	32536608-32539324
415	6S17_2-481d23.q1kw	30661673-30664635	**1289**	S6C_2-291o13.p1kw	32539196-32541992
416	S6C_2-682c04.p1kw	30664440-30666945	**1290**	S6A_2-127n09.p1k	32541661-32544149
417	S6A_2-440o11.q1kw	30666198-30668712	**1291**	S6A_2-485m01.p1kw	32543851-32546046
418	S6C_2-590f14.q1kw	30668130-30670622	**1292**	S6A_2-160p02.q1k	32546536-32549027
419	S6A_2-47a20.p1k	30670375-30672687	**1293**	S6C_2-655g07.p1kw	32549101-32552079
420	6S17_2-154e09.q1kw	30672681-30675554	**1294**	S6C_2-542d02.q1kw	32552075-32554386
421	S6A_2-168i23.q1k	30675002-30677589	**1295**	S6C_3-161p08.p1kw	32553907-32557064
422	6S17_2-578i18.p1kw	30677499-30679491	**1296**	S6C_2-754f14.q1kw	32557020-32559661
423	S6A_3-84h09.p1kw	30678881-30681415	**1297**	S6C_2-558c22.p1kw	32559508-32562044
424	S6A_2-64m14.p1kk	30681160-30683469	**1298**	S6C_3-104n23.q1kw	32561821-32564747
425	S6C_2-510m16.p1kw	30682967-30685552	**1299**	stSG1159378	32564183-32565404
426	S6A_2-317a15.q1k	30685464-30687948	**1300**	S6C_2-494h24.q1kw	32566224-32568770
427	6S17_2-34d21.q1kkw	30687802-30690256	**1301**	S6C_2-213o20.p1kw	32567713-32570098
428	S6A_2-129m07.q1k	30689948-30692394	**1302**	S6C_2-410b14.p1kw	32570284-32572093
429	6S17_2-104a16.q1k	30691343-30693991	**1303**	S6C_2-65n15.p1kkw	32574017-32576550
430	S6A_2-513c24.q1kw	30693812-30696380	**1304**	S6C_2-242o23.q1kw	32574678-32577348
431	S6C_2-359i16.p1kw	30696331-30698309	**1305**	S6C_2-585c14.p1kw	32577343-32579881
432	6S17_2-579m09.p1kw	30698815-30701782	**1306**	S6C_2-371b04.p1kw	32577611-32579425
433	S6C_2-497h09.q1kw	30701596-30704062	**1307**	S6C_2-23j17.p1kkw	32583051-32585482
434	S6A_2-604l08.q1kw	30703929-30706199	**1308**	S6C_2-654j11.p1kw	32585496-32588059
435	6S17_2-606d04.q1ka	30706250-30708860	**1309**	S6C_2-352n06.p1kw	32587814-32590389
436	S6C_2-592h12.p1kw	30708719-30711475	**1310**	S6C_2-266a20.q1kw	32588572-32590988
437	6S17_2-432i09.q1kw	30711444-30713962	**1311**	stSG1159379	32590480-32591619
438	S6A_2-138a12.p1k	30712897-30714595	**1312**	S6C_3-109f13.p1kw	32591170-32594283
439	6S17_2-474m08.p1kw	30714444-30716453	**1313**	S6C_3-125f11.q1kw	32592713-32595798

440	6S17_2-286k07.p1kw	30716726-30719431	**1314**	S6C_2-440h12.q1kw	32595228-32598303
441	6S17_2-106m14.q1k	30719078-30721808	**1315**	S6C_2-701f06.q1ka	32598134-32600400
442	S6C_2-736m04.p1kw	30721858-30724158	**1316**	S6C_2-23a13.p1kkw	32598979-32601716
443	S6A_2-557h08.p1kw	30723587-30725874	**1317**	stSG1159380	32601273-32601860
444	6S17_2-605k18.p1ka	30725120-30727637	**1318**	S6C_2-212a06.p1kw	32603319-32606243
445	S6A_2-169l15.q1k	30727592-30729910	**1319**	S6A_2-718o07.q1kw	32605193-32606885
446	6S17_2-28b16.p1kkw	30729548-30732095	**1320**	S6C_2-763i15.q1kw	32606648-32609256
447	6S17_2-493e01.q1ka	30731648-30734384	**1321**	S6A_2-247f17.p1k	32609013-32611396
448	S6A_2-611m11.q1kw	30733869-30736082	**1322**	S6C_2-394o17.q1kw	32611011-32613607
449	S6C_3-120e01.p1k	30736385-30739485	**1323**	S6C_3-93b19.p1kkw	32613182-32615215
450	S6C_2-652e24.p1kw	30739217-30741637	**1324**	S6A_2-470p08.p1k	32613622-32616563
451	6S17_2-519o08.p1kw	30741586-30744046	**1325**	S6C_2-31e15.p1kkw	32617073-32619269
452	S6C_2-596a06.p1kw	30742569-30745072	**1326**	S6C_2-197c12.q1kw	32617304-32619571
453	S6C_2-153a04.p1kw	30744416-30747127	**1327**	S6A_2-109i04.p1k	32619337-32622559
454	S6A_2-726n04.q1kw	30747104-30749574	**1328**	S6C_2-494l02.q1kw	32621015-32622850
455	6S17_2-783p12.p1kw	30749221-30751728	**1329**	S6C_2-603c08.p1kw	32622631-32625110
456	S6C_2-121d16.q1kw	30751423-30754146	**1330**	S6A_2-155c16.q1k	32624242-32626309
457	S6A_2-485e09.q1kw	30754016-30756025	**1331**	S6A_2-527d02.p1kw	32626531-32628342
458	6S17_2-749c13.p1kw	30754744-30757288	**1332**	stSG1159381	32628159-32629647
459	S6A_2-365l07.p1k	30756515-30758800	**1333**	S6C_2-748n04.q1ka	32629458-32632030
460	S6A_2-617f24.q1kw	30758534-30760818	**1334**	S6C_2-23n12.q1kkw	32629755-32631649
461	S6A_2-608l19.q1kw	30760969-30763083	**1335**	stSG1159382	32631240-32632113
462	S6A_2-126l05.q1k	30763012-30765292	**1336**	stSG1159383	32632094-32633379
463	S6C_2-495l23.q1kw	30765125-30768040	**1337**	stSG1159384	32633359-32634474
464	6S17_2-494h12.p1ka	30767990-30770760	**1338**	S6A_2-112j12.q1k	32633496-32636719
465	S6C_2-243h09.q1kw	30770430-30772995	**1339**	S6C_2-519f13.q1kw	32635458-32637246
466	6S17_2-230b18.p1kw	30772906-30775852	**1340**	S6C_3-129n21.q1kw	32637066-32640334
467	S6A_2-366d09.q1k	30775195-30777418	**1341**	S6C_2-755e01.q1kw	32637942-32640486
468	S6C_2-4d21.p1kkww	30777380-30779889	**1342**	S6C_2-451a13.q1kw	32641050-32643561
469	S6A_2-219b07.q1k	30779529-30781860	**1343**	S6C_2-442e02.q1kw	32642241-32644714
470	S6A_2-635p12.q1kw	30782027-30784613	**1344**	S6C_2-351b16.p1kw	32644074-32646662
471	S6A_2-224o01.p1k	30783876-30786164	**1345**	S6C_2-498k17.q1kw	32646521-32649544
472	S6A_3-52k18.q1kw	30786358-30789092	**1346**	6S17_2-558f21.q1kw	32649832-32652328
473	S6A_2-269o12.p1k	30788411-30790724	**1347**	6S17_2-329d06.q1kw	32651630-32653632
474	S6C_2-50c18.p1kkw	30791075-30793632	**1348**	stSG1159385	32653282-32654222
475	6S17_2-193f12.q1kw	30793632-30796198	**1349**	S6C_2-565j16.q1kw	32653939-32656323
476	S6A_2-100c12.p1k	30796079-30798491	**1350**	S6C_2-670k24.q1kw	32656262-32659045
477	S6A_2-377a10.p1kw	30798378-30800913	**1351**	S6C_2-679p20.q1kw	32657249-32658112
478	S6A_2-34a12.p1kk	30800557-30802795	**1352**	stSG1159386	32657650-32658663
479	S6A_2-621o08.q1kw	30802979-30805417	**1353**	stSG1159387	32658644-32659426
480	S6A_2-372i15.q1kw	30805362-30807102	**1354**	stSG1159388	32659407-32660508
481	S6A_2-241e07.p1k	30807576-30809875	**1355**	S6C_2-744j22.q1kw	32660487-32663275
482	S6C_2-681g09.q1kw	30809836-30812174	**1356**	S6C_2-684n08.p1kw	32663263-32666061
483	S6C_2-753m03.q1kw	30812071-30814586	**1357**	S6C_2-158k03.q1kw	32666007-32668413
484	S6C_2-366p06.p1kw	30814167-30816002	**1358**	6S17_2-498j06.p1ka	32668459-32673858
485	6S17_2-223m24.p1kw	30815969-30818954	**1359**	S6C_3-154p07.p1kw	32673701-32676631
486	S6A_3-28g11.p1kw	30818455-30821315	**1360**	6S17_2-665m03.q1ka	32676160-32678749
487	S6C_2-340j09.p1kw	30821312-30823199	**1361**	S6A_2-374i19.q1kw	32678591-32681243
488	S6C_2-672h21.q1kw	30822901-30825493	**1362**	S6C_2-494b13.p1kw	32680961-32683760

489	S6C_2-242j03.q1kw	30825368-30827875	**1363**	6S17_2-503b15.p1ka	32683574-32686564
490	S6C_2-635b09.p1kw	30827954-30830159	**1364**	S6C_2-650m15.p1kw	32686431-32689080
491	6S17_2-552m05.q1kw	30829832-30832357	**1365**	S6C_2-126m01.q1kw	32689045-32691474
492	S6A_2-238c19.p1k	30832302-30834685	**1366**	S6C_2-22i19.q1kkw	32691590-32694583
493	6S17_2-368f12.q1kw	30834737-30837454	**1367**	S6C_2-651a14.q1kw	32694444-32697209
494	S6C_2-433l09.q1kw	30837308-30839740	**1368**	S6C_2-117g07.p1kw	32696991-32699506
495	6S17_2-713g11.p1kw	30839483-30842254	**1369**	S6C_2-100a10.q1kw	32699542-32702227
496	S6C_2-542h16.q1kw	30842022-30844454	**1370**	S6A_2-297b14.p1k	32701857-32703743
497	6S17_2-461g23.q1kw	30844326-30847065	**1371**	6S17_2-493b24.p1ka	32702876-32705751
498	6S17_2-540d07.p1kw	30846326-30848768	**1372**	S6C_2-53b07.p1kkw	32705613-32708110
499	S6A_2-300p23.p1k	30847921-30849896	**1373**	S6C_2-437n18.q1kw	32707826-32710692
500	S6C_2-491b06.p1kw	30849894-30851788	**1374**	S6A_2-742g13.p1kw	32710133-32712269
501	S6C_2-238i15.q1kw	30851980-30854444	**1375**	S6C_2-313h24.p1kw	32712264-32714547
502	S6A_2-224i23.q1k	30854311-30856717	**1376**	S6A_2-254o14.p1k	32714274-32717018
503	6S17_2-443o13.p1kw	30856421-30858535	**1377**	6S17_2-540i21.q1kw	32716744-32719125
504	S6C_2-139a14.q1kw	30858795-30861512	**1378**	6S17_2-22g19.q1kkw	32718336-32721027
505	S6A_2-220k01.p1k	30861196-30863592	**1379**	S6C_2-247i11.q1kw	32720216-32722920
506	6S17_2-518m10.q1kw	30863518-30866151	**1380**	S6C_2-185f19.p1kw	32722734-32725314
507	S6A_2-715o03.q1kw	30865584-30868163	**1381**	6S17_2-64b02.q1kkw	32724504-32727177
508	6S17_2-506m05.p1ka	30868063-30870686	**1382**	S6C_2-308e07.p1kw	32726637-32729174
509	6S17_2-748e20.q1kw	30870599-30873244	**1383**	S6C_2-724k13.q1kw	32728497-32731051
510	S6C_2-696g02.p1kw	30872234-30874823	**1384**	6S17_2-75a05.q1kkw	32730866-32733779
511	6S17_2-557m16.p1kw	30874781-30877077	**1385**	S6C_2-766n01.p1kw	32733611-32736437
512	6S17_2-688j02.q1kw	30876767-30879336	**1386**	S6A_2-584b12.q1kw	32736096-32738289
513	6S17_2-344b02.p1kw	30879040-30881645	**1387**	6S17_2-681l03.q1kw	32738279-32741157
514	6S17_2-213f19.p1kw	30881555-30884300	**1388**	S6C_2-288m06.q1kw	32740888-32743557
515	6S17_2-515d12.p1kw	30884117-30886506	**1389**	6S17_2-745b24.q1kw	32743165-32746083
516	S6C_2-351a06.q1kw	30886417-30888781	**1390**	6S17_2-649i15.p1kw	32745804-32748726
517	6S17_2-83a03.p1kk	30888462-30891159	**1391**	6S17_2-641c13.p1kw	32748236-32751038
518	6S17_2-62i21.q1kkw	30891136-30893651	**1392**	S6C_2-327b22.q1kw	32750587-32752380
519	S6C_2-458b06.p1kw	30893226-30895910	**1393**	6S17_2-278p22.p1kw	32751956-32754798
520	S6A_2-433k05.p1kw	30895816-30897841	**1394**	S6C_2-356l09.q1kw	32754319-32756817
521	S6A_2-195f18.q1k	30897892-30900087	**1395**	S6C_2-766k17.p1kw	32756715-32759481
522	S6A_2-184f09.q1k	30901287-30903649	**1396**	S6C_2-380f22.q1kw	32759416-32762298
523	6S17_2-337o24.p1kw	30903401-30906093	**1397**	S6C_2-19b23.q1kkw	32761722-32764350
524	6S17_2-773c19.p1kw	30905687-30908256	**1398**	S6A_2-361d06.q1kw	32764348-32767006
525	S6A_2-20p13.q1k	30908280-30910487	**1399**	S6A_2-691a16.q1kw	32766998-32769591
526	S6A_2-520k18.p1kw	30911060-30913484	**1400**	S6C_2-487i03.q1kw	32769075-32771517
527	S6C_2-351b17.q1kw	30913457-30915859	**1401**	S6A_2-253b21.p1k	32771813-32774032
528	S6C_2-386k22.q1kw	30915614-30918252	**1402**	6S17_2-247p13.p1kw	32773440-32776301
529	S6C_2-230f11.p1kw	30917880-30920413	**1403**	S6C_2-575h17.p1kw	32776173-32778703
530	S6A_2-196i12.q1k	30919625-30921968	**1404**	S6A_2-636e10.p1kw	32778597-32781168
531	6S17_2-662k11.p1ka	30921800-30923844	**1405**	6S17_2-783k03.p1kw	32780871-32783266
532	S6A_2-740c04.p1kw	30923216-30925575	**1406**	S6C_2-392f07.p1kw	32783173-32786086
533	S6A_2-14l15.p1k	30925491-30927915	**1407**	S6A_2-319p03.q1kw	32786130-32788393
534	S6A_2-25l19.q1k	30927796-30930045	**1408**	S6A_3-68k17.q1k	32787740-32790461
535	S6C_2-456f05.q1kw	30929953-30932748	**1409**	S6A_2-352m06.p1kw	32790223-32792480
536	6S17_2-105j08.q1k	30932711-30935689	**1410**	S6A_2-32l22.q1kk	32792223-32794599
537	S6C_2-681p03.p1kw	30935107-30937523	**1411**	6S17_2-43d23.q1kkw	32794482-32797049

538	S6A_2-593h07.p1kw	30937423-30939690	**1412**	S6A_2-524h08.q1kw	32796793-32799124
539	6S17_2-743c18.p1kw	30939677-30942406	**1413**	S6C_2-38f08.q1kkw	32799001-32801669
540	S6C_2-38e05.p1kkw	30942377-30944894	**1414**	6S17_2-65g22.p1kkw	32801443-32804134
541	S6A_2-112o09.q1k	30944554-30947737	**1415**	6S17_2-503c16.p1ka	32803977-32805579
542	S6C_2-487m09.q1kw	30947720-30950366	**1416**	6S17_2-355b09.q1kw	32805771-32808229
543	S6C_2-95h02.p1kkw	30950261-30953164	**1417**	S6C_2-673n03.q1kw	32808098-32810522
544	6S17_2-608d19.p1kw	30953134-30955521	**1418**	S6A_3-80h20.q1kw	32810462-32813136
545	S6A_2-390n13.q1kw	30955170-30957387	**1419**	S6C_2-311k23.q1kw	32812745-32815129
546	6S17_2-130a06.p1kw	30958243-30959538	**1420**	S6C_2-396h19.q1kw	32815428-32817674
547	S6A_2-165l18.p1k	30960918-30963025	**1421**	S6C_2-16n14.p1kkw	32817677-32820582
548	6S17_2-223h10.q1kw	30963100-30965641	**1422**	S6C_2-467b14.q1kw	32820315-32822012
549	S6C_2-347e13.q1kw	30965540-30967698	**1423**	S6C_2-165e01.q1kw	32821844-32824227
550	S6A_2-711a01.p1kw	30967454-30969815	**1424**	S6C_2-710h06.p1kw	32825193-32827718
551	S6C_2-647b05.p1kw	30970412-30972863	**1425**	6S17_2-194j14.p1kw	32827724-32830188
552	6S17_2-659i16.q1ka	30971526-30973515	**1426**	S6A_2-202k06.q1k	32829829-32831757
553	stSG1159310	30973452-30974608	**1427**	S6C_2-687a18.q1ka	32831266-32834013
554	S6C_2-746o08.p1kw	30974338-30976991	**1428**	S6C_2-280h09.p1kw	32833558-32836056
555	6S17_2-427a23.q1kw	30975839-30978776	**1429**	S6A_2-707o03.q1kw	32836042-32838492
556	S6C_2-512e02.q1kw	30978723-30981078	**1430**	S6C_3-155c20.q1kw	32838552-32841749
557	S6C_2-468h02.q1kw	30981054-30983803	**1431**	S6C_2-89c13.q1kkw	32840973-32843392
558	S6C_2-357h14.p1kw	30982938-30985380	**1432**	S6A_2-213h05.p1k	32843585-32846054
559	S6C_3-163g12.q1kw	30985302-30988517	**1433**	S6A_2-76a06.p1kk	32845054-32847632
560	S6A_2-539d10.p1kw	30988302-30990472	**1434**	S6C_3-121l19.p1kw	32847268-32850579
561	6S17_2-689o12.q1ka	30989831-30991848	**1435**	S6C_2-533e13.p1kw	32850451-32852327
562	6S17_2-577d11.q1kw	30991536-30994461	**1436**	6S17_2-416a11.p1kw	32852839-32854860
563	S6A_2-593o01.p1kw	30994321-30996758	**1437**	S6C_2-13i19.p1kkw	32854944-32857422
564	6S17_2-297a07.q1kw	30996377-30998924	**1438**	S6A_2-537m15.q1kw	32857226-32859895
565	S6A_3-56b12.q1kw	30997729-31000789	**1439**	S6A_2-495n14.q1kw	32859507-32861730
566	S6C_2-65d23.p1kkw	31000783-31003351	**1440**	S6C_2-8b06.q1k1kw	32861678-32864080
567	S6A_2-308g24.q1k	31003193-31004700	**1441**	6S17_2-4l02.p1kkkw	32864146-32866475
568	S6C_3-155k10.q1kw	31005130-31008143	**1442**	S6A_2-358a03.q1kw	32866691-32868526
569	6S17_2-210i20.p1kw	31008066-31011171	**1443**	S6A_2-71k05.q1kk	32868718-32871367
570	S6A_2-395o17.p1kw	31010755-31013344	**1444**	S6C_2-29d18.p1kkw	32870242-32872810
571	S6C_2-173a10.q1kw	31012161-31014603	**1445**	6S17_2-707a20.q1kw	32872192-32874816
572	S6C_2-461d02.q1kw	31014145-31016926	**1446**	S6C_2-491n17.p1kw	32875022-32877556
573	6S17_2-261e17.q1kw	31016455-31019006	**1447**	S6C_2-73f13.q1kkw	32877232-32879913
574	S6A_2-249k15.q1k	31018945-31021138	**1448**	6S17_2-792p12.p1kw	32879848-32882714
575	S6C_2-106h13.p1kw	31021804-31024362	**1449**	6S17_2-443g24.q1kw	32882666-32885237
576	6S17_2-283h21.q1kw	31023710-31026101	**1450**	6S17_2-489m04.q1ka	32884378-32888315
577	6S17_2-134i19.q1k	31024896-31027536	**1451**	S6A_2-200a10.q1k	32888310-32890611
578	S6C_2-740c20.p1kw	31026926-31029099	**1452**	6S17_2-304j21.q1kw	32890054-32892994
579	S6A_2-122k18.p1k	31028955-31031073	**1453**	S6A_2-219n19.p1k	32892523-32894937
580	S6C_2-24m19.q1kkw	31030830-31033294	**1454**	S6C_2-169h15.p1kw	32894483-32897025
581	6S17_2-552l08.p1kw	31033285-31035132	**1455**	S6C_2-534m22.q1kw	32896974-32899399
582	S6A_2-496n10.p1kw	31035757-31037977	**1456**	6S17_2-196p14.p1kw	32899374-32902066
583	S6A_2-534k20.q1kw	31037242-31039423	**1457**	S6A_2-259p07.q1k	32902016-32904527
584	6S17_2-408d05.p1kw	31039751-31042033	**1458**	S6C_2-573h06.p1kw	32904298-32906120
585	S6A_2-123l03.q1k	31041930-31044323	**1459**	6S17_2-522h15.q1kw	32906204-32908888
586	S6C_2-529h12.q1kw	31044408-31046885	**1460**	S6C_2-404f09.q1kw	32907983-32909931

587	S6A_3-82n18.q1kw	31046807-31049652	**1461**	S6C_2-6b19.p1k1kw	32910640-32913557
588	S6A_2-476f07.p1kw	31049352-31051490	**1462**	S6A_2-479e19.p1kw	32913256-32915385
589	S6C_2-551p22.q1kw	31051409-31054038	**1463**	6S17_2-343c16.q1kw	32915489-32918330
590	S6A_2-69a11.p1kk	31054143-31056020	**1464**	S6A_2-571b17.p1kw	32918067-32920344
591	6S17_2-496g08.p1ka	31056157-31059172	**1465**	S6C_2-269a07.p1kw	32920051-32922458
592	S6C_2-479l10.q1kw	31058865-31061226	**1466**	S6A_2-55j07.q1k	32922257-32924623
593	6S17_2-596e13.q1kw	31061209-31064176	**1467**	S6C_2-422a24.p1kw	32924311-32926079
594	6S17_2-243k16.q1kw	31063977-31066740	**1468**	S6A_2-155a02.q1k	32926466-32928563
595	S6C_2-242b22.q1kw	31065740-31067506	**1469**	S6A_3-29p07.q1kw	32928521-32931366
596	6S17_2-747l02.p1kw	31067896-31070375	**1470**	6S17_2-558e05.p1kw	32931156-32933975
597	6S17_2-111i04.p1k	31070293-31072989	**1471**	S6A_2-366i02.q1k	32934213-32936868
598	6S17_2-41o02.p1kkw	31072846-31075764	**1472**	S6C_2-547g05.q1kw	32936770-32939729
599	S6C_2-109j07.q1kw	31075593-31078313	**1473**	S6A_3-27o21.q1kw	32939311-32941270
600	6S17_2-601c01.p1kw	31077774-31080614	**1474**	S6A_2-19j15.q1k	32941867-32944276
601	6S17_2-553i03.p1kw	31080722-31083306	**1475**	S6A_2-626a17.q1kw	32944237-32946032
602	S6A_2-628k06.p1kw	31082951-31085201	**1476**	S6C_2-582n10.p1kw	32946350-32948854
603	S6A_2-341o10.q1kw	31085463-31087839	**1477**	S6A_2-312i15.p1k	32948866-32951226
604	S6A_2-540a21.q1kw	31087638-31089814	**1478**	6S17_2-651c07.p1kw	32951208-32953571
605	6S17_2-174j09.q1kw	31089661-31092148	**1479**	6S17_2-404o22.q1kw	32953922-32956499
606	6S17_2-277m11.q1kw	31092038-31094660	**1480**	S6C_2-573p22.q1kw	32956699-32959028
607	S6A_3-27m20.p1kw	31094594-31096414	**1481**	6S17_2-425m20.q1kw	32959057-32961622
608	S6A_2-268j06.p1k	31095892-31098083	**1482**	6S17_2-94f17.q1kk	32961629-32963697
609	S6A_2-31c13.q1k	31098259-31100652	**1483**	S6C_2-357m13.p1kw	32962761-32965294
610	6S17_2-575h02.p1kw	31100296-31102131	**1484**	6S17_2-294f12.p1kw	32964422-32967273
611	S6C_2-750m13.q1kw	31102983-31105539	**1485**	S6C_2-335p04.q1kw	32967276-32969811
612	S6A_2-376g17.q1kw	31105233-31107465	**1486**	S6A_2-176g05.p1kw	32968550-32971099
613	6S17_2-512n05.q1ka	31107406-31110072	**1487**	S6C_2-70m16.q1kkw	32970390-32972719
614	S6C_2-175l08.p1kw	31110005-31112753	**1488**	S6C_2-309c03.p1kw	32972559-32975260
615	S6C_2-169c05.q1kw	31112554-31114212	**1489**	S6A_2-136a23.p1kw	32974464-32976746
616	S6A_2-427l24.q1kw	31114131-31116679	**1490**	S6A_2-57j17.q1k	32975782-32978196
617	S6A_2-442i22.q1kw	31116594-31118888	**1491**	S6C_2-742h15.q1kw	32977812-32980308
618	6S17_2-676f20.q1ka	31118993-31121827	**1492**	S6C_2-590p08.p1kw	32980467-32982978
619	6S17_2-463g01.q1kw	31121775-31124316	**1493**	S6C_2-679j03.p1kw	32982897-32985460
620	S6C_2-633n10.p1kw	31124153-31125955	**1494**	S6A_2-210c03.q1k	32985131-32987586
621	S6C_3-165b01.p1kw	31126422-31128177	**1495**	6S17_2-339j05.p1kw	32987255-32990019
622	S6C_2-313m18.p1kw	31128920-31131593	**1496**	S6C_2-295g24.p1kw	32989946-32992530
623	6S17_2-792n19.p1kw	31131448-31133355	**1497**	S6A_2-63j13.p1kk	32992393-32994837
624	S6A_2-501b06.q1kw	31133473-31135674	**1498**	S6C_2-107e13.p1kw	32994469-32996313
625	6S17_2-600c14.p1kw	31135453-31137997	**1499**	6S17_2-175o05.q1kw	32997141-32999893
626	S6A_2-691h12.q1kw	31137718-31140234	**1500**	S6A_2-341a24.q1kw	32999284-33001846
627	S6A_2-408i17.p1kw	31140067-31142747	**1501**	6S17_2-223h03.q1kw	33001360-33003153
628	S6C_2-402f15.p1kw	31142605-31145077	**1502**	S6A_2-703i01.q1kw	33003704-33006056
629	6S17_2-745c05.p1kw	31144549-31147311	**1503**	6S17_2-83m04.p1kk	33006053-33008988
630	S6A_2-443h18.p1kw	31147190-31149630	**1504**	S6C_2-309p12.q1kw	33008444-33010878
631	S6A_2-101p17.p1k	31149238-31151456	**1505**	6S17_2-106c06.p1k	33010869-33013520
632	S6A_2-487i01.q1kw	31151512-31153971	**1506**	6S17_2-555m24.q1kw	33013335-33016294
633	S6A_2-360c02.q1kw	31154147-31156644	**1507**	S6A_2-99j22.q1kk	33015774-33018132
634	S6A_2-29m22.p1kk	31156634-31159116	**1508**	6S17_2-356a13.q1kw	33017693-33020170
635	6S17_2-165i03.p1kw	31159096-31161573	**1509**	6S17_2-227c12.q1kw	33018847-33021797

636	S6C_2-733n22.q1kw	31161570-31164239	**1510**	6S17_2-118i14.q1k	33020486-33022969
637	S6C_2-161h08.q1kw	31163833-31165694	**1511**	S6C_2-552a10.p1kw	33022966-33025488
638	S6C_2-657k11.q1kw	31164441-31167208	**1512**	6S17_2-579l12.p1kw	33025410-33027740
639	S6C_2-106p24.q1kw	31167061-31169514	**1513**	S6A_3-73k11.q1kw	33027231-33028946
640	S6C_2-634b11.q1kw	31169525-31171268	**1514**	S6C_2-760m04.q1kw	33030142-33032566
641	6S17_2-63f24.p1kkw	31171953-31174307	**1515**	S6A_2-473a20.p1kw	33032205-33034703
642	S6C_2-15l14.p1kkw	31174122-31176523	**1516**	S6A_2-739h02.q1kw	33034370-33036962
643	S6A_2-404g15.p1kw	31176621-31179067	**1517**	S6A_2-155n22.q1k	33037346-33039646
644	6S17_2-560h24.p1kw	31179183-31181276	**1518**	S6C_2-157p13.p1kw	33039760-33042545
645	S6A_2-726a13.q1kw	31181088-31183032	**1519**	6S17_2-475p23.q1kw	33042434-33045220
646	S6A_2-443n17.p1kw	31183472-31186095	**1520**	S6A_2-738e03.q1kw	33045191-33047466
647	6S17_2-154o06.q1kw	31185615-31188154	**1521**	6S17_2-408b06.p1kw	33047336-33050005
648	S6C_2-422j01.q1kw	31188134-31190923	**1522**	S6C_2-586p10.p1kw	33049800-33052268
649	6S17_2-388e15.q1kw	31189938-31192798	**1523**	6S17_2-164j19.p1kw	33051852-33053947
650	6S17_2-47d01.q1kkw	31192661-31195203	**1524**	6S17_2-768m02.p1kw	33054039-33055840
651	S6A_2-243n07.p1k	31194823-31197212	**1525**	6S17_2-135p02.q1k	33056054-33058064
652	6S17_2-206a13.q1kw	31197046-31199199	**1526**	6S17_2-414i03.q1kw	33057816-33060600
653	S6C_2-255j16.q1kw	31199321-31201771	**1527**	6S17_2-207h21.q1kw	33060224-33062639
654	S6C_2-392b12.q1kw	31200232-31202762	**1528**	S6C_2-639i04.q1kw	33062605-33065206
655	S6A_2-52c15.q1k	31202242-31204477	**1529**	S6C_2-110e10.q1kw	33065138-33067726
656	S6C_2-167b21.p1kw	31204152-31205988	**1530**	S6A_2-737e23.q1kw	33067567-33070137
657	S6A_2-714f14.p1kw	31205879-31208097	**1531**	S6C_2-518p08.q1kw	33070011-33072400
658	S6C_2-399m23.q1kw	31208146-31210054	**1532**	6S17_2-217b20.q1kw	33072257-33074313
659	S6A_2-669e08.q1kw	31210638-31213069	**1533**	6S17_2-681n12.p1kw	33074648-33077274
660	S6A_2-622e10.p1kw	31212921-31215388	**1534**	S6C_2-512f05.p1kw	33077075-33079961
661	S6A_2-701o19.p1kw	31214656-31216338	**1535**	S6C_2-109m03.p1kw	33079784-33082134
662	S6C_2-648k13.p1kw	31216802-31219415	**1536**	S6A_2-203l11.q1k	33082017-33084690
663	S6A_2-453m14.p1kw	31218410-31220616	**1537**	S6C_2-674e02.q1kw	33084323-33086976
664	S6A_2-236p08.q1k	31220446-31222717	**1538**	S6C_2-549e16.q1kw	33086287-33088714
665	S6C_3-155l19.p1kw	31222362-31224372	**1539**	6S17_2-320l11.q1kw	33087937-33091006
666	S6A_2-413e05.q1kw	31223806-31226366	**1540**	S6C_2-249g19.q1kw	33090674-33093215
667	S6A_3-28b01.q1kw	31225916-31227687	**1541**	6S17_2-485b11.q1kw	33092818-33095473
668	6S17_2-109h09.p1k	31228175-31230000	**1542**	S6A_2-51e24.p1k	33095115-33096836
669	S6A_2-63n06.q1kk	31230075-31232289	**1543**	S6A_2-113b04.q1k	33097613-33099941
670	S6C_2-545i11.q1kw	31232418-31234768	**1544**	6S17_2-789m03.q1kw	33099436-33102011
671	S6A_2-244j06.q1k	31234150-31236355	**1545**	6S17_2-806o23.p1kw	33101501-33103579
672	S6C_2-299a09.p1kw	31236895-31239353	**1546**	S6C_2-493j16.p1kw	33104021-33106350
673	6S17_2-151c03.p1kw	31239086-31242153	**1547**	S6C_2-107k04.p1kw	33106390-33108236
674	6S17_2-234o12.q1kw	31240879-31243323	**1548**	S6C_2-703o23.p1ka	33107152-33109639
675	S6A_3-62p09.p1kw	31243178-31246367	**1549**	S6A_2-243e06.p1k	33109482-33111869
676	6S17_2-205b19.q1kw	31245969-31248699	**1550**	6S17_2-747n05.q1kw	33112049-33114719
677	6S17_2-744m17.p1kw	31248662-31251239	**1551**	S6C_2-365m07.q1kw	33113667-33116173
678	6S17_2-131o19.q1k	31250863-31253884	**1552**	S6A_2-272a11.p1k	33115900-33118153
679	S6A_2-523g07.p1kw	31253774-31256044	**1553**	S6C_2-236e05.p1kw	33117354-33120123
680	S6A_2-37f08.q1kk	31256049-31258433	**1554**	6S17_2-96g02.p1kk	33119492-33121227
681	6S17_2-262d14.p1kw	31258475-31261419	**1555**	S6A_2-673f06.p1kw	33121204-33123602
682	6S17_2-202c02.p1kw	31261110-31263621	**1556**	S6A_2-458p15.q1kw	33123473-33125541
683	6S17_2-209o15.p1kw	31262795-31265512	**1557**	6S17_2-537g22.p1ka	33125489-33127433
684	S6C_2-509p24.q1kw	31265504-31267886	**1558**	S6A_2-534n13.q1kw	33128270-33130623

685	6S17_2-249o01.q1kw	31267843-31270674	**1559**	S6A_2-29i03.p1kk	33130078-33132394
686	6S17_2-363i22.p1kw	31270669-31273172	**1560**	S6A_2-135h18.p1kw	33132309-33134479
687	6S17_2-457g21.p1kw	31272355-31275387	**1561**	S6A_2-317b17.q1k	33133928-33138288
688	S6A_2-635f19.p1kw	31275343-31277509	**1562**	S6C_2-647g11.q1kw	33138219-33141006
689	S6C_2-218i07.p1kw	31277684-31280326	**1563**	6S17_2-618j17.q1kw	33141083-33142900
690	S6C_2-191e11.p1kw	31279197-31281009	**1564**	6S17_2-124e21.q1k	33142984-33145436
691	6S17_2-659l11.q1ka	31282010-31284107	**1565**	S6A_2-693p14.p1kw	33144119-33146299
692	S6C_3-133b12.q1kw	31285006-31288198	**1566**	S6C_2-495l17.p1kw	33146226-33148958
693	S6A_2-517f09.p1kw	31288155-31290534	**1567**	S6C_2-261i05.q1kw	33148418-33151260
694	S6C_2-184k17.q1kw	31290270-31293226	**1568**	6S17_2-77b10.q1kkw	33150708-33153101
695	6S17_2-106j08.p1k	31292775-31295165	**1569**	S6C_2-296n21.p1kw	33152888-33155357
696	6S17_2-284a02.q1kw	31295127-31297047	**1570**	6S17_2-190j14.q1kw	33155406-33158145
697	6S17_2-806m20.p1kw	31297137-31298930	**1571**	6S17_2-250c19.q1kw	33157976-33160566
698	6S17_2-304j16.q1kw	31299583-31302103	**1572**	S6A_2-594m04.q1kw	33159764-33161477
699	S6A_2-672b02.p1kw	31302095-31304664	**1573**	stSG1159389	33161371-33162818
700	6S17_2-762l22.p1kw	31304652-31307456	**1574**	6S17_2-109l12.p1k	33162178-33164006
701	S6C_2-84b09.p1kkw	31306864-31309399	**1575**	S6C_2-220g01.p1kw	33163960-33166516
702	S6C_2-291f21.q1kw	31309154-31310921	**1576**	S6A_2-269p11.p1k	33166439-33168753
703	6S17_2-411o22.p1kw	31311254-31313868	**1577**	S6A_2-553k12.p1kw	33168409-33170259
704	6S17_2-251i18.p1kw	31313866-31315916	**1578**	S6A_2-215a19.q1k	33169768-33172038
705	S6C_2-136n04.p1kw	31315627-31318295	**1579**	S6C_2-741o21.p1kw	33171878-33174286
706	6S17_2-568i13.p1kw	31317159-31321576	**1580**	S6C_2-513a18.q1kw	33174199-33176819
707	S6A_2-323m06.p1k	31321337-31323848	**1581**	S6A_2-256b09.p1k	33176769-33178915
708	S6A_2-80h01.p1kk	31323764-31326217	**1582**	6S17_2-143c10.q1kw	33179389-33182056
709	S6C_2-64d13.q1kkw	31325778-31328534	**1583**	S6A_2-269g05.p1k	33182207-33184791
710	S6A_3-85a12.p1kw	31328363-31331256	**1584**	S6C_2-560c24.p1kw	33184714-33187171
711	6S17_2-428p01.p1kw	31331246-31333604	**1585**	S6A_2-200e21.p1k	33187152-33188915
712	S6C_2-574b21.q1kw	31333527-31335887	**1586**	S6C_2-333e17.q1kw	33190199-33192634
713	6S17_2-641j16.p1kw	31335975-31338861	**1587**	6S17_2-705l03.q1ka	33192620-33193912
714	6S17_2-467o10.q1kw	31338592-31340579	**1588**	6S17_2-806h02.p1kw	33194560-33196721
715	S6A_2-89n04.p1kk	31340738-31342871	**1589**	6S17_2-45m23.q1kkw	33196915-33199698
716	S6C_2-414g11.q1kw	31343087-31345560	**1590**	S6C_2-760k02.p1kw	33198578-33201144
717	S6A_2-447o17.q1kw	31345147-31347528	**1591**	6S17_2-685o15.p1ka	33201104-33203350
718	S6C_2-100k04.p1kw	31347352-31349944	**1592**	S6A_2-564p14.p1kw	33203545-33205377
719	S6C_2-242e22.q1kw	31349918-31352712	**1593**	6S17_2-174o15.p1kw	33205658-33208356
720	6S17_2-646n05.q1kw	31352523-31355086	**1594**	6S17_2-704j05.q1ka	33208179-33210083
721	S6A_2-753n21.p1kw	31354494-31357371	**1595**	S6A_2-42f12.p1k	33210173-33212682
722	S6A_2-11m01.q1k	31356275-31358547	**1596**	S6A_2-551o02.p1kw	33211780-33213487
723	S6A_2-146n23.q1k	31358328-31360082	**1597**	S6A_2-62g11.q1k	33213814-33215866
724	6S17_2-642d20.q1kw	31360825-31362921	**1598**	S6A_2-97b07.q1kk	33215866-33218460
725	6S17_2-597a10.p1kw	31362788-31365470	**1599**	S6A_2-629l11.q1kw	33217907-33219670
726	S6A_2-579i17.q1kw	31365145-31367681	**1600**	6S17_2-690m19.p1kw	33219995-33222707
727	S6A_2-151a18.p1k	31367358-31369739	**1601**	S6C_2-173c11.p1kw	33222660-33225492
728	S6C_2-328g03.q1kw	31369850-31372247	**1602**	S6C_2-562a24.q1kw	33225441-33227983
729	S6C_2-118e16.p1kw	31372023-31374900	**1603**	S6C_2-464m12.q1kw	33227950-33230409
730	6S17_2-539d20.p1kw	31373910-31376551	**1604**	6S17_2-599d16.p1kw	33230323-33232862
731	S6A_3-76a07.q1kw	31376096-31377899	**1605**	S6C_2-188n16.q1kw	33232836-33235623
732	6S17_2-132e21.q1k	31377505-31380155	**1606**	S6A_2-623p03.q1kw	33236058-33238366
733	S6A_2-527e19.q1kw	31379976-31382140	**1607**	6S17_2-436l23.p1kw	33238447-33240806

734	6S17_2-114e12.p1k	31381877-31384179	**1608**	6S17_2-378a20.q1kw	33240701-33243474
735	6S17_2-560n07.q1kw	31383618-31385658	**1609**	6S17_2-472j14.p1kw	33242318-33244782
736	6S17_2-684m23.q1kw	31385692-31388400	**1610**	6S17_2-699o21.q1kw	33244158-33246922
737	S6A_3-10p04.q1kw	31387943-31390679	**1611**	S6A_2-495p21.p1kw	33246190-33248772
738	6S17_2-604m07.q1kw	31389893-31392559	**1612**	S6C_2-322l01.q1kw	33248190-33249957
739	S6A_2-393k13.p1kw	31392265-31394713	**1613**	S6C_2-173b04.q1kw	33250488-33252770
740	6S17_2-281f10.q1kw	31394279-31397156	**1614**	S6C_2-387b11.p1kw	33252634-33254951
741	S6C_2-127c21.p1kw	31397092-31399917	**1615**	S6C_2-476j16.p1kw	33255894-33258084
742	S6C_2-52a11.p1kkw	31399278-31403895	**1616**	S6C_2-523j21.p1kw	33258306-33261017
743	S6C_2-398j12.p1kw	31403562-31405377	**1617**	S6A_2-33i07.p1k	33260428-33262435
744	S6C_2-41h09.p1kkw	31405420-31408180	**1618**	S6C_2-239d21.q1kw	33262162-33264179
745	6S17_2-556c06.p1kw	31407745-31410625	**1619**	6S17_2-349p20.p1kw	33263540-33266027
746	S6A_2-205l16.p1k	31410312-31412594	**1620**	S6A_2-718o10.q1kw	33265657-33267969
747	S6C_2-525h16.q1kw	31410804-31413338	**1621**	S6C_2-547n02.p1kw	33267769-33270333
748	S6A_2-583l01.q1kw	31413230-31416000	**1622**	6S17_2-605c04.p1ka	33270548-33273058
749	S6A_3-69h21.q1k	31415829-31418487	**1623**	S6C_2-619j20.q1kw	33272867-33275324
750	S6A_2-229o17.p1k	31417219-31419500	**1624**	S6A_2-8k14.p1k	33274525-33276622
751	S6C_2-315o12.q1kw	31419326-31421777	**1625**	S6A_2-575c03.q1kw	33276854-33279042
752	S6C_2-686e07.q1kw	31421730-31424152	**1626**	S6C_2-141a12.p1kw	33279164-33281784
753	6S17_2-489c22.p1ka	31423462-31425292	**1627**	S6C_3-128c17.q1kw	33281188-33283958
754	S6A_2-697o17.p1kw	31425276-31427539	**1628**	6S17_2-355a04.p1kw	33283836-33286387
755	S6C_2-328g10.p1kw	31427156-31429633	**1629**	S6C_2-551e11.p1kw	33286034-33288603
756	S6C_2-448h13.q1kw	31429070-31431658	**1630**	S6A_2-263p12.q1k	33288292-33290935
757	S6C_2-437h19.p1kw	31431405-31434315	**1631**	S6C_2-417b17.p1kw	33289579-33292051
758	S6A_2-523o03.p1kw	31433998-31436656	**1632**	S6C_2-63h24.q1kkw	33292021-33293767
759	6S17_2-683e04.p1kw	31435990-31438961	**1633**	S6C_2-494i08.p1kw	33294111-33296809
760	S6C_2-433f21.p1kw	31438478-31440903	**1634**	S6A_2-373b05.q1kw	33296228-33297864
761	S6A_2-180o24.p1k	31441096-31443372	**1635**	S6C_2-667p14.q1kw	33298375-33301049
762	S6A_2-596o19.p1kw	31442467-31444925	**1636**	S6C_2-64k23.q1kkw	33300951-33303804
763	S6A_2-304h03.p1k	31444860-31447238	**1637**	S6C_2-212b13.q1kw	33303485-33305809
764	6S17_2-642p02.p1kw	31447054-31449127	**1638**	6S17_2-563p18.q1kw	33305348-33308026
765	6S17_2-331p08.p1kw	31449326-31451794	**1639**	S6C_2-338c19.p1kw	33307247-33309867
766	6S17_2-30e24.p1kkw	31451728-31454419	**1640**	6S17_2-431d15.p1kw	33309748-33312124
767	S6C_2-84a09.p1kkw	31454436-31456982	**1641**	S6A_2-602d01.p1kw	33311515-33313909
768	S6C_2-545g21.q1kw	31456974-31459366	**1642**	S6A_2-122a05.p1k	33313472-33315325
769	S6A_2-553l01.p1kw	31459216-31461762	**1643**	S6A_2-363j09.q1kw	33315842-33317981
770	6S17_2-786k20.p1kw	31461623-31464713	**1644**	S6C_2-40n03.q1kkw	33318535-33321050
771	S6C_3-126a12.p1kw	31463966-31467008	**1645**	6S17_2-301i14.p1kw	33320016-33322458
772	S6C_3-114o20.p1k	31466903-31470124	**1646**	S6A_2-270o06.q1k	33322331-33324713
773	S6C_2-311i13.q1kw	31470091-31472561	**1647**	S6A_2-233i02.q1k	33324387-33326855
774	S6C_2-324h03.p1kw	31472505-31475307	**1648**	S6C_2-117k15.q1kw	33326481-33329320
775	S6C_2-2h19.p1k1kw	31474983-31477045	**1649**	6S17_2-760c09.p1kw	33328484-33331034
776	S6A_2-137n09.p1k	31477351-31479645	**1650**	S6C_2-250d23.p1kw	33331019-33333605
777	S6A_2-240h04.p1k	31479362-31481941	**1651**	S6C_2-352o04.p1kw	33333357-33335680
778	S6A_2-420i23.p1kw	31481894-31483829	**1652**	S6C_2-80j01.q1kkw	33335676-33338157
779	6S17_2-339f11.q1kw	31482771-31485215	**1653**	6S17_2-326i18.q1kw	33338315-33340658
780	6S17_2-431p03.q1kw	31485229-31487901	**1654**	6S17_2-356g24.q1kw	33340424-33343221
781	S6A_2-755o05.q1kw	31487731-31490992	**1655**	S6C_2-54g22.p1kkw	33343143-33345886
782	S6A_2-574h15.q1kw	31490983-31493112	**1656**	S6C_2-712a15.p1kw	33345817-33348484

783	S6A_3-71c12.q1k	31492606-31495592	**1657**	S6A_2-353i24.q1k	33348267-33350788
784	S6A_2-515h01.q1kw	31494840-31497029	**1658**	S6C_3-142p06.q1kw	33350713-33353847
785	S6C_2-462a18.q1kw	31496569-31498908	**1659**	6S17_2-470i24.p1kw	33352730-33355282
786	S6A_2-173a20.q1k	31498765-31501407	**1660**	S6C_2-450i05.p1kw	33355252-33357951
787	S6A_2-424b19.p1kw	31501428-31503919	**1661**	S6A_2-324b05.p1kw	33357745-33360383
788	S6A_2-263b12.p1k	31501672-31503750	**1662**	6S17_2-150j22.p1kw	33360060-33362545
789	6S17_2-421j19.p1kw	31505209-31507825	**1663**	S6C_2-212a02.q1kw	33362395-33365052
790	S6A_2-209i18.q1k	31507238-31509555	**1664**	6S17_2-685i13.p1ka	33365027-33366857
791	6S17_2-763n22.q1ka	31509279-31511644	**1665**	S6A_2-467m07.p1k	33366393-33368870
792	S6A_3-64a01.q1kw	31511491-31514354	**1666**	S6A_2-691m12.p1kw	33368638-33371042
793	S6A_2-152g09.p1kw	31513524-31515946	**1667**	6S17_2-106e19.p1k	33370646-33372739
794	S6A_2-415c09.q1kw	31515789-31518599	**1668**	S6C_2-440i18.q1kw	33372651-33375048
795	S6C_2-450h05.p1kw	31517732-31520447	**1669**	6S17_2-163a14.q1kw	33374801-33377421
796	S6A_2-211e08.p1k	31520143-31522818	**1670**	6S17_2-759b13.q1kw	33377380-33379900
797	S6A_2-195b05.p1k	31522428-31524251	**1671**	S6A_2-494k23.p1kw	33379710-33382163
798	S6A_2-29k22.q1kk	31524921-31527446	**1672**	6S17_2-240f19.p1kw	33381961-33384834
799	S6C_2-655b12.q1kw	31527486-31529675	**1673**	S6C_2-148n15.q1kw	33384751-33387417
800	6S17_2-165k08.q1kw	31529042-31534960	**1674**	6S17_2-205b08.p1kw	33387409-33389702
801	6S17_2-98g13.q1kk	31534938-31537493	**1675**	S6A_2-182a16.q1k	33389687-33392295
802	S6C_2-387j18.q1kw	31536940-31539145	**1676**	S6A_3-52b11.q1kw	33391099-33394400
803	S6A_2-112a20.p1k	31539384-31542372	**1677**	6S17_2-187k03.p1kw	33394268-33396753
804	6S17_2-704e03.p1ka	31541574-31544203	**1678**	S6C_3-118k06.q1k	33397103-33400166
805	S6C_2-323p21.q1kw	31544177-31546543	**1679**	S6C_3-100a24.p1kw	33400120-33401889
806	S6A_2-649c07.p1kw	31546522-31549182	**1680**	S6C_2-730m19.p1kw	33402283-33404883
807	S6C_2-331b01.p1kw	31548571-31550755	**1681**	6S17_2-65h12.p1kkw	33404647-33406909
808	S6A_2-480m10.p1kw	31551026-31552843	**1682**	S6A_3-31l21.p1kw	33406383-33409272
809	6S17_2-40d18.p1kkw	31553280-31555425	**1683**	S6C_2-185c06.p1kw	33409216-33411913
810	S6A_2-585h14.p1kw	31555714-31557747	**1684**	S6C_2-623j19.q1kw	33411226-33413741
811	S6A_2-285a02.q1k	31558217-31560371	**1685**	S6A_2-107f11.q1k	33413392-33416765
812	S6C_2-422p06.q1kw	31559795-31562434	**1686**	6S17_2-344g06.p1kw	33416544-33419346
813	S6A_2-245f06.p1k	31562288-31564901	**1687**	6S17_2-211f01.q1kw	33418703-33421177
814	6S17_2-516j14.p1kw	31564829-31567403	**1688**	6S17_2-17p09.p1kkw	33420924-33423511
815	S6C_2-497m03.p1kw	31567390-31569981	**1689**	S6C_2-37h08.q1kkw	33423446-33426238
816	S6C_2-165l22.q1kw	31569152-31571627	**1690**	S6A_2-143b07.p1kw	33425991-33428532
817	S6C_2-500e18.q1kw	31570582-31572998	**1691**	S6A_3-16n09.q1kw	33428168-33431405
818	6S17_2-461n18.p1kw	31572759-31575340	**1692**	S6A_2-341d02.q1kw	33431263-33433534
819	S6C_2-770h15.p1kw	31575231-31578232	**1693**	S6C_2-121d04.p1kw	33433496-33436132
820	S6A_2-335a24.q1kw	31578226-31580534	**1694**	S6C_2-642f18.q1kw	33435835-33438369
821	6S17_2-523h22.q1kw	31581123-31584021	**1695**	S6C_2-329k09.q1kw	33438295-33441008
822	S6A_2-5d19.p1k	31583533-31585907	**1696**	S6A_2-76k03.p1kk	33440884-33443383
823	S6A_2-64a13.q1kk	31586135-31588613	**1697**	S6A_3-68i20.p1k	33443201-33446017
824	S6C_2-207b20.p1kw	31588415-31591252	**1698**	6S17_2-719c10.p1kw	33445832-33448263
825	6S17_2-153a03.p1kw	31591171-31593942	**1699**	S6C_2-350f07.p1kw	33448064-33450859
826	S6A_2-602c13.q1kw	31593932-31596449	**1700**	S6A_2-188l24.p1k	33450625-33452501
827	S6C_2-530o15.p1kw	31595921-31598452	**1701**	S6A_2-62e18.p1k	33453010-33455403
828	6S17_2-792d24.q1kw	31598450-31601042	**1702**	6S17_2-72j09.q1kkw	33455266-33457876
829	S6A_3-58e13.p1kw	31600714-31603500	**1703**	S6C_2-605l03.q1kw	33457235-33459637
830	S6A_2-505f15.q1kw	31602298-31604502	**1704**	6S17_2-146i11.p1kw	33459300-33462283
831	S6A_2-415h04.q1kw	31604437-31607304	**1705**	S6C_2-420g20.q1kw	33462560-33465285

832	S6A_2-385h12.q1kw	31607131-31609387	**1706**	S6A_2-82k10.q1kk	33463903-33466555
833	6S17_2-18o11.p1kkw	31609652-31612281	**1707**	S6C_2-550k12.q1kw	33466498-33468984
834	S6A_2-611k13.p1kw	31612719-31614689	**1708**	S6C_2-437e15.q1kw	33469103-33471584
835	S6C_2-216a10.p1kw	31614898-31617590	**1709**	6S17_2-176l13.q1kw	33471362-33473730
836	S6A_2-172p21.q1k	31617564-31620016	**1710**	S6A_2-339j01.p1k	33473556-33475839
837	S6C_2-225p03.p1kw	31619220-31621528	**1711**	6S17_2-707d09.p1kw	33475862-33478335
838	6S17_2-238h24.p1kw	31621456-31623166	**1712**	S6A_2-527d21.q1kw	33478219-33480655
839	S6A_2-28p19.p1k	31624227-31626500	**1713**	S6C_2-321d06.q1kw	33480339-33482959
840	S6A_2-631l19.p1kw	31626425-31628785	**1714**	S6C_2-297j01.p1kw	33482783-33485490
841	S6A_2-203k21.p1k	31628748-31631153	**1715**	6S17_2-265n22.p1kw	33484055-33486337
842	6S17_2-428j05.q1kw	31630655-31633551	**1716**	S6C_2-476o22.p1kw	33486314-33488262
843	6S17_2-622j13.p1kw	31633077-31634986	**1717**	S6C_2-247m14.q1kw	33488661-33491053
844	S6C_2-682i12.p1kw	31635389-31637920	**1718**	S6C_2-707g09.p1kw	33490963-33493613
845	6S17_2-414a03.q1kw	31637916-31640706	**1719**	S6C_2-176n16.q1kw	33493246-33495524
846	6S17_2-43g16.q1kkw	31640554-31642280	**1720**	S6C_2-260l12.q1kw	33495473-33497978
847	S6A_2-526n02.p1kw	31641500-31644075	**1721**	6S17_2-62i20.q1kkw	33497634-33500208
848	S6C_2-205e06.q1kw	31643852-31646335	**1722**	S6A_2-222f12.q1k	33498741-33500976
849	S6A_2-550c18.p1kw	31647311-31649827	**1723**	6S17_2-537l09.p1ka	33501985-33503886
850	S6C_2-591j16.q1kw	31649837-31652271	**1724**	S6C_2-232h16.p1kw	33503008-33505329
851	6S17_2-558f04.p1kw	31651482-31654336	**1725**	S6A_2-588i03.q1kw	33504498-33506676
852	S6C_2-377j17.p1kw	31653977-31656641	**1726**	6S17_2-304k12.q1kw	33506716-33509202
853	6S17_2-283o09.p1kw	31656398-31658063	**1727**	S6C_2-267n12.q1kw	33509038-33511425
854	S6A_2-676b19.p1kw	31658687-31661288	**1728**	S6A_2-45a04.q1kk	33511328-33513089
855	S6A_2-294i05.q1k	31661214-31662958	**1729**	6S17_2-705p22.p1ka	33513248-33516058
856	6S17_2-63h20.p1kkw	31662312-31665020	**1730**	S6C_2-27o04.q1kkw	33515150-33517773
857	S6C_2-465p11.p1kw	31664610-31667272	**1731**	S6A_2-100j09.p1k	33518216-33520763
858	S6A_2-35c03.q1kk	31667243-31669668	**1732**	S6C_2-624p15.p1kw	33520343-33522986
859	S6C_2-18i18.p1kkw	31669661-31672263	**1733**	6S17_2-655j23.q1ka	33522488-33524201
860	S6C_2-96o12.q1kkw	31671730-31673485	**1734**	S6C_2-440i03.p1kw	33523883-33525523
861	6S17_2-677h04.p1ka	31673197-31676154	**1735**	S6A_2-182k21.q1k	33525617-33527854
862	S6C_2-696e10.p1kw	31676093-31678464	**1736**	6S17_2-397g03.p1kw	33528186-33530929
863	S6A_2-278l01.p1k	31678683-31681025	**1737**	S6C_2-417o08.q1kw	33529999-33532371
864	S6A_2-751a07.p1kw	31679841-31681916	**1738**	S6A_2-395c21.p1kw	33531720-33534078
865	S6C_2-649k23.p1kw	31682232-31685102	**1739**	S6A_2-3b11.q1k	33534211-33536223
866	S6C_2-380h19.p1kw	31684907-31687727	**1740**	6S17_2-483a04.q1kw	33536400-33539103
867	S6C_2-547i07.p1kw	31687714-31690387	**1741**	6S17_2-222m10.p1kw	33538830-33541653
868	6S17_2-203n20.q1kw	31689689-31692751	**1742**	S6C_2-182d13.q1kw	33541330-33543791
869	S6C_3-101m14.q1kw	31691844-31694777	**1743**	S6C_2-334e12.q1kw	33543877-33546708
870	S6A_2-694n21.p1kw	31694041-31696414	**1744**	6S17_2-713p24.q1kw	33546168-33548761
871	S6A_2-52n07.p1k	31696264-31698456	**1745**	S6A_2-218f17.q1k	33547521-33549822
872	S6A_2-666b08.p1kw	31697728-31700057	**1746**	S6A_2-466c09.p1k	33549821-33552084
873	6S17_2-368a11.p1kw	31700030-31702827	**1747**	S6C_2-470m11.p1kw	33552081-33554763
874	S6C_2-628n07.p1kw	31702678-31705254			

Table 2.2. **Names and chromosome 6 coordinates (NCBI_35) of the clones used for the MHC tiling array**.

	CD8 v PLACENTA			
	Start.coord	End.coord	M	P.Value
1	30228982	30231712	0.653629	0.000611
	LIVER v PLACENTA			
	Start.coord	End.coord	M	P.Value
2	29889483	29892066	0.738334	0.000869
3	30491424	30493923	0.761044	0.000197
4	31709197	31711626	-0.872107	0.000162
5	32056738	32058031	-0.963175	8.14E-05
6	32067481	32068550	-0.714901	2.81E-05
7	32074474	32074660	-0.912389	3.39E-05
8	32077678	32079121	-0.978122	8.72E-06
9	32081199	32081780	-0.770113	0.00076
10	32090749	32092076	-0.811636	0.000459
11	32104734	32105602	-0.55281	0.000383
12	32107212	32107398	-1.117908	1.49E-08
13	32110416	32111859	-0.85967	1.67E-05
14	32590480	32591619	-0.958434	1.65E-05
	LIVER v CD8			
	Start.coord	End.coord	M	P.Value
15	30247370	30249040	0.813238	7.91E-06
16	30565890	30568365	0.635978	9.96E-05
17	32056738	32058031	-0.803751	0.000119
18	32067481	32068550	-0.654797	3.71E-05
19	32074474	32074660	-0.743694	0.000274
20	32077678	32079121	-0.919853	4.12E-05
21	32088718	32090526	-0.886511	0.000224
22	32107212	32107398	-0.831638	3.15E-07
23	32110416	32111859	-0.766263	3.65E-06
24	32590480	32591619	-0.619532	0.000469
25	33372651	33375048	-0.819691	1.98E-05
	LIVER v SPERM			
	Start.coord	End.coord	M	P.Value
26	29823989	29826356	0.65412	0.000573
27	30247370	30249040	1.555232	1.33E-07
28	30527803	30529467	0.894699	0.000198
29	30731648	30734384	1.458403	1.46E-08
30	30891136	30893651	0.798895	1.45E-05
31	31092038	31094660	0.867882	0.000286
32	31270669	31273172	0.7429	1.25E-05
33	31709197	31711626	-0.72996	0.000348
34	31803609	31806450	1.300837	0.000273
35	32020686	32023216	-1.222297	6.42E-05
36	32056738	32058031	-0.904856	1.59E-05
37	32067481	32068550	-0.762318	1.59E-05
38	32071709	32072864	-0.756704	1.40E-05
39	32073608	32074514	-0.71949	0.000216
40	32074474	32074660	-0.987143	5.42E-05
41	32077678	32079121	-1.333444	2.96E-09
42	32088659	32090434	-0.884048	0.000159
43	32092057	32093147	-0.82539	0.000796
44	32094350	32095101	-0.677409	0.000259
45	32098656	32099323	-0.730227	8.63E-05
46	32099573	32100214	-0.875286	4.03E-05
47	32104734	32105602	-0.713212	1.34E-05
48	32107212	32107398	-0.944333	1.47E-07
49	32109195	32110435	-0.770992	0.000114
50	32119000	32120024	-0.570658	0.000326
51	32590480	32591619	-0.95534	1.51E-06
52	32622631	32625110	0.658602	0.000744
53	32817677	32820582	0.844115	9.91E-06
54	32836042	32838492	1.38817	3.03E-06
55	33389687	33392295	1.15599	2.62E-06

	PLACENTA v SPERM			
	Start.coord	End.coord	M	P.Value
56	29937894	29939594	0.962559	0.00069976
57	30000805	30003606	0.898938	0.00059084
58	30228982	30231712	-0.744124	8.74E-05
59	30484481	30486798	-0.714068	0.00025428
60	30491424	30493923	-0.778861	9.83E-05
61	30526624	30528439	1.490191	6.55E-05
62	30534798	30537070	-0.911697	0.00026108
63	30731648	30734384	1.29065	3.22E-06
64	30881555	30884300	0.771825	0.00018371
65	30891136	30893651	0.853398	2.39E-05
66	31092038	31094660	0.82443	0.00090522
67	31270669	31273172	0.814419	1.19E-05
68	31454436	31456982	-0.553736	0.00091332
69	31841070	31843352	0.871871	0.00070662
70	32115381	32116535	-0.85392	0.00010511
71	32223988	32226638	0.943871	0.00025358
72	32836042	32838492	1.499562	1.61E-06
73	33132309	33134479	-0.987847	0.00050575
74	33389687	33392295	1.426845	1.69E-07
75	33450625	33452501	0.965143	0.00027171
	CD8 v SPERM			
	Start.coord	End.coord	M	P.Value
76	29823989	29826356	0.686032	0.00080629
77	29830203	29832660	0.802217	0.00065693
78	29937894	29939594	1.138717	0.0007233
79	30527803	30529467	0.898271	9.03E-05
80	30565890	30568365	-0.662875	9.24E-05
81	30721858	30724158	0.814142	0.00025511
82	30731648	30734384	1.364174	2.61E-06
83	30881555	30884300	0.63042	0.00042592
84	30891136	30893651	0.686268	8.80E-05
85	31270669	31273172	0.669456	5.03E-05
86	31803609	31806450	1.269115	0.00068925
87	32836042	32838492	1.729655	2.77E-07
88	33192620	33193912	0.771141	0.00075793
89	33389687	33392295	1.560515	3.74E-07
90	32659407	32660508	0.84688	0.00035068

Table 4.1 tDMRs within the MHC region. A total of 90 tDMRs were identified. Six pair-wise comparisons were performed and, in total, 90 tDMRs were identified using t-statistics. tDMRs of

each comparison and their co-ordinates on chromosome 6 are provided. M values which are equivalent to the $\log_2$ ratio of the two corresponding methylation profiles in each comparison are shown. A threshold of p-value <0.001 was used. P-values of the 90 tDMRs are provided.

Clone name	chromosome 6 coordinate (NCBI_35)	
6S17_2_149n23	30527803	30529467
6S17_2_213f19	30881555	30884300
6S17_2_580e24	29937894	29939594
6S17_2_705l03	33192620	33193912
S6A_2_188l24	33450625	33452501
S6A_2_367m01	31841070	31843352
S6A_2_454k03	30247370	30249040
S6A_2_48e04	32088718	32090526
S6A_2_50m21	29889483	29892066
S6A_2_707o03	32836042	32838492
S6C_2_161i01	30000805	30003606
S6C_2_310e17	30228982	30231712
S6C_2_736m04	30721858	30724158
S6C_3_122j09	30526624	30528439
stSG1159328	32079102	32080248
stSG1159349	32098656	32099323
stSG1159370	32115381	32116535
stSG1159388	36659407	32660508

Table 5.1 **DMRs common in both tDMR and pDMR screen.** A total of 18 DMRs identified in section 5.5.2 had been identified as tDMRs in chapter 4. These DMRs were removed from any further analysis for the pDMR screen (chapter 5).

Table 5.2

	CCRF-CEM				
	Clone Name	**Start**	**End**	**M-value**	**p-value**
1	mtp_S6C_2_295c12	29767842	29770217	-0.56719	0.0002804
2	stSG1159305	29799299	29800711	0.690492	4.07E-07
3	mtp_S6A_2_349p03	29852518	29854940	0.595634	0.0007958
4	mtp_6S17_2_523e17	29899083	29901168	0.598125	0.0007759
5	mtp_6S17_2_333l22	29908506	29911028	0.480597	0.0004993
6	mtp_S6A_2_427m23	29921905	29924681	0.416954	0.0005401
7	mtp_S6C_2_233b21	29952327	29954750	0.763758	0.0003412
8	mtp_S6C_2_252b19	30081271	30083717	0.994879	2.07E-05
9	mtp_S6A_2_302b02	30083166	30085450	0.738726	5.81E-06
10	mtp_S6C_2_651k20	30152988	30155591	0.688175	0.0004019
11	mtp_6S17_2_550d16	30178743	30181378	1.397924	1.10E-08
12	mtp_S6C_2_724m20	30243167	30246046	0.558438	0.0007535
13	mtp_6S17_2_432i09	30711444	30713962	-0.46115	0.000808
14	mtp_S6A_2_126l05	30763012	30765292	1.62006	2.00E-10
15	mtp_6S17_2_130a06	30958243	30959538	0.732888	1.50E-06

16	mtp_6S17_2_261e17	31016455	31019006	0.709016	3.54E-05
17	mtp_S6C_2_24m19	31030830	31033294	-0.42393	2.04E-05
18	mtp_6S17_2_641j16	31335975	31338861	0.807199	0.0001693
19	mtp_S6C_2_437h19	31431405	31434315	0.926176	7.47E-06
20	mtp_S6C_2_323p21	31544177	31546543	-0.66098	0.0003248
21	mtp_S6A_2_285a02	31558217	31560371	-0.46492	0.0006089
22	mtp_6S17_2_406p23	31765370	31767911	-0.37426	0.0003661
23	mtp_S6A_2_474a15	31801630	31803851	-0.55334	0.0006669
24	mtp_S6C_2_47j02	31830687	31833596	-0.65185	0.0003632
25	mtp_S6A_2_139f17	32238133	32240410	-0.46266	0.0003004
26	mtp_S6A_2_518p02	32404753	32407328	0.625894	0.0007431
27	mtp_S6A_3_52o24	32476215	32479059	-0.60195	0.0001485
28	mtp_6S17_2_455p07	32491122	32493607	0.667301	6.70E-05
29	mtp_S6C_2_291o13	32539196	32541992	-0.561	0.0003876
30	mtp_S6A_2_718o07	32605193	32606885	0.768783	4.42E-05
31	mtp_S6C_2_766n01	32733611	32736437	0.606751	0.0004482
32	mtp_6S17_2_707a20	32872192	32874816	-0.49818	0.0008148
33	mtp_6S17_2_304j21	32890054	32892994	0.814173	0.000167
34	mtp_S6A_3_29p07	32928521	32931366	0.837205	0.000581
35	mtp_S6A_2_366i02	32934213	32936868	-0.64186	0.0002129
36	mtp_6S17_2_118i14	33020486	33022969	1.241087	4.06E-07
37	mtp_S6C_2_512f05	33077075	33079961	-0.59716	0.0001125
38	mtp_S6C_2_495l17	33146226	33148958	1.064771	3.58E-05
39	mtp_S6C_2_261i05	33148418	33151260	1.14691	0.0002159
40	mtp_6S17_2_109l12	33162178	33164006	-0.67207	1.90E-05
41	mtp_S6C_3_128c17	33281188	33283958	0.57968	0.0009564
42	mtp_S6C_2_551e11	33286034	33288603	0.761003	0.0002226
43	mtp_S6A_2_353i24	33348267	33350788	0.630111	1.54E-05
44	mtp_S6C_2_420g20	33462560	33465285	0.69955	7.90E-05
45	mtp_S6C_2_437e15	33469103	33471584	-0.71327	5.05E-05
46	mtp_6S17_2_537l09	33501985	33503886	0.667891	0.0002164
	Colo-205				
	Clone Name	**Start**	**End**	**M-value**	**p-value**
47	mtp_S6A_2_126l05	30763012	30765292	1.21117	1.35E-08
48	mtp_6S17_2_118i14	33020486	33022969	1.326516	1.38E-08
49	mtp_6S17_2_577d11	30991536	30994461	-1.35874	2.84E-07
50	mtp_S6C_2_176n16	33493246	33495524	0.969393	3.85E-07
51	mtp_S6C_2_591j16	31649837	31652271	0.889856	1.26E-06
52	mtp_S6C_2_724m20	30243167	30246046	0.978553	2.24E-06
53	mtp_S6A_2_742g13	32710133	32712269	1.019544	3.51E-06
54	mtp_S6A_2_99j22	33015774	33018132	1.067542	5.12E-06
55	mtp_S6C_2_291o13	32539196	32541992	-0.81429	8.32E-06
56	mtp_S6A_3_29p07	32928521	32931366	1.142544	8.69E-06
57	mtp_S6C_2_525h16	31410804	31413338	-1.13893	8.94E-06
58	mtp_S6A_2_247f17	32609013	32611396	-0.74061	9.92E-06
59	mtp_6S17_2_75k18	30283371	30285180	-0.71881	1.59E-05
60	mtp_S6C_2_495l17	33146226	33148958	1.217834	1.73E-05
61	mtp_S6A_2_366o15	32203258	32205842	-1.07394	2.17E-05
62	mtp_S6C_2_256g20	29960874	29962955	0.687232	2.35E-05

63	mtp_S6C_2_494b13	32680961	32683760	0.621659	2.64E-05
64	mtp_6S17_2_304j21	32890054	32892994	1.080267	2.66E-05
65	mtp_6S17_2_163a14	33374801	33377421	-0.55412	3.12E-05
66	mtp_6S17_2_558f04	31651482	31654336	0.887192	4.93E-05
67	mtp_S6A_2_19j15	32941867	32944276	1.024239	5.56E-05
68	mtp_S6C_2_261i05	33148418	33151260	1.370677	7.68E-05
69	mtp_6S17_2_406p23	31765370	31767911	-0.5321	9.63E-05
70	mtp_S6C_2_728o04	31784795	31786680	-0.96111	9.87E-05
71	mtp_6S17_2_227c12	33018847	33021797	0.788601	0.0001023
72	mtp_6S17_2_537l09	33501985	33503886	0.615933	0.000138
73	mtp_6S17_2_461g23	30844326	30847065	-0.74669	0.0001416
74	mtp_S6A_2_550c18	31647311	31649827	0.816073	0.0002
75	mtp_6S17_2_333n04	32323976	32326426	-1.07325	0.000231
76	mtp_6S17_2_491n23	29863681	29866461	-1.14484	0.0002416
77	mtp_S6C_2_309c03	32972559	32975260	0.508227	0.0002526
78	stSG1159389	33161371	33162818	-0.6743	0.0002961
79	mtp_S6A_2_738e03	33045191	33047466	0.651116	0.0003096
80	mtp_S6A_2_155a02	32926466	32928563	0.659656	0.000343
81	mtp_6S17_2_150b10	31962270	31964146	-0.54269	0.0003518
82	mtp_S6C_2_323p21	31544177	31546543	-0.60766	0.0003693
83	mtp_S6C_2_468h02	30981054	30983803	-0.57288	0.0003835
84	mtp_S6C_2_106h13	31021804	31024362	0.434185	0.0003983
85	mtp_S6C_2_169c05	31112554	31114212	0.462286	0.0004366
86	mtp_S6A_2_593o01	30994321	30996758	-0.6159	0.0005327
87	mtp_6S17_2_705p22	33513248	33516058	-0.55752	0.000537
88	mtp_S6C_2_126m01	32689045	32691474	0.813405	0.0005809
89	mtp_6S17_2_689o12	30989831	30991848	-0.62209	0.0006024
90	mtp_6S17_2_503c16	32803977	32805579	0.797316	0.0006535
91	mtp_S6C_2_405j01	30476804	30479649	1.467248	0.0006538
92	mtp_S6A_2_401f24	31867881	31870208	-0.45313	0.0006707
93	mtp_S6A_2_495n14	32859507	32861730	1.215167	0.0007131
94	mtp_S6C_2_173a10	31012161	31014603	0.491818	0.0007713
95	mtp_6S17_2_355b09	32805771	32808229	0.736536	0.0008333
96	mtp_S6C_2_24m19	31030830	31033294	-0.36284	0.0008357
97	mtp_S6C_2_630p01	31849432	31852366	-0.76832	0.0009198
98	mtp_S6A_2_42g10	32222119	32224613	0.556036	0.0009527
99	mtp_6S17_2_77b10	33150708	33153101	0.83274	0.0009703
	H69				
	Clone Name	**Start**	**End**	**M-value**	**p-value**
100	mtp_S6A_2_617f24	30758534	30760818	1.81176	4.18E-09
101	mtp_S6A_2_126l05	30763012	30765292	1.228218	7.13E-09
102	mtp_6S17_2_109l12	33162178	33164006	-1.08565	1.21E-08
103	mtp_S6C_2_591j16	31649837	31652271	1.188759	2.58E-07
104	mtp_S6A_3_28g11	30818455	30821315	0.92168	5.53E-07
105	mtp_6S17_2_707a20	32872192	32874816	-1.00553	1.51E-06
106	mtp_6S17_2_124e21	33142984	33145436	-1.10912	1.58E-06
107	mtp_S6A_2_152g09	31513524	31515946	-0.94512	1.98E-06
108	mtp_6S17_2_278p22	32751956	32754798	0.959251	3.85E-06
109	mtp_S6A_2_353i24	33348267	33350788	1.087473	4.87E-06

110	mtp_S6C_2_754f14	32557020	32559661	-1.18712	8.06E-06
111	mtp_S6C_2_291o13	32539196	32541992	-0.73957	8.35E-06
112	mtp_6S17_2_558f04	31651482	31654336	0.953425	8.97E-06
113	mtp_6S17_2_522h15	32906204	32908888	-0.71227	1.31E-05
114	mtp_S6A_3_29p07	32928521	32931366	1.116248	1.70E-05
115	mtp_S6A_2_724m04	30350008	30351777	0.52074	2.68E-05
116	mtp_S6A_2_584b12	32736096	32738289	-1.24846	4.48E-05
117	mtp_S6C_2_323p21	31544177	31546543	-1.05423	5.82E-05
118	mtp_S6C_2_309c03	32972559	32975260	0.589118	7.68E-05
119	mtp_6S17_2_537l09	33501985	33503886	0.657134	8.15E-05
120	mtp_S6C_3_114o20	31466903	31470124	-0.78067	8.48E-05
121	mtp_S6C_2_599m10	32471036	32473567	-0.76463	8.70E-05
122	mtp_S6A_2_200a10	32888310	32890611	-1.44944	9.58E-05
123	mtp_6S17_2_579l12	33025410	33027740	1.150113	0.0001153
124	mtp_6S17_2_111f06	30134479	30136131	0.758627	0.0001167
125	mtp_S6A_2_485e09	30754016	30756025	0.779481	0.000131
126	mtp_S6A_2_245f06	31562288	31564901	-0.84827	0.0001339
127	mtp_S6A_2_247f17	32609013	32611396	-0.91501	0.0001496
128	stSG1159333	32083780	32085032	-0.52852	0.0001612
129	mtp_6S17_2_355b09	32805771	32808229	0.749548	0.0002615
130	mtp_6S17_2_34d21	30687802	30690256	0.817429	0.0002806
131	mtp_S6A_2_673h09	30034394	30036661	0.606668	0.0002892
132	mtp_S6C_2_35n12	31904599	31907111	-0.62012	0.0003299
133	mtp_6S17_2_172f10	31815961	31818685	0.63943	0.0003398
134	stSG1159311	31903338	31904796	-0.77202	0.0003435
135	mtp_6S17_2_227c12	33018847	33021797	0.599893	0.0003601
136	mtp_S6C_2_176n16	33493246	33495524	0.710887	0.0004165
137	mtp_S6C_2_525h16	31410804	31413338	-0.77281	0.0004209
138	mtp_S6A_2_755o05	31487731	31490992	-1.08131	0.0004368
139	stSG1159344	32094951	32095618	0.638461	0.0004405
140	mtp_S6A_2_607b18	31892543	31894559	-0.87294	0.0004616
141	mtp_S6C_2_494h24	32566224	32568770	0.857864	0.0004902
142	mtp_S6C_2_249g19	33090674	33093215	-0.83823	0.0005037
143	mtp_S6A_2_203l11	33082017	33084690	-1.03336	0.0005155
144	mtp_6S17_2_40d18	31553280	31555425	-0.70576	0.0005245
145	mtp_6S17_2_203n20	31689689	31692751	0.723136	0.0006501
146	mtp_S6C_2_567l15	32484275	32487774	-1.01229	0.0006631
147	mtp_S6A_3_77e12	30096934	30100100	0.56266	0.0006754
148	mtp_6S17_2_118i14	33020486	33022969	0.767671	0.0006897
149	mtp_S6A_2_693p14	33144119	33146299	-1.19236	0.0007169
150	mtp_S6C_2_551e11	33286034	33288603	0.719353	0.000776
151	mtp_6S17_2_283o09	31656398	31658063	0.78074	0.0007777
152	mtp_6S17_2_163a14	33374801	33377421	-0.5063	0.0008214
153	mtp_S6A_2_365l07	30756515	30758800	0.560907	0.0008969
154	mtp_S6C_2_24m19	31030830	31033294	-0.39812	0.0009504
	MDA-MB-231				
	Clone Name	**Start**	**End**	**M-value**	**p-value**
155	mtp_S6A_2_126l05	30763012	30765292	1.18811	8.13E-08
156	mtp_S6C_2_591j16	31649837	31652271	1.201073	1.10E-07

157	mtp_S6C_2_495l17	33146226	33148958	1.301633	6.97E-07
158	mtp_6S17_2_118i14	33020486	33022969	1.428598	1.30E-06
159	mtp_6S17_2_227c12	33018847	33021797	0.972723	2.94E-06
160	mtp_6S17_2_111f06	30134479	30136131	0.894931	4.03E-06
161	mtp_6S17_2_707l19	31995564	31998405	0.594004	2.85E-05
162	mtp_6S17_2_558f04	31651482	31654336	0.892191	3.20E-05
163	mtp_S6A_2_200e21	33187152	33188915	0.722338	3.66E-05
164	mtp_S6C_2_261i05	33148418	33151260	1.261192	4.43E-05
165	mtp_S6C_2_176n16	33493246	33495524	0.847578	4.59E-05
166	mtp_S6C_2_291o13	32539196	32541992	-0.55691	4.64E-05
167	mtp_6S17_2_304j21	32890054	32892994	1.032476	5.42E-05
168	mtp_S6C_2_295c12	29767842	29770217	-0.65879	5.82E-05
169	mtp_S6A_3_29p07	32928521	32931366	1.000062	5.92E-05
170	mtp_S6C_2_63h24	33292021	33293767	-1.0433	6.56E-05
171	mtp_S6A_2_19j15	32941867	32944276	0.791763	7.30E-05
172	mtp_6S17_2_337o24	30903401	30906093	0.486788	0.0001157
173	mtp_S6C_2_651k20	30152988	30155591	0.692531	0.0001259
174	mtp_S6A_2_593o01	30994321	30996758	-0.56731	0.0001529
175	mtp_S6A_2_617f24	30758534	30760818	0.991063	0.0001707
176	mtp_S6A_2_572p22	31854646	31857207	-0.76015	0.0002103
177	mtp_6S17_2_579l12	33025410	33027740	1.01135	0.00025
178	mtp_S6C_2_296n21	33152888	33155357	0.638952	0.0002898
179	mtp_S6C_2_242j03	30825368	30827875	-0.65592	0.0003419
180	mtp_S6A_3_59l07	30555778	30557696	0.513929	0.0003455
181	mtp_S6A_2_724m04	30350008	30351777	0.550353	0.0003629
182	mtp_6S17_2_747l02	31067896	31070375	-0.67933	0.0004386
183	mtp_6S17_2_283o09	31656398	31658063	0.814487	0.0004443
184	mtp_6S17_2_203n20	31689689	31692751	0.688619	0.0005062
185	mtp_S6C_2_242e07	29814777	29817114	0.555024	0.0005125
186	mtp_S6A_2_403c13	30433512	30435982	0.927802	0.0005354
187	mtp_6S17_2_355b09	32805771	32808229	0.550376	0.0006068
188	stSG1159306	29823382	29824715	-0.45434	0.0006593
189	mtp_S6A_2_203l11	33082017	33084690	-0.52996	0.0006766
190	mtp_S6A_2_99j22	33015774	33018132	0.837434	0.0008397
191	mtp_6S17_2_749c22	30583516	30586461	0.49832	0.0008852
192	mtp_S6A_2_268j06	31095892	31098083	-0.53211	0.0008925
193	mtp_S6A_2_71a13	29929108	29931705	0.466542	0.0009068
194	mtp_S6C_2_437h19	31431405	31434315	0.66889	0.0009391
195	mtp_S6C_2_119a05	30345571	30347925	0.594424	0.000967
	MDA-MB-361				
	Clone Name	**Start**	**End**	**M-value**	**p-value**
196	mtp_6S17_2_118i14	33020486	33022969	1.524417	1.48E-08
197	mtp_S6A_2_617f24	30758534	30760818	1.589697	2.06E-08
198	stSG1159381	32628159	32629647	1.212893	8.84E-08
199	mtp_S6A_2_126l05	30763012	30765292	1.344771	1.55E-07
200	mtp_S6C_2_176n16	33493246	33495524	1.228532	9.08E-07
201	mtp_S6C_2_591j16	31649837	31652271	1.203571	3.06E-06
202	mtp_6S17_2_227c12	33018847	33021797	0.758475	9.18E-06
203	mtp_S6C_2_495l17	33146226	33148958	1.334531	1.23E-05

204	mtp_S6A_2_718o07	32605193	32606885	1.18814	1.63E-05
205	mtp_S6A_3_29p07	32928521	32931366	1.14799	2.03E-05
206	mtp_S6A_2_742g13	32710133	32712269	1.050884	2.07E-05
207	mtp_S6A_2_99j22	33015774	33018132	1.184914	2.07E-05
208	mtp_S6C_2_126m01	32689045	32691474	0.956218	2.43E-05
209	mtp_S6A_2_353i24	33348267	33350788	0.677166	5.92E-05
210	mtp_6S17_2_163a14	33374801	33377421	-0.62735	6.28E-05
211	mtp_S6A_2_607b18	31892543	31894559	-1.08672	8.39E-05
212	mtp_S6C_2_252b19	30081271	30083717	0.674057	9.14E-05
213	mtp_6S17_2_304j21	32890054	32892994	1.00715	0.0001135
214	mtp_S6C_2_261i05	33148418	33151260	1.34449	0.000131
215	mtp_S6A_3_10p04	31387943	31390679	1.371339	0.0001676
216	mtp_S6A_2_393k13	31392265	31394713	0.975536	0.0001773
217	mtp_S6A_2_152g09	31513524	31515946	-0.51419	0.0002072
218	mtp_S6C_2_437h19	31431405	31434315	0.806833	0.0002355
219	mtp_S6C_2_672h21	30822901	30825493	-0.62056	0.0002374
220	mtp_S6A_2_593o01	30994321	30996758	-0.72539	0.0002463
221	mtp_6S17_2_558f04	31651482	31654336	1.084652	0.000283
222	mtp_S6A_2_485e09	30754016	30756025	0.690791	0.0002857
223	mtp_6S17_2_75k18	30283371	30285180	-0.66476	0.0003405
224	mtp_6S17_2_283o09	31656398	31658063	0.909426	0.0003737
225	mtp_S6A_2_263p12	33288292	33290935	0.759434	0.000422
226	mtp_6S17_2_244b17	30041663	30044107	-0.48621	0.0005006
227	stSG1159344	32094951	32095618	0.76621	0.0005217
228	stSG1159309	30370522	30371723	0.746106	0.0006274
229	mtp_6S17_2_707l19	31995564	31998405	0.500099	0.0006637
230	mtp_S6A_2_649c07	31546522	31549182	-0.58717	0.0006647
231	mtp_S6C_2_269h18	30404296	30406670	-0.52764	0.0008381
232	mtp_S6A_2_19j15	32941867	32944276	0.760213	0.0009152
233	mtp_S6A_2_200e21	33187152	33188915	0.730549	0.0009207
234	mtp_S6A_2_42g10	32222119	32224613	0.481033	0.0009589
	MCF7				
	Clone Name	**Start**	**End**	**M-value**	**p-value**
235	mtp_S6A_2_617f24	30758534	30760818	1.722349	9.90E-11
236	mtp_S6C_2_495l17	33146226	33148958	1.638079	5.62E-10
237	mtp_S6C_2_542d02	32552075	32554386	-1.26969	1.25E-09
238	mtp_S6A_2_126l05	30763012	30765292	1.060891	1.40E-09
239	mtp_S6C_2_446o03	30129527	30132152	-0.95654	6.32E-09
240	stSG1159389	33161371	33162818	-1.06777	1.52E-08
241	mtp_S6C_2_173b09	32063457	32066073	-1.25293	2.54E-08
242	mtp_S6A_2_593o01	30994321	30996758	-0.79813	2.75E-08
243	mtp_S6C_2_591j16	31649837	31652271	0.886516	8.53E-08
244	mtp_6S17_2_118i14	33020486	33022969	1.093815	1.02E-07
245	mtp_S6C_2_417b10	30023644	30025314	1.418453	1.11E-07
246	mtp_S6C_2_35n12	31904599	31907111	-1.44894	1.13E-07
247	stSG1159377	32124830	32125663	-0.98314	1.25E-07
248	mtp_S6A_2_673h09	30034394	30036661	-1.03355	1.40E-07
249	mtp_S6A_2_149a10	29861411	29863644	-0.7115	1.47E-07
250	mtp_6S17_2_560n07	31383618	31385658	0.75882	1.56E-07

251	mtp_6S17_2_558f04	31651482	31654336	0.989128	1.82E-07
252	mtp_S6C_2_256g20	29960874	29962955	0.848121	2.20E-07
253	mtp_S6C_2_126m01	32689045	32691474	0.958427	2.84E-07
254	mtp_6S17_2_227c12	33018847	33021797	0.767396	3.32E-07
255	mtp_S6C_2_247i11	32720216	32722920	-0.82355	4.08E-07
256	mtp_S6C_2_494b13	32680961	32683760	0.729892	4.18E-07
257	mtp_S6A_2_577p21	30363052	30365623	0.717306	4.58E-07
258	mtp_6S17_2_583k01	30231506	30234359	1.309995	4.97E-07
259	mtp_S6C_2_261i05	33148418	33151260	1.449423	6.46E-07
260	mtp_6S17_2_704e03	31541574	31544203	-0.70854	6.96E-07
261	mtp_S6A_3_29p07	32928521	32931366	1.109096	7.91E-07
262	mtp_6S17_2_537l09	33501985	33503886	0.645086	8.24E-07
263	mtp_6S17_2_40d18	31553280	31555425	-0.87511	8.64E-07
264	mtp_S6C_2_252b19	30081271	30083717	0.741594	1.05E-06
265	mtp_6S17_2_143c10	33179389	33182056	-0.67008	1.66E-06
266	mtp_S6A_2_607b18	31892543	31894559	-1.62095	2.02E-06
267	mtp_6S17_2_646n05	31352523	31355086	-0.88519	2.10E-06
268	mtp_S6A_2_571b17	32918067	32920344	1.540323	2.34E-06
269	mtp_S6C_2_328g03	31369850	31372247	1.305149	2.61E-06
270	mtp_S6C_2_242j03	30825368	30827875	-0.86811	4.03E-06
271	mtp_S6A_3_76a07	31376096	31377899	0.622509	5.02E-06
272	mtp_S6A_2_29i03	33130078	33132394	-0.95538	8.98E-06
273	mtp_6S17_2_163a14	33374801	33377421	-0.63635	1.19E-05
274	mtp_S6C_2_291o13	32539196	32541992	-0.51466	1.34E-05
275	mtp_6S17_2_278p22	32751956	32754798	0.627347	1.43E-05
276	mtp_6S17_2_536j18	32505710	32507577	0.478069	1.72E-05
277	mtp_S6C_2_47o13	30341155	30343559	-0.57607	1.93E-05
278	mtp_S6A_2_319p03	32786130	32788393	0.62126	1.95E-05
279	mtp_6S17_2_150b10	31962270	31964146	-0.54188	2.27E-05
280	mtp_S6C_2_323p21	31544177	31546543	-0.69278	2.41E-05
281	mtp_S6A_2_435c02	29997684	29999912	-0.76466	2.44E-05
282	mtp_6S17_2_691p19	32333324	32335035	-0.58101	2.55E-05
283	mtp_S6A_2_495p21	33246190	33248772	0.557239	2.70E-05
284	mtp_6S17_2_283o09	31656398	31658063	0.753481	2.72E-05
285	mtp_6S17_2_339j05	32987255	32990019	-1.00603	3.06E-05
286	mtp_S6A_2_427m23	29921905	29924681	-0.61879	3.08E-05
287	mtp_S6C_2_169c05	31112554	31114212	0.520293	3.36E-05
288	mtp_S6C_2_725k15	30351301	30353113	1.225248	3.44E-05
289	mtp_6S17_2_523e17	29899083	29901168	-0.76674	3.50E-05
290	mtp_6S17_2_130a06	30958243	30959538	-0.65883	3.66E-05
291	mtp_S6A_2_485e09	30754016	30756025	0.614172	3.87E-05
292	mtp_6S17_2_788a04	30087895	30090090	-0.79337	3.98E-05
293	mtp_S6A_2_550c18	31647311	31649827	0.9494	4.15E-05
294	mtp_S6A_2_66m22	29947487	29949977	-0.6585	4.19E-05
295	mtp_6S17_2_214d05	30146157	30148833	0.428611	4.22E-05
296	mtp_S6A_2_353i24	33348267	33350788	-0.64813	4.24E-05
297	stSG1159311	31903338	31904796	-0.95195	4.28E-05
298	mtp_S6C_2_479j24	32496153	32498835	-0.69457	4.35E-05
299	mtp_S6A_2_209i18	31507238	31509555	-0.98144	4.47E-05

300	mtp_6S17_2_705p22	33513248	33516058	-0.57214	4.50E-05
301	mtp_S6A_2_151a18	31367358	31369739	0.690009	5.05E-05
302	mtp_S6A_2_99j22	33015774	33018132	0.992915	5.91E-05
303	mtp_S6C_2_442e02	32642241	32644714	-0.89555	7.32E-05
304	mtp_6S17_2_408b06	33047336	33050005	-0.71171	7.41E-05
305	mtp_S6A_2_349p03	29852518	29854940	-0.67915	7.77E-05
306	mtp_S6A_2_579i17	31365145	31367681	-0.48871	8.34E-05
307	mtp_S6C_2_451a13	32641050	32643561	-0.94326	8.58E-05
308	mtp_S6C_2_581h23	30496479	30499147	0.506153	8.83E-05
309	mtp_S6C_2_420g20	33462560	33465285	0.512422	9.09E-05
310	mtp_S6A_2_195b05	31522428	31524251	0.442649	9.84E-05
311	mtp_6S17_2_550d16	30178743	30181378	0.635713	0.0001068
312	mtp_S6C_2_296i15	29805657	29808379	-0.62679	0.0001087
313	mtp_S6C_2_560j06	31822009	31824451	-0.52368	0.0001099
314	mtp_S6A_2_365l07	30756515	30758800	0.590558	0.0001146
315	mtp_S6C_2_602b15	30521587	30523578	0.718527	0.0001247
316	mtp_S6A_2_180o24	31441096	31443372	-0.78154	0.0001341
317	mtp_S6C_2_266a20	32588572	32590988	-0.47288	0.0001537
318	mtp_6S17_2_431p03	31485229	31487901	-0.54793	0.0001632
319	mtp_S6A_2_174l24	30173168	30175684	0.380024	0.000166
320	mtp_S6C_2_674e02	33084323	33086976	0.637764	0.0001664
321	mtp_S6A_2_415h04	31604437	31607304	-0.463	0.0001747
322	mtp_S6C_2_84b09	31306864	31309399	-0.66905	0.0001842
323	mtp_6S17_2_368a11	31700030	31702827	-0.52412	0.000188
324	mtp_S6A_3_70g05	30523998	30526686	0.844319	0.0002068
325	stSG1159381	32628159	32629647	-0.51668	0.0002098
326	mtp_6S17_2_477f16	30509530	30512280	0.6886	0.000222
327	mtp_S6A_2_84i07	29788550	29790980	-0.91074	0.0002331
328	mtp_S6C_2_450i05	33355252	33357951	-0.60344	0.0002342
329	mtp_S6A_2_400k18	31791865	31794379	-0.58838	0.0002603
330	mtp_S6A_2_223f06	31902447	31904569	-0.76213	0.0002793
331	mtp_S6A_2_507a06	30498694	30501279	0.43934	0.0002968
332	mtp_6S17_2_203n20	31689689	31692751	0.645595	0.0003015
333	mtp_6S17_2_9m02	29975451	29978299	-0.61241	0.0003346
334	mtp_S6A_2_71k05	32868718	32871367	-0.83589	0.0003368
335	mtp_S6C_3_147l15	31933254	31936222	-0.40006	0.0003516
336	mtp_S6A_2_446h15	30424262	30426665	0.908199	0.0004169
337	mtp_S6C_2_311i13	31470091	31472561	-0.82808	0.0004354
338	mtp_6S17_2_685i13	33365027	33366857	-0.94413	0.0004496
339	mtp_S6C_2_158k03	32666007	32668413	-0.53493	0.0004514
340	stSG1159309	30370522	30371723	0.562395	0.0004606
341	mtp_S6C_2_169h15	32894483	32897025	-0.40184	0.0004631
342	mtp_S6A_2_211a07	29884167	29886552	0.509612	0.0004699
343	mtp_S6A_2_238l14	30233200	30235491	-0.62232	0.0004742
344	mtp_S6A_2_534n13	33128270	33130623	-0.61796	0.0004872
345	mtp_S6C_2_672h21	30822901	30825493	-0.75586	0.0004888
346	mtp_6S17_2_749c13	30754744	30757288	0.649079	0.0004914
347	mtp_S6A_2_377g19	30078444	30080712	-1.11138	0.0004997
348	mtp_6S17_2_556c06	31407745	31410625	0.68503	0.0005032

349	mtp_S6A_2_596o19	31442467	31444925	-0.88855	0.0005103
350	mtp_S6A_2_724m04	30350008	30351777	0.497283	0.0005295
351	mtp_6S17_2_30e24	31451728	31454419	0.876509	0.0005372
352	mtp_6S17_2_617i02	30238940	30240972	0.803218	0.0005497
353	mtp_S6C_2_728o04	31784795	31786680	0.586009	0.000567
354	mtp_S6A_2_165l18	30960918	30963025	-1.63084	0.0005768
355	mtp_S6A_2_131p01	32261170	32263480	-0.42238	0.0006133
356	mtp_S6C_2_233b21	29952327	29954750	-0.72725	0.0006166
357	mtp_S6C_2_405j01	30476804	30479649	1.423038	0.0006381
358	mtp_6S17_2_624p03	30428243	30430343	0.467783	0.0006676
359	mtp_6S17_2_435e01	30020915	30023760	-0.73822	0.0006679
360	mtp_6S17_2_577d11	30991536	30994461	0.529195	0.0006714
361	mtp_6S17_2_494h12	30767990	30770760	0.564341	0.0006943
362	mtp_S6A_2_403c13	30433512	30435982	0.821549	0.0007068
363	mtp_S6A_2_649c07	31546522	31549182	-0.55807	0.0007201
364	mtp_S6C_2_529n06	30131866	30134499	-0.5302	0.0007319
365	mtp_S6A_2_594m04	33159764	33161477	-0.75746	0.0007896
366	mtp_6S17_2_608m07	32455394	32458106	0.466302	0.000814
367	mtp_S6C_2_630p01	31849432	31852366	-0.69456	0.0008157
368	mtp_S6A_2_701o19	31214656	31216338	0.370916	0.0008342
369	mtp_S6C_2_573h06	32904298	32906120	1.107249	0.00089
370	mtp_6S17_2_244b17	30041663	30044107	-0.38159	0.0008919
371	mtp_S6C_2_269h18	30404296	30406670	-0.39783	0.0009188
372	mtp_S6A_3_6j09	31717156	31720176	-0.39535	0.0009473
373	mtp_S6C_2_628n07	31702678	31705254	-0.51633	0.0009511
374	mtp_S6C_2_242e22	31349918	31352712	-0.91514	0.0009541
375	mtp_6S17_2_205b08	33387409	33389702	-0.59709	0.0009612
	T47D				
	Clone Name	**Start**	**End**	**M-value**	**p-value**
376	mtp_S6C_2_291o13	32539196	32541992	-1.29528	3.97E-09
377	mtp_S6A_2_617f24	30758534	30760818	1.782922	1.07E-08
378	mtp_S6A_2_126l05	30763012	30765292	1.699656	5.72E-08
379	mtp_6S17_2_118i14	33020486	33022969	1.401021	1.39E-06
380	mtp_S6A_2_422n17	32430334	32433086	-1.08039	1.77E-06
381	mtp_S6C_2_285g11	30519080	30521624	-0.86139	1.92E-06
382	mtp_6S17_2_558f04	31651482	31654336	1.041974	5.91E-06
383	mtp_S6C_2_323p21	31544177	31546543	-0.92859	1.27E-05
384	mtp_6S17_2_111f06	30134479	30136131	1.286751	1.52E-05
385	mtp_S6C_2_189h20	29942189	29945148	-0.80317	3.10E-05
386	mtp_6S17_2_227c12	33018847	33021797	0.962292	3.33E-05
387	mtp_S6A_3_29p07	32928521	32931366	1.232809	3.85E-05
388	mtp_6S17_2_124e21	33142984	33145436	-1.00387	4.19E-05
389	mtp_S6A_2_607b18	31892543	31894559	-1.20159	4.69E-05
390	stSG1159382	32631240	32632113	1.010522	5.99E-05
391	mtp_S6C_2_420g20	33462560	33465285	0.922306	6.29E-05
392	mtp_S6C_2_591j16	31649837	31652271	1.118047	9.12E-05
393	mtp_S6C_2_494h24	32566224	32568770	1.177862	9.49E-05
394	mtp_S6C_2_567l15	32484275	32487774	-0.90546	0.0001398
395	mtp_S6C_2_235c10	30094409	30096974	0.799617	0.0001422

396	mtp_S6A_2_137k10	29983949	29986575	-0.79445	0.0001804
397	mtp_6S17_2_707a20	32872192	32874816	-0.69772	0.0001899
398	mtp_6S17_2_34c02	29939562	29942347	-0.94461	0.0001906
399	mtp_S6A_2_550c18	31647311	31649827	1.003426	0.0001997
400	mtp_S6C_2_392f07	32783173	32786086	-0.6499	0.0002078
401	mtp_S6C_2_29d18	32870242	32872810	-0.72618	0.0002366
402	mtp_S6C_2_169c05	31112554	31114212	0.537283	0.00026
403	mtp_S6A_2_374i19	32678591	32681243	1.270246	0.0003693
404	mtp_6S17_2_414a03	31637916	31640706	0.531428	0.0003995
405	mtp_S6C_2_461d02	31014145	31016926	0.635657	0.0004075
406	mtp_S6C_2_672h21	30822901	30825493	-0.68673	0.0004805
407	mtp_S6C_2_495l17	33146226	33148958	1.027689	0.0005442
408	mtp_S6C_2_351b16	32644074	32646662	-0.79282	0.0005524
409	mtp_S6A_2_485e09	30754016	30756025	1.032661	0.0005525
410	mtp_S6C_2_417b10	30023644	30025314	1.463841	0.0007582
411	mtp_6S17_2_583k01	30231506	30234359	1.10007	0.0007721
412	mtp_S6A_3_30g20	32533849	32536651	-0.70346	0.0008137
413	mtp_S6A_2_693p14	33144119	33146299	-1.03754	0.0008252
414	mtp_6S17_2_403h19	29945051	29947511	-0.58579	0.0008952
415	mtp_S6C_2_754f14	32557020	32559661	-0.74717	0.00096
416	mtp_S6A_2_99j22	33015774	33018132	1.27525	0.0009647
417	mtp_S6C_2_63h24	33292021	33293767	-0.67812	0.0009838
418	mtp_S6C_2_482e09	29967686	29969637	-0.69363	0.0009839
	K562				
	Clone Name	**Start**	**End**	**M-value**	**p-value**
419	mtp_6S17_2_550d16	30178743	30181378	1.813617	3.27E-09
420	mtp_S6A_2_203l11	33082017	33084690	-1.57977	1.59E-08
421	mtp_S6A_2_63e09	30288220	30290560	1.814325	6.36E-08
422	mtp_S6A_3_29p07	32928521	32931366	2.342967	1.24E-07
423	stSG1159377	32124830	32125663	-1.42949	3.88E-07
424	mtp_S6A_2_215a19	33169768	33172038	-0.86194	4.87E-07
425	mtp_6S17_2_111f06	30134479	30136131	1.302455	5.14E-07
426	mtp_S6C_2_249g19	33090674	33093215	-1.25453	2.13E-06
427	mtp_6S17_2_134i19	31024896	31027536	-0.93995	2.71E-06
428	mtp_S6C_2_252b19	30081271	30083717	0.996822	3.04E-06
429	mtp_6S17_2_130a06	30958243	30959538	1.1478	3.17E-06
430	mtp_6S17_2_40d18	31553280	31555425	-1.13414	3.90E-06
431	mtp_S6C_2_35n12	31904599	31907111	-1.24066	7.09E-06
432	mtp_S6A_2_126l05	30763012	30765292	1.238969	7.19E-06
433	stSG1159311	31903338	31904796	-1.26344	9.72E-06
434	mtp_S6A_2_577p21	30363052	30365623	0.874226	1.27E-05
435	mtp_6S17_2_337o24	30903401	30906093	0.995116	1.69E-05
436	mtp_S6A_2_152g09	31513524	31515946	-0.79528	1.81E-05
437	mtp_S6A_2_607b18	31892543	31894559	-1.2635	2.33E-05
438	mtp_S6A_2_571b17	32918067	32920344	1.734007	3.04E-05
439	mtp_S6C_2_417b10	30023644	30025314	1.208653	4.14E-05
440	mtp_6S17_2_283o09	31656398	31658063	1.033447	4.32E-05
441	mtp_S6C_2_495l17	33146226	33148958	1.321642	6.85E-05
442	mtp_6S17_2_558f04	31651482	31654336	1.040009	7.24E-05

443	mtp_6S17_2_124e21	33142984	33145436	-1.24287	8.26E-05
444	mtp_S6A_2_352g13	32278686	32281326	-0.72338	9.16E-05
445	mtp_6S17_2_206g17	30264102	30266980	-0.94293	9.17E-05
446	mtp_6S17_2_583k01	30231506	30234359	1.260341	0.0001286
447	mtp_S6A_2_422n17	32430334	32433086	-0.89926	0.0001517
448	mtp_S6C_2_512f05	33077075	33079961	-0.83076	0.0001791
449	mtp_S6A_2_693p14	33144119	33146299	-1.55943	0.0001888
450	mtp_S6C_2_323p21	31544177	31546543	-0.89927	0.0002395
451	mtp_6S17_2_47d01	31192661	31195203	-0.84057	0.0002441
452	mtp_S6C_2_446o03	30129527	30132152	1.038804	0.000261
453	mtp_6S17_2_154o06	31185615	31188154	-1.0366	0.0002681
454	mtp_S6A_2_99j22	33015774	33018132	0.929407	0.0002871
455	mtp_S6A_2_180o24	31441096	31443372	-0.87963	0.0003012
456	stSG1159329	32080229	32081243	0.844391	0.0003174
457	mtp_6S17_2_283h21	31023710	31026101	-1.19789	0.0003211
458	mtp_S6C_2_291o13	32539196	32541992	-0.65126	0.0003295
459	mtp_S6A_2_540a21	31087638	31089814	-0.66246	0.0003502
460	mtp_S6C_3_128c17	33281188	33283958	0.705128	0.0003914
461	mtp_S6C_2_328g03	31369850	31372247	1.144393	0.0004181
462	mtp_6S17_2_676f20	31118993	31121827	-0.76444	0.0004221
463	mtp_S6A_2_594m04	33159764	33161477	-1.61745	0.0004365
464	mtp_S6A_2_29i03	33130078	33132394	-1.13731	0.0004972
465	stSG1159389	33161371	33162818	-1.63193	0.0005346
466	mtp_S6A_2_434k14	29965444	29967775	-0.98072	0.0005607
467	mtp_S6C_2_261i05	33148418	33151260	1.101245	0.0005824
468	mtp_6S17_2_403h19	29945051	29947511	-0.80451	0.0006158
469	stSG1159367	32111840	32112986	0.721595	0.0006469
470	mtp_6S17_2_106c06	33010869	33013520	-0.76766	0.000657
471	mtp_S6A_2_223f06	31902447	31904569	-0.93172	0.0007029
472	mtp_6S17_2_704e03	31541574	31544203	-1.03204	0.0007468
473	mtp_S6C_2_109m03	33079784	33082134	-0.87375	0.0008087
474	mtp_S6A_2_724m04	30350008	30351777	0.580665	0.0008155
475	mtp_S6C_2_437h19	31431405	31434315	0.79726	0.0008557
476	mtp_6S17_2_806h02	33194560	33196721	0.503952	0.0008652
477	mtp_S6C_2_63h24	33292021	33293767	-0.81228	0.0008962
478	mtp_6S17_2_707a20	32872192	32874816	-0.62536	0.0009228
	578T				
	Clone Name	**Start**	**End**	**M-value**	**p-value**
479	mtp_S6A_2_77l14	29741918	29744577	0.763344	0.0004559
480	mtp_S6C_2_33f20	29784008	29786547	-0.96811	0.0007055
481	mtp_S6C_2_296i15	29805657	29808379	-0.91	5.92E-05
482	mtp_S6C_2_256g20	29960874	29962955	0.87112	0.0001627
483	mtp_S6C_2_417b10	30023644	30025314	1.209422	7.52E-05
484	mtp_S6C_2_252b19	30081271	30083717	0.942966	0.0001421
485	mtp_6S17_2_111f06	30134479	30136131	0.871317	2.89E-05
486	mtp_6S17_2_214d05	30146157	30148833	1.046351	8.81E-08
487	mtp_6S17_2_550d16	30178743	30181378	1.450958	4.60E-08
488	mtp_6S17_2_624p03	30428243	30430343	0.625393	0.0007955
489	mtp_S6A_2_485e09	30754016	30756025	1.364416	2.16E-05

490	mtp_S6A_2_126l05	30763012	30765292	1.140752	2.78E-06
491	mtp_6S17_2_494h12	30767990	30770760	0.711924	0.0001308
492	mtp_6S17_2_337o24	30903401	30906093	0.724276	8.92E-06
493	mtp_6S17_2_130a06	30958243	30959538	1.052614	6.86E-08
494	mtp_6S17_2_575h02	31100296	31102131	0.763887	0.0005684
495	mtp_S6A_3_76a07	31376096	31377899	-0.68428	0.0006986
496	mtp_S6A_2_205l16	31410312	31412594	-0.74116	0.0008045
497	mtp_S6C_2_525h16	31410804	31413338	-0.89887	9.83E-05
498	mtp_S6C_2_315o12	31419326	31421777	-0.94361	0.0007341
499	mtp_S6C_2_437h19	31431405	31434315	0.930959	0.0007604
500	mtp_S6A_2_596o19	31442467	31444925	-0.83344	0.0006928
501	mtp_S6A_2_152g09	31513524	31515946	-1.03619	4.78E-06
502	mtp_S6C_2_591j16	31649837	31652271	0.900304	3.18E-05
503	mtp_6S17_2_558f04	31651482	31654336	1.128676	1.35E-05
504	mtp_6S17_2_283o09	31656398	31658063	0.848681	0.0005942
505	mtp_S6A_2_607b18	31892543	31894559	-1.30215	2.30E-05
506	mtp_S6C_2_35n12	31904599	31907111	-0.94557	0.0004561
507	mtp_S6C_2_173b09	32063457	32066073	-0.9907	8.76E-05
508	stSG1159344	32094951	32095618	-0.54195	0.0006025
509	stSG1159377	32124830	32125663	-1.03526	3.58E-05
510	mtp_S6A_2_528m17	32288063	32290295	-0.77037	0.0001326
511	mtp_6S17_2_700n22	32293344	32295765	-0.88109	5.29E-05
512	mtp_6S17_2_601o04	32298082	32300874	-0.86989	0.0009984
513	mtp_S6A_2_422n17	32430334	32433086	-1.06942	2.06E-06
514	mtp_S6C_2_599m10	32471036	32473567	-0.8953	0.0002523
515	mtp_S6C_2_567l15	32484275	32487774	-1.15683	0.0004177
516	mtp_S6A_2_69d24	32487094	32489228	-1.00168	0.0005821
517	mtp_6S17_2_536j18	32505710	32507577	0.681998	0.0001884
518	mtp_S6C_2_291o13	32539196	32541992	-0.89436	0.0002175
519	mtp_S6C_2_542d02	32552075	32554386	-0.89816	0.0006355
520	mtp_S6C_3_125f11	32592713	32595798	-1.18136	0.0001557
521	stSG1159380	32601273	32601860	-1.26308	0.0005372
522	mtp_S6A_2_247f17	32609013	32611396	-0.80472	0.0001054
523	stSG1159384	32633359	32634474	-0.71199	0.0005897
524	mtp_S6C_3_129n21	32637066	32640334	-0.87328	7.72E-05
525	mtp_S6C_2_442e02	32642241	32644714	-0.79022	0.0009418
526	mtp_S6C_2_351b16	32644074	32646662	-1.01415	0.0001885
527	mtp_S6C_2_158k03	32666007	32668413	-0.88331	0.0004025
528	mtp_6S17_2_540i21	32716744	32719125	-1.03478	9.01E-05
529	mtp_S6C_2_247i11	32720216	32722920	-0.99852	0.0001093
530	mtp_S6C_2_766n01	32733611	32736437	-0.87053	0.0001096
531	mtp_S6C_2_29d18	32870242	32872810	-0.66463	0.0003428
532	mtp_S6A_2_200a10	32888310	32890611	-1.42085	0.0005849
533	mtp_S6A_2_571b17	32918067	32920344	1.532234	0.0001507
534	mtp_S6A_3_29p07	32928521	32931366	1.122592	2.15E-05
535	mtp_S6A_2_203l11	33082017	33084690	-1.16469	0.0001271
536	mtp_S6C_2_249g19	33090674	33093215	-1.53323	0.0001774
537	mtp_S6A_2_113b04	33097613	33099941	-1.17848	3.34E-05
538	mtp_S6A_2_29i03	33130078	33132394	-0.90704	0.0001379

539	mtp_6S17_2_124e21	33142984	33145436	-1.5521	5.18E-06
540	mtp_S6A_2_693p14	33144119	33146299	-1.56936	0.0001033
541	mtp_S6A_2_594m04	33159764	33161477	-1.32693	3.88E-05
542	stSG1159389	33161371	33162818	-1.40478	3.20E-07
543	mtp_6S17_2_109l12	33162178	33164006	-1.45179	1.06E-06
544	mtp_S6A_2_215a19	33169768	33172038	-0.86117	4.32E-06
545	mtp_S6A_2_33i07	33260428	33262435	-0.82609	0.0005795
546	mtp_S6C_2_141a12	33279164	33281784	1.292865	9.87E-05
547	mtp_S6C_3_128c17	33281188	33283958	0.861494	1.32E-05
548	mtp_S6C_2_551e11	33286034	33288603	0.83157	0.0002175
549	mtp_S6C_2_63h24	33292021	33293767	-0.98491	0.0004232
550	mtp_6S17_2_205b08	33387409	33389702	1.150282	3.40E-05
551	mtp_S6C_2_420g20	33462560	33465285	0.840402	6.72E-05
552	mtp_S6C_2_176n16	33493246	33495524	0.790378	9.14E-06

Table 5.2 **DMRs between each of the cancer cell lines and the shared controls.** Chromosome 6 coordinates (NCBI_35), M- and p-values are given.